

**MECHANISMS OF AUTOPHAGY CONTROL THROUGH MICRORNAS
UNDER CELLULAR STRESS**

by
DENIZ GULFEM OZTURK

Submitted to the Faculty of Engineering and Natural Sciences
in partial fulfillment of
the requirements for the degree of
Doctor of Philosophy

Sabanci University

July 2019

TITLE OF THE THESIS/DISSERTATION

APPROVED BY:

Prof. Dr. Devrim Gözûaçık
(Thesis Supervisor)



Prof. Dr. Ali Koşar



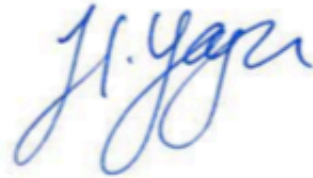
Assoc. Prof. Dr. Özlem Kutlu



Assoc. Prof. Dr. Hilal Kazan



Assoc. Prof. Dr. Havva Funda Yağcı Acar



DATE OF APPROVAL: 19/07/2019

© Deniz Glfem ztrk 2019
All Rights Reserved

ABSTRACT

DENİZ GÜLFEM ÖZTÜRK

Ph.D. Dissertation, July 2019

Thesis Supervisor: Prof. Devrim Gozuacik

Keywords: autophagy, cellular stress, lysosome, microRNA, MITF, mTOR, RICTOR

Macroautophagy (autophagy) is an evolutionarily conserved stress response mechanism that is necessary for the maintenance of cellular homeostasis. Autophagic activity in cells is regulated by various upstream signaling pathways including mTOR. Stress-mediated inhibition of mTOR complex 1 (mTORC1) results in the nuclear translocation of the TFE/MITF family of transcriptional factors, and triggers an autophagy- and lysosomal-related gene transcription program. In this thesis work, we introduce a specific and rate-limiting role for MITF in autophagy regulation that requires transcriptional activation of *MIR211*. Under stress conditions including starvation and mTOR inhibition, a MITF-*MIR211* axis constitutes a novel feed-forward loop that controls autophagic activity in cells. Direct targeting and downregulation of mTORC2 binding partner RICTOR by *MIR211* attenuated mTORC1 signal through AKT-mediated crosstalk. Under these conditions, the transcription factor MITF translocated from cytosol to the nucleus, and amplified autophagic activity. All together, the outcome of this thesis is the identification of MITF-*MIR211* axis as a novel autophagy amplification mechanism required for optimal autophagy activation under cellular stress conditions.

ÖZET

DENİZ GÜLFEM ÖZTÜRK

Doktora Tezi, Temmuz 2019

Tez Danışmanı: Prof. Devrim Gözüaçık

Anahtar kelimeler: otofaji, hücrel stres, lizozom, mikroRNA, MITF, mTOR, RICTOR

Makrotofaji (otofaji) evrimsel olarak korunan bir geri dönüşüm ve stres yanıt mekanizmasıdır. Hücrel otofajik aktivite, mTOR dahil olmak üzere çeşitli sinyal yolları ile düzenlenir. mTOR kompleksi 1'in (mTORC1) stres kaynaklı inhibisyonu, MITF/TFE transkripsiyonel faktör ailesinin nükleer translokasyonu ile sonuçlanır, ve otofaji ve lizozomal ilişkili bir gen transkripsiyon programını tetikler. Bu tez çalışmasında, ilk defa MITF için otofaji kontrolünde *MIR211*'in transkripsiyonel düzenlemesini içeren spesifik ve oran sınırlayıcı bir rol ortaya koyuyoruz. Açlık ve mTOR inhibisyonu stres koşullarını altında, MITF-*MIR211* ekseninin hücrelerde otofajik aktiviteyi kontrol eden yeni ve özgün bir ileri besleme döngüsü oluşturduğunu gösterdik. mTORC2 bileşeni RICTOR'un *MIR211* ile doğrudan hedeflenmesi; mTORC1 yolağının AKT aracılığıyla inhibe edilmesine, dolayısıyla MITF'in hücre çekirdeğine göçüne ve otofaji amplifikasyon döngüsünün tamamlanmasına yol açmıştır. Sonuç olarak, bu tez çalışmasından elde edilen verilerle MITF-*MIR211* eksenini yeni bir otofaji amplifikasyon mekanizması olarak tanımlanmıştır ve bu eksenin hücrel stres koşulları altında optimal otofaji aktivasyonu için gerekliliği ispatlanmıştır.

*Dedicated to
Bayram Öztürk and Recep Akbıyık*

“Her eđitimli kadının bu Cumhuriyet’e borcu vardır.”

Türkan Saylan

ACKNOWLEDGEMENTS

First and foremost, I would like to express my very great gratitude to my thesis supervisor Prof. Devrim Gozuacik. I appreciate all his contributions of time, ideas, and funding to make my PhD experience productive and stimulating. Without his endless support, patient guidance and encouragement, this thesis would not have been possible. It is truly an honor to complete my PhD thesis under his supervision.

Besides my advisor, I would like to thank the rest of my thesis committee: Asst. Prof. Hilal Kazan, Assoc. Prof. Havva Funda Yağcı Acar, Assoc. Prof. Özlem Kutlu and Prof. Ali Koşar for their encouragement and insightful comments.

A very special gratitude goes out to Muhammed Koçak. It was a great relief and comfort to know that he was there for me no matter what. This journey would not be easy without him, I was so lucky. My heartfelt thanks to my given brother.

I would like to express my sincere appreciation to Dr. Gözde Korkmaz, my very first mentor in the lab. I could never ask a better mentor than her who was so generous in sharing her knowledge in science and life.

I would like to thank all former and present Gozuacik Lab members. It was great sharing laboratory with all of them during these years.

My special thanks are extended to Nur Kocatürk, Yunus Akkoç and Seçil Erbil for sharing all the joy and pain we have had in the last seven years. This would not have been possible without their unwavering love and support given to me at all times.

Finally, to my family, because I owe it all to you.

Thank you.

TABLE OF CONTENTS

| | |
|--|-----------|
| 1. INTRODUCTION | 1 |
| 1.1. Autophagy | 2 |
| 1.1.1 <i>Microautophagy</i> | 2 |
| 1.1.2 <i>Chaperone-mediated autophagy</i> | 4 |
| 1.1.3 <i>Macroautophagy</i> | 5 |
| 1.1.3.1 Core autophagy proteins | 6 |
| 1.1.3.2 Initiation and formation of the autophagosome | 7 |
| 1.1.3.3 Elongation of the autophagosome | 9 |
| 1.1.3.4 Maturation and fusion with the lysosomes | 10 |
| 1.1.3.5 Selective autophagy and autophagy receptors..... | 11 |
| 1.2 mTOR Regulation of Autophagy | 13 |
| 1.2.1 <i>mTOR structure and organization into complexes</i> | 13 |
| 1.2.2 <i>mTORC1: Functions and signaling pathways</i> | 15 |
| 1.2.3 <i>mTORC2: Functions and signaling pathways</i> | 19 |
| 1.2.4 <i>mTOR and autophagy</i> | 22 |
| 1.3 Transcriptional Control of Autophagy: MiT/TFE Transcription Factors | 25 |
| 1.3.1 <i>MITF/TFE Family of Transcription Factors</i> | 26 |
| 1.3.2 <i>Regulation of MITF/TFE activity</i> | 33 |
| 1.3.2.1 Nutrient deprivation and mTORC-1 dependent regulation | 34 |
| 1.3.2.2 Cellular Stress | 36 |
| 1.3.2.3 mTORC1-independent regulation | 38 |
| 1.3.3 <i>Lysosomal and autophagy-related targets of MITF/TFE family</i> | 41 |
| 1.4 Epigenetic Regulation of Autophagy: microRNAs | 46 |
| 1.4.1 <i>microRNAs</i> | 46 |
| 1.4.2 <i>microRNA Biogenesis</i> | 47 |
| 1.4.3 <i>Autophagy-regulating microRNAs</i> | 50 |
| 1.4.4 <i>Autophagy-regulating microRNAs and cancer</i> | 51 |
| 1.4.5 <i>MIR211</i> | 52 |
| 1.5 Role of autophagy in cancer development and progression | 55 |
| 1.5.1 <i>Autophagy as a tumor suppressor</i> | 55 |
| 1.5.2 <i>Autophagy as a tumor promoter</i> | 57 |
| 1.5.3 <i>Autophagy and cancer treatment</i> | 59 |
| 2. MATERIALS AND METHODS..... | 60 |
| 2.1 Plasmid and constructs | 60 |
| 2.2 Cell Culture..... | 60 |

| | |
|---|------------|
| 2.2.1 Cell Line Maintenance | 60 |
| 2.2.2 <i>Transient and stable transfections</i> | 61 |
| 2.2.3 <i>Autophagy induction in cell culture</i> | 61 |
| 2.3 Protein isolation and immunoblotting..... | 61 |
| 2.4 Immunofluorescence tests..... | 62 |
| 2.4.1 <i>Immunofluorescence analyses.....</i> | 62 |
| 2.4.2 <i>Quantitative GFP-LC3, GFP-WIP1, RFP-GFP-LC3, RFP-LAMP1 analyses.....</i> | 63 |
| 2.5 Bioinformatics analyses | 63 |
| 2.6 RNA isolation and RT-PCR analyses | 64 |
| 2.7 Dual luciferase reporter assay..... | 65 |
| 2.8 Antagomir and siRNA tests | 65 |
| 2.9 Chromatin immunoprecipitation (ChIP) and ChIP-qPCR..... | 66 |
| 2.10 Human tissue samples..... | 67 |
| 2.11 Statistical analyses..... | 67 |
| 3. RESULTS..... | 68 |
| 3.1 MITF is required for starvation and mTOR- dependent autophagy | 69 |
| 3.1.1 <i>Effect of MITF overexpression on autophagy</i> | 70 |
| 3.1.2 <i>Effect of MITF silencing on autophagy</i> | 76 |
| 3.2 Role of MITF-dependent transcriptional activation in autophagy control | 89 |
| 3.3 <i>MIR211</i> induced autophagy..... | 98 |
| 3.3.1 <i>Effect of MIR211 on basal autophagy</i> | 99 |
| 3.3.2 <i>Effect of MIR211 on torin1-induced autophagy.....</i> | 101 |
| 3.3.3 <i>Effect of MIR211 on starvation-induced autophagy.....</i> | 106 |
| 3.4 Inhibition of <i>MIR211</i> suppressed starvation- and MTOR-dependent autophagy. ... | 114 |
| 3.4.1 <i>Effect of AN211 on torin1-induced autophagy</i> | 115 |
| 3.4.2 <i>Effect of AN211 on starvation-induced autophagy.....</i> | 121 |
| 3.4.3 <i>Regulation of autophagy through MITF/MIR211 axis</i> | 124 |
| 3.5 RICTOR was an autophagy-related target of <i>MIR211</i>..... | 125 |
| 3.5.1 <i>Target prediction using bioinformatics tools.....</i> | 126 |
| 3.5.2 <i>Effect of MIR211 on target mRNA and protein levels.....</i> | 126 |
| 3.5.3 <i>Luciferase activity assay to demonstrate direct binding of MIR211 to RICTOR.....</i> | 130 |
| 3.5.4 <i>Rescue assay to demonstrate RICTOR is a rate-limiting target</i> | 133 |

| | |
|--|------------|
| 3.6 <i>MIR211</i> regulated the mTORC1 pathway through RICTOR | 136 |
| 3.8 Other autophagy-related miRNAs targeting RICTOR | 144 |
| 3.9 Model for novel autophagy-regulating axis during cellular stress: MITF/<i>MIR211</i>. 146 | |
| 4. DISCUSSION | 147 |
| 5. CONCLUSION and FUTURE PROSPECTS | 152 |
| 6. REFERENCES | 154 |
| APPENDIX A – Chemical and material list | 177 |
| APPENDIX B- Publications | 180 |
| <i>Research and Review Articles</i> | <i>180</i> |
| <i>Poster Presentations.....</i> | <i>181</i> |
| <i>Patents.....</i> | <i>181</i> |

LIST OF FIGURES

| | |
|---|----|
| Figure 1.1.1 1: Microautophagy mechanism | 3 |
| Figure 1.1.2 1: Chaperone-mediated autophagy (CMA) mechanism..... | 4 |
| Table 1.1.3.1 1 Core autophagy proteins and their functions | 6 |
| Figure 1.1.3.2 1: Membrane sources for phagophore formation | 8 |
| Figure 1.1.3.4 1: Molecular regulators involved in different stages of autophagy | 11 |
| Figure 1.1.3.5 1: Model for selective autophagy of ubiquitinated substrates. | 12 |
| Figure 1.2.1 1: Structure of mTORC1 and domains of mTOR.. | 14 |
| Figure 1.2.1 2: Structure of mTORC2 and domains of mTOR.. | 15 |
| Figure 1.2.2 1: Upstream regulation of mTORC1 pathway..... | 17 |
| Figure 1.2.2 1: The major signaling pathways regulated by mTORC1 | 19 |
| Figure 1.2.3 1: Activation of mTORC2 by interaction with ribosome | 19 |
| Figure 1.2.3 2: TSC1-TSC2 complex regulates mTORC1 negatively whereas promotes mTORC2 activity. | 20 |
| Figure 1.2.3 4: mTOR signaling pathway | 21 |
| Figure 1.2.4 1: Regulation of autophagy by mTORC1. | 23 |
| Figure 1.3.1 1: Multiple sequence alignment of MITF/TFE family members (MITF, TFEB, TFEC and TFE3) and homologs in <i>C. elegans</i> (<i>HLH-30</i>) and <i>D. Melanogaster</i> (<i>Mitf</i>). | 26 |
| Figure 1.3.1 2: Alternative promoter usage and spliced mRNAs of human MITF isoforms. | 28 |
| Figure 1.3.1 3: TFEB-mediated cellular clearance in diseases..... | 29 |
| Figure 1.3.1 4 Role of TFE3 in metabolic response to environmental cues. | 30 |
| Figure 1.3.1 5: MITF is involved in the induction of melanoma, melanocyte differentiation, cell-cycle progression and survival | 32 |
| Figure 1.3.2 1: Sequence conservation of TFEB, TFE3, MITF and TFEC phosphorylation sites..... | 33 |
| Figure 1.3.2.1 1: Amino acid signaling to mTORC1 | 34 |
| Figure 1.3.2.1 2: mTORC1-dependent signaling mechanism that regulate TFEB nuclear translocation | 36 |
| Figure 1.3.2.2 1: TFEB and TFE3 respond to ER-Stress in a PERK-dependent manner. | 37 |
| Figure 1.3.2.3 1: Highly conserved GSK3 phosphorylation sites in MITF and its paralogues TFEB, TFE3 and TFEC..... | 38 |
| Figure 1.3.2.3 2: Positive feedback loop between MITF and Wnt signaling in melanoma | 39 |
| Figure 1.4.1: microRNA biogenesis and mechanism of action..... | 49 |
| Figure 1.4.5 1: Stem-loop sequence of MIR211 and mature sequences.. | 53 |
| Figure 1.5 1: Autophagy impacts several aspects of cancer progression | 55 |
| Figure 3.1.1: The pipeline of the experiments performed for MITF regulation of autophagy analysis. | 69 |
| Figure 3.1.1 1: Nuclear translocation of MITF-A upon torin1 treatment. | 70 |
| Figure 3.1.1 2: Nuclear translocation of MITF-A upon starvation. | 71 |
| Figure 3.1.1 3: Nuclear translocation of MITF-A upon torin1 treatment in SK-MEL-28 cells..... | 72 |
| Figure 3.1.1 4: Effect of MITF-A overexpression on torin1-induced autophagy..... | 74 |
| Figure 3.1.1 5: Effect of MITF-A overexpression on starvation-induced autophagy..... | 75 |
| Figure 3.1.2 1: Effect of siRNA against MITF on <i>MITF</i> mRNA.. | 76 |

| | |
|---|-----|
| Figure 3.1.2 2: Effect of <i>siMITF</i> on GFP-LC3 dot formation following torin1 treatment in HeLa cells..... | 78 |
| Figure 3.1.2 3: Effect of <i>siMITF</i> on GFP-LC3 dot formation following torin1 treatment in SK-MEL-28 cells.. | 79 |
| Figure 3.1.2 4: Effect of <i>siMITF</i> on LC3-II accumulation following torin1 treatment in HeLa cells..... | 80 |
| Figure 3.1.2 5: Effect of <i>siMITF</i> on LC3-II accumulation following torin1 treatment in SK-MEL-28 cells.. | 81 |
| Figure 3.1.2 6: Effect of <i>siMITF</i> on LC3-II accumulation following starvation treatment in HeLa cells..... | 82 |
| Figure 3.1.2 7: Effect of <i>siMITF</i> on LC3-II accumulation following starvation treatment in SK-MEL-28 cells. | 83 |
| Figure 3.1.2 8: Confirmation of MITF knockdown using siRNA on MITF protein level). | 84 |
| Figure 3.1.2.9: Effect of MITF knockdown on GFP-WIP1 puncta formation following torin1 treatment..... | 85 |
| Figure 3.1.2.10: Effect of MITF knockdown on GFP-WIP1 puncta formation following starvation treatment..... | 86 |
| Figure 3.1.2 11: Effect of MITF knockdown on GFP-RFP-LC3 colocalization following torin1 treatment..... | 88 |
| Figure 1.3.2 12: Effect of MITF knockdown on GFP-LC3 lysosomal delivery and proteolysis. | 88 |
| Figure 3.2 1: Effect of MITF silencing on expression of autophagy-related genes. | 90 |
| Figure 3.2 2: Effect of MITF silencing on MIR211 expression..... | 90 |
| Figure 3.2 3: MITF-MIR211 promoter interaction analysis using ChIP assays. | 91 |
| Figure 3.2 4: MITF-LC3 promoter interaction analysis using ChIP.. | 92 |
| Figure 3.2 5: Correlation of endogenous <i>MIR211</i> and <i>MITF</i> mRNA levels in various cell lines.. | 93 |
| Figure 3.2 6: Correlation of endogenous <i>MIR211</i> and <i>MITF</i> mRNA levels in human.... | 94 |
| tissues from 4 different cadavers. | 94 |
| Figure 3.2 7: Correlation of <i>MIR211</i> and MITF mRNA expression using NCI-60 expression dataset..... | 95 |
| Figure 3.2 8: Correlation of <i>MIR211</i> and MITF mRNA expression using TCGA SKCM expression dataset..... | 96 |
| Figure 3.2 9: Correlation of <i>MIR211</i> and MITF mRNA expression using various TCGA expression datasets.. | 97 |
| Figure 3.3 1: The pipeline of experiments demonstrating the effect <i>MIR211</i> overexpression on autophagy. | 98 |
| Figure 3.3.1 1: Effect of <i>MIR211</i> on GFP-LC3 dot formation following lysosomal inhibition in HeLa cells..... | 99 |
| Figure 3.3.1 2: Effect of <i>MIR211</i> on LC3-II accumulation following lysosomal inhibition in HeLa cells..... | 100 |
| Figure 3.3.1 3: Effect of <i>MIR211</i> on GFP-LC3 dot formation following lysosomal inhibition in SK-MEL-28 cells.. | 100 |
| Figure 3.3.1 4: Effect of <i>MIR211</i> on LC3-II accumulation following lysosomal inhibition in SK-MEL-28 cells.. | 101 |
| Figure 3.3.2 1: Effect of <i>MIR211</i> on LC3-II accumulation following torin1 treatment in HeLa cells..... | 102 |
| Figure 3.3.2 2: Effect of <i>MIR211</i> on LC3-II accumulation following torin1 treatment in SK-MEL-28 cells.. | 103 |

| | |
|--|-----|
| Figure 3.3.2 3: Confirmation of <i>MIR211</i> overexpression in Figure 3.3.2 1 and 3.3.2 2.. | 104 |
| Figure 3.3.2 4: Effect of <i>MIR211</i> overexpression on GFP-WIPI1 puncta formation following torin1 treatment..... | 105 |
| Figure 3.3.3 1: Effect of <i>MIR211</i> on LC3-II accumulation following starvation treatment in HeLa cells..... | 106 |
| Figure 3.3.3 2: Effect of <i>MIR211</i> on LC3-II accumulation following starvation treatment in SK-MEL-28 cells. | 107 |
| Figure 3.3.3 3: Confirmation of <i>MIR211</i> overexpression in Figure 3.3.3 1 and 3.3.3 2. | 108 |
| Figure 3.3.3 4: Effect of <i>MIR211</i> overexpression on GFP-WIPI1 puncta formation following starvation..... | 109 |
| Figure 3.3.3 5: Effect of <i>MIR211</i> overexpression on GFP-RFP-LC3 colocalization following torin1 treatment..... | 111 |
| Figure 3.3.3 6: Effect of <i>MIR211</i> overexpression on GFP-LC3 and RFP-LAMP1 colocalization..... | 112 |
| Figure 3.3.3 7: Effect of <i>MIR211</i> on GFP-LC3 lysosomal delivery and proteolysis. | 113 |
| Figure 3.4 1: The pipeline of experiments demonstrating the effect of antagomir-mediated <i>MIR211</i> silencing on autophagy | 114 |
| Figure 3.4 2: Confirmation of <i>MIR211</i> overexpression and antagomir (<i>ANT211</i>)-mediated silencing.. | 115 |
| Figure 3.4.1 1: Effect of <i>ANT211</i> on GFP-LC3 dot formation following torin1 treatment in HeLa cells..... | 116 |
| Figure 3.4.1 2: Effect of <i>ANT211</i> on GFP-LC3 dot formation following torin1 treatment in SK-MEL-28 cells.. | 117 |
| Figure 3.4.1 3: Effect of <i>ANT211</i> on LC3-II accumulation following torin1 treatment in HeLa cells.. | 118 |
| Figure 3.4.1 4: Effect of <i>ANT211</i> on LC3-II accumulation following torin1 treatment in SK-MEL-28 cells.. | 119 |
| Figure 3.4.1 5: Effect of <i>ANT211</i> on GFP-WIPI1 puncta formation following torin1 treatment.. | 120 |
| Figure 3.4.2 1: Effect of <i>ANT211</i> on LC3-II accumulation following starvation treatment in HeLa cells..... | 121 |
| Figure 3.4.2 2: Effect of <i>ANT211</i> on LC3-II accumulation following starvation in SK-MEL-28 cells.. | 122 |
| Figure 3.4.3 1: MITF regulates autophagy through <i>MIR211</i> | 124 |
| Figure 3.5 1: The pipeline of experiments demonstrating target prediction and validation for <i>MIR211</i> functional analysis. | 125 |
| Figure 3.5.1 1: Target prediction using bioinformatics tools. | 126 |
| Figure 3.5.2 1: Effect of <i>MIR211</i> overexpression on RICTOR mRNA levels..... | 127 |
| Figure 3.5.2 2: Effect of <i>MIR211</i> overexpression on RICTOR protein levels.. | 128 |
| Figure 3.5.2 3: Effect of <i>ANT211</i> on RICTOR protein levels..... | 129 |
| Figure 3.5.3 1: Linker primer cloning strategy for RICTOR 3'UTR into luciferase vector. | 130 |
| Figure 3.5.3 2: A scheme representing luciferase constructs. | 131 |
| Figure 3.5.3 3: Luciferase activity assay in HEK293T cells. | 131 |
| Figure 3.5.4 1: Rescue assay and GFP-LC3 dot formation assay.. | 134 |
| Figure 3.5.4 2: Rescue assay and LC3 shift assay. | 135 |
| Figure 3.6 1: Effect of <i>MIR211</i> overexpression on AKT phosphorylation.. | 136 |
| Figure 3.6 2: Effect of <i>MIR211</i> overexpression on MTOR pathway.. | 137 |
| Figure 3.6 3: Effect of <i>shRICTOR</i> on mTOR pathway.. | 138 |
| Figure 3.6 4: Determination of RICTOR activity on AKT phosphorylation. | 139 |

| | |
|---|------------|
| Figure 3.6 5: Effect of RICTOR knockdown on GFP-LC3 puncta formation..... | 140 |
| Figure 3.6 6: Effect of RICTOR knockdown on LC3-II accumulation..... | 141 |
| Figure 3.7 1: Effect of <i>MIR211</i> overexpression of TFEB nuclear translocation.. | 142 |
| Figure 3.7 2: Effect of <i>MIR211</i> overexpression of MITF nuclear translocation.. | 143 |
| Figure 3.8 1: Regulation of other RICTOR targeting miRNAs upon torin1 treatment and starvation. | 145 |
| Figure 3.9 1: A model depicting the MITF-<i>MIR211</i> autophagy feed-forward regulation pathway. | 146 |

LIST OF TABLES

| | |
|---|-----------|
| Table 1.1.3.1 1: Core autophagy proteins and their functions..... | 6 |
| Table 1.3 1: Transcriptional regulation of autophagy..... | 25 |
| Table 1.3.3 1: Reported lysosomal and autophagy-related targets of TFEB, TFE3 and MITF | 43 |

LIST OF ABBREVIATIONS

ACTB: actin beta

AIMs: ATG8-interacting motifs

AGO: argonaute

AKT: AKT serine/threonine kinase

AKT1S1/PRAS40: AKT1 substrate 1

AMPK: AMP-activated protein kinase

ATF4: activating transcription factor 4

ATG: Autophagy-related genes

ATM: Ataxia telangiectasia mutated ser/thr kinase

BECN1: beclin 1

BNIP3L: BCL2/adenovirus E1B-interacting protein 3-like

CMA: chaperone mediated autophagy

CLEAR: coordinated Lysosomal Expression and Regulation

DEPTOR: DEP domain containing MTOR interacting protein

DMEM: Dulbecco's modified eagle medium

DMSO: dimethyl sulfoxide

DGCR8: DiGeorge syndrome critical region gene 8 or Pasha

EBSS: Earl's balanced salt solution

ER: endoplasmic reticulum

ERK: extracellular-signal-regulated kinase

FIP200: focal adhesion kinase-family interacting protein of 200 kDa

GABARAP: GABA type A receptor-associated protein

GAP: GTPase activating protein

GFP: green fluorescent protein

GSK3: glycogen synthase kinase 3

HBS: HEPES-buffered saline

HLH: helix loop helix

HIF1a: hypoxia inducible factor 1 alpha subunit

LAMP1: lysosomal associated membrane protein 1

LIR: LC3-interacting region

MAP1LC3B/LC3B: microtubule associated protein 1 light chain 3 beta

MAPK: mitogen-activated protein kinase

MCOLN1: mucolipin 1

MDM2: E3 ubiquitin-protein ligase Mdm2

MITF: melanogenesis associated transcription factor

MLST8 : mTOR associated protein, LST8 homolog

MRE: miRNA response element

mSIN1: MAPKAP1, mitogen-activated protein kinase-associated protein 1

mTOR: mechanistic target of rapamycin kinase

mTORC1: mTOR complex 1

mTORC2: mTOR complex 2

NBR1: neighbor of BRCA1 gene 1 protein

NDP52: Nuclear dot protein 52

OPTN: Optineurin

PAS: Phagophore assembly site

PBS: phosphate-buffered saline

PDA: pancreatic adenoductal carcinoma

PE: phosphotidyl ethanolamine

PERK: eukaryotic translation initiation factor 2-alpha kinase

PKC: protein kinase C

PI3K: Class-III-Phosphotidyl inostiol-3-Kinase

PI3P: phosphotidyl inositol-3-phosphate

PINK1: PTEN Induced Putative Kinase 1

PRAS40: proline-rich Akt substrate of 40 kDa

Protor1/2: protein observed with Rictor 1/2

PRR5/Protor 1 proline rich 5

PRR5L/Protor 2 proline rich 5 like

pVHL: von Hippel-Lindau tumor suppressor protein

RACK1: receptor for activated C kinase 1

RANKL1: receptor activator of nuclear factor kappa-B ligand

RHEB: Ras homolog enriched in brain

RICTOR: RPTOR independent companion of MTOR complex 2

RISC: RNA induced silencing complex

ROS: Reactive oxygen species

RPS6KB/p70S6K: ribosomal protein S6 kinase

RPTOR: regulatory associated protein of MTOR complex 1

RT-qPCR: quantitative reverse transcription-polymerase chain reaction

SQSTM1 sequestosome 1

STK11/LKB1: serine/threonine kinase 11

STUBLs: SUMO-targeted ubiquitin ligases

SUMO: Small Ubiquitin-like modifier

TFE3: transcription factor binding to IGHM enhancer 3

TFEB: transcription factor EB

TFEC: transcription factor EC

TRPM1: transient receptor potential cation channel subfamily M member 1

TSC1/2: TSC complex subunit 1/2

Ub: ubiquitin

ULK1: unc-51 like autophagy activating kinase 1

UPS: Ubiquitin-proteasome system

UVRAG: UV radiation resistance associated

VIM: vimentin

VPS11: VPS11, CORVET/HOPS core subunit

VPS18: VPS18, CORVET/HOPS core subunit

WIPI2: WD repeat domain, phosphoinositide interacting 2

1. INTRODUCTION

Autophagy is an evolutionarily conserved catabolic pathway to maintain cellular homeostasis by degrading cellular constituents such as long-lived proteins and intracellular organelles. These substrates are engulfed by structures called phagophores which are nucleated and elongated to become autophagosomes, the hallmark of autophagy. Eventually, autophagosomes fuse with lysosomes and form autolysosomes for degradation of autophagic substrates by the lysosomal hydrolases and release of degraded components in the cytoplasm by lysosomal efflux transporters. Being a highly complex process, autophagy is regulated through autophagy-related ATG proteins, and also several key upstream pathways including mTOR pathway. Dysregulation of autophagy causes multiple human pathologies such as cancer, lysosomal disorder diseases, neurodegenerative diseases and infection. Thus, autophagy must be under strict control.

Autophagy requires constant fine-tuning and is tightly regulated at multiple levels including transcriptional and post-transcriptional. The research on transcriptional regulation of autophagy has gained importance as TFEB, the member of MITF/TFE family of transcription factors, is identified as master regulator of lysosomal biogenesis and autophagy. Hence, TFEB and other factors of the MITF/TFE family, MITF and TFE3, have the ability to rapidly induce autophagy by transcriptionally targeting autophagy-related proteins that are involved in all steps of the process. Moreover, recent studies introduced microRNAs (miRNAs) as new players in the post-transcriptional control of autophagy. MiRNAs are 18-21 base pair protein non-coding small RNAs that fine tune cellular levels of transcripts. They do so through modulation of messenger RNA (mRNA) stability and/or through inhibition of protein translation. Indeed, players in various steps of autophagy, including upstream regulatory pathways and core autophagy components, were reported to be targets of different miRNAs.

In this study, I will first briefly define autophagic machinery, and then discuss transcriptional and epigenetic regulation of autophagy. Finally, I will introduce a novel and universal mechanism required for optimal autophagy activation under cellular stress: MITF/MIR211 axis.

1.1. Autophagy

Anabolic and catabolic processes are key events that are important for cellular homeostasis. Hence, synthetic and degradative pathways are highly regulated in cells. The two major catabolic mechanisms in cells are ubiquitin-proteasome system (UPS) and autophagy. The UPS is responsible for the degradation of ubiquitin-conjugated and short-lived proteins in the multimeric protease complex called “proteasome”. On the other hand, autophagy is a lysosomal degradation mechanism, through which long-lived proteins and organelles such as mitochondria, are engulfed by double membrane autophagic vesicles (autophagosomes) and delivered to and degraded by lysosomes, allowing recycling of cellular building blocks (Mizushima & Komatsu, 2011). The term “*autophagy*” denotes “self-eating” and derived from Greek words *auto* (self) and *phagein* (to eat). This concept invented by Christian de Duve, the Nobel Laureate of 1960 for his work on lysosomes.

According to morphological and mechanistic features, autophagy is categorized into three subtypes: microautophagy, chaperone mediated autophagy (CMA), macroautophagy. In this chapter, first I will briefly introduce microautophagy and CMA, then I will mainly focus on macroautophagic and cytoplasmic regulation of the autophagic machinery through *Atg* genes.

1.1.1 Microautophagy

The non-selective lysosomal degradative process, microautophagy, involves the direct engulfment of cytosolic components by lysosomal action in mammalian cells and vacuolar action in plants/fungi. Microautophagy is originally described in yeast and conserved from yeast to mammals. Our understanding of microautophagy has come about almost entirely from studies carried out in *S. Cerevisiae* and detailed studies has remained limited in mammalian cells (Mijaljica, Prescott, & Devenish, 2011)

In microautophagy, the lysosomal/vacuolar membrane is randomly invaginated or projected arm-like protrusions to enclose cytosolic components in vesicles that pinch off into

the lumen (Figure 1.1.1 1) (W. W. Li, Li, & Bao, 2012). Several organelles were identified as microautophagy targets such as mitochondria, nucleus, peroxisomes, the ER and lipid droplets (Oku et al., 2017). Coordinated with other types of autophagy, microautophagy can function in the control of vacuole size, membrane homeostasis and composition, organelle degradation and cell survival under nitrogen deprivation. In yeast, microautophagy is regulated by TOR (the target of rapamycin) and EGO (exit from rapamycin-induced growth arrest) complexes (Dubouloz, Deloche, Wanke, Cameroni, & De Virgilio, 2005). In yeast, three different forms of selective microautophagy have been identified depending on the particular microautophagic cargo: Micropexophagy, micronucleophagy and micromitophagy (W. W. Li et al., 2012). Damaged peroxisomes or cluster of peroximes are engulfed and sequestered by vacuolar membranes during micropexophagy. In micronucleophagy, nuclear components are separated from proteins, and delivered into the vacuole for turnover. Damaged and dysfunctional mitochondria are selectively degraded through micromitophagy.

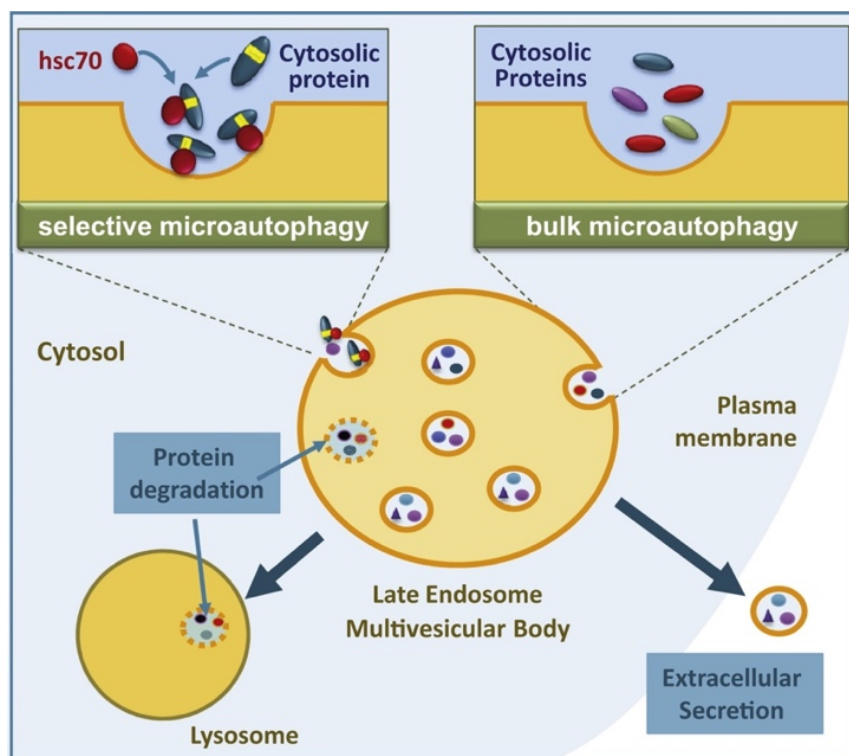


Figure 1.1.1 1: Microautophagy mechanism (retrieved from Sahu et al., 2011).

1.1.2 Chaperone-mediated autophagy

Chaperone-mediated autophagy (CMA) is a selective type of autophagy by which specific soluble proteins are recognized for lysosomal delivery with the involvement of a degradation tag and transported across the lysosomal membrane for degradation (Majeski & Fred Dice, 2004). Similar to and often synchronized with macroautophagy, CMA is active at basal level in many cell types and can be further activated upon cellular stresses leading to protein damage and nutritional stress or starvation (Orenstein & Cuervo, 2010). Differing from macroautophagy, CMA is extremely selective for cytosolic proteins and cannot degrade damaged or dysfunctional organelles. Moreover, it does not involve the formation of autophagosomes, and the cargo is directly delivered into the lysosomal lumen (Kaushik & Cuervo, 2012).

The selectivity of CMA depends on a pentapeptide KFERQ motif present in the amino acid sequences of CMA substrate proteins (Fred Dice, 1990; Wing, Chiang, Goldberg, & Dice, 1991). This motif is necessary for targeting unfolded or misfolded proteins to lysosomes. The KFERQ motif in the substrate proteins is recognized through the binding of a constitutive chaperone, the heat shock-cognate protein of 70 kDa (HSC70), to form the complex HSC70-substrate (Chiang, Terlecky, Plant, & Dice, 1989). Then, HSC70 targets the CMA substrate to the lysosomal membrane where it interacts with the cytosolic tail of lysosome-associated membrane type 2A (LAMP-2A) (Cuervo & Dice, 1996; Rout, Strub, Piszczek, & Tjandra, 2014). The assembly of LAMP-2A to HSC70-substrate complex drives the translocation of the substrate protein into the lysosome lumen (Detailed representation given in Figure 1.1.2 1).

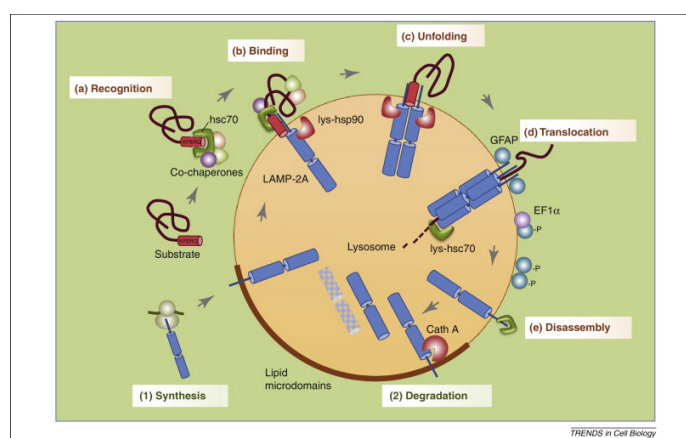


Figure 1.1.2 1: Chaperone-mediated autophagy (CMA) mechanism (retrieved from (Kaushik & Cuervo, 2012)).

1.1.3 Macroautophagy

Macroautophagy (autophagy herein) is an evolutionarily conserved catabolic pathway that is necessary for the maintenance of cellular homeostasis through degrading waste materials in cells and recycling some cellular organelles including mitochondria and peroxisomes (Mizushima & Komatsu, 2011).

Active at a basal level, autophagy may be upregulated in response to cellular stress conditions, including nutrient (e.g., amino acid) and growth factor deprivation, changes in ATP:ADP ratios, unfolded, misfolded or mutant protein accumulation, oxidative stress and hypoxia (Devrim Gozuacik & Kimchi, 2004). Following autophagy activation, double-membrane compartments termed phagophores are formed in the cytosol, engulfing cytosolic components as well as organelles, such as mitochondria. The phagophores subsequently mature into autophagosomes. Fusion of autophagosomes with lysosomes results in the delivery of autophagy targets to lysosomes and allows their degradation and recycling (Oral, Akkoc, Bayraktar, & Gozuacik, 2016).

During autophagy, the cargo is engulfed by and delivered to lysosomes by unique vesicles composed of double membrane bilayers called “autophagic vesicles or autophagosomes” (B. et al., 2010). Fusion of the outer bilayer with the membrane of the lysosomes, releases the cargo in the inner autophagosomal membrane layer to the lumen of the organelle and result in the formation of the so called “autolysosomes”. Together with the autophagy components, the cargo is then degraded as a result of the activity of lysosomal hydrolases. Products of degradation, for example amino acids are produced from whole proteins, are recycled back to the cytoplasm in order to allow the reuse of the components by the cell. By this way, autophagy provides nutrients and energy through the use of cells’ internal resources, allowing them to survive unfavorable conditions such as starvation, growth factor deprivation and detachment from natural environment etc. Autophagy is also the only way to clear and recycle bulky cellular components, including organelles, aggregates or intracellular parasites, destruction of which is important for cellular health (B. et al., 2010). For example, depolarized and damaged mitochondria are sources of reactive oxygen radicals that might be detrimental to the cell. By a specialized autophagy process called “mitophagy”, those damaged mitochondria are cleared and further damage to the cell is avoided. As such, autophagy is a cellular stress response and a mechanism protecting cellular homeostasis and well-being.

1.1.3.1 Core autophagy proteins

More than 30 *ATG* genes (autophagy-related genes) were identified from the baker's yeast and plants to man, in all organisms that were analyzed, revealing the conservation of this process during evolution (Nakatogawa, Suzuki, Kamada, & Ohsumi, 2009). In addition to *ATG* proteins, several others were implicated in autophagy regulation (Dikic & Elazar, 2018). These proteins are essential for autophagosome formation and lysosomal delivery and serve at different stages of autophagy, namely, initiation and formation of the autophagosome, elongation, maturation and fusion with the lysosomes (See also Table 1).

Table 1.1.3.1 1 Core autophagy proteins and their functions

| Protein | Function |
|--|--|
| Initiation and formation of the autophagosome | |
| ULK1 and ATG1 | Serine/threonine kinase; regulates autophagy by phosphorylating downstream components of the autophagy machinery |
| FIP200 | Member of ULK1-kinase complex, ULK-interacting protein, localizes to the isolation membrane |
| ATG13 | Member of ULK1-kinase complex, Bridges the interaction between ULK1 and FIP200 |
| ATG101 | Member of ULK1-kinase complex, Atg13-interacting protein, stabilizes ATG13 and ULK1 |
| VPS34 | Lipid kinase, catalytic component of PI3K complex, generates PI3P in the phagophore |
| Beclin-1 | Regulatory subunit of VPS34 complex |
| ATG14 | Connector to form PI3K complex, translocates to the initiation site, targeting PI3K complex to the PAS |
| ATG9 | Transmembrane protein, directing membrane material for phagophore expansion |
| WIPI1/2 | Essential PtdIns3P effectors, recruits ATG5-12-16L complex by direct binding to ATG16L |

| Elongation of the autophagosome | |
|---|---|
| ATG4 | Cysteine protease that processes pro-ATG8s; also, deconjugation of lipidated LC3 and ATG8s |
| ATG7 | E1-like enzyme; activation of ATG8/LC3; conjugation of ATG12 to ATG5 |
| ATG3 | E2-like enzyme; conjugation of activated ATG8s to membranal PE |
| ATG10 | E2-like enzyme that conjugates ATG12 to ATG5 |
| ATG12~ATG5-ATG16L | E3-like complex that mediates the lipidation of ATG8/LC3 |
| PE-conjugated ATG8/LC3 | Membrane protein of mature autophagosome, specific cargo recognition, adaptor protein docking, membrane tethering |
| ATG9 | Delivery of membrane material to the phagophore |
| Maturation and fusion with the lysosomes | |
| SNAREs | Mediate vesicular fusion events |
| ATG8/LC3 | Required for autophagosome formation, tethering and hemifusion |
| ATG14 | Promotes SNARE-driven tethering and fusion |
| RAB7 | Microtubular bidirectional transport of autophagosomes |
| LAMP-2 | Dynein-mediated transport of lysosomes to perinuclear regions for autophagosome fusion |

1.1.3.2 Initiation and formation of the autophagosome

The origin of the autophagosome membrane is still not clear which may be due to cell dependent and/or context dependent manner, yet, a number of recent studies provided the evidence that autophagosome formation is related to pre-existing membranous compartments. Omegasomes, which are enriched for PI3P and marked by the PI3P-binding protein zinc-finger FYVE domain-containing protein 1 (DFCP1) serve as a cradle for preautophagosome membrane formation and referred to as the phagophore or isolation membrane. Various different membrane sources from endomembrane system contribute to the further elongation of phagophores including ER domains, the Golgi apparatus, ERGIC, endosomes and mitochondria (Figure 1.1.3.2 1) (Carlsson & Simonsen, 2015; Weidberg, Shvets, & Elazar, 2011).

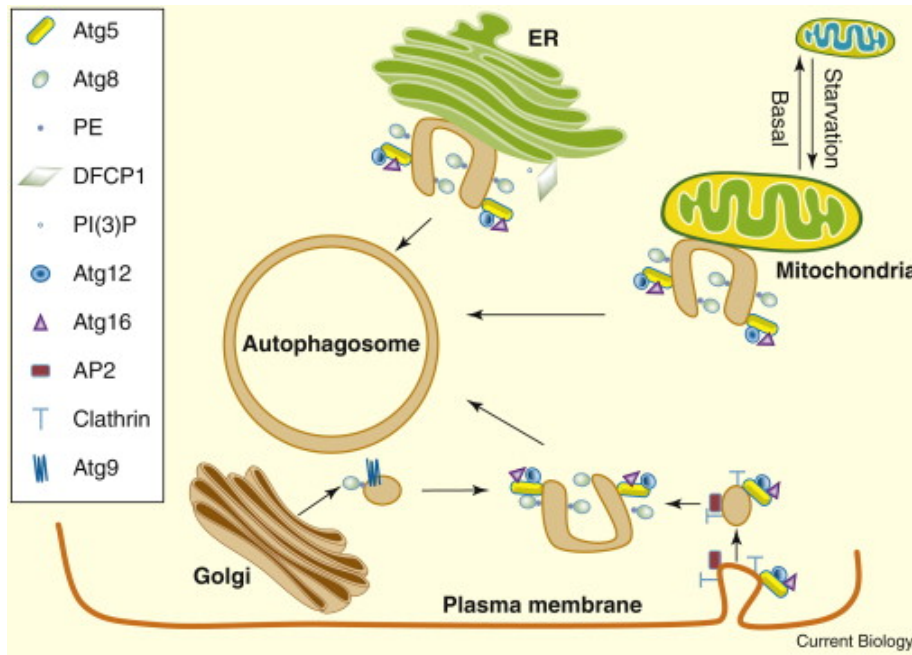


Figure 1.1.3.2 1: Membrane sources for phagophore formation (Retrieved from (Rubinsztein, Shpilka, & Elazar, 2012)).

Whatever might be the origin, several upstream signals leading to autophagosome formation (see below) converge at the signaling complex TORC1 (mTORC1 in mammals). This protein complex possesses serine/threonine kinase activity due to its central kinase component mTOR. TORC1 was shown to play a role in cellular growth, cell cycle progression and protein synthesis. When cellular and organismal conditions are favorable, mTOR complex is active allowing protein synthesis and cellular growth. Since autophagic activity above basal levels is not required under favorable conditions, TORC1 directly blocks autophagy (Laplante & Sabatini, 2012). In fact, mTOR kinase regulates the activity of the autophagy-related ATG1 kinase (or ULK1/2 in mammals) complex. ATG1 kinase complex consists of ATG1-13-17-29-31 in yeast, and its mammalian counterpart, ULK1/2 complex is composed of ULK1/2-ATG13-ATG101-FIP200 proteins (Mizushima & Komatsu, 2011). This multimeric complex is responsible for initiation of the autophagic activity. mTOR phosphorylation of ATG13 regulates ULK1/2-ATG1 activity. Under stress conditions, mTORC1 is blocked leading to ATG13 hypophosphorylation. ATG13 binds to ULK1/2 in its hypophosphorylated state and mediates the interaction with FIP200, leading to the phosphorylation of FIP200 by ULK1/2. Under these circumstances, FIP200-ATG1-ATG13 complex triggers cascades that result in autophagosome initiation and nucleation.

The class III phosphatidylinositol 3-kinase (PI3K) complex consists of VPS34 (the PI3K), VPS30, ATG14/Barkor, VPS15 and ATG6 / BECN1 (Beclin1) (Funderburk, Wang, & Yue, 2010). AMBRA1 was also shown as one of the regulators of the complex in the mammalian system (Mehrpour, Esclatine, Beau, & Codogno, 2010). The VPS34-PI3K complex is responsible for the formation of phosphatidylinositol 3-phosphate (PI3P) from phosphatidylinositols found on cellular membranes. This lipid decoration serves as a landing path for the recruitment of the other ATG proteins to the site of autophagosome formation (PAS (preautophagosomal structure) in the yeast or omegasome / cradle in mammals).

ATG18 or mammalian counterparts WIPI 1-4 are PI3P-binding and WD-repeat containing proteins that localize to PAS or omegasomes and regulate the autophagic activity (Mauthe et al., 2011). ATG2 protein is also another component that interacts with ATG18 and it is important for ATG18 localization to PI3P-rich membranes. Although the exact role is not yet clear, ATG2-ATG18 complex is believed to play a role in formation of autophagosomes. In line with this, the mammalian WIPI1 and 2 were shown to colocalize with proteins ATG14 and ATG16L1 proteins involved initiation and elongation stages. Another important protein, ATG9 (mammalian homolog: ATG9L1) is a multipass transmembrane protein that is present on endosomes, Golgi and also autophagic membranes (A. R. J. Young, 2006). ATG9 is believed to be involved in lipid delivery to the autophagosome formation centers.

1.1.3.3 Elongation of the autophagosome

Following priming of PAS or omegasomes with appropriate protein complexes mentioned above, autophagic membrane elongation begins. During this step, two ubiquitination-like conjugation systems namely the ATG12-ATG5-ATG16 and ATG8 (MAP1LC3, or briefly LC3 in mammals) systems are involved (Mizushima & Komatsu, 2011).

ATG12-ATG5-ATG16 is the system where ATG12 is conjugated to ATG5 through activation by ATG7 (E1-like enzyme) and followed by transfer to the E2-like enzyme, ATG10. Then, ATG10 triggers ATG12 conjugation to a central lysine residue of ATG5. Formation of a large multimeric complex (300 kDa complex in the yeast and 800 kDa complex in mammals) requires the coiled coil protein ATG16 (ATG16L1 in mammals). Resulting ATG12-ATG5-ATG16 complex possesses an E3-like enzyme activity for the second conjugation system.

The second system involves the conjugation of LC3/ATG8 to a lipid molecule, phosphatidylethanolamine (PE) (Hanada et al., 2007). After cleavage of the carboxyl-terminus of LC3 by the cysteine protease ATG4, a glycine residue is exposed, resulting in the formation of so called LC3-I cytosolic form. LC3-I-lipid conjugation requires the activity of ATG7 (E1-like) and ATG3 (E2-like), then leads to the formation of the lipid-conjugated and autophagic membrane-bound form, LC3-II. Consequently, detection of LC3-I conversion into LC3-II is commonly used as a marker of autophagy activation. There are several mammalian LC3 orthologues with overlapping but somewhat different functions in autophagy and other vesicular events, including LC3A-D, GABARAP (GABA-A receptor associated protein) and GATE-16 (Golgi associated ATPase enhancer of 16 kDa) (Shpilka, Weidberg, Pietrokovski, & Elazar, 2011). As autophagosome biogenesis and clearance is a dynamic process, LC3-II formation and recycling is regulated on a tight schedule, where the same ATG4 enzymes cleave the lipid bond to allow detachment and recycling of LC3 from mature autophagosomes (Kabeya, 2004; Kirisako et al., 2000).

1.1.3.4 Maturation and fusion with the lysosomes

Fully mature autophagosomes move within the cell to meet late endosomes or lysosomes (vacuole in the yeast) for delivering their cargo to be degraded. Homotypic fusion events play an important role in the autophagosome and lysosome fusion process, and proteins such as vacuolar syntaxin homologue Vam3, SNAP-25 homologue Vam7, the Rab family GTP-binding protein Ypt7 and Sec18 are required for the process in the yeast. In mammals, together with the integral lysosome membrane protein LAMP2 and the SNARE machinery, Rab7, Rab22 and Rab24 were shown to play important roles in fusion (Jager, 2004; Tanaka et al., 2000). Moreover, dyneins are necessary for the transport of autophagosomes along microtubules to allow them to meet acidic compartments. Following fusion, the cargo is degraded through the action of lysosomal enzymes including cathepsins, and the monomers that are generated such as aminoacids are recycled to cytosol and reused by the cell in various synthetic processes (Tanida, Ueno, & Kominami, 2004).

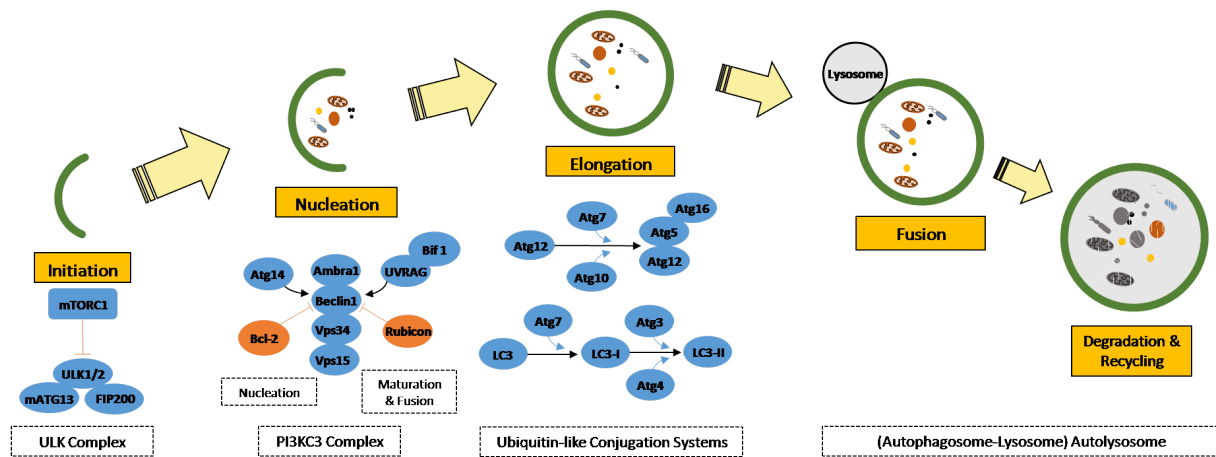


Figure 1.1.3.4 1: Molecular regulators involved in different stages of autophagy. (Retrieved from (Gozuacik et al., 2017))

1.1.3.5 Selective autophagy and autophagy receptors

Autophagy was believed to be a non-selective phenomenon. More recent studies describe several selective autophagy pathways including protein aggregates (aggrephagy) (Lamark & Johansen, 2012), mitochondria (mitophagy) (Okamoto, Kondo-Okamoto, & Ohsumi, 2009), ribosomes (ribophagy), pathogens (xenophagy) (Wileman, 2013), peroxisomes (pexophagy) (Till, Lakhani, Burnett, & Subramani, 2012), endoplasmic reticulum (reticulophagy), nuclear envelope (nucleophagy), liposomes (lipophagy), and lysosomes (lysophagy). Specific cargo recognition is mediated through a family of proteins called autophagy receptors which are able to recognize degradation signals on cargo proteins and simultaneously bind ATG8-family proteins on the autophagosome (Zaffagnini & Martens, 2016).

Several receptor proteins recognize cargos for selective autophagy through most prevalent autophagy-targeting signal, poly-ubiquitin chains. Indeed, autophagy receptors including p62/SQSTM1 (p62), optineurin (OPTN) and NDP52 (nuclear dot protein 52 kDa) contain both Ub-binding domains and LC3-interacting regions (LIR domain).

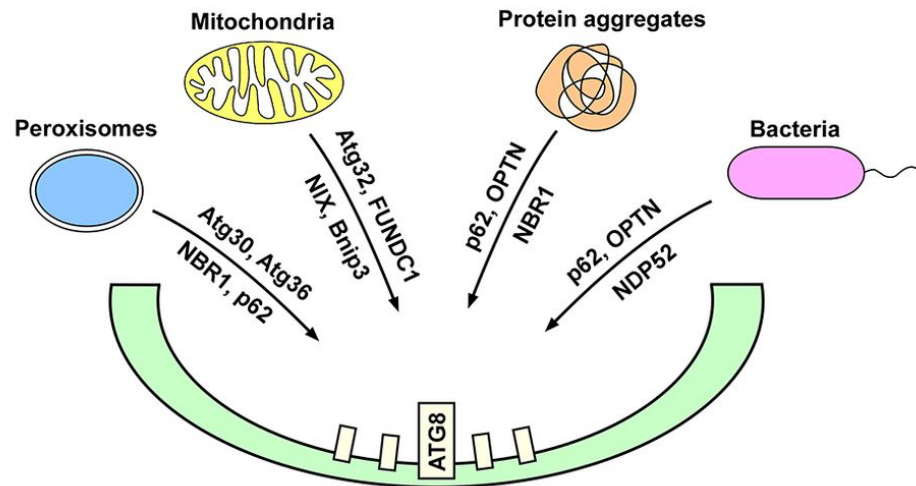


Figure 1.1.3.5 1: Model for selective autophagy of ubiquitinated substrates (Retrieved from (Svenning & Johansen, 2013)).

The best characterized autophagy receptor, p62, serves as a sensor/scaffold for sequestration of aggregated proteins and pathogens by the phagophore (Pankiv et al., 2007). It also participates in aggregate formation by delivering misfolded aggregated proteins to the aggresome (Seibenhener et al., 2004). After recognizing polyubiquitinated cargo through non-covalent binding via C-terminal UBA domain, p62 delivers the cargo to the autophagosome via a short LIR (LC3-interacting region) sequence responsible for LC3 interaction (Ciani, Layfield, Cavey, Sheppard, & Searle, 2003). Knockout studies in *Drosophila* and mice and mutations studies in the UBA domain results in impaired autophagy and in a spectrum of multisystem proteinopathies (Goode et al., 2014; Komatsu et al., 2007; Nezis et al., 2008). Homeostatic level of p62 is regulated by autophagy since it is also a substrate during autophagic degradation.

Similarly, OPTN and NDP52 have been described as autophagy receptors that drives the clearance of pathogens (Thurston, 2009; Wild et al., 2011), aggregates (K. Lu, Psakhye, & Jentsch, 2014) and mitochondria (Lazarou et al., 2015; Sarraf et al., 2013). Peroxisomes are recognized and sequestered by the phagophore by binding capacity of NBR1 (Deosaran et al., 2013).

1.2 mTOR Regulation of Autophagy

Several key adaptor pathways such as mTOR, AKT/PKB and growth factors, FOXO, AMPK, Inositol and p53 pathways regulate autophagy. Among them, mammalian target of rapamycin (mTOR) pathway have a great importance by being at the crossroad of major eukaryotic signaling pathways including cellular growth, cell cycle progression, proliferation and survival.

Studies from dozens of labs have revealed that several major intracellular and extracellular signals such as growth factors, energy status, oxygen and amino acids levels are integrated through mTOR pathway and it plays a fundamental role in cellular physiology through the regulation of key metabolic events such as protein synthesis, lipid synthesis, autophagy, lysosomal biogenesis and energy metabolism.

In this chapter, I will describe the structure of two distinct mTOR complexes, emphasize their functions and signaling pathways, and conclude with their roles in autophagy.

1.2.1 mTOR structure and organization into complexes

Evolutionary conserved serine-threonine kinase mTOR, which belongs to the phospho-inositide 3-kinase (PI3K)-related kinase family (PIKK), comprises two structurally and functionally distinct multi-protein complexes: mTOR complex 1 (mTORC1) and mTOR complex 2 (mTORC2).

mTORC1 have three core components: the catalytic subunit mTOR, Raptor (regulatory protein associated with mTOR) and mLST8 (mammalian lethal with Sec 13 protein 8). Raptor regulates the assembly of the complex and recruits substrate for mTOR by binding Tor signaling motif found on mTORC1 substrates (Hara et al., 2002; D. H. Kim et al., 2002). Although genetic studies proposed that mLST8 is dispensable for mTORC1 activity, it associates with the catalytic domain of mTOR and stabilizes the kinase activation loop (Guertin et al., 2006; Yang et al., 2013). In addition to the core subunits, there are two inhibitory subunits PRAS40 (proline

rich AKT substrate of 40 kDa) (Haar, Lee, Bandhakavi, Griffin, & Kim, 2007; Sancak et al., 2007; Wang, Harris, Roth, & Lawrence, 2007) and DEPTOR (DEP domain containing mTOR interacting protein) (Peterson et al., 2009). Upon mTORC1 activation, mTORC1 directly phosphorylates PRAS40 and Deptor, which reduces their physical interaction with mTORC1 and further activates mTORC1 signaling (Figure 1.2.1 1) (Peterson et al., 2009; Wang et al., 2007).

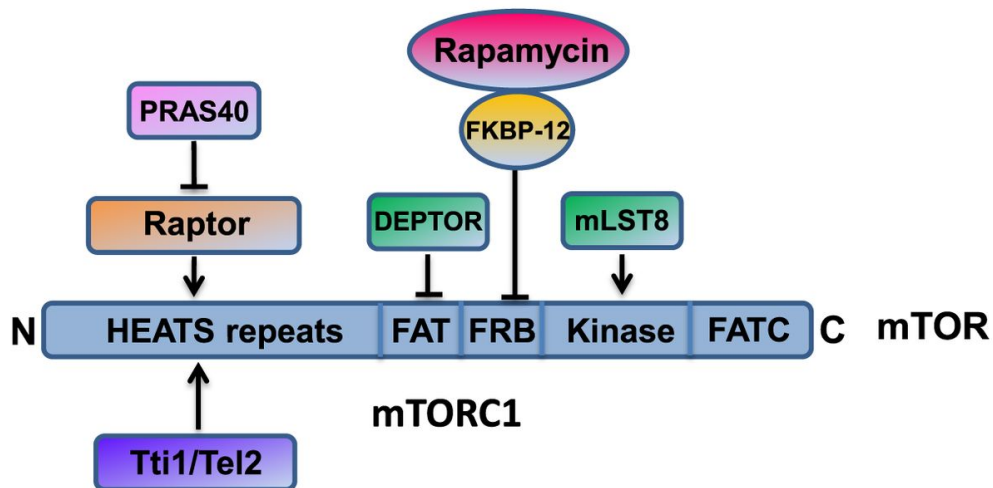


Figure 1.2.1 1: Structure of mTORC1 and domains of mTOR. Subunits of mTORC1 complex are mTOR, Raptor, DEPTOR, PRAS40 and mLST8 (Retrieved from Bartolome et al., 2014)).

mTORC2 is characterized by its insensitivity to rapamycin treatment. Instead of Raptor, mTORC2 contains the protein called rapamycin-insensitive companion of mTOR (Rictor), which is a scaffold protein playing a role in mTORC2 assembly and activation (Dos et al., 2004; Jacinto et al., 2006). mTORC2 also consists of common proteins with mTORC1 including mTOR, DEPTOR and mLST8. Being the only inhibitor subunit of mTORC2, Deptor negatively regulates mTORC2 activity (Peterson et al., 2009). Knockout studies show that mLST8 is critical for mTORC2 stability and activity (Guertin et al., 2006). Unlike mTORC1, mTORC2 also consists of mSin1 (mammalian stress-activated protein kinase interacting protein) (mSIN1) and Protor1/2 (protein observed with Rictor). Structure of mTORC2 is maintained by the stabilizing activity of two scaffold proteins in the complex, Rictor and mSIN1 onto each other (Figure 1.2.1 2) (Jacinto et al., 2006).

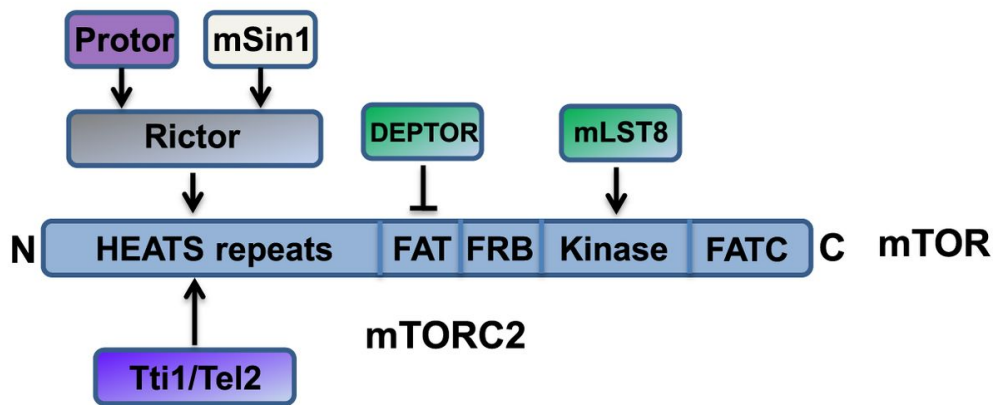


Figure 1.2.1 2: Structure of mTORC2 and domains of mTOR. Subunits of mTORC2 complex are mTOR, Rictor, DEPTOR, Protor1/2, mSin1 and mLST8 (Retrieved from Bartolome et al., 2014)).

mTORC1 and mTORC2 can be distinguished on the basis of their sensitivity to rapamycin which only inhibits mTORC1 (Sarbasov et al., 2006). The two complexes are responsive to different signals and produce different downstream targets. While mTORC2 mainly regulates cytoskeleton organization and cell survival, the major cellular role of mTORC1 is the control of cell growth, protein synthesis and autophagy.

1.2.2 mTORC1: Functions and signaling pathways

mTORC1 functions in macromolecule biosynthesis, autophagy, cell cycle, growth and metabolism once it is activated by the amino acids, cellular energy level, oxygen, stress and growth factors.

Upstream Regulators

mTORC1 has several intracellular and extracellular upstream regulators. Major signals are growth factors, energy status, oxygen, stress and amino acids. One of the most important sensors involved in the regulation of mTORC1 activity is the tuberous sclerosis complex (TSC), which is a heterodimeric complex comprised of TSC1, TSC2 and TBC1D7 (Dibble & Manning, 2010). TSC1/2 complex functions as a GTPase activating protein (GAP) for the small GTPase Rheb (Ras homolog enriched in brain) (Inoki, Li, Xu, & Guan, 2003). TSC1/2 is inactivated

once it is phosphorylated on multiple sites. Upon TSC1/2 inactivation, GTP-bound and activated Rheb directly binds and stimulates the kinase activity of mTORC1 (Long, Ortiz-Vega, Lin, & Avruch, 2005; Sancak et al., 2007).

Stimulation of mTORC1 via TSC1/2 dependent manner includes the insulin/insulin-like growth factor-1 (IGF-1) pathway, which resulted in the Akt-dependent multisite phosphorylation of TSC2. Phosphorylated TSC dissociates from the lysosomal membrane, where at least some fraction of cellular Rheb localizes (Menon et al., 2014).

Another road for growth factors to stimulate mTORC1 activity via TSC1/TSC2 mechanism is the phosphorylation of TSC1 by I κ B kinase β (IKK β) and leads TSC1/2 inhibition (D. F. Lee et al., 2007). As a substrate of AKT, GSK3B has been also identified as a mTORC1 upstream regulator. Glycogen synthase kinase 3 β (GSK3 β) phosphorylates TSC2 and promotes the TSC1/2 activity which in turn inhibits mTORC1 activity (Inoki et al., 2006). mTORC1 can also be activated by growth factors via TSC1/2 independent pathway. As AKT is phosphorylated and activated by growth factors; PRAS40 which is negatively regulating mTORC1 activity by inhibiting the substrate binding, can be phosphorylated and dissociated from the complex (Sancak et al., 2007).

mTORC1 activity is inhibited by receiving the intracellular energy status signals through AMP activated protein kinase, AMPK pathway. Upon the ratio ATP/ADP decreases, AMPK pathway is activated. Activated adenylyl cyclase phosphorylates TSC2 and GDP bound RHEB reduces the activity of mTORC1 (Inoki, Zhu, & Guan, 2003). Moreover, Raptor is also a target for AMPK. Phosphorylation of Raptor by AMPK results in reduction of mTORC1 activity (Gwinn et al., 2008).

Intracellular amino acid levels can also act upon mTORC1 activation through TSC1/2 independent pathway. It has been discovered that Rag GTPases are essential for amino acid dependent activation of mTORC1 (Sancak et al., 2008). In response to amino acid rich condition, RAG GTPases are activated via GTP loading. RagA or RagB is loaded with GTP and RagC or RagD is loaded with GDP. This results in translocation of mTORC1 from cytosol to lysosomes and, interaction and activation by GTP bound RHEB. Upon amino acid deprivation, Rags are inactivated. RagA or RagB is loaded with GDP and RagC or RagD is loaded with GTP. Thus, mTORC1 is inactivated and transported to cytosol.

Hypoxia is another key regulator of mTORC1. One of the major responses for hypoxia is the block in mitochondrial respiration. First, AMPK pathway is activated due to the low ATP levels, then TSC1/2 complex activity is initiated and mTORC1 activity is abolished. REDD1, DNA damage response 1, is also a target for hypoxia to induce TSC1/2 assembly by disrupting the interaction between TSC2 and cytosolic chaperone 14-3-3 (Brugarolas et al., 2004). Another major response to hypoxia-related stress is the stabilization of the hypoxia inducible factor-1a (HIF-1a) (He & Klionsky, 2009). HIF-1a induces transcription of a Bcl-2 family member BNIP3 which disrupts the interaction between mTOR and Rheb, thus reduces mTORC1 activity (Bellot et al., 2009).

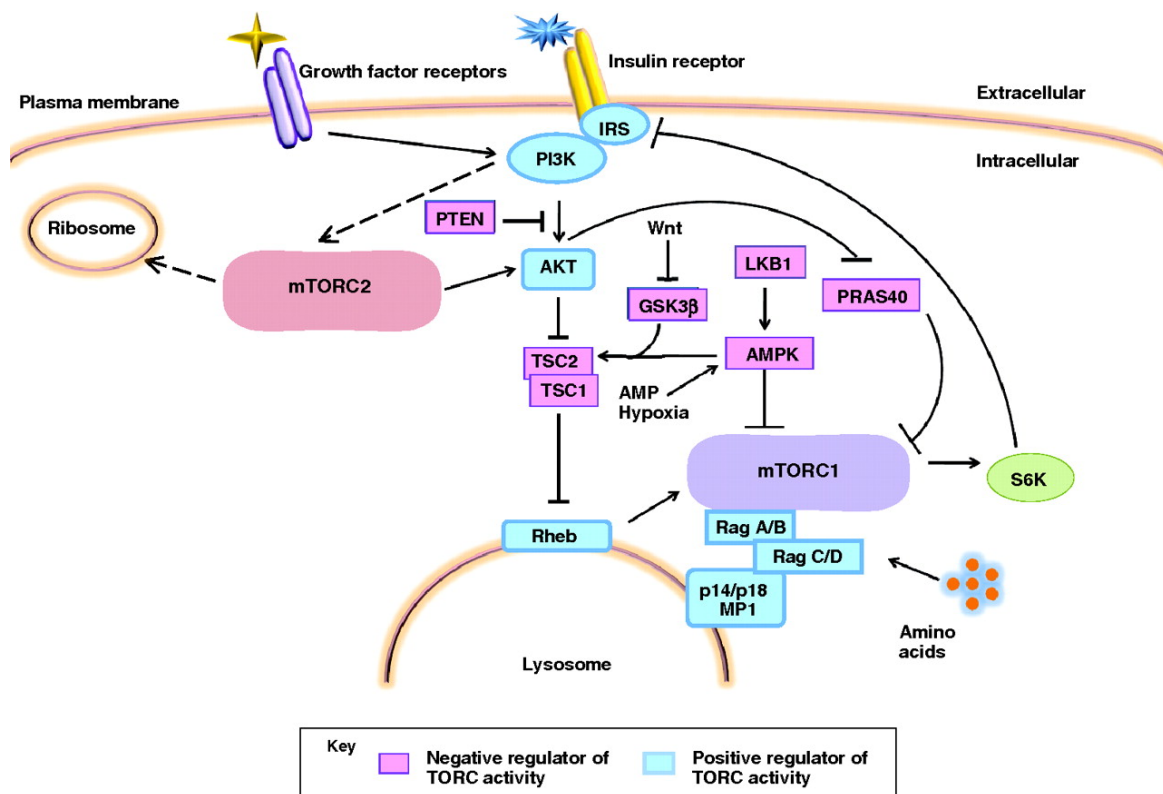


Figure 1.2.2 1: Upstream regulation of mTORC1 pathway (Retrieved from (Russell, Fang, & Guan, 2011)).

Outputs of mTORC1 signaling

mTORC1 regulates several highly significant cellular processes such as protein synthesis, lipid synthesis, autophagy, lysosomal biogenesis and energy metabolism (Sarbasov, Ali, & Sabatini, 2005). Promoting protein synthesis which is essential for cellular growth is one of the well-

studied functions of mTORC1 via inducing ribosomal biogenesis and mRNA translation. This is occurred due to the direct binding of S6K1 (ribosomal S6 kinase) on its hydrophobic motif site, Thr 389. This enables its subsequent phosphorylation and activation by PDK1. Active S6K1 promotes mRNA translation initiation via phosphorylation of several substrates including EIF4B, that positively controls 5' cap binding eIF4F complex (Holz, Ballif, Gygi, & Blenis, 2005). Moreover, an inhibitor of eIF4B, PCDC4 is also phosphorylated and degraded by S6K1 (Dorrello et al., 2006). Additionally, S6K1 promotes translation efficiency of spliced mRNAs by interacting with SKAR, an exon-junction complex member (X. M. Ma, Yoon, Richardson, Jülich, & Blenis, 2008). mTORC1 also promotes protein synthesis through targeting 4EBP1. 4EBP1, which has a translation inhibitory function, is phosphorylated at multiple sites and released from eIF4E, eukaryotic translation initiation factor. This allows 5'cap-dependent mRNA translation to occur (Brunn et al., 1997; Gingras et al., 1999).

Other anabolic processes, such as nucleotide and lipid synthesis are also stimulated by mTORC1. Pyrimidine synthesis is promoted through phosphorylation and activation of carbamoyl-phosphate synthetase (CAD) that is a key component of the de novo pyrimidine synthesis pathway (Robitaille et al., 2013). Lipid biosynthesis, which is required for cell growth and proliferation, is also one of the significant outputs of mTORC1 signaling pathway. mTORC1 takes a role in lipid synthesis via activating sterol regulatory element binding protein (SREBP1) through S6K1 (Düvel et al., 2010; Porstmann et al., 2008). Also, mTORC1 performs activating lipid biosynthesis function by inhibiting LIPIN1 translocation to nucleus which will downregulate SREBP1 activity (Peterson et al., 2011).

In addition to the stimulatory effects on anabolic processes, mTORC1 also function as the major negative regulator of lysosome biogenesis and autophagy. (see below for further detail).

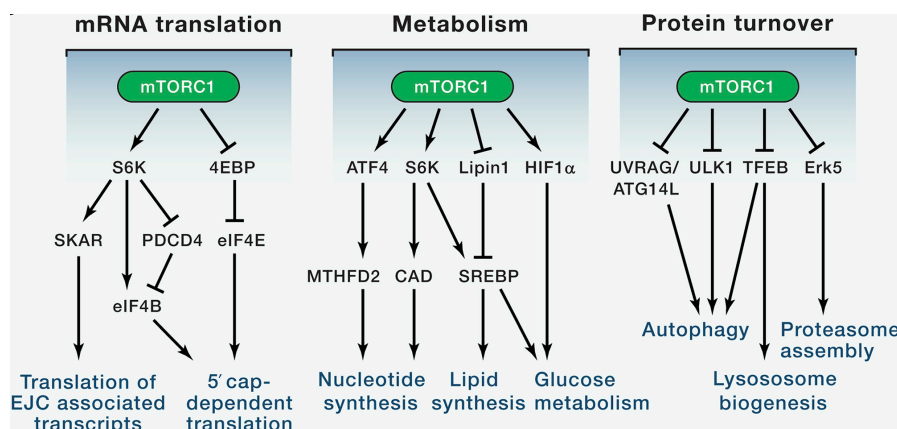


Figure 1.2.2 1: The major signaling pathways regulated by mTORC1 (Retrieved from (Saxton & Sabatini, 2017))

1.2.3 mTORC2: Functions and signaling pathways

Although the signaling pathways related to mTORC1 is well-characterized, limited information is provided for mTORC2 functions and signaling pathways which causes mTORC2 to be remained as the “black box”.

Upstream regulators

Similar to mTORC1, mTORC2 activity is also regulated by various upstream stimuli, including insulin/PI3K signaling and growth factors. Growth factors activate mTORC2 via PI3K signaling. Studies in yeast and mammalian cells showed that ribosomes are required for mTORC2 signaling and active mTORC2 physically interacts with the ribosomes (Figure 1.2.3 1). Their interaction is promoted by insulin-stimulated PI3K signaling (Zinzalla, Stracka, Oppliger, & Hall, 2011). Another PI3K-dependent mechanism for mTORC2 activation is dependent on the interaction between PtdIns(3,4,5)P3 and mSin1, the subunit that negatively regulates mTORC2 activity (Yuan & Guan, 2015).

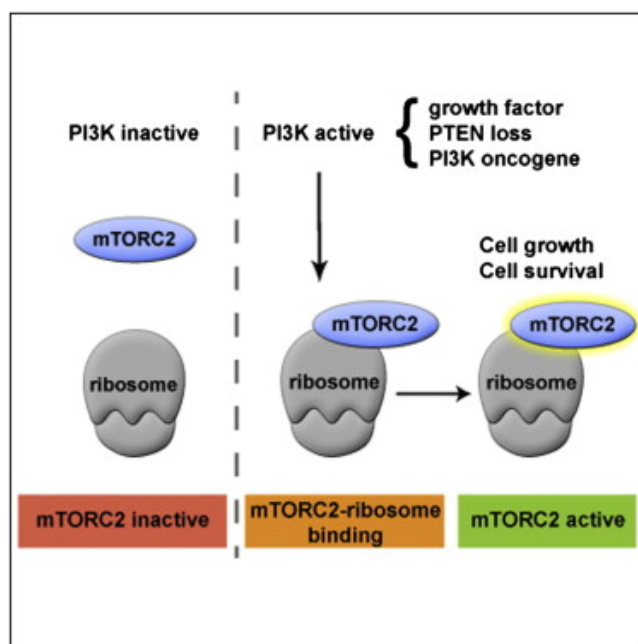


Figure 1.2.3 1: Activation of mTORC2 by interaction with ribosome (Retrieved from (Zinzalla et al., 2011)).

Feedback signals from mTORC1 and its downstream target S6K1 were shown to negatively modulate insulin/PI3K signaling through phosphorylation of its regulators, affecting mTORC2 activity. For example, the negative regulator GRB10, was phosphorylated and activated by mTORC1 (P. P. Hsu et al., 2011; Yu et al., 2011). Moreover, S6K1, which directly phosphorylates and promotes the degradation of IRS1 (insulin receptor substrate 1) (Harrington et al., 2004; Shah, Wang, & Hunter, 2004).

The TSC1-TSC2 complex plays opposing roles in the regulation of mTOR complexes (Figure 1.2.3 2). Surprisingly, TSC1-TSC2 complex promote mTORC2 activity. One Inhibition of Rheb and mTORC1 results in the relief of mTORC1-dependent feedback mechanism. Furthermore, TSC1-TSC2 complex physically associates with and activates mTORC2. Attenuation of mTORC2 kinase activity upon disruption of TSC1-TSC2 complex is independent of its GAP activity and Rheb, that results in reduction in Akt phosphorylation (J. Huang & Manning, 2008).

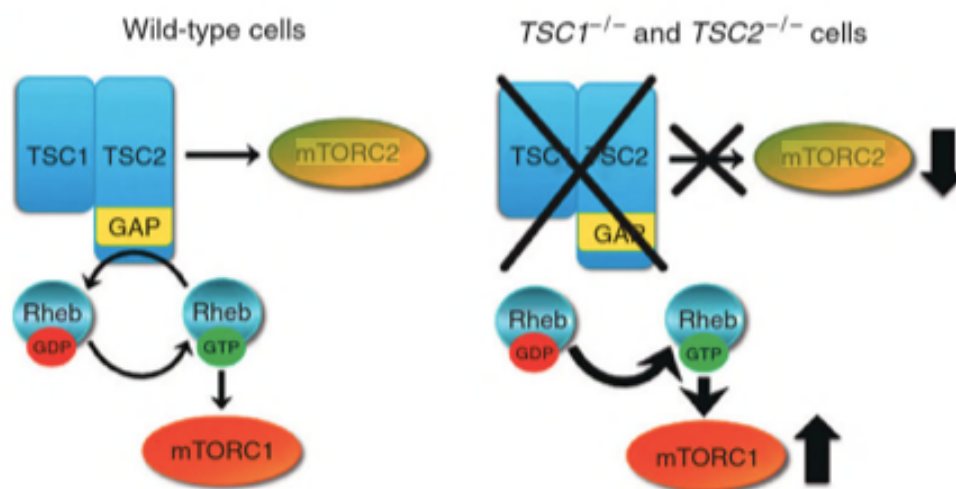


Figure 1.2.3 2: TSC1-TSC2 complex regulates mTORC1 negatively whereas promotes mTORC2 activity (Retrieved from (Dibble & Manning, 2010)).

Outputs of mTORC2 signalling

The best characterized mTORC2 substrates are components of AGC protein kinase family, including Akt, SGK1 (serum- and glucocorticoid-induced protein kinase 1), and PKC- α (protein kinase C- α) (Oh & Jacinto, 2011). mTORC2 phosphorylates Akt at Ser473 and increases its phosphorylation at Thr308 by PDK1 which in turn results in the Akt activation and cell survival (Guertin et al., 2006; Sarbassov, Guertin, Ali, & Sabatini, 2005). However, Akt and expression of its downstream targets are not completely blocked in the loss of mTORC2 (Oh et al., 2010). SGK1, that controls ion transport and cellular growth, is also identified as a target of mTORC2 (Aoyama et al., 2005). Knockdown of mTORC2 results in the absence of SGK1 phosphorylation and complete blockage of its activity, and increased cell death (García-Martínez & Alessi, 2008). Moreover, mTORC2-mediated phosphorylation of PKC prevents its degradation and promotes its kinase activity. PKC seems to control actin cytoskeleton organization by mTORC2 (Xin et al., 2014). Similarly, animal model with Rictor knockout showed decreased levels of PKC α and its activity in the hypothalamus (Kocalis et al., 2014).

mTORC2 is also implicated in lipid biogenesis via activation of SREBP1c through phosphorylated Akt (Hagiwara et al., 2012).

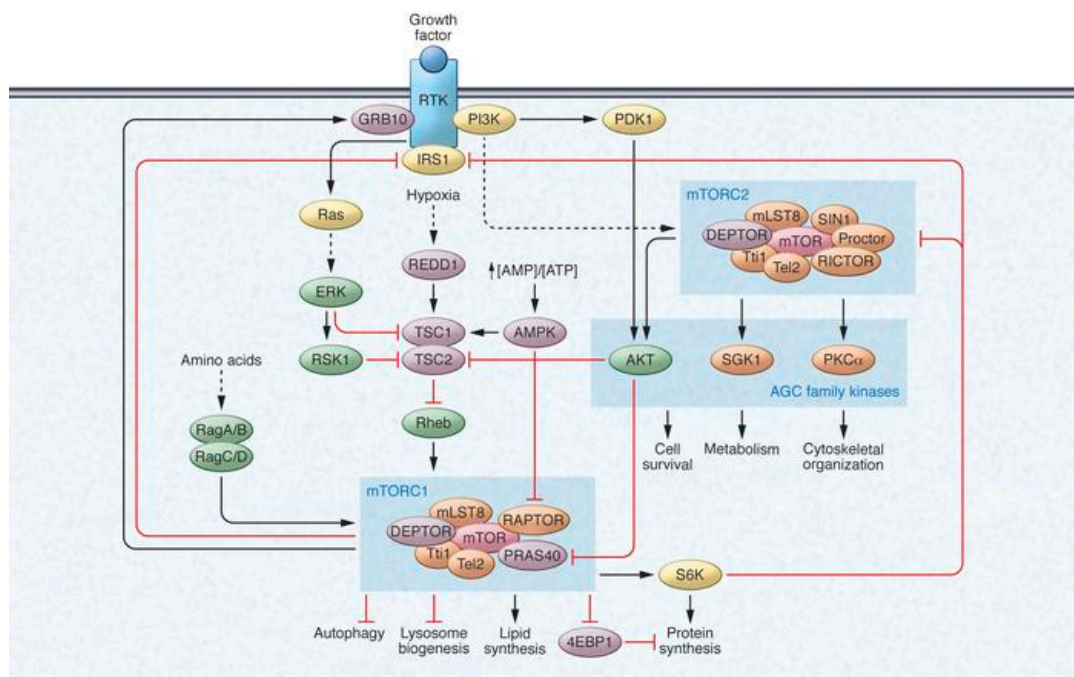


Figure 1.2.3 4: mTOR signaling pathway (Retrieved from Kim, 2015)

1.2.4 mTOR and autophagy

Studies have shown that mTORC1 is the major inhibitor of autophagy pathway and inhibition of mTORC1 reduces autophagic activity. In mammals, under aminoacid-rich conditions, autophagy is directly regulated by mTORC1 through phosphorylation of ULK1 at Ser757. mTORC1 directly binds, phosphorylates and inactivates the kinase activity of ULK1 which is required for autophagy initiation. On sensing a decrease in amino acid levels, mTORC1 is inactivated and dissociates from the ULK1 complex which leads to ULK1/ATG13/FIP200 complex formation and initiation of autophagy via ULK1 autophosphorylation and phosphorylation of its binding partners (Hosokawa et al., 2009; Mizushima, 2010). Hence, cascades that result in autophagosome initiation and nucleation are triggered.

Moreover, AMPK, the energy sensor of the cell, is another player in the control of autophagy through ULK1 and mTORC1. AMPK is activated in response to the increase in AMP:ATP ratio upon energy starvation. Under these conditions, AMPK promotes autophagy by activating ULK1 through direct phosphorylation at Ser555, Ser317 and Ser777 residues (Joungmok Kim, Kundu, Viollet, & Guan, 2011; J. W. Lee, Park, Takahashi, & Wang, 2010; Shang & Wang, 2011). Moreover, the interaction between ULK1 and AMPK is distorted when active mTORC1 phosphorylates ULK1 (Joungmok Kim et al., 2011).

AMPK-activated ULK1 contributes to mTORC1 inactivation through phosphorylation of Raptor which creates a negative feedback loop to maintain mTORC1 inhibition under energy-limited conditions (Dunlop, Hunt, Acosta-Jaquez, Fingar, & Tee, 2011). Another negative feedback loop on autophagy induction is created when active ULK1 inhibits AMPK activation through repressive phosphorylation (Löffler et al., 2011).

In addition, mTORC1 inhibits ULK1 stability through phosphorylation of AMBRA1, which activates VPS34, a class III PI3K critical for autophagosome formation (Nazio et al., 2013). A component of VPS34 complex, ATG14, is phosphorylated by mTOR to control autophagy level by inhibiting its lipid kinase activity under nutrient-rich conditions (Yuan, Russell, & Guan, 2013). Subsequent studies revealed that several other mechanisms are included in mTORC1-mediated autophagy regulation including death-associated protein 1

(DAP1), a novel mTOR substrate (Koren, Reem, & Kimchi, 2010) and WD repeat domain phosphoinositide-interaction protein 2 (WIPI2) (P. P. Hsu et al., 2011).

Regulation of MITF/TFE transcription factors by mTORC1 will be covered in the next chapter.

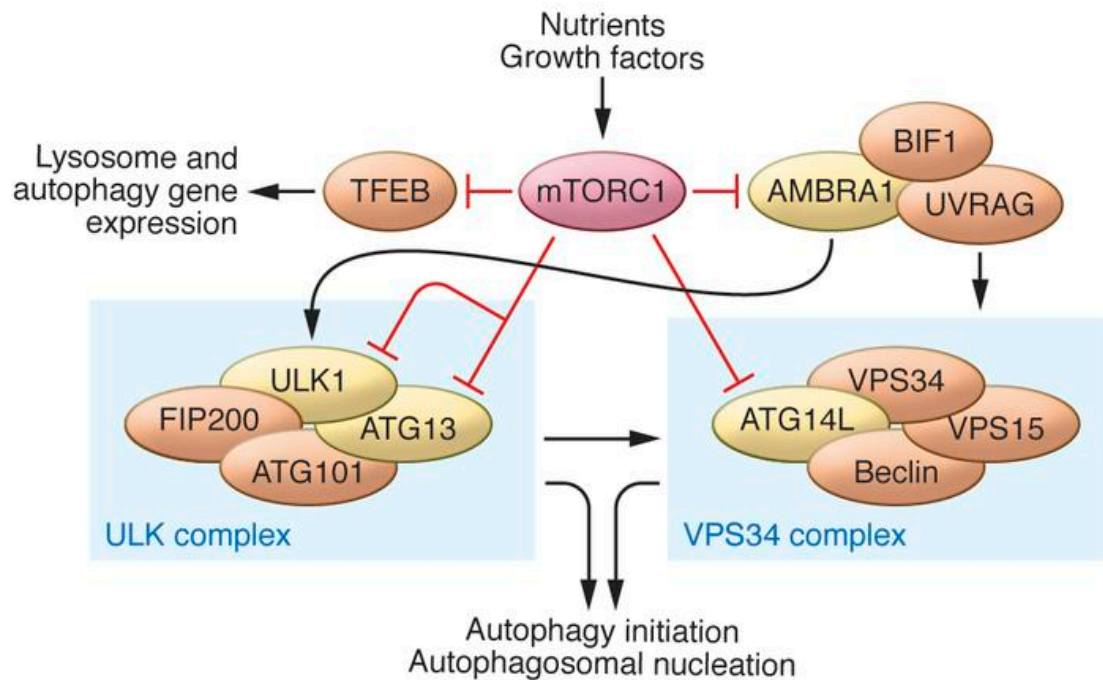


Figure 1.2.4 1: Regulation of autophagy by mTORC1 (Retrieved from (Y. C. Kim & Guan, 2015)).

Although the connection between mTORC1 and autophagy is well established, much less is known about the role of mTORC2 effect on autophagy regulation. Yet, mTORC2-RICTOR complex was found to be necessary for the phosphorylation of Akt at Serine 473 in vitro (Sarbasov, Guertin, et al., 2005). Activation of Akt/PKB effector inhibits the activation of transcription factor FoxO3 and consequently the transcription inhibition of autophagy related genes including LC3 and BNIP3 (Mammucari et al., 2007). It has been shown that silencing of Rictor evoked autophagy in neuroblastoma x glioma hybrid cell line (Chin et al., 2010). In addition, the inactivation of mTORC2 by targeted deletion of RICTOR in myocytes from adult heart result in increased levels of cleaved caspase-3 and LC3-II indicating the induction in both apoptosis and autophagy (Shende et al., 2016). mTORC2 was also reported to indirectly suppress autophagy through the activation of mTORC1. The PI3K signaling axis activates mTORC2, which, in turn, phosphorylates AKT at two different sites, leading to AKT/mTORC1

signaling axis activation (Oh et al., 2010; Zinzalla et al., 2011). In this context, mTORC2 can be defined as a negative regulator of autophagy, as mTORC1.

In line with this, in the recent study of Arias et al., lysosomal mTORC2, Akt, and PHLPP are shown to regulate the activity of chaperone mediated autophagy, a selective type of lysosomal degradation that is a selective component of the cellular stress response (Arias et al., 2015). They identified PHLPP1 and TORC2 as endogenous CMA stimulator and inhibitor, respectively, and unveiled how their opposite effects on Akt act coordinately in the modulation of basal and inducible CMA activity. The stress-induced increase in the association of the phosphatase with the Mb and the modulation of its stability in this compartment by the GTPase, Rac1, contribute to neutralize the endogenous inhibitory effect of lysosomal mTORC2/Akt on CMA (Arias et al., 2015).

1.3 Transcriptional Control of Autophagy: MiT/TFE Transcription Factors

Early studies about autophagic machinery mainly focused on the cytoplasmic regulation of autophagy through ATG family of proteins that mediate dynamic membrane rearrangements. Indeed, nuclear regulation of autophagy was neglected. However, lately it has been gained increased attention that the control center of autophagy is found in the nucleus and several transcription factors function in the longer-term transcriptional regulation of autophagy. There are more than 20 transcription factors that have been shown to be in control of the autophagic process and lysosomal biogenesis (Table 1.3 1) (reviewed in (Füllgrabe, Ghislat, Cho, & Rubinsztein, 2016; Pietrocola et al., 2013). Some of the transcription factors promote induction of autophagy (E2F1, GATA1 and FOXO family members, others repress (GATA4, FXR, ATF5 and ZKSCAN1), and a few have a dual inhibitory/activating function (TP53/p53 and NFkB) (Table 1.3 1).

Table 1.3 1 Transcriptional regulation of autophagy

| Transcription factor | Impact on autophagy | Targets |
|-----------------------------|-----------------------------|--|
| TFEB | Upregulation | ATG4, ATG9, BCL2, LC3, SQSTM1, Wipi1, UVRAG |
| TFE3 | Upregulation | TG16L1, ATG9B, GABARAP-L1, WIPI, UVRAG |
| ZKSCAN3 | Downregulation | MAPLC3B, ULK1, ATG18b, DFCP1 |
| FXR | Downregulation | ATG4, ATG7, ATG10, Wipi1, Dfcp1, ULK1, LAMP2, P62, PI3KCIII, Bnip3 |
| PPAR alpha | Upregulation/Downregulation | ATG2, ATG4, ATG12, ATG16, Pink1, Bnip3, Wipi1, LC3, P13KCIII |
| NF-kappa B | Upregulation/Downregulation | BCL2, Bnip3, BECN1, SQSTM1 |
| HIF-1alpha | Upregulation | Bnip3, BCL2, LC3, Beclin1, PI3KCIII |
| P53 | Upregulation/Downregulation | ATG2, ATG4, ATG7, ATG10, BCL2, ULK1, DRAM1, AMPK |
| FOXO | Upregulation | ATG8, ATG12, ATG4B, Gabarapl1, VSP34, BECLINI |
| E2F | Upregulation/Downregulation | Bnip3, LC3, ULK1, DRAM, ATG1, ATG5 |
| STAT | Downregulation | ATG3, ATG12, BCL2, Bnip3, BECN1 |
| GATA | Upregulation/Downregulation | ATG4, ATG8, LC3, ATG12, Bnip3, ATG5, ATG7, BECN1 |
| ATF4 | Upregulation | HRK, PUMA, NOXA, MAPLC3B, ULK1 |
| ATF5 | Downregulation | mTOR |
| C/EBPb | Upregulation | ULK1, BNIP3, LC3, ATG4 |

In 2011, a landmark paper by Settembre and his colleagues introduced transcription factor EB (TFEB), that belongs to MITF/TFE transcription factor family, as a master regulator of wide-range of genes in autophagy in coordination with the genes involved in lysosomal biogenesis and function (Settembre et al., 2011) TFEB enables a rapid induction of autophagy-related proteins that are functioning in all steps of the autophagic machinery. Considerable work has sought to understand the role of MITF/TFE family in cellular metabolism.

In this chapter, I will describe the structure, expression pattern and functions of four members of MITF/TFE family of transcription factors, analyze the regulation of MITF/TFE activity, and summarize the current knowledge transcriptional control of autophagy and lysosomal biogenesis through MiT/TFE family.

1.3.1 MITF/TFE Family of Transcription Factors

Evolutionary conserved MITF/TFE family of transcription factors encodes four distinct genes: MITF (Microphthalmia-associated transcription factor), TFEB (Transcription factor EB), TFEC and TFE3 (Hemesath et al., 1994). Homologs of the family were identified in *C. elegans* (HLH-30) (Rehli, 1999) and *Drosophila* (*Mitf*) (Figure 1.3.1 1) (Hallsson et al., 2004). Structurally, all the four family members constitute three critical regions; a basic helix-loop-helix (bHLH) leucine zipper (LZ) motif, a transactivation domain, and a domain required for DNA binding (Figure 1.3.1 1) (Beckmann, Su, & Kadesch, 1990; Sato et al., 1997; Eiríkur Steingrímsson, Copeland, & Jenkins, 2004).

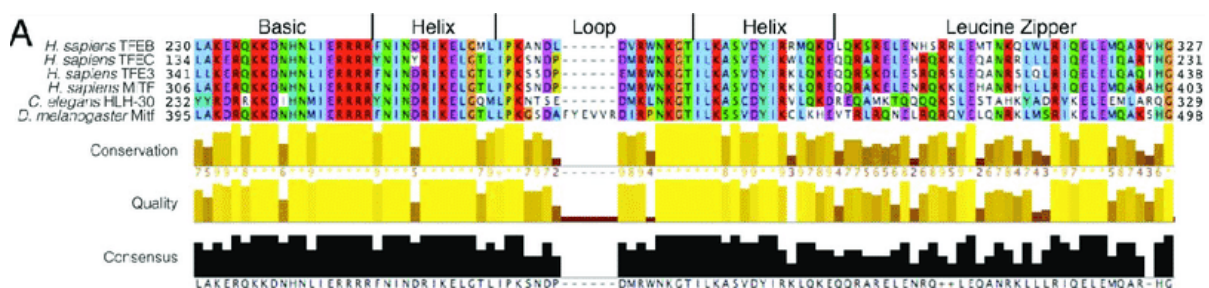


Figure 1.3.1 1: Multiple sequence alignment of MITF/TFE family members (MITF, TFEB, TFEC and TFE3) and homologs in *C. elegans* (HLH-30) and *D. Melanogaster* (*Mitf*) (Retrieved from (Bouché et al., 2016).

The members of MITF/TFE family can form homodimers or heterodimers through their HLH-LZ motif with another member of the family to activate transcription. However, MITF/TFE family members cannot form homo/heterodimers with other related bHLH proteins including c-Myc, Max or USF (Hemesath et al., 1994; Pogenberg et al., 2012).

MITF/TFE family members specifically bind to promoter region of their downstream target genes through E-box (CANNTG) and M-box (AGTCATGTGCT) response elements (Aksan & Goding, 2015). The function of MITF/TFE family members, especially TFEB remained unknown until a landmark paper published in 2009 that showed transcriptional regulation of numerous lysosomal and autophagy-related genes by TFEB via their binding to the E-box type element called Coordinated Lysosomal Expression and Regulation (CLEAR) element (GTCACGTGAC) (Sardiello & Ballabio, 2009). Several follow-up studies revealed that MITF and TFE3 could also bind the CLEAR element and regulate lysosome biogenesis in several different cell types (José A. Martina, Diab, Li, & Puertollano, 2014; Ploper & De Robertis, 2015).

TFEB and TFE3 expression have been detected in several different cell types, hence they show a ubiquitous pattern of expression, whereas TFEC is the macrophage-restricted member of the family (Rehli, Den Elzen, Cassady, Ostrowski, & Hume, 1999). TFE3 gene seems to be under control of a single promoter, whereas TFEB and TFEC contain multiple alternative first exons.

The MITF gene is expressed by alternative promoter usage from at least four promoters and their consecutive first exons (exons 1A, 1H, 1B and 1M) that results in several MITF isoforms sharing important functional domains of MITF but differing in their N termini (Udono et al., 2000). There are at least nine isoforms of MITF currently identified (Figure 1.3.1 2). The amino-termini of MITF-M is encoded by melanocyte-specific exon 1 (exon 1M). Common to all isoforms, exon 2-9 encode the functionally important regions, including b-HLH-Zip domain, transactivation domain and several phosphorylation consensus sequences (Hershey & Fisher, 2005). However, all isoforms except B- and M-isoforms, exon 1 is formed from a unique exon spliced to exon 1B1b, common region of 83 amino acid residues. This domain is significantly similar to the one in TFEB (Amae et al., 1998) and TFE3 (Amae et al., 1998; Rehli et al., 1999). The M-isoform does not contain exon 1B whereas the B-isoforms has the entire exon 1B.

MITF isoforms except MITF-M are widely expressed in many cell types including RPE cells, cervical cancer, osteoclasts, and mast cells (Amae et al., 1998; Fuse et al., 1999; Udono et al., 2000). MITF-D is generally expressed in RPE cells and monocyte lineage (Kazuhisa Takeda et al., 2002), while MITF-Mc is a novel mast cell isoform (Takemoto, Yoon, & Fisher, 2002). MITF-A and MITF-H has ubiquitous expression pattern due to their promoters lacking a typical TATA-box at the usual position which is commonly seen in many housekeeping genes (Udono et al., 2000). However, MITF-M promoter is under separate control that shows the melanocyte-specific function and MITF-M is highly expressed exclusively in melanocytes but not in other cell types. Thus, it has been identified as specific marker for melanocyte-lineage cells (Fuse, Yasumoto, Suzuki, Takahashi, & Shibahara, 1996; Shibahara, 2001).

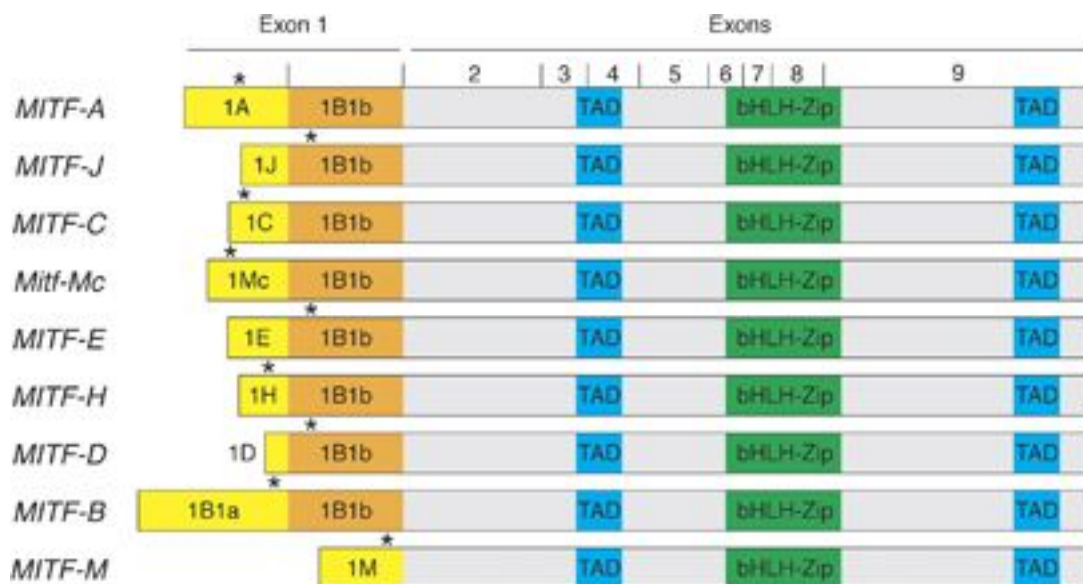


Figure 1.3.1 2: Alternative promoter usage and spliced mRNAs of human MITF isoforms. (Retrieved from (Kawakami et al., 2017)).

Numerous studies demonstrated the significant role of MITF/TFE family of transcription factors in many cellular and physiological processes. TFEB is well-characterized as the master regulator of lysosomal function and autophagy by coordinating expression of lysosomal-autophagic pathway. Moreover, some studies reveal a role of TFEB in immune response, demonstrating TFEB function in the regulation of the innate immune response to pathogen infection in activated macrophages (Pastore et al., 2016), and antigen presentation during adaptive immune response (Samie & Cresswell, 2015). Furthermore, glucose and lipid

metabolism also are controlled by TFEB transcriptional activity. Thereby, TFEB allows cells to adapt to changing environmental cues. Overexpression of TFEB improves outcomes in various diseases associated protein aggregation, including Parkinson's disease, Huntington disease, X-linked spinal and bulbar muscular atrophy (Napolitano & Ballabio, 2016). Moreover, TFEB alleviates pathology in models of alpha-1-anti-trypsin deficiency, and lysosomal storage disorders including Pompe disease (Spampanato et al., 2013) and multiple sulfatase deficiency mucopolysaccharidosis type IIIA (Soria & Brunetti-Pierri, 2018). Taken together, TFEB has a crucial function in various pathological conditions through regulation of lysosomal function and autophagy (Figure 1.3.1 3).

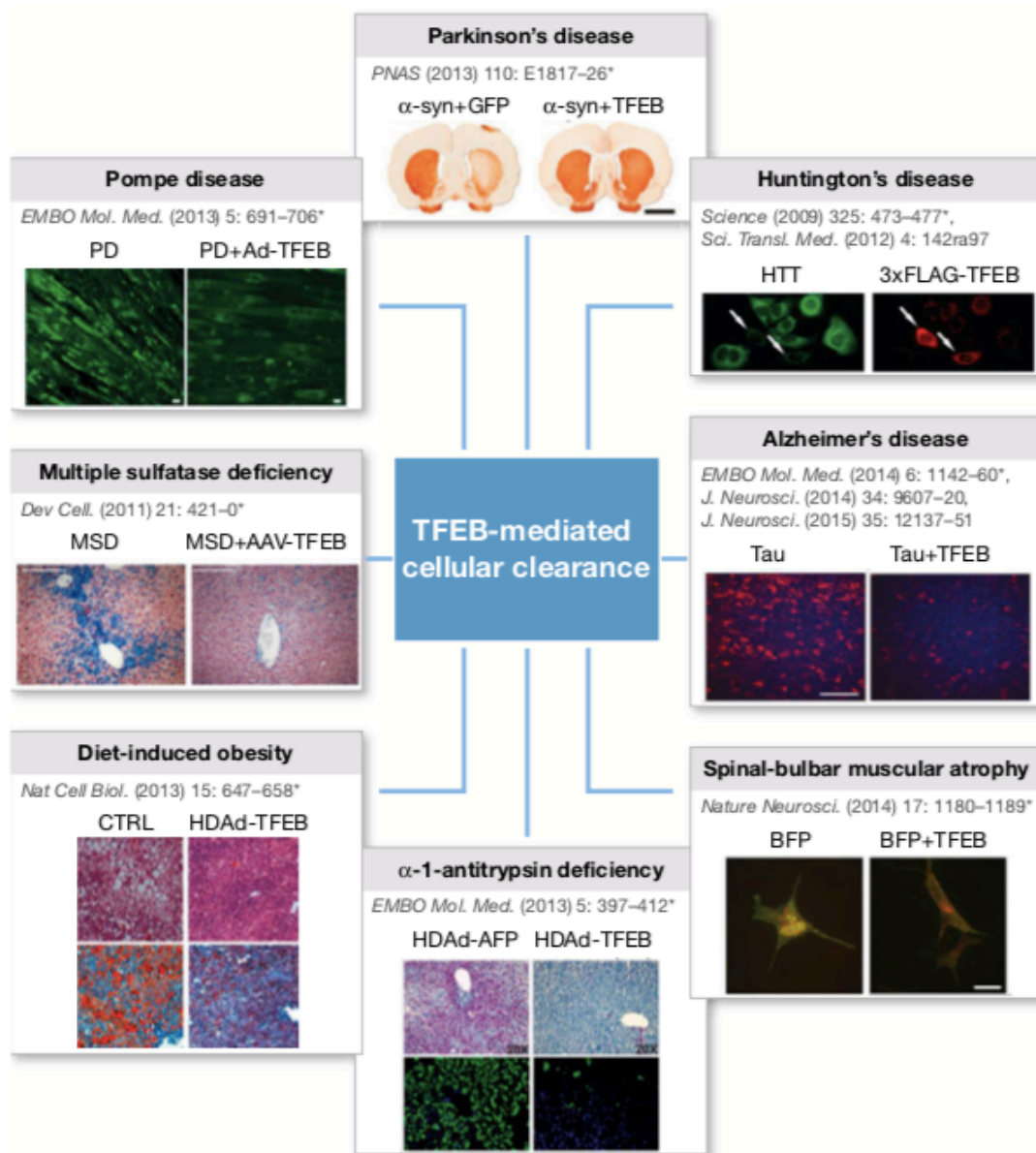


Figure 1.3.1 3: TFEB-mediated cellular clearance in diseases (Retrieved from (Ballabio, 2016).

TFE3 also plays a critical role in the lysosomal function and autophagy, as well as in the regulation of glucose homeostasis, lipid metabolism and mitochondrial dynamics (Pastore et al., 2017). TFE3 knockout experiments in mice showed that it can be a novel therapeutic target for diet-induced obesity and diabetes. Hence, it cooperates with TFEB to ensure metabolic adaptation to environmental cues (Figure 1.3.1 4).

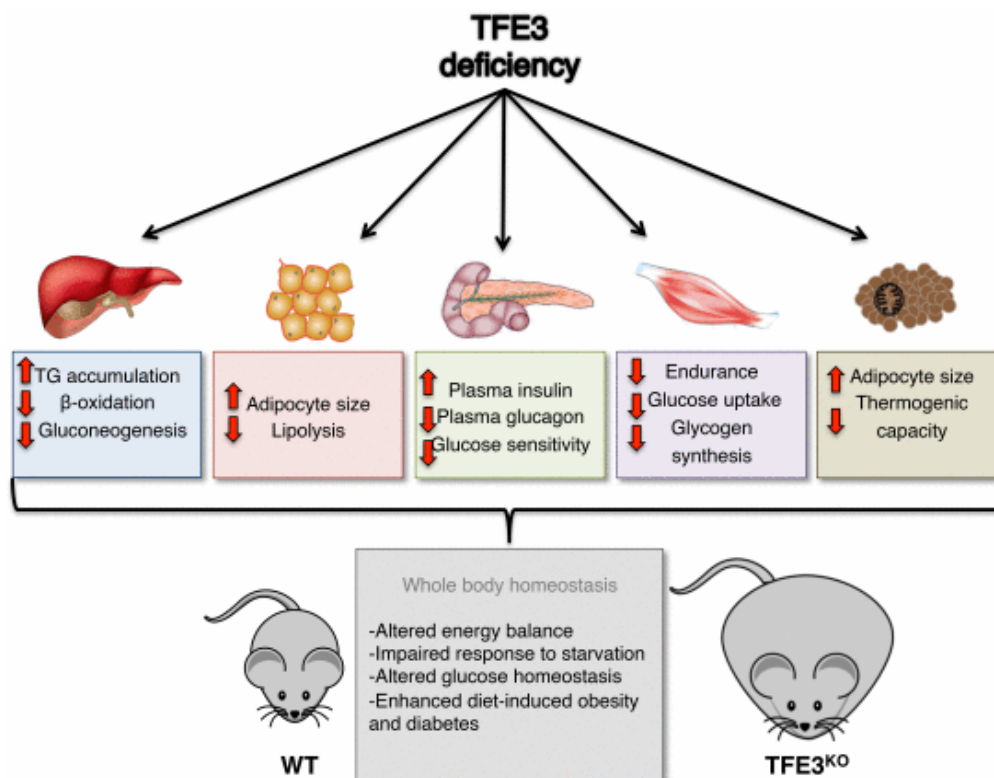


Figure 1.3.1 4: Role of TFE3 in metabolic response to environmental cues (Retrieved from (Pastore et al., 2017)).

MITF, on the other hand, is mainly characterized as the regulator of melanosome biogenesis, and development, survival, and differentiation of neural crest-derived melanocytes and retinal pigmented epithelium (RPE). These processes are highly dependent on proper lysosomal pH and autophagic activity. Interestingly, in recent studies, MITF has been shown to play a role in the transcriptional regulation of lysosomal biogenesis and, to some extent, autophagic activity like TFEB and TFE3. In collaboration with TFE3, MITF also regulates osteoclastogenesis (Hershey & Fisher, 2004) and mast cell differentiation (Weilbaecher et al., 2001). Moreover, some target genes of MITF are involved in cell proliferation and survival mechanisms.

Mutations in MITF gene can result in white coat color and deafness in mice and rats that also present microphthalmia (Hodgkinson et al., 1993). Heterozygous mutations in MITF can cause Waardenburg Syndrome type 2, which is characterized as a hypopigmentation and deafness disorder (Tassabehji, Newton, & Read, 1994). On the other hand, Tietz Syndrome, that is also characterized by generalized depigmentation and deafness, is caused by dominant-negative mutations in human MITF gene (Smith, Kelley, Kenyon, & Hoover, 2000).

Several studies argue that MITF/TFE family of transcription factors are oncogenes. TFEB and TFE3 are driven by translocations in pediatric renal cell carcinomas (RCC) and alveolar soft part sarcomas (ASPS) (Argani, 2015; Ramphal, Pappo, Zielenska, Grant, & Ngan, 2006).

However, the expression levels of MITF appear to have different downstream effects in melanoma. It has been shown to promote oncogenesis in melanoma by regulating key processes in carcinogenesis involving proliferation, invasiveness, survival, oxidative stress and DNA repair (Haq & Fisher, 2011). MITF amplification has been identified in 20% of melanomas as lineage specific oncogene (Garraway et al., 2005). Thereby, the expression of transcriptional targets of MITF that are involved in cell proliferation (CDK2), cell survival (BCL2), invasiveness (cMET) and cell-cycle arrest (p21, p16) are increased. Conversely, some studies suggest that high levels of MITF attenuates proliferation, invasiveness and tumor development. Interestingly, it has been described that, MITF, when expressed at very low levels, causes p27-dependent cell cycle arrest with increased invasiveness properties, whereas intermediate levels of MITF result in proliferation and high levels of MITF activity initiate differentiation (Carreira et al., 2006).

Recently, MITF, TFEB and TFE3 overexpression was detected in pancreatic adenoductal carcinoma (PDA) cell lines and patient tumors in which constitutive activation of autophagy is required to maintain metabolic homeostasis in PDA (Perera et al., 2015). Moreover, these transcription factors were found in nucleus constitutively, similar to that seen in RCC and ASPs. Importantly, MITF, TFEB and TFE3 were shown to promote lysosomal function and autophagy in PDA.

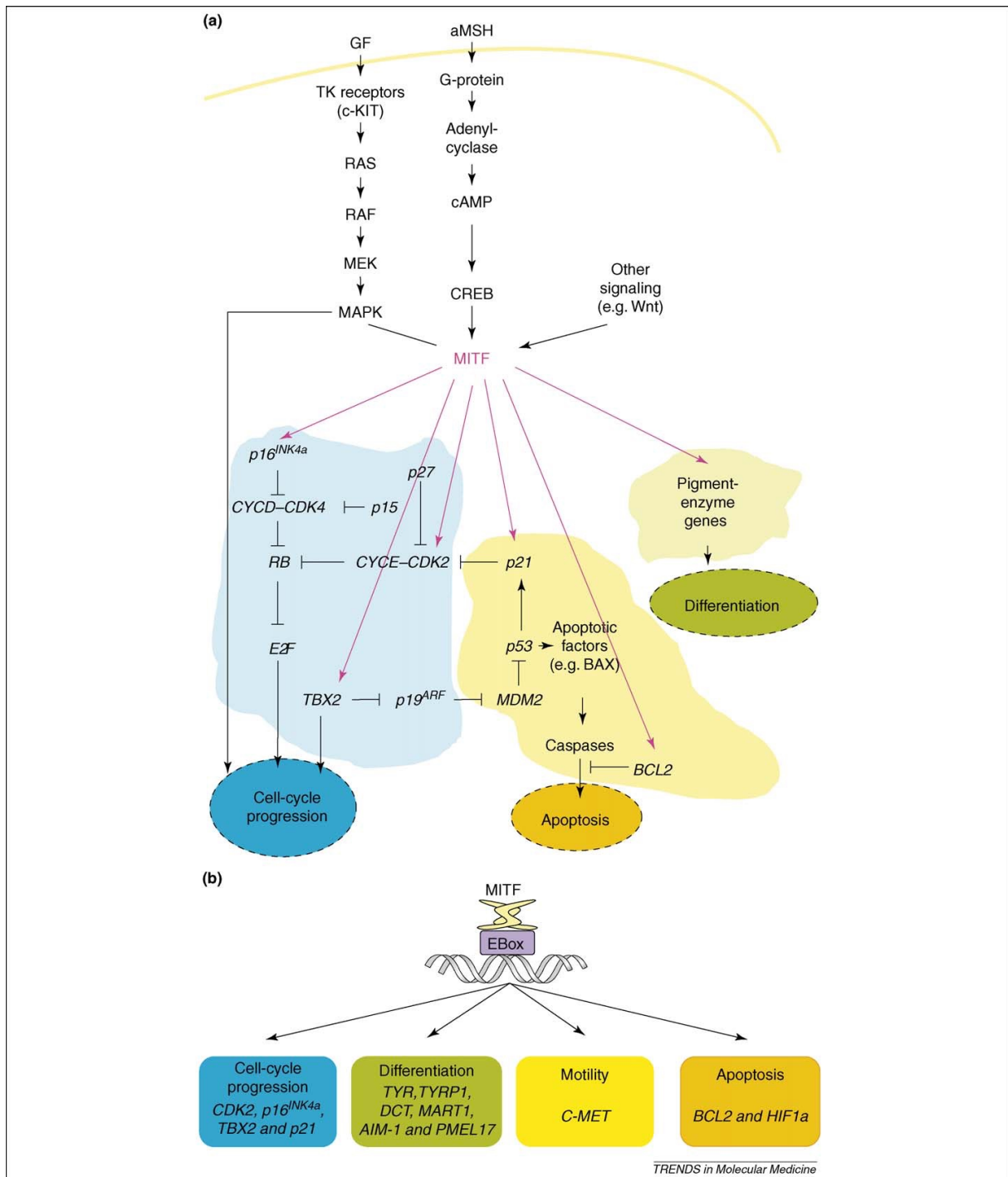


Figure 1.3.1 5: MIF is involved in the induction of melanoma, melanocyte differentiation, cell-cycle progression and survival (Retrieved from (Levy, Khaled, & Fisher, 2006))

1.3.2 Regulation of MITF/TFE activity

MITF/TFE family of transcription factors are regulated in response to extracellular signals such as nutrient availability and various forms of cell stress. Such regulation mechanism involves shuttling of transcription factors between lysosomal membranes, the cytoplasm, and the nucleus that is mediated by phosphorylation of multiple conserved aminoacids (Figure 1.3.2 1). Major kinases responsible for MITF-TFE phosphorylation include mTOR, ERK, GSK3 and AKT.

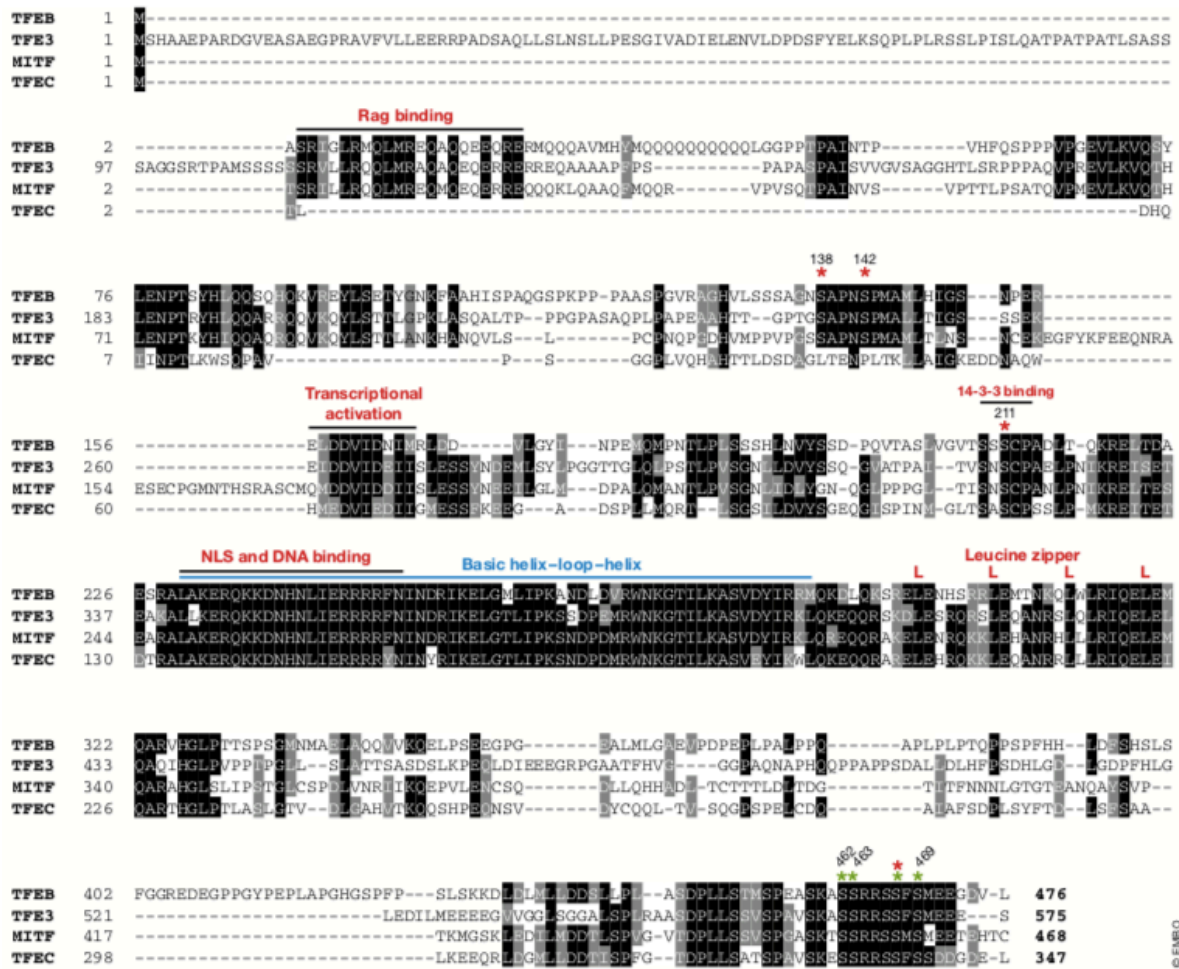


Figure 1.3.2 1: Sequence conservation of TFEB, TFE3, MITF and TFEC phosphorylation sites. Phosphorylation sites that inhibit nuclear translocation of TFEB are shown with red asterisks, while those have been found to promote TFEB nuclear localization are shown with green asterisks (Retrieved from (Puertollano, Ferguson, Brugarolas, & Ballabio, 2018)).

1.3.2.1 Nutrient deprivation and mTORC-1 dependent regulation

A key point in understanding the role of MITF/TFE family in lysosomal biogenesis and autophagy was the identification of the mechanism for TFEB activation in response to nutrient deprivation. Subsequent studies indicate that TFEB is regulated by mammalian target of rapamycin complex 1 (mTORC1) (Jose A. Martina, Chen, Gucek, & Puertollano, 2012; Settembre et al., 2012). Under nutrient-rich conditions, TFEB is phosphorylated by mTORC1 at S122, S142 or S211 but only S211 phosphorylation creates a docking sites for the cytosolic chaperone 14-3-3 (Jose A. Martina et al., 2012; Roczniak-Ferguson et al., 2012; Settembre et al., 2011; Vega-Rubin-de-Celis, Peña-Llopis, Konda, & Brugarolas, 2017). Binding of 14-3-3 causes sequestration of TFEB in the cytosol and keeps it inactive, most probably via masking the nuclear import signal. Mutations of S142A or S211A resulted in a constitutively active TFEB in nucleus which is a similar response to mTOR inhibitor Torin1 (Settembre et al., 2012).

Remarkably, mTORC1 regulation in response to nutrient status is mediated by RAG GTPases that sense amino acid availability and control subcellular localization of mTORC1 (Sancak et al., 2010). In the presence of amino acids, mTORC1 complexes are recruited to lysosome membranes through active RAG GTPase heterodimers (RAGA/B-GTP and RAGC/D-GDP), leading to their activation by RHEB proteins (Sancak et al., 2010; Zoncu et al., 2011). Interestingly, active RAG GTPases bind and recruit TFEB to lysosomes, promoting its mTORC1-dependent phosphorylation (Figure 1.3.2.1 1). This suggests that mTORC1-mediated TFEB phosphorylation can occur at the lysosomal membrane.

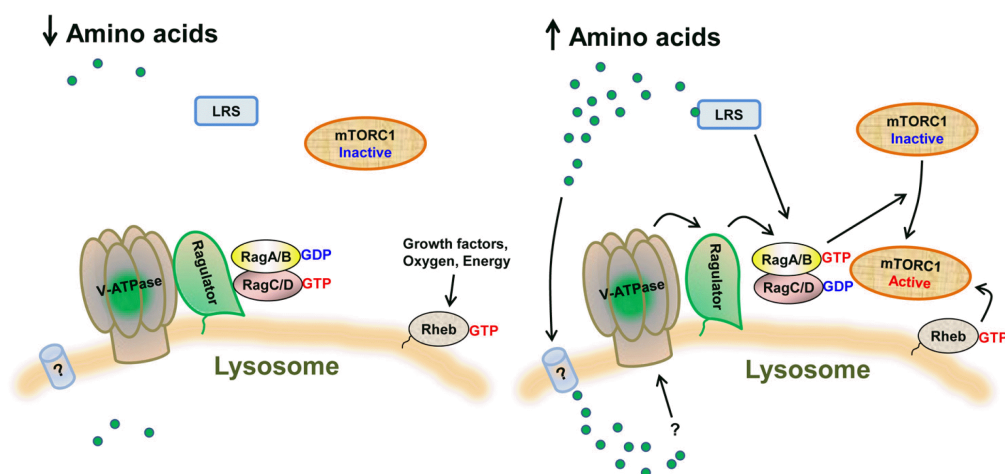


Figure 1.3.2.1 1: Amino acid signaling to mTORC1 (Retrieved from (S. G. Kim, Buel, & Blenis, 2013))

Conversely, starvation or lysosomal stress shuts-off RRAG proteins, resulting in the release of mTORC1 from the lysosomal membrane. Consequently, non-phosphorylated TFEB is free to translocate to the nucleus and activate the target genes in lysosomal biogenesis and autophagy that will assist in cellular survival during starvation conditions (Figure 1.3.2.1 2). Interestingly, in response to nutrient deprivation, lysosomal calcium is released through calcium channel mucolipin 1 (MCOLN1), which in turn activates phosphatase calcineurin (CaN) to directly dephosphorylate TFEB (Medina et al., 2015). Indeed, TFEB activation and autophagy induction upon nutrient deprivation is prevented in the absence of MCOLN1. TFEB nuclear localization and activation is also triggered by the TOR inhibitors rapamycin and Torin-1.

Very recently, MAP4K3 was identified as a key node in the amino acid-mediated regulation of TFEB subcellular localization (C. L. Hsu et al., 2018). Direct phosphorylation of TFEB serine 3 by MAP4K3 is essential for the interaction of TFEB with the mTORC1-Rag GTPase complex by likely contributing to the recruitment of TFEB to lysosomal membranes. Indeed, S3 phosphorylation is necessary for TFEB serine 211 phosphorylation by mTORC1 and cytosolic sequestration of TFEB with 14-3-3.

Studies in several cellular systems revealed that similar mTORC1-dependent mechanism controlling TFEB activity also appear to regulate subcellular localization of other MITF/TFE members, MITF and TFE3, in response to nutrient starvation and mTORC1 inhibition (José A. Martina, Diab, Lishu, et al., 2014). Indeed, TFEB serine residues phosphorylated by mTORC1 are conserved in MITF and TFE3. In response to the changes in the nutrient levels, MITF is also recruited to the lysosomal surface where mTORC1 phosphorylates the serine 280 residue and create a binding site for 14-3-3. In the case of TFE3, active mTORC1 phosphorylates serine 321 residue. mTORC1-dependent phosphorylation results in sequestration of MITF and TFE3 in the cytosol. Conversely, when nutrients are deprived, mTORC1 inactivation and dephosphorylation of Ser280 for MITF and Ser321 for TFE3 result in the rapid accumulation of these transcription factors in the nucleus. Similar activation mechanisms for different members of MITF/TFE family suggests a similar function for TFEB, MITF and TFE3.

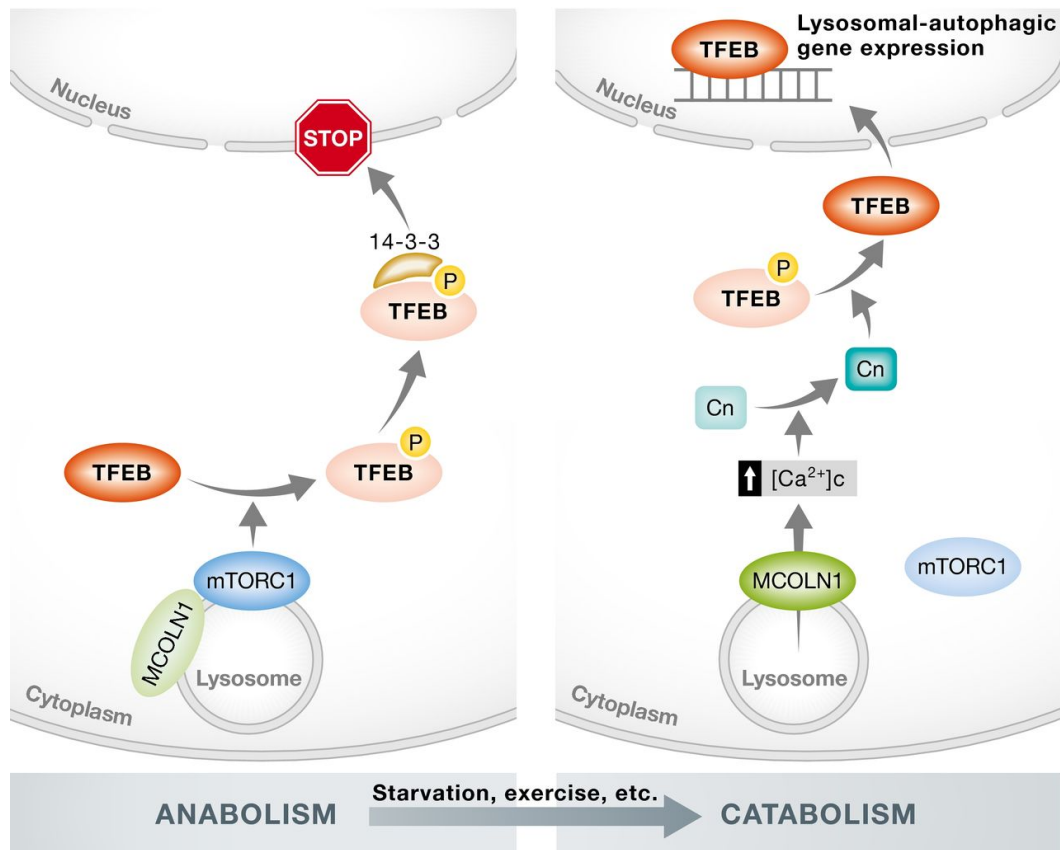


Figure 1.3.2.1 2: mTORC1-dependent signaling mechanism that regulate TFEB nuclear translocation (Retrieved from (Ballabio, 2016)).

1.3.2.2 Cellular Stress

Several studies showed that MITF/TFE family of transcription factors, especially TFEB, responds to a variety of cellular stresses including lysosomal stress, mitochondrial stress, endoplasmic reticulum (ER) stress, and reactive oxygen species (ROS).

TFEB responds to lysosomal status in mTORC1-dependent manner, as mTORC1 is inactivated upon lysosomal stress and released from the lysosomal membrane (Sancak et al., 2010). Moreover, treatment with lysosomal inhibitors such as chloroquine or Bafilomycin-1 can trigger the nuclear localization of TFEB (Roczniak-Ferguson et al., 2012; Settembre et al., 2012).

Unlikely, TFEB and TFE3 responds to mitochondrial stress in a mTORC1-independent manner such that nuclear translocation of TFEB and TFE3 upon mitophagy induction by oligomycin and antimycin A is dependent on PINK1, Parkin, ATG5 and ATG9A (Nezich, Wang, Fogel, & Youle, 2015). Further studies showed that peroxisome proliferator-activated receptor gamma coactivator-1 alpha (PGC-1 α) transactivates TFEB expression to induce mitophagy and ameliorate Huntington's Disease neurodegeneration (Tsunemi et al., 2012). Interestingly, a feed-forward loop has been generated through PGC-1 α being a direct target gene for TFEB with three CLEAR sites in its promoter (Settembre et al., 2013).

Furthermore, in response to endogenous and exogenous ROS treatment, TFEB is activated following MCOLN1 mediated lysosomal calcium release and calcineurin activation (X. Zhang et al., 2016).

Recently, ER stress has been found to regulate TFEB and TFE3 nuclear translocation in an mTORC1-independent manner (Figure 1.3.2.2 1). In this case, activation of one of the key mediators of integrated stress response, PERK (kinase double-stranded RNA activated protein kinase-like ER kinase), results in upregulation of ATF4 (activating transcription factor 4), which in turn induces calcineurin activation and promotes nuclear translocation of TFEB and TFE3 (J. A. Martina, Diab, Brady, & Puertollano, 2016). However, the exact mechanism of PERK-dependent activation of TFEB and TFE3 is still needed to be discovered.

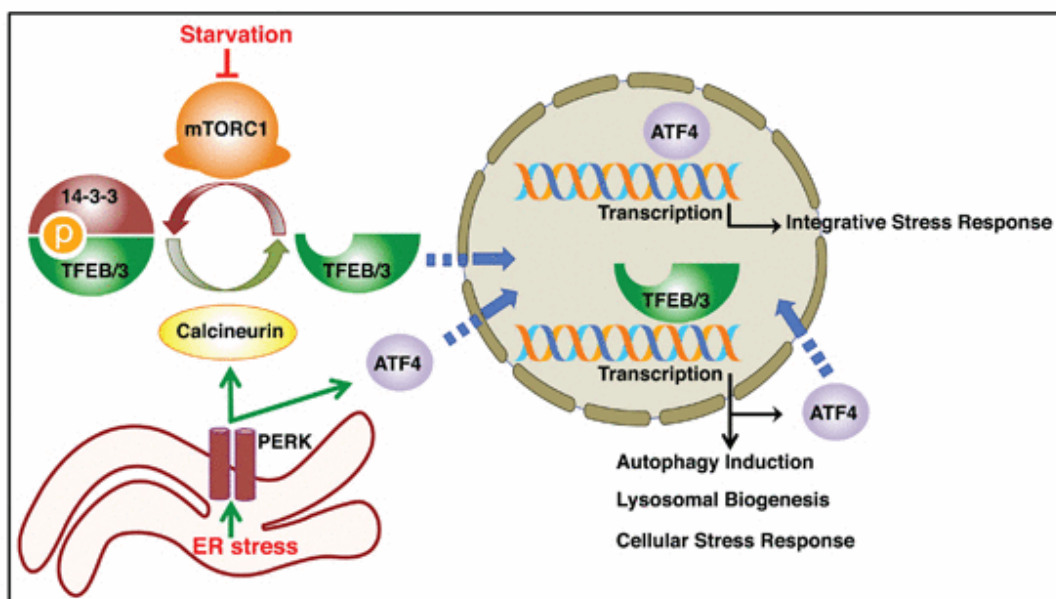


Figure 1.3.2.2 1: TFEB and TFE3 respond to ER-Stress in a PERK-dependent manner. (Retrieved from Martina et al., 2016).

1.3.2.3 mTORC1-independent regulation

Along with mTORC1, other growth-regulating kinases glycogen synthase kinase 3 (GSK3) and MAPK kinase (MEK)/extracellular signal-regulated kinase (ERK) also control subcellular localization of MITF/TFE family members. Indeed, as shown in Fig. 1.3.2.3 1, GSK3-regulated phosphoproteome showed that MITF/TFE family of transcription factors consist the most conserved GSK3 phosphorylation sites in the carboxy-terminus (Ploper & De Robertis, 2015).

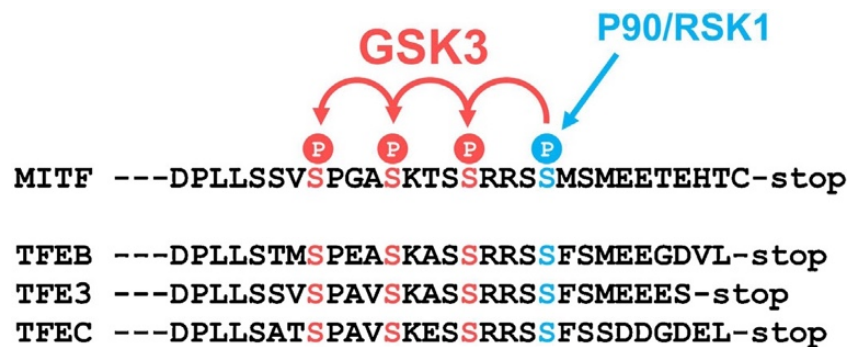


Figure 1.3.2.3 1: Highly conserved GSK3 phosphorylation sites in MITF and its paralogues TFEB, TFE3 and TFEC (retrieved from (Ploper et al., 2015)).

Recently, it was shown that TFEB is phosphorylated by GSK β at serine 134 and serine 138, directing TFEB to the lysosomal surface by an unknown mechanism and facilitating mTORC1-mediated phosphorylation. Following PKC α and PKC δ -mediated inhibition of GSK3 β , TFEB, rather than TFE3, TFEB is no longer localized at lysosomal membrane, freely translocates to nucleus and activated (Y. Li et al., 2016).

Furthermore, nuclear export signal of TFEB was found to be regulated through a mechanism involving phosphorylation at S138 by GSK3 β which is primed by phosphorylation at S142 by ERK/mTORC1. Whether TFEB is retained in the nucleus will be dependent on the phosphorylation status of S138 and S142. Absence of phosphorylation of S138 or S142 will lead to nuclear retention. Although S142 should be dephosphorylated to promote TFEB nuclear entry, there is no must for S138 to be dephosphorylated for nuclear translocation of TFEB. Moreover, glucose limitation activates mTORC2-Akt-GSK3 β axis that results in the inhibitory phosphorylation of GSK3 β , hence preventing nuclear export of TFEB (Li et al., 2018).

Moreover, MITF in proliferative stages of melanoma was also shown to be regulated through GSK3 β phosphorylation via a positive-feedback loop (Figure 1.3.2.3 2). Without Wnt signaling, serine 405, 401 and 397 residues of MITF are phosphorylated by GSK3 β promoting degradation of the MITF protein in proteasomes. Upon Wnt ligand binding, GSK3 β is inhibited, phosphorylation of serine residues at MITF C-terminal is abolished, and MITF protein is stabilized. Hence, MITF constitutively translocate into the nucleus and expands late endosomes which can further sequester destruction complex components and enhance the Wnt signal (Ploper et al., 2015).

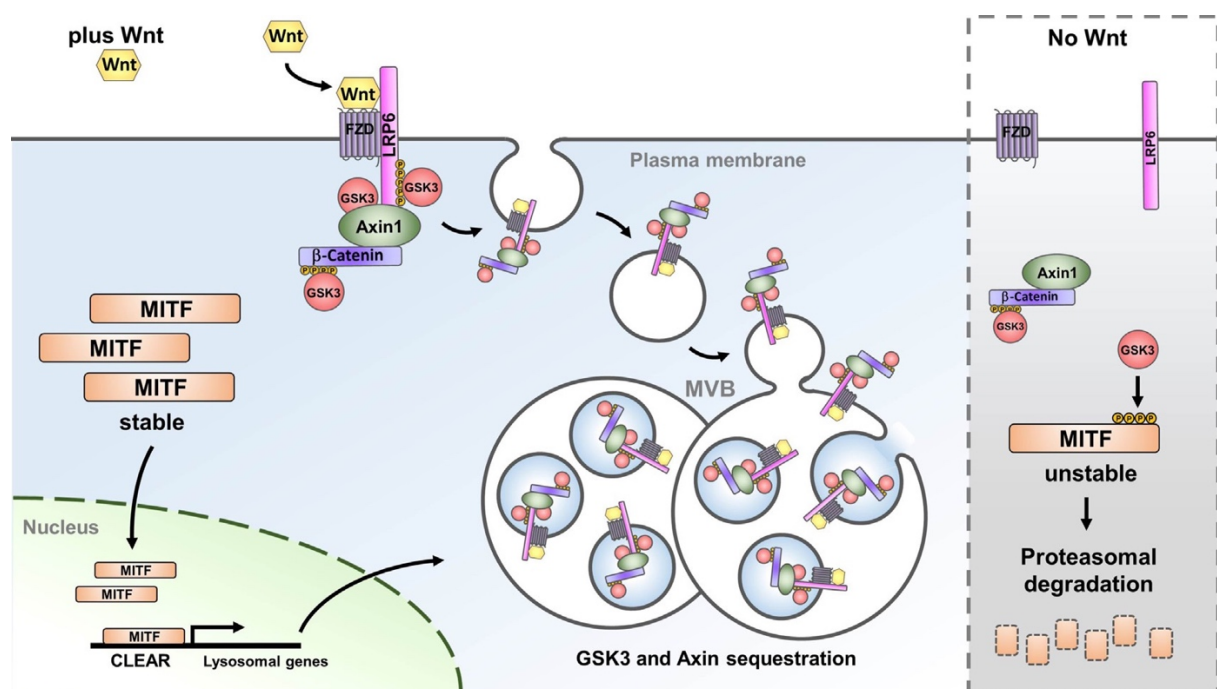


Figure 1.3.2.3 2: Positive feedback loop between MITF and Wnt signaling in melanoma (Retrieved from Ploper et al., 2015)

In addition, serine 298 residue of MITF, that is mutated in individuals with Waardenburg syndrome type 2 (WS2), is also a target for GSK3 β phosphorylation in melanoma, thereby enhancing the interaction of MITF to the promoter of its target, tyrosinase (K. Takeda, 2000).

Notably, a recent study identified Akt as an mTORC1-independent regulator of TFEB activity through phosphorylation at serine 467. Indeed, pharmacological inhibition of Akt induces TFEB-mediated cellular clearance in models of lysosomal storage diseases (M. et al., 2017).

Another kinase ERK2 was also shown to phosphorylate TFEB at serine 142 that promotes TFEB cytoplasmic retention (Settembre et al., 2011). Similarly, ERK-mediated phosphorylation of the homologous serine 73 site in the melanocyte-specific MITF isoform, MITF-M, enhances recruitment of p300/CBP (CREB-binding protein) to MITF and modulates transcriptional activity (Wu et al., 2000). Moreover, activated ERK1/2 can further promote its downstream kinase p90-RSK1 which can also phosphorylate MITF at serine 409 (Wu, 2000). Additionally, another study showed that BRAF/MAPK and GSK3-mediated phosphorylation mechanisms converge to regulate MITF nuclear export (Ngeow et al., 2018). Phosphorylation of MITF-M isoform by ERK on S73 in response to BRAF/MAPK signaling primes for phosphorylation by GSK3 β on S69. Hence, this mechanism was reported to control transcriptional activity and protein stability of MITF-M by regulating its ubiquitination on K201 and proteosomal degradation.

Several different kinases were shown to be involved MITF/TFE regulation in osteoclast differentiation. Various studies demonstrate that RANKL1, osteoclast differentiation factor, promotes lysosomal biogenesis in osteoclast differentiation through TFEB and MITF activation. For instance, RANKL induces PKC β -mediated phosphorylation of TFEB on S462/S463/S467/S469 in the C-terminal region, hence stabilizes and increases the activity of TFEB (Ferron et al., 2013). Moreover, MITF is also phosphorylated in response to RANKL signaling. Phosphorylation of serine 307 residue is mediated by p38 MAPK, which promotes MITF activity (Mansky, Sankar, Han, & Ostrowski, 2002). Additionally, subcellular localization of MITF in osteoclast differentiation is also controlled by C-TAK1 (Cdc25-associated kinase) by generating 14-3-3 binding sites and promoting cytosolic retention of MITF. Upon RANKL treatment, interaction between C-TAK1 and MITF is disturbed, and MITF freely translocates to the nucleus (Bronisz, 2006; Schwarz, Murphy, Sohn, & Mansky, 2010).

1.3.3 Lysosomal and autophagy-related targets of MITF/TFE family

Members of the MITF-TFE family of transcription factors have a large degree of overlap in their regulatory mechanisms (as described in previous section) and functions. MITF-M is the exception since it is melanocyte-specific isoform of MITF and constitutively localized in the nucleus (Selzer et al., 2002). The function of MITF-M as regulator of melanoblast survival and differentiation, melanosome biogenesis and eye development has been broadly explored but functions of other isoforms has been more subtle.

Detailed insights into the function of MITF/TFE family has been revealed when TFEB was characterized as a major transcription factor regulating lysosomal biogenesis and further studies unravel its function in autophagic machinery by coordinating the expression of genes involved in all steps of the autophagy process, from initiation and autophagosome formation to autolysosomal degradation. TFEB regulates expression of lysosomal and autophagy-related targets through binding to the E-box type CLEAR elements (GTCACGTGAC) in their promoter regions (Sardiello & Ballabio, 2009). Several follow-up studies revealed that MITF and TFE3 display conserved regulation by mTOR, and also bind to similar CLEAR elements found on targets genes of TFEB. Thereby, all these factors have overlapping but not identical functions in lysosomal biogenesis and autophagy in several different cell types (Table 1.3.3 1).

TFEB overexpression results in a significant increase in total lysosome amount in the cell through its contribution to the transcriptional activation of numerous lysosomal genes, including several subunits of the v-ATPase, lysosomal transmembrane proteins and lysosomal hydrolases (Sardiello & Ballabio, 2009). In addition, TFEB overexpression leads to enhanced clearance of long-lived proteins (Settembre et al., 2011), lipid droplets and dysfunctional mitochondria (Nezich et al., 2015; Settembre et al., 2013) indicating that it also regulates autophagy. Furthermore, TFEB mediates lysosomal docking to the plasma membrane and promotes their fusion through raising Ca^{2+} levels through MCOLN1. Indeed, TFEB overexpression induces lysosomal exocytosis and modulate cellular clearance in lysosomal storage diseases (LSDs) both *in vitro* and *in vivo* (Medina et al., 2011). The ability of TFEB to regulate lysosomal biogenesis, autophagy and lysosomal exocytosis is of great importance because it reveals a transcriptional program controlling the main cellular degradative pathways.

More recently, Martina et al. reported that TFE3 also promoted the expression of genes involved in lysosomal and autophagy-related pathways in ARPE-19 cells in response to starvation and lysosomal stress (José A. Martina, Diab, Lishu, et al., 2014). mTORC1-dependent regulatory mechanism of TFEB is also shared by TFE3, and upon nutrient deprivation TFE3 rapidly translocated to the nucleus and bound to the CLEAR elements found in the promoter region of its target genes. Furthermore, overexpression of TFE3 induces lysosomal exocytosis and promotes cellular clearance in a cell model of lysosomal storage disorder, Pompe disease. Despite their conserved regulation and overlapping targets, TFEB and TFE3 must have distinct functions in particular cell types or during development, as depletion of *Tfeb*-null mice show embryonic lethality (E Steingrímsson, Tessarollo, Reid, Jenkins, & Copeland, 1998), whereas knockout of *Tfe3* has no apparent phenotype (Steingrímsson et al., 2002).

Whereas the role of TFEB and TFE3 in this context has been studied in detail, whether MITF is indispensable and has a distinct function in autophagy regulation is yet to be established. The difficulty comes from alternative splicing and multiple isoform formation of MITF. A study with *Drosophila melanogaster* reported that the lysosomal-autophagy pathway is controlled by *Mitf* gene, the single member of MITF-TFE family in the fruit fly genome (Bouché et al., 2016). *Mitf* transcriptionally regulates genes involved in lysosomal-autophagy pathway such as orthologs of mammalian MCOLN1, UVRAG, GABARAP, WIPI1 and ATG9A, consistent with TFEB network in mammalian. Accordingly, *Mitf*-knockdown flies show impaired autophagic flux and abnormal lysosomes during nutrient deprivation. Moreover, overexpression of *Mitf* display a higher number of autophagosomes under both basal and starved conditions which shows that *Mitf* is required for starvation-induced fusion of autophagosomes and lysosomes. Furthermore, subcellular localization of *Mitf* in *Drosophila* is regulated by MTORC1-dependent mechanism similar to that in mammalian system. Another study using *Drosophila* model organism showed that *Mitf* directly regulates all V-ATPase subunits and lysosomal metabolism (T. Zhang et al., 2015).

Interestingly, MITF-A overexpression in ARPE-19 cells promotes expression of several autophagy genes but does not effectively increase lysosomal gene expression (José A. Martina, Diab, Lishu, et al., 2014). Furthermore, an inducible MITF melanoma model as well as HEK293T cells transiently transfected with MITF, showed upregulation of many, but not all,

lysosomal gene transcripts including CTSA, MCOLN1, PSAP, GNS, SCPEP1, NEU1 and GLA through direct activation of CLEAR element in their promoters (Ploper et al., 2015).

Table 1.3.3 1 Reported lysosomal and autophagy-related targets of TFEB, TFE3 and MITF

| | TFEB | | | TFE3 | | | MITF | | |
|-------------------------|---------------|-----------|----------|--------------|-----------|---------|---------------|-----------|--------|
| | TARGET | CELL LINE | METHOD | TARGET | CELL LINE | METHOD | TARGET | CELL LINE | METHOD |
| Lysosomal Hydrolases | <i>ASAH1</i> | HeLa | Chip-Seq | <i>CTSS</i> | ARPE-19 | qPCR | <i>CTSS</i> | 8902 | ChIP |
| | <i>CTSA</i> | HeLa | Chip-Seq | <i>CTSD</i> | ARPE-19 | qPCR | <i>CTSD</i> | PL18 | qPCR |
| | <i>CTSB</i> | HeLa | Chip-Seq | <i>GAA</i> | ARPE-19 | qPCR | <i>NAGLU</i> | C32 | qPCR |
| | <i>CTSD</i> | HeLa | Chip-Seq | <i>GBA</i> | ARPE-19 | qPCR | <i>PSAP</i> | C32 | qPCR |
| | <i>CTSF</i> | HeLa | Chip-Seq | <i>GLA</i> | ARPE-19 | qPCR | <i>NEU1</i> | C32 | qPCR |
| | <i>GAA</i> | HeLa | Chip-Seq | <i>CTSA</i> | ARPE-19 | qPCR | <i>GLA</i> | C32 | qPCR |
| | <i>GALNS</i> | HeLa | Chip-Seq | <i>CTSF</i> | ARPE-19 | qPCR | <i>GBA</i> | C32 | qPCR |
| | <i>GBA</i> | HeLa | Chip-Seq | <i>HEXA</i> | ARPE-19 | qPCR | <i>SCPEP1</i> | C32 | qPCR |
| | <i>GLA</i> | HeLa | Chip-Seq | <i>GALC</i> | 8988T | RNA-Seq | <i>HPRT1</i> | C32 | qPCR |
| | <i>GLB1</i> | HeLa | Chip-Seq | <i>GM2A</i> | 8988T | RNA-Seq | | | |
| | <i>GNS</i> | HeLa | Chip-Seq | <i>GNS</i> | 8988T | RNA-Seq | | | |
| | <i>GUSB</i> | HeLa | Chip-Seq | <i>HEXB</i> | 8988T | RNA-Seq | | | |
| | <i>HEXA</i> | HeLa | Chip-Seq | <i>IDS</i> | 8988T | RNA-Seq | | | |
| | <i>HEXB</i> | HeLa | Chip-Seq | <i>AGA</i> | 8988T | RNA-Seq | | | |
| | <i>IFI30</i> | HeLa | Chip-Seq | <i>ARL8B</i> | 8988T | RNA-Seq | | | |
| | <i>NAGLU</i> | HeLa | Chip-Seq | <i>ARSA</i> | 8988T | RNA-Seq | | | |
| | <i>NEU1</i> | HeLa | Chip-Seq | <i>ASAH1</i> | 8988T | RNA-Seq | | | |
| | <i>PLBD2</i> | HeLa | Chip-Seq | | | | | | |
| | <i>PPT1</i> | HeLa | Chip-Seq | | | | | | |
| | <i>PSAP</i> | HeLa | Chip-Seq | | | | | | |
| | <i>SCPEP1</i> | HeLa | Chip-Seq | | | | | | |
| <i>SGSH</i> | HeLa | Chip-Seq | | | | | | | |
| <i>TPP1</i> | HeLa | Chip-Seq | | | | | | | |

| Lysosomal Membrane | TFEB | | | TFE3 | | | MITF | | |
|--------------------|----------------|------|----------|---------------|---------|------|---------------|-----|------|
| | <i>TMEM55B</i> | HeLa | Chip-Seq | <i>CLCN7</i> | ARPE-19 | qPCR | <i>CLCN7</i> | C32 | qPCR |
| | <i>LAMP1</i> | HeLa | Chip-Seq | <i>CLCN3</i> | ARPE-19 | qPCR | <i>MCOLN1</i> | C32 | qPCR |
| | <i>SLC36A1</i> | HeLa | Chip-Seq | <i>LAMP1</i> | ARPE-19 | qPCR | | | |
| | <i>MCOLN1</i> | HeLa | Chip-Seq | <i>CD63</i> | ARPE-19 | qPCR | | | |
| | <i>CTNS</i> | HeLa | Chip-Seq | <i>MCOLN1</i> | ARPE-19 | qPCR | | | |
| | <i>CLCN3</i> | HeLa | Chip-Seq | | | | | | |
| | <i>CLCN7</i> | HeLa | Chip-Seq | | | | | | |
| | <i>CD63</i> | HeLa | Chip-Seq | | | | | | |
| | <i>C1orf85</i> | HeLa | Chip-Seq | | | | | | |

| Lysosomal Acidification | TFEB | | | TFE3 | | | MITF | | |
|-------------------------|-----------------|----------|----------|-----------------|-------|---------|----------------|------|------|
| | <i>ATP6V1H</i> | HeLa | Chip-Seq | <i>ATPV1C1</i> | 8988T | RNA-Seq | <i>ATP6V1H</i> | 8902 | ChIP |
| | <i>ATP6V1G1</i> | HeLa | Chip-Seq | <i>ATPV1D</i> | 8988T | RNA-Seq | | | |
| | <i>ATP6V1E1</i> | HeLa | Chip-Seq | <i>ATP6V1D</i> | 8988T | RNA-Seq | | | |
| | <i>ATP6V1D</i> | HeLa | Chip-Seq | <i>ATP6V1E1</i> | 8988T | RNA-Seq | | | |
| | <i>ATP6V1C1</i> | HeLa | Chip-Seq | <i>ATP6V1G1</i> | 8988T | RNA-Seq | | | |
| | <i>ATP6V1B2</i> | HeLa | Chip-Seq | <i>ATP6V1H</i> | 8988T | RNA-Seq | | | |
| | <i>ATP6V1A</i> | HeLa | Chip-Seq | | | | | | |
| | <i>ATP6V0E1</i> | HeLa | Chip-Seq | | | | | | |
| | <i>ATP6V0D2</i> | HeLa | Chip-Seq | | | | | | |
| | <i>ATP6V0D1</i> | HeLa | Chip-Seq | | | | | | |
| | <i>ATP6V0C</i> | HeLa | Chip-Seq | | | | | | |
| | <i>ATP6V0B</i> | HeLa | Chip-Seq | | | | | | |
| | <i>ATP6V0A1</i> | HeLa | Chip-Seq | | | | | | |
| <i>ATP6AP1</i> | HeLa | Chip-Seq | | | | | | | |

| | TFEB | | | TFE3 | | | MITF | | |
|----------------|-----------|--------------|----------|------------------|---------------|---------|---------------|----------------|---------|
| | Autophagy | <i>WDR45</i> | HeLa | Chip-Seq | <i>SQSTM1</i> | Panc1 | ChIP | <i>ATG16L1</i> | ARPE-19 |
| <i>VPS35</i> | | HeLa | Chip-Seq | <i>ATG9B</i> | Panc1 | ChIP | <i>ATG3</i> | ARPE-19 | qPCR |
| <i>VPS33A</i> | | HeLa | Chip-Seq | <i>ULK2</i> | 8988T | RNA-Seq | <i>ATG9B</i> | ARPE-19 | qPCR |
| <i>VPS26A</i> | | HeLa | Chip-Seq | <i>LC3A</i> | ARPE-19 | qPCR | <i>BCL2</i> | ARPE-19 | qPCR |
| <i>VPS18</i> | | HeLa | Chip-Seq | <i>ATG10</i> | ARPE-19 | qPCR | <i>UVRAG</i> | ARPE-19 | qPCR |
| <i>VPS11</i> | | HeLa | Chip-Seq | <i>ATG16L1</i> | ARPE-19 | qPCR | <i>WIPI1</i> | ARPE-19 | qPCR |
| <i>VPS8</i> | | HeLa | Chip-Seq | <i>ATG9B</i> | ARPE-19 | qPCR | <i>ATG4A</i> | ARPE-19 | qPCR |
| <i>UVRAG</i> | | HeLa | Chip-Seq | <i>UVRAG</i> | ARPE-19 | qPCR | <i>SQSTM1</i> | 8902 | ChIP |
| <i>STK4</i> | | HeLa | Chip-Seq | <i>GABARAPL1</i> | ARPE-19 | qPCR | <i>LC3A</i> | PL18 | qPCR |
| <i>SQSTM1</i> | | HeLa | Chip-Seq | <i>WIPI</i> | ARPE-19 | qPCR | <i>ATG10</i> | PL18 | qPCR |
| <i>RRAGC</i> | | HeLa | Chip-Seq | | | | | | |
| <i>RAB7A</i> | | HeLa | Chip-Seq | | | | | | |
| <i>PRKAG2</i> | | HeLa | Chip-Seq | | | | | | |
| <i>NRBF2</i> | | HeLa | Chip-Seq | | | | | | |
| <i>HIF1A</i> | | HeLa | Chip-Seq | | | | | | |
| <i>GABARAP</i> | | HeLa | Chip-Seq | | | | | | |
| <i>BECN1</i> | | HeLa | Chip-Seq | | | | | | |
| <i>LC3A</i> | | 8902 | qPCR | | | | | | |
| <i>CTSD</i> | | 8902 | qPCR | | | | | | |
| <i>ATG10</i> | | 8902 | qPCR | | | | | | |
| <i>ATG3</i> | | 8902 | qPCR | | | | | | |
| <i>ATP6V1H</i> | | 8902 | qPCR | | | | | | |
| <i>SQSTM1</i> | | 8902 | qPCR | | | | | | |
| <i>WIPI</i> | | HeLa | qPCR | | | | | | |
| <i>LC3B</i> | | HeLa | qPCR | | | | | | |
| <i>ATG9B</i> | | HeLa | qPCR | | | | | | |
| <i>ATG16L1</i> | | ARPE-19 | qPCR | | | | | | |
| <i>SNCA</i> | | ARPE-19 | qPCR | | | | | | |

1.4 Epigenetic Regulation of Autophagy: microRNAs

microRNAs (miRNAs) are best characterized members of the small RNA world which also includes small interfering RNAs (siRNAs) and PIWI-interacting RNAs (piRNAs). miRNAs mainly act on post-transcriptional regulation of genes by affecting messenger RNA (mRNA) stability and/or by blocking protein translation.

Being endogenous regulators of gene expression, several miRNAs were recently shown to play a role in the regulation of cellular pathways. Indeed, independent studies demonstrated that, core autophagy-related genes (*ATG* genes) and upstream mediators were targeted by microRNAs, revealing the presence of a novel and intricate miRNA network that is tightly regulating autophagy under physiological conditions. Moreover, dysregulation of miRNA expression was reported under various pathological conditions, including cancer, neurodegenerative diseases, cardiac and metabolic disorders. Most autophagy-related miRNAs were shown to be up or down-regulated in response to autophagy-inducing stress signals. In order to achieve a dynamic and context-dependent regulation, stress responsiveness may be an important property of autophagy modulation by miRNAs.

In this chapter, I will describe post-transcriptional control of autophagy through microRNAs and give details about microRNA biogenesis as well as autophagy-regulating microRNAs and their implications in cancer, and finally will focus on *MIR211*.

1.4.1 microRNAs

miRNAs are evolutionary conserved family of single stranded non-coding RNA molecules of 17-25 nucleotides in length. They regulate biological events through post-transcriptional gene silencing (Bartel, 2004). These endogenous regulators of gene expression are coded by the genome of various organisms ranging from *C. elegans* to mammals (John Kim et al., 2004). The first microRNA, *lin-4*, is discovered in *Caenorhabditis elegans* by the Ambros and Ruvkun groups in 1993 (R. C. Lee, Feinbaum, & Ambros, 1993; Wightman, Ha, & Ruvkun, 1993). The miRNA repository miRBase database (v22), updated in 2018, currently contains 1917

annotated precursor miRNAs (pre-miRNAs), and 2654 mature miRNA sequences for human genome (Kozomara, Birgaoanu, & Griffiths-Jones, 2019). Computational predictions revealed that more than 60% of human protein-coding genes contain conserved miRNA-binding site. Considering that various non-conserved miRNA binding sites also exist, most protein-coding genes may be under the control of miRNAs (Friedman, Farh, Burge, & Bartel, 2009).

In the genome, miRNAs are encoded as individual genes (monocistronic), as gene clusters (polycistronic) or in introns of host genes (intronic) (MacFarlane & R. Murphy, 2010). MiRNAs residing in the same cluster might share same transcriptional regulatory units. Hence, miRNAs may be expressed as polycistronic transcripts, allowing a coordinated expression pattern for functionally-related miRNAs (Mathelier & Carbone, 2013). Cellular levels of intronic miRNAs usually depend on the expression of the host protein-coding gene. Isolated miRNA genes exist as well; these genes possess their own promoters and can be expressed independently (Monteys et al., 2010; Oszolak et al., 2008).

1.4.2 microRNA Biogenesis

miRNAs are generally transcribed in an RNA polymerase II (Pol II)-dependent manner as capped and polyadenylated primary miRNAs (pri-miRNAs) which are 60-70 nucleotides length RNA transcripts (Y. Lee et al., 2003). However, transcription of some miRNA types may depend on RNA polymerase III (Pol III) (Borchert, Lanier, & Davidson, 2006). Following transcription, protein complexes showing ribonuclease III activity lead to the processing of pri-miRNAs into small hairpin-shaped pre-miRNAs in the nucleus (Denli, Tops, Plasterk, Ketting, & Hannon, 2004). The core ribonuclease complex (The microprocessor complex) consists of a heterotetramer of Drosha and DGCR8 (DiGeorge syndrome critical region gene 8 or Pasha) proteins (Han et al., 2004; Y. Lee et al., 2003). Pre-miRNAs are then exported to the cytoplasm by an exportin 5(XPO5)/RanGTP complex (Okada et al., 2009). Following transport to the cytoplasm, DICER protein further cleaves the hairpin, leading to the formation of a double-stranded 21–22-nt-long mature miRNA/miRNA* duplex (Koscianska, Starega-Roslan, & Krzyzosiak, 2011). Then, one of the mature miRNA strands is loaded onto RNA Induced Silencing Complex (RISC) containing an Argonaute protein (AGO), that guides the mature miRNA strand to its target messenger RNAs (mRNAs). Both 5p and 3p strands derived from the mature miRNA duplex can be loaded into the AGO proteins (AGO 1-4 in human) in an

ATP-dependent manner (Yoda et al., 2010). Thermodynamic stability at the 5' ends of the miRNA duplex determines the fate of 5p or 3p strand to be loaded (Khvorova, Reynolds, & Jayasena, 2003). Loaded strand is named as the guide strand whereas the unloaded one is called the passenger strand. Passenger strand is generally removed and degraded by cellular machinery.

Matching between a functionally important region of the miRNA, namely “the seed sequence” consisting of around 6–8 nucleotides, and complementary “miRNA response elements” (MRE) on the target mRNA sequences (mainly in the 3' UTR regions) determines the target specificity of the miRNA. Depending on the complementarity, the end result is a translational repression (partial complementarity) and/or mRNA cleavage (near perfect complementarity) (MacFarlane & R. Murphy, 2010). In near perfect complementarity, base-pairing with the guide miRNA result in an endonuclease-dependent cleavage of the target mRNA. MiRNA-directed deadenylation of the target mRNA may precede the degradation process. If the complementarity between the seed sequence and MRE on the target mRNA is partial, which is in the most cases, miRNAs inhibit translation of target mRNAs into proteins at translation initiation and elongation steps (Huntzinger & Izaurralde, 2011). Both mechanisms result in the downregulation of target protein levels and affect cellular functions that they control (Figure 1.4.1 1).

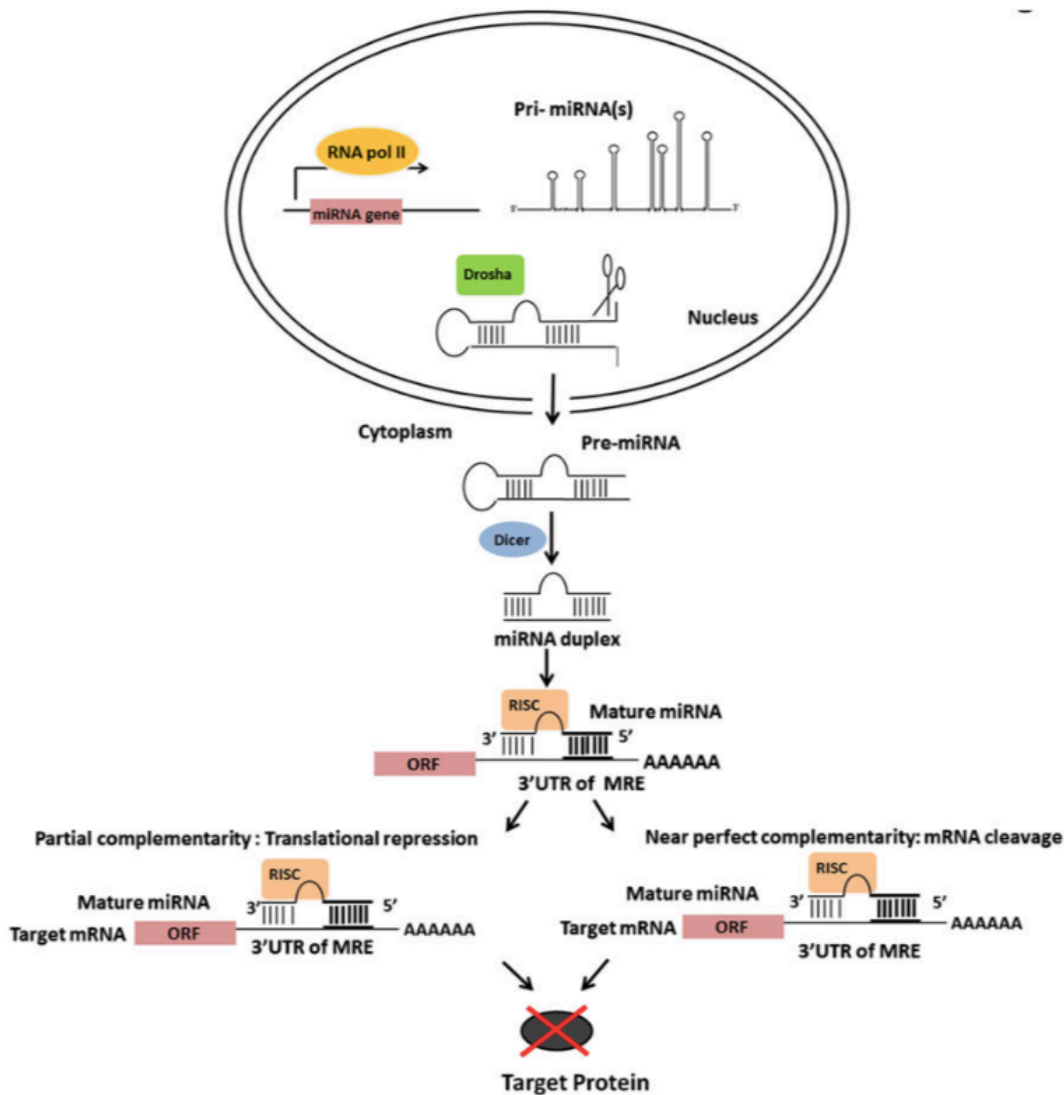


Figure 1.4.1: microRNA biogenesis and mechanism of action. The long primary miRNA transcript (pri-miRNA) are transcribed from miRNA genes in an RNA polymerase II (Pol II)-dependent manner and form a local hairpin structure called pri-miRNA. Following transcription, evolutionarily conserved mechanisms of human miRNA biogenesis give rise to mature miRNAs following nuclear and subsequent cytoplasmic cleavage events: Following transcription, the nuclear RNase III Drosha cleaves and forms pre-miRNAs with a ~60–100 nt hairpin structures. Pre-miRNAs are then transported into the cytoplasm through exportin-5-dependent nuclear export. In the cytoplasm, pre-miRNAs are subject to a second processing event that is catalyzed by Dicer enzymes. Double-stranded ~22 ntRNAs are then produced. They consist of a mature miRNA guide strand and a miRNA* passenger strand. The mature miRNA guide strand is chosen by the RNA-induced silencing complex (RISC). MiRNAs guide the RISC to mRNA targets and eventually lead to gene silencing through their degradation or translation inhibition. (Retrieved from (Tekirdag et al., 2013)).

1.4.3 Autophagy-regulating microRNAs

Studies over the last decade introduced miRNAs as new players in the regulation of autophagy. mRNA of proteins playing a role in various steps of autophagy, from proteins functioning in the upstream stimulatory or inhibitory pathways to the final stages of autophagic degradation, were reported to be miRNA targets (Frankel & Lund, 2012). microRNA studies so far reveal that we are only beginning to understand stress-related miRNA networks controlling cellular responses, including autophagy. Several autophagy-related miRNAs were also shown to affect other biological responses, such as apoptosis, growth or proliferation. Moreover, while only one autophagy-related target was reported for some miRNAs, others affected intracellular levels of proteins playing key roles in more than one stage of the autophagy pathway.

The first study about microRNA regulation of autophagy was published in 2009 (Zhu et al., 2009). Zhu *et al.* first revealed a role for *MIR30A* in the regulation of rapamycin-induced autophagy. They showed that the miRNA targeted BECN1 and inhibited autophagy in MCF-7 cells. Since then, huge amount of data has been published about microRNAs and autophagy.

Previous studies in our lab unravel that microRNAs have direct implications in autophagy through regulating core known components of autophagic machinery. The members of the *MIR376* family, *MIR376A* and *MIR376B*, were shown to regulate autophagy through their effect on BECN1 and ATG4C in breast and liver cancer cells (Korkmaz et al., 2013; Korkmaz, Le Sage, Tekirdag, Agami, & Gozuacik, 2012). *MIR376A* and *B* directly targeted the 3'UTR sequences of BECN1 (has a role in autophagosome initiation and formation) and ATG4C (has a role in autophagosome elongation) and regulate starvation and mTOR inhibition-related autophagy (Tekirdag, Akkoc, Kosar, & Gozuacik, 2016). Moreover, we have showed that ubiquitin-like conjugation system components functioning in autophagosome elongation step were also shown to be miRNA targets. *MIR181A* was shown to regulate cellular levels of the Atg5 protein. mTOR-dependent autophagy was blocked by the overexpression of *MIR181A* in different cell lines, including breast cancer, hepatocellular carcinoma and leukemia cells. *MIR181A* was directly targeting the ATG5 3'UTR (Tekirdag, Korkmaz, Ozturk, Agami, & Gozuacik, 2013).

It is highly critical to understand the physiological role of the miRNA-autophagy interconnection in stress response, adaptation and in the development of human diseases such as cancer, neurodegenerative diseases, cardiac diseases and metabolic disorders.

1.4.4 Autophagy-regulating microRNAs and cancer

Among autophagy-related microRNAs, many of them were involved in different stages of cancer formation and progression (Devrim Gozuacik, Akkoc, Ozturk, & Kocak, 2017). These miRNAs were shown to influence cancer growth, cancer cell metabolism, hypoxia responses and neovascularization, cancer cell migration and metastasis, and even response to drugs and radiotherapy. Moreover, some autophagy-related microRNAs were tested as anticancer agents or cancer biomarkers. In many studies, it was suggested that the effects miRNAs on autophagy genes and proteins were critical for cancer-related outcomes. Moreover, targeting of miRNAs or miRNA-related components by autophagic degradation systems were decisive in the control of cancer progression. Autophagy competence is important for the growth and survival of cancer cells. A number of miRNAs were shown to regulate autophagy and control tumor cell growth and proliferation. Several studies in the literature implicated autophagy-related miRNAs in the regulation of metabolism and metabolic stress responses of cancer cells. Furthermore, miRNAs can result in growth inhibition in different cancer cell types. Tumor cells face hypoxia as a result of abnormal vascularization and irregular blood supply. Under these circumstances, hypoxic tumor cells rely on autophagy for survival. A number of microRNAs were reported to control hypoxia-induced responses in cancer cells, including those that regulated autophagy in this context. Additionally, many microRNAs were reported to affect cell motility, invasion and metastatic spread of cancer cells. Some of the miRNAs that regulate autophagy also had an influence on cancer cell migration and metastasis.

In the following table, I summarize the existing literature that mainly implicates autophagy-related roles of these microRNAs in cancer biology and clinical outcomes (Table 1.4.4 1) (Devrim Gozuacik et al., 2017).

1.4.5 *MIR211*

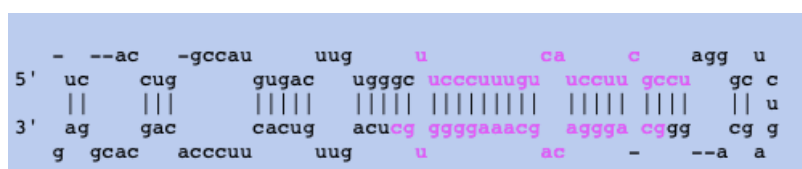
Following an unbiased screen that was performed using a microRNA library provided by Reuven Agami from Netherlands Cancer Institute (NKI), several microRNAs were revealed as a potential candidate to regulate stress-induced autophagy in Gozuacik laboratory. Under either fed or starved condition, miRNAs that induce autophagy in fed state or inhibit starvation induced autophagy were searched in that screen and *MIR211* was identified as an autophagy-inducer miRNA under fed conditions.

The microRNA *MIR211* is embedded in intron 6 of *TRPM1* gene, melastanin, at locus 15q13-q14 (Mazar et al., 2010). Melastanin is a member of the transient receptor potential (TRPM) cation channel family and a target gene of MITF (microphthalmia associated transcription factor) (Miller et al., 2004; Zhiqi et al., 2004). *TRPM1* has been shown to greatly downregulated in invasive melanomas compared to benign and dysplastic nevi and melanocytes. Its expression is inversely correlated with melanoma progression.

Stem-loop sequence, structure and mature sequences for *MIR211* is given in Figure 1.4.5

1.

MIR211 stem-loop sequence



Mature Strand *MIR211* (hsa-miR-211-5p)

26 - uccuuugucauccuucgcu - 47

Mature Strand *MIR211* (hsa-miR-211-3p)

63 - gcagggacagcaaggggugc - 83

Figure 1.4.5 1: Stem-loop sequence of MIR211 and mature sequences. Sequences of MIR211 were taken from MIRBASE <http://www.mirbase.org/>. Accession number: MI0000287.

Several studies point out the functions and the effect of loss-of-function for *MIR211* in normal and cancer cells and tissues. Both oncogenic and tumor-suppressive functions and dysregulated expression pattern in various cancer types have been shown for *MIR211*. In most melanoma cases, *MIR211* was down-regulated in melanoma cells and melanoblasts compared to melanocytes. Previous studies demonstrated that upregulation of *MIR211* in melanoma cells caused suppression of tumor invasion of cells by targeting *KCNMA1* (Levy et al., 2010), *IGF2R*, *TGFBR2*, *NFAT5* (Mazar et al., 2010), *BRN2* (Boyle et al., 2011) and *NUAK1* (Bell et al., 2014). Furthermore, dysregulation of *MIR211* expression has been also found in epithelial ovarian cancer. In EOC cells, *MIR211* inhibited proliferation and induced apoptosis by directly targeting *Cyclin D1* and *CDK6*, thereby reduced EOC tumorigenesis in vivo (Xia, Yang, Liu, & Lou, 2015). Moreover, in glioblastoma multiforme, *MIR211* induced glioma cell apoptosis by directly targeting of *MMP-9*, an important oncogene that enhances invasiveness (Asuthkar, Velpula, Chetty, Gorantla, & Rao, 2012). Their results revealed that either restoring *MIR211* or downregulating *MMP-9* could have therapeutic applications. Conversely, others reported that *MIR211* promoted cell proliferation, tumor growth and cell migration in vitro and in vivo by directly targeting *CHD5* mRNA in colorectal cancer (Cai et al., 2012), while upregulated *MIR211* enhanced invasion and migration of colorectal cancer cells by targeting *FABP4*, a fatty acid binding protein (Zhao, Ma, Li, & Lu, 2019). Moreover, enforced *MIR211* expression increased migration, proliferation and anchorage-independent colony formation of oral carcinoma cells (Chang et al., 2008). Furthermore, functional screening assay using a library of miRNA inhibitors showed *MIR211* inhibition decreased cell growth in HeLa cells (Cheng, Byrom, Shelton, & Ford, 2005). Also, ectopically induced *MIR211* was shown to stimulate

cellular proliferation and its down-regulation decreased colony number and size of MCF-10A, MCF-7 and MDA-MB-231 breast cancer cells (H. Lee, Lee, Bae, Kang, & Kim, 2016). Interestingly, Chitnis et al. proposed a model in which *MIR211* is a pro-survival miRNA that is expressed in PERK (aka EIF2AK3, Eukaryotic translation initiation factor 2-alpha kinase)-ATF4-dependent manner and decreases ER-stress-dependent expression of the proapoptotic transcription factor chop/gadd153 in mouse embryonic fibroblasts (Chitnis et al., 2012). *MIR211* prevented temporal accumulation of chop and thereby function as a key regulator of PERK-dependent pro-survival signaling.

1.5 Role of autophagy in cancer development and progression

Studies in the literature draw a complex picture about the involvement of autophagy in cancer formation and progression. The role of autophagy seems to be context- and tumor type-dependent such that early versus late stage disease or slow versus fast growing tumors show of different degrees of autophagy dependence. Autophagy exerts inhibitory effect on cancer by limiting cell proliferation and genomic instability before the onset of tumorigenesis. Yet, in well-established tumors autophagy plays a protective role in cancer cells to satisfy the metabolic needs of proliferating tumorigenic cells (Figure 1.5 1).

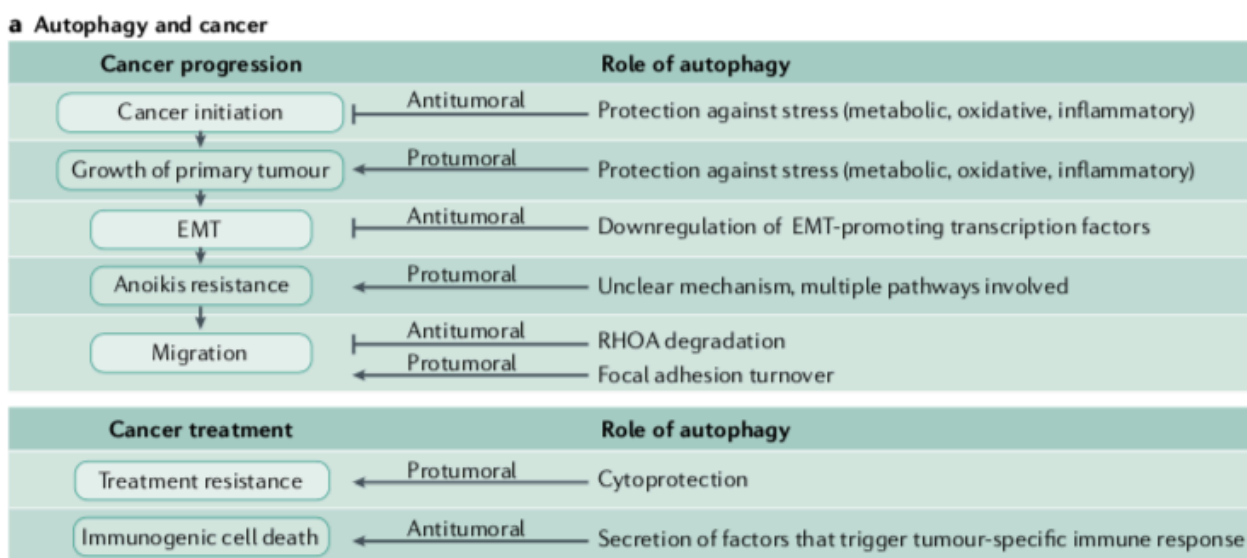


Figure 1.5 1: Autophagy impacts several aspects of cancer progression (Retrieved from (Dikic & Elazar, 2018)).

1.5.1 Autophagy as a tumor suppressor

Studies focusing on early stages of cancer formation indicate a tumor-suppressor role of autophagy during malignant transformation. For example, haploinsufficiency of *ATG6/BECN1* in genetically modified mice resulted in the formation of tumors in several tissues, including lung adenocarcinomas, hepatocellular carcinomas (HCCs), and lymphomas (Qu et al., 2003;

Yue, Jin, Yang, Levine, & Heintz, 2003). Similarly, *ATG5* and *ATG7* deletions in the liver resulted in the formation of liver adenomas (Takamura et al., 2011). *Atg4C*-deficient mice were prone to develop fibrosarcomas that were induced by chemical carcinogens (Mariño et al., 2007). In line with these results, *UVRAG* expression suppressed and *Bif1* deletion enhanced tumor formation in mice (Liang et al., 2006; Takahashi et al., 2007). Analysis of a series of human tumors confirmed these experimental results. Monoallelic deletions and lower *BECN1* protein levels were found in human prostate, breast, and ovarian cancers tissues that were analyzed (Qu et al., 2003; Yue et al., 2003). Similarly, *ATG5* expression was lost in human gastric, colorectal, and hepatocellular carcinoma specimen and monoallelic mutations of *UVRAG* were reported to be frequent in human colon cancers (Ionov, Nowak, Perucho, Markowitz, & Cowell, 2004).

Mechanisms of cancer suppression by autophagy were studied as well. Autophagy is responsible for the degradation of abnormally folded and/or mutant proteins and damaged organelles (e.g mitochondria) that in fact constitute a major source of reactive oxygen species (ROS). Consequently, elimination of these sources of ROS induction by autophagy was shown to alleviate DNA damage accumulation and prevent genomic instability (Mathew et al., 2009). Targeted elimination of some cancer-related proteins by autophagy was also reported. Autophagy-dependent selective elimination of oncogenic p62, PML-RARA, mutant p53 and BCR-ABL1 proteins may be cited as prominent examples (Choudhury, Kolukula, Preet, Albanese, & Avantaggiati, 2013; Duran et al., 2008; Goussetis et al., 2012). Autophagic degradation of hypoxia-inducible and proangiogenic HIF2 α protein in a constitutive manner was also reported to suppresses kidney tumorigenesis (Liu et al., 2015).

Moreover, while autophagy mainly acts as a pro-survival mechanism and a stress response, autophagy activation under certain conditions was connected to cell death (Berry & Baehrecke, 2007; Devrim Gozuacik & Kimchi, 2004; Levine & Yuan, 2005). Hence at least in some contexts, autophagic cell death might also contribute to the tumor-suppressive function. In line with this view, blockage of autophagy in some contexts prevented death of cancer cells (e.g. (Elgendy, Sheridan, Brumatti, & Martin, 2011; Lamy et al., 2013). Furthermore, several tumor suppressor and death-related proteins, including DAPK, DRP1, ZIPK, and a p19ARF form triggered a non-apoptotic and autophagy dependent cell death in cancer cells (D. Gozuacik et al., 2008; Inbal, Bialik, Sabanay, Shani, & Kimchi, 2002). Oncogene-induced senescence

that eventually lead to cell death was also shown to depend on autophagy (Andrew R.J. Young et al., 2009).

Anticancer immunosurveillance that involves recognition and elimination of nascent cancerous cells by the immune system may be dually regulated by autophagy in different cell types (e.g. development and maturation of immune system components versus hijacking of the immune system by tumor autophagy) (Y. Ma, Chen, Xu, & Lin, 2013; Viry et al., 2014). Additionally, autophagy was shown to limit inflammation that, in especially a chronic form, is a major trigger for some types of cancer like HCC. Elimination of inflammasomes and limitation of pro-inflammatory interleukins (Nakahira et al., 2011; Zitvogel, Kepp, Galluzzi, & Kroemer, 2012), and NF- κ B signaling (Paul et al., 2012) as well as inhibition of pro-inflammatory signals controlled by pattern recognition receptors (Jounai et al., 2007; Saitoh et al., 2009) and prevention of metabolic stress and inflammatory cell infiltration to tissues (Degenhardt et al., 2006) depended on intact autophagy function.

1.5.2 Autophagy as a tumor promoter

In established and especially fast-growing tumors, survival-related role of autophagy predominates. Cancer cells face with unfavorable conditions that challenge their endurance to stress. Abnormal and insufficient tumor vascularization leads to hypoxia, changes in local pH, scarce nutrient, growth factor and hormone supply, while energy and oxygen demands increase due to fast proliferation. Therefore, the tumor environment imposes high levels of metabolic stress upon malignant cells. Autophagy supports tumor cell survival and growth under these harsh conditions. For example, in oncogenic RAS- or RAF-driven fast-growing tumors, autophagy allowed tumor cell proliferation and survival, and mitochondrial quality control and maintenance of energy and building block levels by autophagy were crucial to support metabolic activities of cancer cells (Strohecker et al., 2013). Elevation of basal autophagy levels was especially indispensable for the survival of tumor cells that were found in the interior parts of solid tumors (Degenhardt et al., 2006).

Cells from invasive and metastatic tumors face with conditions that are related to detachment from neighboring cells in the tissue and from the basal lamina, evasion from the primary sites, shear forces in the blood stream, invasion and spread (Levine et al., 2007). Under

these conditions, autophagy provided resistance to metabolic stress and anoikis (detachment-induced cell death) allowing cancer cell survival (Fung, Lock, Gao, Salas, & Debnath, 2007). Autophagic capacity of tumor cells was reported as a determining factor during epithelial-mesenchymal transition (EMT), metastasis and dormancy of tumor cells in some contexts (Gewirtz, 2009; Gugnoni, Sancisi, Manzotti, Gandolfi, & Ciarrocchi, 2016). Yet in hepatocellular carcinoma cells, EMT and migration properties was not affected but anoikis resistance and distant metastasis capacity was reduced when autophagy was suppressed (Peng et al., 2013). In another study, knockdown of ATG5 in melanoma cells decreased their capacity to survive metabolic stress and to colonize lungs in mice following intravenous injection (Maes et al., 2014). Similarly, depletion of ATG12 decreased the invasive capacity of glioma cells (Macintosh et al., 2012). But, motility, invasion and metastatic capacity of oncogenic RAS-transformed tumor cells depended on their autophagy competence and autophagy-dependent production of secreted factors (Lock, Kenific, Leidal, Salas, & Debnath, 2014). Establishment of the dormancy state and survival of dormant cancer cells seem to depend on autophagy competence. For example, induction of autophagy by ARHI/DIRAS3 was essential for dormancy of ovarian cancer cell micro metastases in xenograft models (Z. Lu et al., 2008).

Autophagy plays a critical role in endothelial cell biology as well as tumor vascularization. Although endothelial deletion of the key autophagy gene *Atg7* in mice did not result in any prominent vascular abnormality or vascular density change, but there were abnormalities in endothelial cell function such as defect in the maturation and secretion of von Willebrand factor (Torisu et al., 2013). In the context of cancer, selective degradation of angiogenesis regulators such as gastrin-releasing peptide or HIF2 α by autophagy affected tumor vasculature and limited tumor growth (K. W. Kim, Paul, Qiao, Lee, & Chung, 2013; Liu et al., 2015). In line with these observations, BECN1/Beclin1 heterozygous mice had higher levels of circulating erythropoietin and HIF2 α that led to an increase in angiogenesis under hypoxia and enhance in tumor growth compared to wild-type mice (S. J. Lee, Kim, Jin, Choi, & Ryter, 2011). ATG5 knockdown in B16-F10 melanoma cells increased tumor vessel tortuosity; on the other hand, endothelial cell-specific deletion of ATG5 led to formation of smaller and less mature tumor vasculature with endothelial cell lining and perfusion defects (Maes et al., 2014). Therefore, autophagic activity is important for angiogenesis under physiological conditions and affects tumor neovascularization.

1.5.3 Autophagy and cancer treatment

An important response of cancer cells to treatment with anticancer agents and radiation is autophagy activation. In most cases, autophagy confers resistance to anticancer therapy, yet in some tumor types activation of autophagy was reported to have lethal effects on cancer cells. In any case, strategies aiming at the modulation of autophagy have the potential to improve responses to classical anticancer approaches. Choice of the best strategy seems to depend on tumor type, stage and specific treatment. Additionally, autophagy manipulation renders otherwise resistant cancer types to therapeutic agents and might be used to overcome drug resistance (Zhou et al., 2012).

Sensitization to chemotherapy is of the most studied topics in the autophagy field. In the scientific literature, beneficial effects of the combination of autophagy modulators on chemotherapy or radiotherapy was extensively studied. In many cancer types, usage of the PI3K inhibitors (e.g. 3-MA or LY294002) in experimental systems enhanced the efficacy of various chemotherapeutic agents and radiation therapy through their autophagy blocking effects. For example, treatment with 3-MA sensitized esophageal squamous carcinoma cells to radiation therapy (Chen et al., 2011). Similarly, administration of 3-MA enhanced the efficacy of 5-Fluorouracil and cisplatin and promoted apoptosis in colon and lung cancer cells (J. Li et al., 2009). On the other hand, lysosomotropic agents (e.g. Chloroquine (CQ) or hydroxychloroquine (HQ)) that neutralize the pH of lysosomes and prevent autolysosome formation were shown in numerous publications to exert anticancer effects and/or enhance the efficacy of antineoplastic treatments (Selvakumaran, Amaravadi, Vasilevskaya, & O'Dwyer, 2013; Sotelo, Briceño, & López-González, 2006). For instance, in non-small-cell lung cancer bevacizumab plus CQ combination was found to increase the efficacy of cancer treatment (Selvakumaran et al., 2013). Concomitantly, CQ and HCQ potentiated cytotoxic effects of p53 and alkylating agents in a mouse model of lymphoma (Amaravadi et al., 2007). siRNA-based depletion of autophagy modulators was also able to sensitize carcinoma cells from different origins to chemotherapy and radiation treatment (Apel, Herr, Schwarz, Rodemann, & Mayer, 2008)

2. MATERIALS AND METHODS

2.1 Plasmid and constructs

The pMSCV-miR plasmids containing 443 different human miRNA minigene sequences mimicking pri-miRNAs including *MIR211* were constructed as described previously (Voorhoeve et al., 2007). The plasmid encoding the control human telomerase (hTR) genomic region (a nontranslated RNA coding for hTR RNA) was used as control for (*MIR-CNT*) (Voorhoeve et al., 2007). pEGFP-1-N1-MITF-A (38132) (Roczniak-Ferguson et al., 2012), pEGFP-N1-TFEB (38119) (Roczniak-Ferguson et al., 2012), pRK-5-MYC-RICTOR (11367) (Dos et al., 2004), pLKO.1-RICTOR shRNA (1853) (Sarbasov, Guertin, et al., 2005), and LAMP1-RFP (1817) (Sherer et al., 2003) were purchased from Addgene. GFP-LC3 and RFP tandemly tagged LC3 (tfLC3 or RFP-GFP-LC3) were also described (Kabeya, 2000; Kimura, Fujita, Noda, & Yoshimori, 2009).

For luciferase tests, 3' UTR segments containing MRE sequences of *RICTOR* and mutant versions were synthesized as sense and antisense linkers. The linker primers were: *RICTOR* primers 5' CTAGACCTGAAGCATAATCTTATCAAAGGGATGTAACT-3', 5'-CTAGAGTTAACATCCCTTTGATAAGATTATGCTTCAGGT-3'. Mutant *RICTOR* primers 5'-CTAGACCTCTACCAAAAATCTTATGTTACCCATGTAACT-3', 5'-CTAGAGTTAACATGGGTAACATAAGATTTTGGTAGAGGT-3'.

Double-stranded DNA linkers with added sticky *Xba*I sites were created by annealing complementary strands following incubation at 95°C and slow cooling at RT. Linkers were cloned into the luciferase reporter pGL3-control vector (Promega, E1741) in the 3' UTR region of the luciferase gene into *Xba*I sites between the stop codon and the polyadenylation signal.

2.2 Cell Culture

2.2.1 Cell Line Maintenance

HeLa cervix cancer cells, HEK293T human embryonic kidney cells and MCF-7 breast cancer cells were cultured in Dulbecco's modified Eagle's medium (DMEM; Biological Industries, BI01-050-1A) supplemented with 10% (v:v) fetal bovine serum (PAN, P30-3302), antibiotics

(penicillin/streptomycin; Biological Industries, BI03-031-1B) and L-glutamine (Biological Industries, BI03-020-1B) in a 5% CO₂ humidified incubator at 37°C. The melanoma cell line SK-MEL-28 and breast cancer cell line MDA-MB-231 were cultured in DMEM medium additionally supplemented with 1% non-essential amino acids (Gibco, 11140-035). SHSY-5Y neuroblastoma cells were cultured in fully supplemented DMEM low glucose (1000 mg/l) medium.

2.2.2 Transient and stable transfections

HeLa and HEK293T cells were transiently transfected using the calcium phosphate method according to standard protocols (Jordan, 1996). SK-MEL-28 and MCF-7 cells were transiently transfected using the polyethylenimine (PolySciences Inc., 23966) transfection method according to Foley et al (Foley et al., 2008). Stable RFP-GFP-LC3 HeLa monoclonal cells were created by 4 weeks of G418 (Roche, 04727894001) selection following transfection of cells with the construct.

2.2.3 Autophagy induction in cell culture

For induction of autophagy, cells were incubated in culture media containing torin1 (200 nM; Tocris, 4247) dissolved in DMSO (Sigma, VWRSA2650), or cells were starved in Earle's Balanced Salt solution (Biological Industries, BI02-010-1A) for 4 h. Autophagic flux experiments were performed in the presence or absence of lysosomal protease inhibitors E64D (10 µg/ml; Santa Cruz Biotechnology, SC201280A) and pepstatin A (10 µg/ml; Sigma, P5318) for 4 h.

2.3 Protein isolation and immunoblotting

Cells were lysed at the indicated time points in RIPA buffer (50 mM TRIS-HCl, pH 7.4, 150 mM NaCl [Applichem, A2942], 1% NP40 [Sigma, 74385], 0.25% Na-deoxycholate [Sigma, 30970]) supplemented with a complete protease inhibitor cocktail (Sigma, P8340) and 1 mM phenylmethylsulfonyl fluoride (Sigma, P7626). Protein extracts (30 µg per well for autophagy assays, and 80 µg per well for MTOR pathway assays) were separated using 6-15% SDS-polyacrylamide gels, and then transferred onto nitrocellulose membranes (Millipore,

IPVH00010). Membranes were blocked in 5% nonfat milk (Applichem, A0830) or in 3% BSA (Capricorn, BSA-1T) in PBS-T (3.2 mM Na₂HPO₄[Sigma, S5136], 0.5 mM KH₂PO₄[Sigma, 4243], 1.3 mM KCl [Sigma, P9333], 135 mM NaCl, 0.05% Tween 20[Sigma, P5927], pH 7.4) for 1 h, and then incubated with primary antibodies in a 3% BSA-PBS-T solution. Following PBS-T washes, membranes were incubated with horseradish peroxidase-coupled secondary anti-mouse (Jackson Immunoresearch Laboratories, 115035003) or anti-rabbit (Jackson Immunoresearch Laboratories, 111035144) antibodies. Anti-LC3B (Novus, 2331), anti-RICTOR (Cell Signaling Technology, 2114S), anti-phospho-MTOR (Ser2448; Cell Signaling Technology, 5536), anti-MTOR (Cell Signaling Technology, 2972), anti-RPS6KB/p70S6K (Cell Signaling Technology, 2708), anti-phospho-RPS6KB/p70S6K (Thr389; Cell Signaling Technology, 9205), anti-AKT (Cell Signaling Technology, 9272S), anti-phospho-AKT (Ser473;Cell Signaling Technology, 587F11), anti-MITF clone 5 (Millipore, MAB3747-I), anti-TFEB (Cell Signaling Technology, 4240), anti-GFP (Roche, 11814460001), anti-ACT/ β -ACTIN (Sigma, A5441) or anti-VIM/vimentin (Sigma, V6630) antibodies were used. ImageJ software was used to quantify protein band intensities (Abràmoff, Magalhães, & Ram, 2004).

2.4 Immunofluorescence tests

2.4.1 Immunofluorescence analyses

Cells were cultured on cover slides and fixed in an ice-cold 4% paraformaldehyde-PBS solution (pH 7.4). For indirect immunostaining experiments, following fixation, cells were permeabilized in PBS containing 0.1% BSA (Sigma, A4503) and 0.1% saponin (Sigma, 84510). As primary antibodies, anti-MITF clone 5, and anti-TFEB were used. Anti-mouse Alexa Fluor 594 (Invitrogen, A11005) and anti-rabbit Alexa Fluor 594 (Invitrogen, A11002) were used as secondary antibodies. When indicated, nuclei were stained using Hoechst dye in 1x PBS. Coverslides were mounted onto glass slides, and samples were analyzed using a BX60 fluorescence microscope (Olympus, BX60).

For experiments with fluorescent protein fusions, cells stably expressing RFP-GFP-LC3 or cells transiently transfected with a plasmid encoding GFP-LC3, RFP-LAMP1, or GFP-MITF-A, GFP-TFEB or GFP-WIP1 plasmids were used. After 48 h, cells were fixed in ice-

cold 4% paraformaldehyde-PBS. Coverslips were then mounted onto glass slides, and samples were analyzed using a BX60 fluorescence microscope (Olympus, BX60) or a Carl Zeiss LSM 710 confocal microscope (Zeiss, Germany).

2.4.2 Quantitative GFP-LC3, GFP-WIPI1, RFP-GFP-LC3, RFP-LAMP1 analyses

Dot counts were performed in RFP-GFP-LC3 stable HeLa cells or GFP-LC3-transfected SK-MEL-28 cells or GFP-WIPI1-transfected HeLa cells. Basal autophagy threshold was determined as 15 GFP-LC3 dots per RFP-GFP-LC3 stable HeLa cell, and 5 GFP-LC3 dots per SK-MEL-28 cell. At least 150 GFP-positive cells per condition were analyzed, and results were expressed as percentage of GFP-LC3 dot-positive cells (above the thresholds) versus total number of transfected cells. For GFP-WIPI1 tests, at least 40 GFP-positive cells per condition were analyzed and quantified by ImageJ analyses, and results were expressed as number of GFP-WIPI1 puncta per cell.

For RFP-GFP-LC3 tests, at least 30 RFP-GFP-positive HeLa cells for each experimental condition were analyzed under a fluorescence microscope (Olympus BX60, Japan) using a 60x magnification. Autophagosomes gave both RFP and GFP signals, while autolysosomes were defined as RFP-positive dots. The number of autolysosomes was calculated by subtracting GFP-positive dot numbers from RFP-positive dot numbers. For GFP-LC3 and RFP-LAMP1 colocalization tests, at least 20 cells for each experimental condition were analyzed under a Carl Zeiss LSM 710 confocal microscope (Zeiss, Germany).

2.5 Bioinformatics analyses

miRNA targets were identified using publicly available bioinformatics tools FindTar3 (<http://bio.sz.tsinghua.edu.cn>), TargetScan Human (www.targetscan.org/), miRanda (www.microrna.org), miRDB (<http://mirdb.org/>) and RNA22 (cm.jefferson.edu/rna22). Pearson correlation analysis of MITF and *MIR211* expression across NCI-60 cell lines was performed using bioinformatic tools available on the CellMiner website (<https://discover.nci.nih.gov/cellminer/analysis.do>). Detailed information on multiple platform analysis tools were previously published (Reinhold et al., 2012).

For TCGA analyses (<http://cancergenome.nih.gov/>), datasets of *MITF* and *MIR211* expression were downloaded using FireBrowse RESTful API (<http://firebrowse.org/api-docs/>). Datasets were selected according to the following criteria: (i) the number of samples that have missing values for *MIR211* expression less than 40% of all samples; and (ii) the number of samples with both *MITF* and *MIR211* expression larger than 100. Pearson correlation analyses were performed using datasets meeting the criteria above: Skin Cutaneous Melanoma, Glioma, Pan-kidney Cohort, Testicular Germ Cell Tumors, and Ovarian Serous Cystadenocarcinoma.

2.6 RNA isolation and RT-PCR analyses

Total RNA was extracted using TRIzol reagent (Sigma, T9424) according to the manufacturer's instructions. cDNA was reverse transcribed from DNase 1 (Thermo Fischer Scientific, EN0521)-treated total RNA using M-MuLV reverse transcriptase (Fermentas, EP0351) and random hexamers (Invitrogen, 48190-011). For real-time RT-PCR quantification of mRNA levels, the SYBR Green Quantitative RT-PCR kit (Roche, 04-913-914-001) and LightCycler 480 (Roche) were used. To activate the SYBR Green, an initial cycle of 95°C, 10 min was performed. PCR reactions were as follows: 95°C for 15 sec and 60°C for 1 min. (40 cycles). Then a thermal denaturation protocol was used to generate the dissociation curves for the verification of amplification specificity (a single cycle of 95°C for 60 sec, 55°C for 60 sec and 80 cycles of 55°C for 10 sec). Changes in mRNA levels were quantified using the $2^{-\Delta\Delta CT}$ method using *GAPDH* (glyceraldehyde-3-phosphate dehydrogenase) mRNA as control. Primers used were: *RICTOR* primers 5'-AGTGAATCTGTGCCATCGAGT -3', 5'-AGTAGAGCTGCTGCCAAACC -3'; Pan-*MITF* primers 5'-TTCACGAGCGTCCTGTATGCAGAT-3', 5'-TTGCAAAGCAGGATCCATCAAGCC-3'; *MITF-M* primers 5'-TCTACCGTCTCTCACTGGATTGG-3', 5'-GCTTTACCTGCTGCCGTTGG-3'; *MITF-A* primers 5'-GCAGTGGAAGGACGGGAAG-3', 5'-CAGGATGCTCGGCGGAAC-3'; *ATG10* primers 5'-GTCACATCTAGGAGCATCTACCC-3', 5'-CATCCAAGGGTAGCTCGAAA-3'; *LC3B* primers 5'-GAGAAGCAGCTTCCTGTTCTGG-3', 5'-GTGTCCGTTACCAACAGGAAG-3'; *GAPDH* primers 5'-AGCCACATCGCTCAGACAC-3', 5'-GCCCAATACGACCAAATCC-3'; *MIR155* stem-loop primer, 5'-GTCGTATCCAGTGCAGGGTCCGAGGTATTCGCACTGGATACGACACCCCTA-3',

MIR155 forward primer, 5'-GTTGGGTTAATGCTAATCGTGA-3'; *MIR15A* stem-loop primer, 5'-GTCGTATCCAGTGCAGGGTCCGAGGTATTTCGCACTGG ATACGACCACAAAC-3', *MIR15A* forward primer, 5'-GGGTAGCAGCACATAATG-3'; *MIR16* stem-loop primer, 5'-GTCGTATCCAGTGCAGGGTCCGAGGTATTTCGCACTGG ATACGACCACAAAC-3', *MIR16* forward primer, 5'-GTTTGGTAGCAGCACGTAAAT-3'; *MIR185* stem-loop primer, 5'-GTCGTATCCAGTGCAGGGTCCGAGGTATTTCGCACTGGATACGACTCAGGAA-3', *MIR185* forward primer, 5'-GTGTGGAGAGAAAGGCAG-3'; Universal reverse primer, 5'-GTGCAGGGTCCGAGGT-3'.

TaqMan RT-qPCR reactions were performed using FastStart Universal Probe Master kit (Roche, 04913957001) and LightCycler 480 according to previously described protocols (Korkmaz, 2013). Primers and the probe used during the study were: *MIR211* stem-loop primer, 5'-GTCGTATCCAGTGCAGGGTCCGAGGTATTTCGCACTGGATACGACAGGCGA-3'; *MIR211* forward primer, 5'-GGGTCCCTTTGTCATCCT-3'; Universal reverse primer, 5'-GTGCAGGGTCCGAGGT-3'; *MIR211* TaqMan Probe, 5'-(6-FAM)-CGCACTGGATACGACAGGCGAAG-(TAMRA-sp)-3'.

2.7 Dual luciferase reporter assay

Luciferase vectors containing wild-type or mutant *MIR211* MREs from the *RICTOR* 3' UTR were co-transfected with *MIR211* or *ANT211* and a Renilla luciferase construct into HeLa and SK-MEL-28 cells. HEK293T cells were co-transfected with *MIR211* and a Renilla luciferase construct. After 48 h, cells were lysed. Firefly and Renilla luciferase activities were measured using a dual luciferase-reporter assay system (Promega, E1910) and a luminometer (Thermo Fischer Scientific, Fluoroskan Ascent FL). Results were calculated following normalization of the firefly luciferase activity to the renilla luciferase activity.

2.8 Antagomir and siRNA tests

miRIDIAN microRNA Hairpin Inhibitors (antagomirs) against *MIR211* (hsa-*MIR211*, IH-300566-05-0005) and a control antagomir (miRIDIAN microRNA hairpin inhibitor negative control, IN001005-01-05) were purchased from Dharmacon. The control antagomir sequence

was based on *miR-67 C. elegans* microRNA which has minimal sequence similarity with known human miRNAs. Transfection of antagomirs (200 nM per point) was performed using either the polyethylenimine transfection or calcium phosphate protocols as previously explained [23]. Pan-*MITF* siRNA (siGenome SMARTPool Human MITFsiRNA, M-008674-00-0005) and control siRNA (D-001210-01-20) were purchased from Dharmacon, and 40 nM/well siRNA was transfected.

2.9 Chromatin immunoprecipitation (ChIP) and ChIP-qPCR

For ChIP, HeLa and SK-MEL-28 cells were cultured for 48 h and either incubated for 4 h with DMSO or torin1 (200 nM) and subsequently crosslinked in 1% formaldehyde (Sigma, F8775) at room temperature for 10 min. Fixation was stopped by adding 125 mM glycine (Applichem, A1067). Cells were then harvested and lysed in 2 ml of ChIP lysis buffer (50 mM HEPES [Sigma, 54457], 150 mM NaCl, 1% Triton X-100 [Applichem, A4975], 0.1% Na-deoxycholate, 1 mM EDTA [Calbiochem, 324503] containing 0.25% SDS [Applichem, A2572] and protease inhibitor cocktail [Sigma, P8340]). The lysates were subjected to sonication to shear DNA to the length of approximately 150-900 base pairs using a Q700 Sonicator (QSonica). An aliquot (20%) of the supernatant fraction from the chromatin was used as the “input sample”. For IP, MITF antibody (5 µg/sample; Millipore, MAB3747-I) was incubated with 50 µL of protein-G Dynabeads (Invitrogen, 10003D) overnight at 4°C and washed 3 times with ChIP lysis buffer containing protease inhibitor cocktail. A fraction (500 µg) of the resulting sheared chromatin samples were incubated with MITF antibody-coupled magnetic beads or with beads only (for background control) for 2 h at room temperature. Beads were washed 2x with ChIP lysis buffer, 2x with high salt wash buffer (ChIP lysis buffer containing 500 mM NaCl) and 2x with Tris-EDTA (10 mM Tris-Cl, 1 mM EDTA, pH 8). Immunocomplexes were eluted using 100 µL Tris-EDTA at 95°C for 10 min. After elution, crosslink was reversed by adding NaCl of 200 mM final concentration and incubated with proteinase K (Thermo Fisher Scientific, EO0491) overnight at 65°C. DNA fragments were purified by phenol-chloroform extraction, air-dried, and redissolved in H₂O. Quantitative real-time PCR was performed using a SYBR Green Quantitative RT-PCR kit (Roche, 04-913-914-001) and a LightCycler 480. Primers used were: *MIR211* promoter-specific primers, 5'-CATCGCTTCACAGCAATCATGAGG-3', 5'-ATCTGAGCTTACCTGCCACAGCA-3'; *LC3B* promoter-specific primers, 5'-CATGCC TTGGGACACCAGAT-3', 5'-ACCTTCTTCAAGTGCTGTTTGT-3'; *HSPA/HSP70*

promoter-specific primers, 5'-CCTCCAGTGAATCCCAGAAGACTCT-3', 5'-TGGGACAACGGGAGTCACTCTC-3'. The results are presented as percentage of input.

2.10 Human tissue samples

Human tissue sample collection and experiments were conducted in accordance with the guidelines set by the Turkish Republic Ministry of Health, and approved by the Ethics Committee of Dr. Sadi Konuk Research and Training Hospital and Sabanci University. Samples were drop frozen in liquid nitrogen shortly after admission of cadavers to the Council of Forensic Medicine. RNA isolation and protein analyses were performed from frozen tissue powders according to the protocols above.

2.11 Statistical analyses

Statistical analyses were performed using Student's two-tailed t-test. Data were represented as means of \pm SD of n independent experiments (biological replicates). Values of $p < 0.05$ were considered as significant.

3. RESULTS

Proposed novel autophagy-regulating axis during cellular stress: MITF/*MIR211*

In this PhD study, previously unidentified and novel pathway of autophagy amplification was investigated under basal and cellular stress-inducing conditions. Along with this thesis, rate-limiting function of MITF was verified in starvation and mTOR inhibition-mediated autophagy through knockdown studies. Furthermore, *MIR211*, previously reported direct transcriptional target of MITF, was discovered as a novel autophagy-regulating microRNA in melanoma and epithelial cells. Several independent autophagy assays confirmed that overexpression of *MIR211* potentiated both basal and MTOR-dependent autophagy, and its downregulation resulted in a decrease in the amplitude of autophagy. Functional analysis was carried out to understand the mechanism behind the regulatory role of *MIR211* on autophagy through identification and validation of its direct target, RICTOR. The effect of *MIR211* on mTORC1 pathway and nuclear translocation of MITF were also evaluated. *In silico* data showing co-expression of MITF and *MIR211* in various cancer types was also verified in the molecular data obtained *in vitro*.

Altogether, findings of this thesis suggest an intriguing and new molecular system amplifying autophagy involving MITF/*MIR211* axis. The proposed feed-forward amplification mechanism, that is MITF-specific and *MIR211*-dependent, is required for optimal autophagy activation under cellular stress conditions.

This novel mechanism could suggest an extra layer of importance for understanding the role of transcriptional control and epigenetics in autophagy regulation.

3.1 MITF is required for starvation and mTOR- dependent autophagy

Recent evidences suggest that MITF/TFE family of transcription factors play a critical role in organelle biogenesis and cellular homeostasis. Under nutrient-rich conditions, TFEB and MITF transcription factors are phosphorylated by mTORC1 and sequestered in the cytosol (Martina, 2014). Conversely, upon cellular stress such as starvation or lysosomal stress, mTORC1 dissociates from the lysosomal membrane and becomes inactivate. Then, non-phosphorylated TFEB and MITF translocate to the nucleus and activate several lysosome and autophagy-related target genes. In subsequent studies, TFEB was characterized as the master regulator of lysosomal biogenesis through transcriptionally regulating numerous lysosomal genes. (Sardiello, 2009; Napolitano, 2016). Along with TFEB and TFE3 that can also coordinate autophagosome formation, some studies indicate that MITF contributes to autophagy regulation (Martina, 2013; Perara, 2015; Bouche, 2016). Yet, detailed analyses are missing. Several independent autophagy tests were performed in order to evaluate whether MITF is indispensable for autophagy and that it has a specific function in autophagy regulation (Figure 3.1.1).

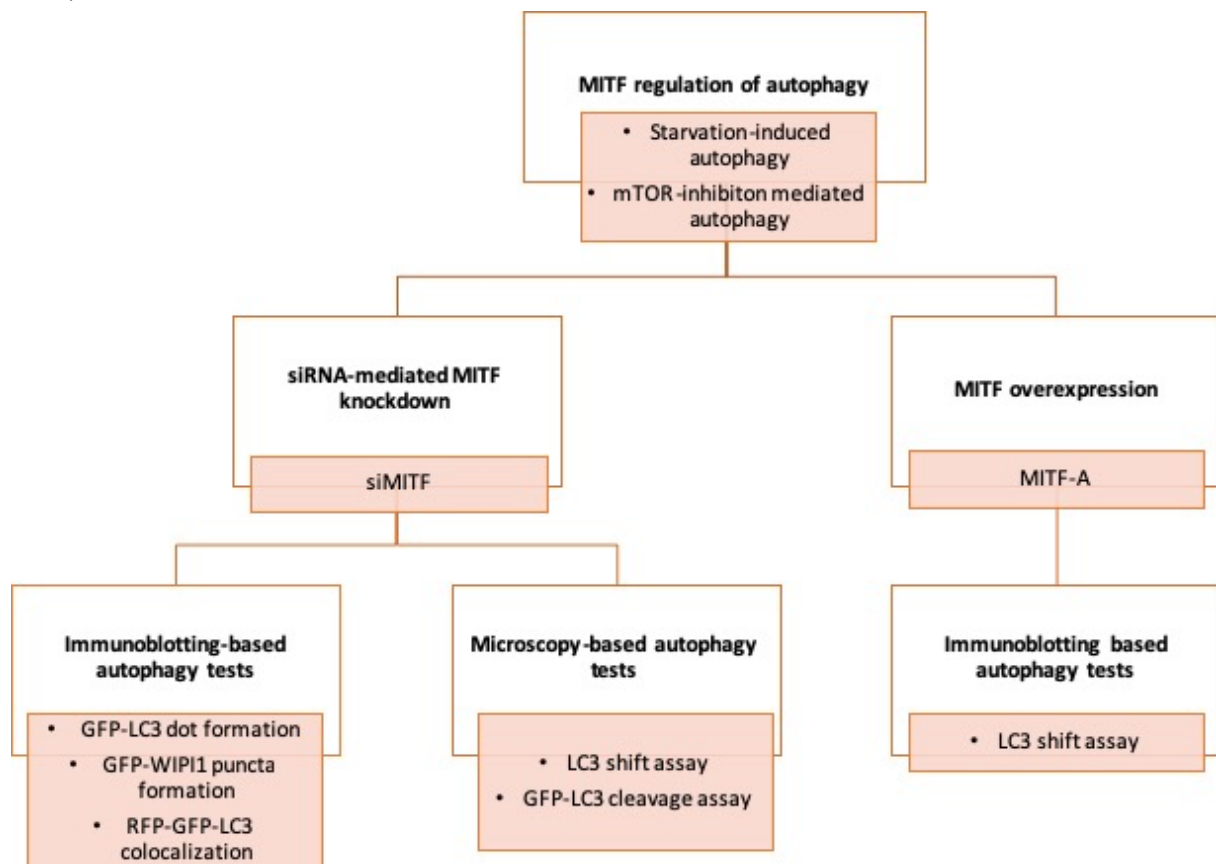


Figure 3.1.1: The pipeline of the experiments performed for MITF regulation of autophagy analysis.

3.1.1 Effect of MITF overexpression on autophagy

In order to confirm nuclear translocation of MITF in our experimental conditions, immunofluorescence analyses were performed. First, GFP-fused constructs of MITF-A were overexpressed in HeLa cells. MITF proteins were cytosolic, and they were excluded from the nucleus under fed conditions (Figure 3.1.1 1 and Figure 3.1.1 2). MITF translocated to nuclei of HeLa cells following mTOR inhibitor torin1 treatment (Figure 3.1.1 1).

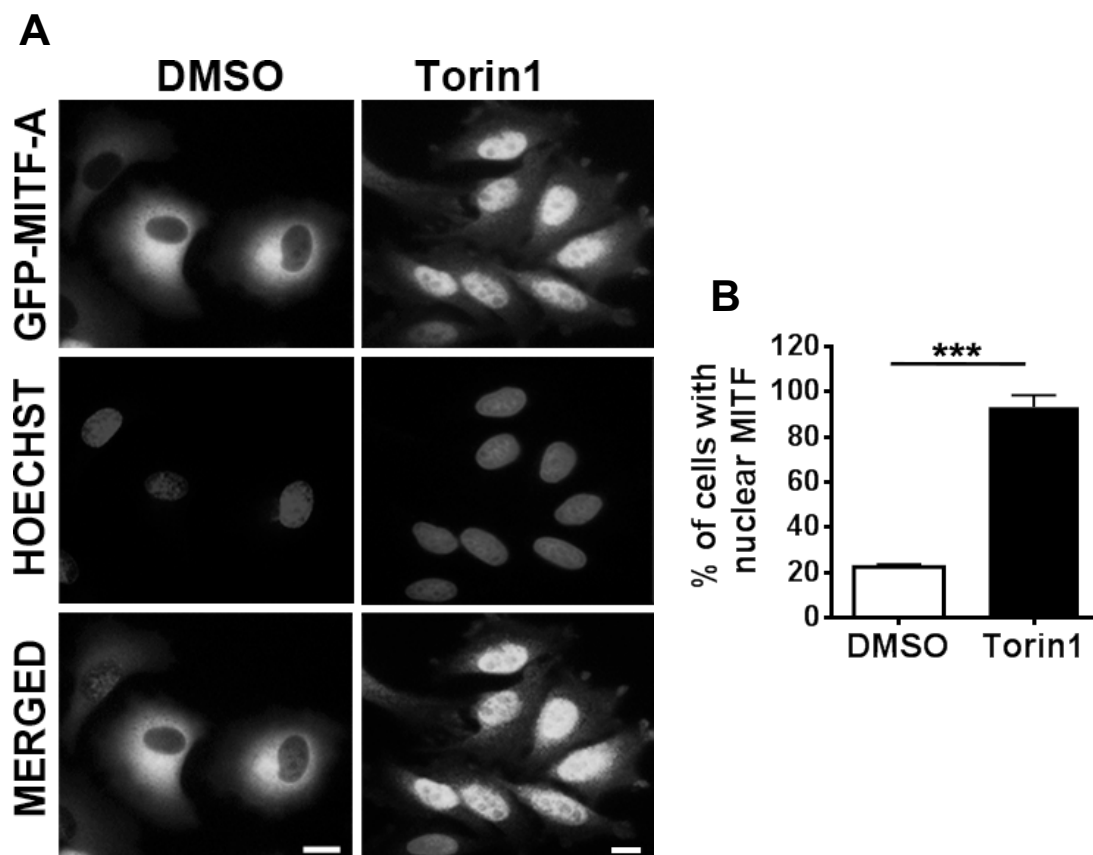


Figure 3.1.1 1: Nuclear translocation of MITF-A upon torin1 treatment.

(A) MITF translocated to nuclei of cells following torin1 (MTOR inhibitor) treatment. HeLa cells were transiently transfected with GFP-MITF-A vector and incubated with torin1 (200 nM, 4 h) and analyzed under a fluorescence microscope. DMSO, carrier control. Hoechst dye was used to stain the nuclei (blue). Scale bar, 10 μ m. (B) Quantitative analysis of MITF nuclear translocation in the experimental set-up shown in A and B (mean \pm SD of n=3 independent experiments, ***p<0.01)

Similar immunofluorescence analysis was performed with starvation as an autophagy-inducer. According to the results in Figure 3.1.1 2, nutrient deprivation also promotes nuclear translocation of overexpressed MITF-A isoform in HeLa cells.

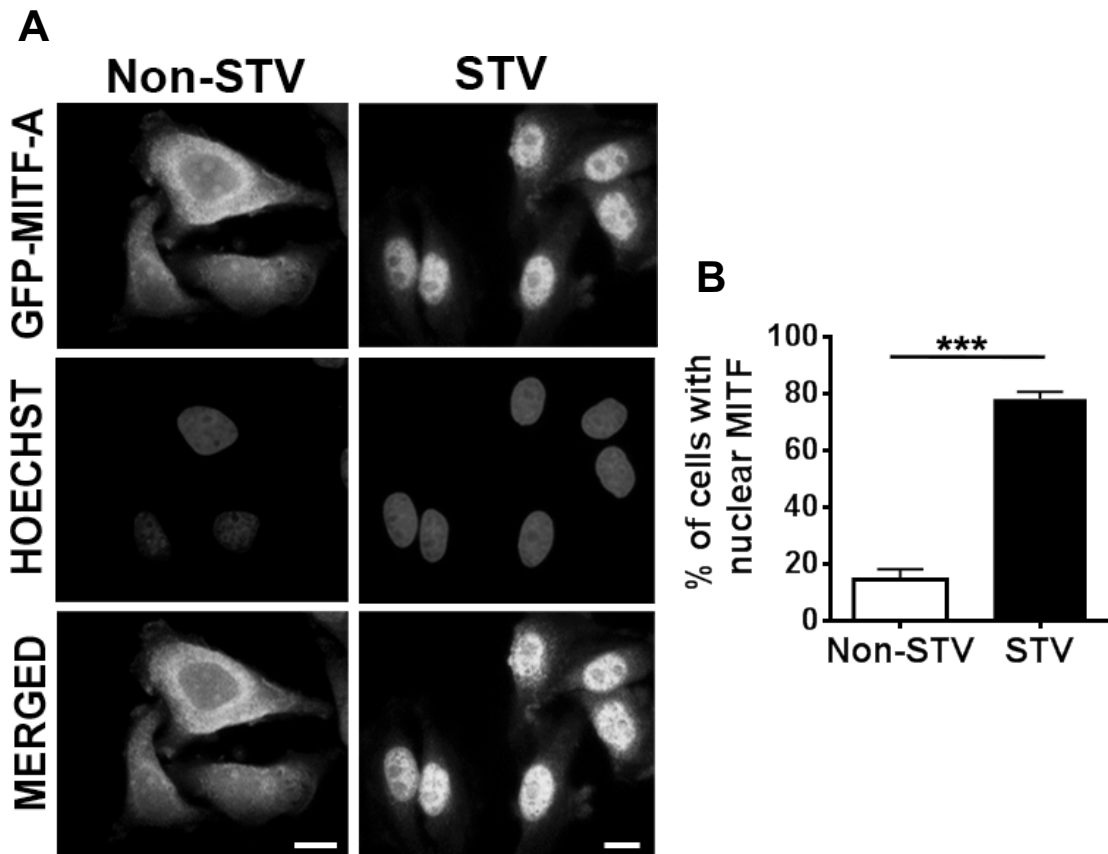


Figure 3.1.1 2: Nuclear translocation of MITF-A upon starvation. (A) MITF translocated to nuclei of cells following starvation treatment. HeLa cells were transiently transfected with GFP-MITF-A vector and incubated with starvation medium (Earle's Balanced Salt solution, 4 h, STV) and analyzed under a fluorescence microscope. Non-STV, non-starved. Hoechst dye was used to stain the nuclei (blue). Scale bar, 10 μ m. (B) Quantitative analysis of MITF nuclear translocation in the experimental set-up shown in A and B (mean \pm SD of n=3 independent experiments, ***p<0.01)

Moreover, similar results were observed in immunofluorescence experiments performed in another cell line, SK-MEL-28. Upon torin1 treatment, overexpressed GFP-MITF-A constructs translocated to the nuclei of cells as can be seen in Figure 3.1.1 3.

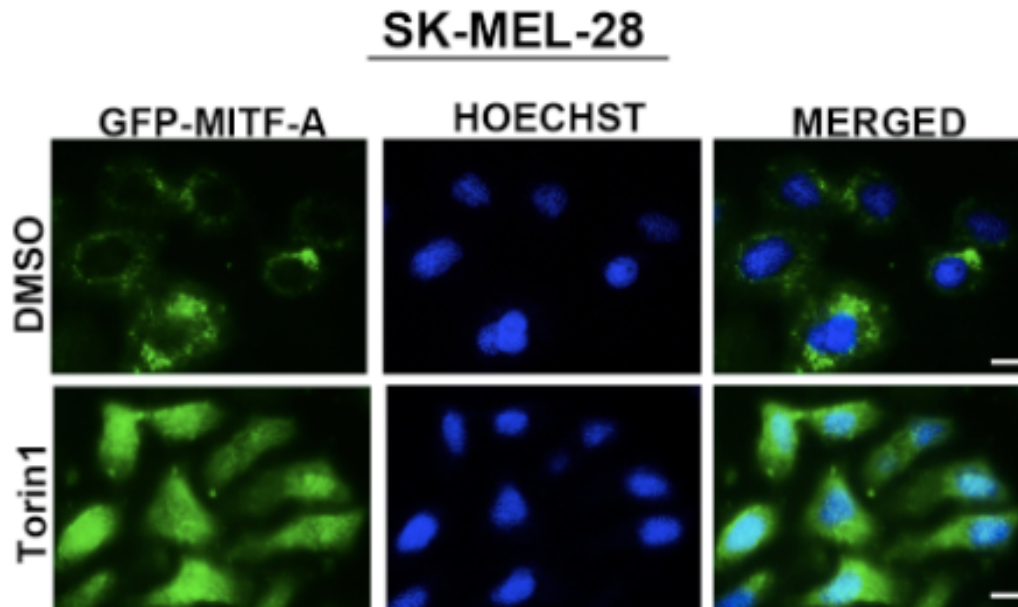


Figure 3.1.1 3: Nuclear translocation of MITF-A upon torin1 treatment in SK-MEL-28 cells. (A) MITF translocated to nuclei of cells following torin1 (MTOR inhibitor) treatment. SK-MEL-28 cells were transiently transfected with GFP-MITF-A vector and incubated with torin1 (200 nM, 4 h) and analyzed under a fluorescence microscope. DMSO, carrier control. Hoechst dye was used to stain the nuclei (blue). Scale bar, 10 μ m. (B) Quantitative analysis of MITF nuclear translocation in the experimental set-up shown in A and B (mean \pm SD of n=3 independent experiments, ***p<0.01)

Hence, in response to the changes in the nutrient levels and mTORC1 inhibition, MITF is translocated to the cell nucleus.

Autophagic activity in HeLa cells was analyzed in order to elucidate the role of MITF in autophagy context. The effect of the overexpression of MITF-A (an alternative splicing isoform of MITF) in HeLa cells was tested using the LC3 shift assay. As it is mentioned above, cysteine protease ATG4 enzymes cleave cytosolic pro-LC3 protein into LC3-I cytosolic form. Lipid-conjugated and autophagic membrane-bound form, LC3-II is formed upon conjugation of a lipid molecule (PE). The PE-conjugated form of LC3-II shows faster electrophoretic mobility in SDS-PAGE gels. Consequently, LC3-II is the only protein marker associated with growing and mature autophagosomes and used as gold-standard and widely used autophagic test.

In order to enlighten whether the observed accumulation of the LC3-II form of the protein was a result of increased autophagic activity, and not a result of a block in autophagosome-lysosome fusion, the experiments were performed in the presence or absence of the lysosomal protease inhibitors E64D-pepstatin A (E+P).

Following mTOR inhibition by torin1 treatment, extracts from cells that overexpressed MITF had higher levels of LC3-II and further accumulation was observed upon lysosomal inhibition by E64D+pepstatin A. Hence, these results are presented in Figure 3.1.1 4 and confirm that MITF stimulated autophagosome formation and did not prominently affect autophagosome-lysosome fusion.

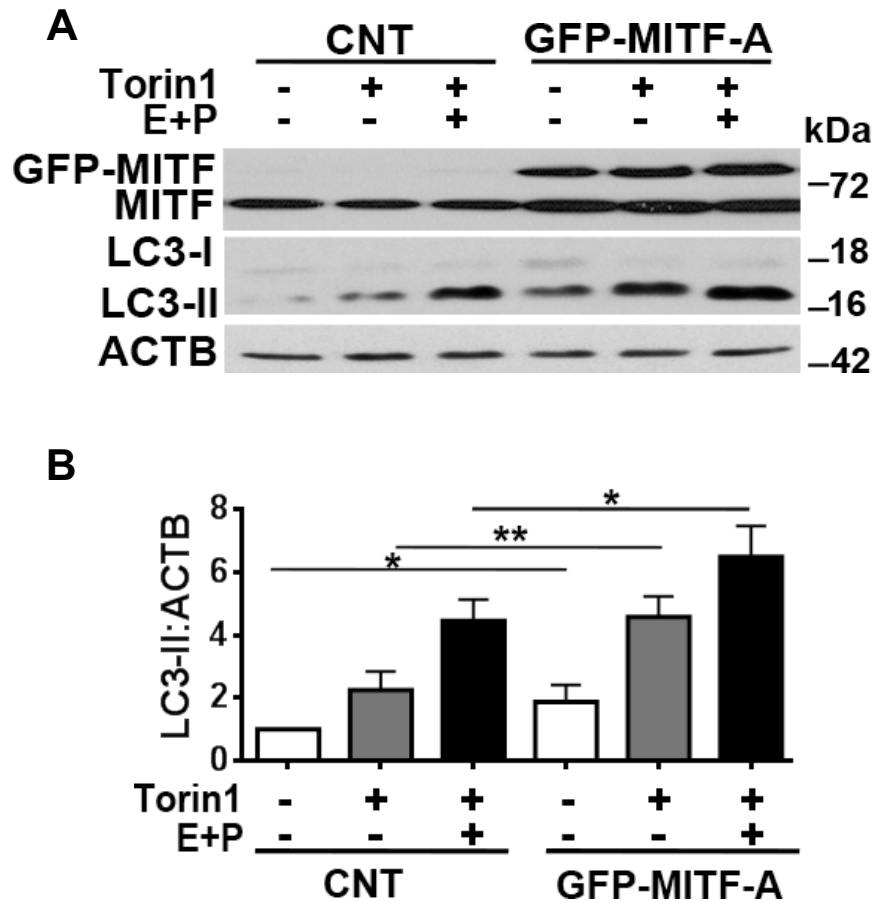


Figure 3.1.1 4: Effect of MITF-A overexpression on torin1-induced autophagy. (A) Overexpression of MITF-A amplified torin1-induced LC3-II (lipid-conjugated and autophagosome-associated LC3 form) formation in HeLa cells. LC3-I, free LC3 form. E+P, E64D (10 μ g/ml) and pepstatin A (10 μ g/ml) were used as lysosomal protease inhibitors. (B) Graph depicting quantification of LC3-II:ACTB ratios in the experimental set-up shown in E (mean \pm SD, n=3 independent experiments, **p<0.03, *p<0.05).

Similar with the effect on torin1-induced autophagy, overexpression of MITF-A increased starvation-induced LC3-II formation in HeLa cells and further accumulation was observed upon lysosomal inhibition (Figure 3.1.1 5).

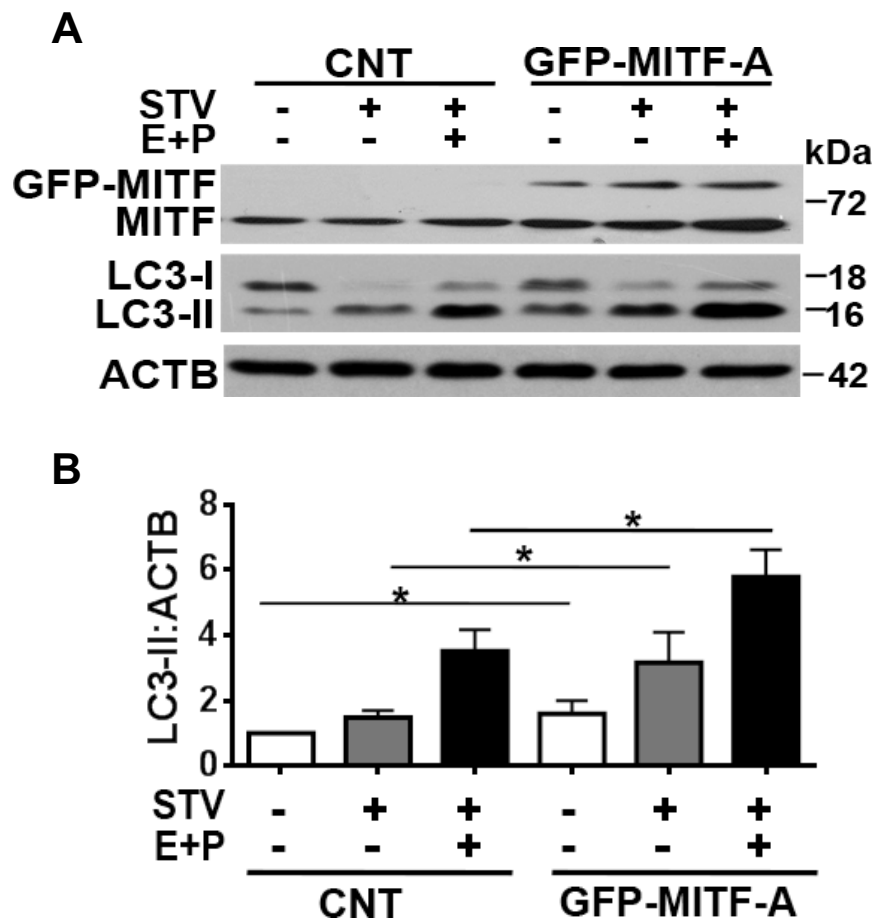


Figure 3.1.1 5: Effect of MITF-A overexpression on starvation-induced autophagy. (A) Overexpression of MITF-A amplified starvation-induced LC3-II (lipid-conjugated and autophagosome-associated LC3 form) formation in HeLa cells. STV, 4 hr. LC3-I, free LC3 form. E+P, E64D (10 μ g/ml) and pepstatin A (10 μ g/ml) were used as lysosomal protease inhibitors. (B) Graph depicting quantification of LC3-II:ACTB ratios in the experimental set-up shown in E (mean \pm SD, n=3 independent experiments, **p<0.03, *p<0.05).

To conclude, classical autophagic tests revealed that MITF-A overexpression further amplifies mTOR-inhibition-mediated and starvation-induced autophagosome formation.

3.1.2 Effect of MITF silencing on autophagy

To check whether endogenous MITF was a rate-limiting factor in autophagy activation by stress, HeLa and SK-MEL-28 cells were transfected with siRNAs targeting *MITF* (*siMITF*) or non-targeting control siRNAs (*siCNT*). First, we confirmed that pan-MITF siRNAs that were used in following experiments could target all endogenous isoforms of *MITF* in HeLa (Figure 3.1.2 1A). and SK-MEL-28 (human skin malignant melanoma cell line) (Figure 3.1.2 1B).

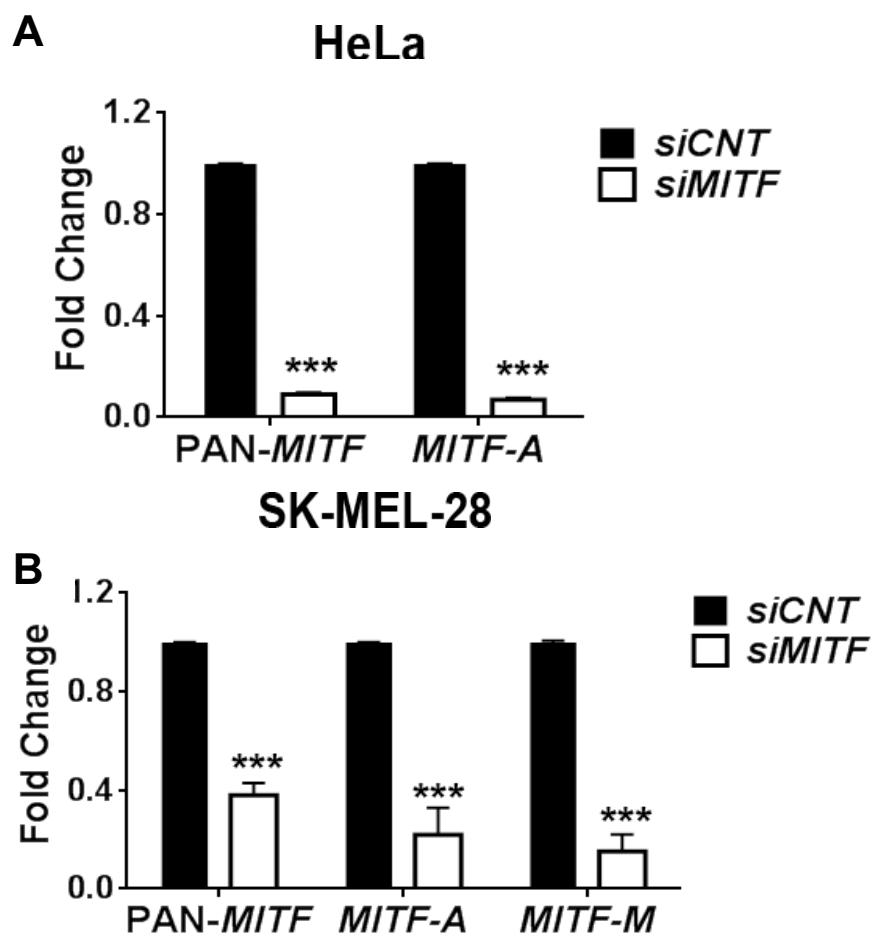


Figure 3.1.2 1: Effect of siRNA against MITF on *MITF* mRNA. *MITF* mRNA expression levels were quantified by RT-qPCR in HeLa (A) and SK-MEL-28 (B) cells transfected with *siCNT* or *siMITF*. Pan-*MITF*-, *MITF-A*- or *MITF-M*-specific primer pairs were used. Data were normalized to *GAPDH* (mean \pm SD of n=3 independent experiments, ***p<0.01).

After confirmation of efficiency of MITF silencing by siRNAs, autophagy levels were checked under basal conditions or with autophagy inducers and in the presence or absence of the lysosomal inhibitors E64D-pepstatin A.

The effect of MITF knockdown on torin1-induced autophagy was evaluated in HeLa cells and SK-MEL-28 cells by GFP-LC3 dot formation assay. GFP-LC3 shows a punctuate pattern and localized in autophagosome membranes in the cell upon autophagy activation and lipid conjugation. Moreover, larger autophagosomes are detected due to autophagosome-lysosome fusion when autophagosome-lysosome fusion is blocked by lysosomal inhibitors.

First, threshold dot number was determined by counting the number of GFP-LC3 dots in each cell under basal condition. For stable HeLa-GFP-LC3 cells, basal dot number was identified as 15. For transiently-transfected SK-MEL-28 cells, 5 GFP-LC3 dots per cell was identified as threshold.

GFP-LC3 dot formation analysis showed that knockdown of MITF significantly attenuated autophagy that was stimulated by torin1 in HeLa (Figure 3.1.2 2). Interestingly, MITF downregulation could even suppress autophagy at basal levels.

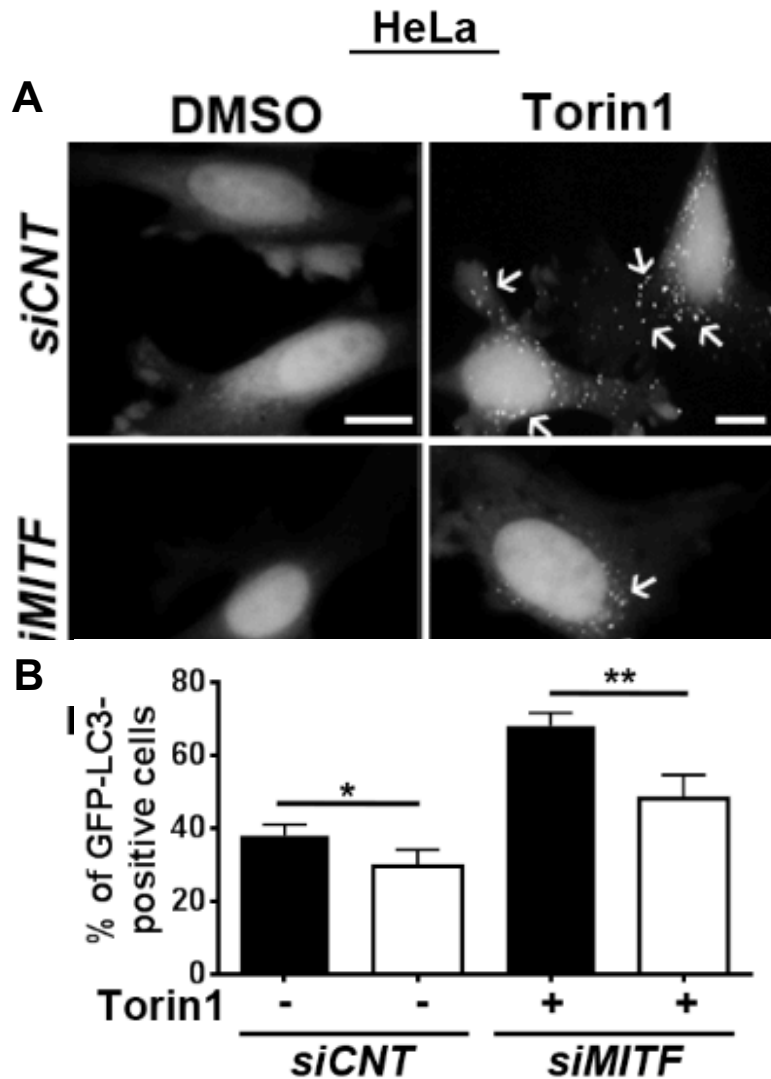


Figure 3.1.2 2: Effect of *siMITF* on GFP-LC3 dot formation following torin1 treatment in HeLa cells. (A) HeLa-GFP-LC3 stable cells transfected with either *siCNT* (control siRNA) or *siMITF*, incubated with torin1 (200 nM, 4 h) and analyzed under a fluorescence microscope. DMSO, carrier control. White arrows indicate the GFP-LC3 dots in the cells. Scale bar, 10 μ m. (B) Quantitative analysis of GFP-LC3 dots in the experimental set-up shown in A (mean \pm SD of n=3 independent experiments, **p<0.03, *p<0.05).

Similarly, MITF knockdown by *siMITF* attenuated torin1-induced GFP-LC3 dot formation compared to control siRNA (*siCNT*)-transfected SK-MEL-28 cells (Figure 3.1.2 3).

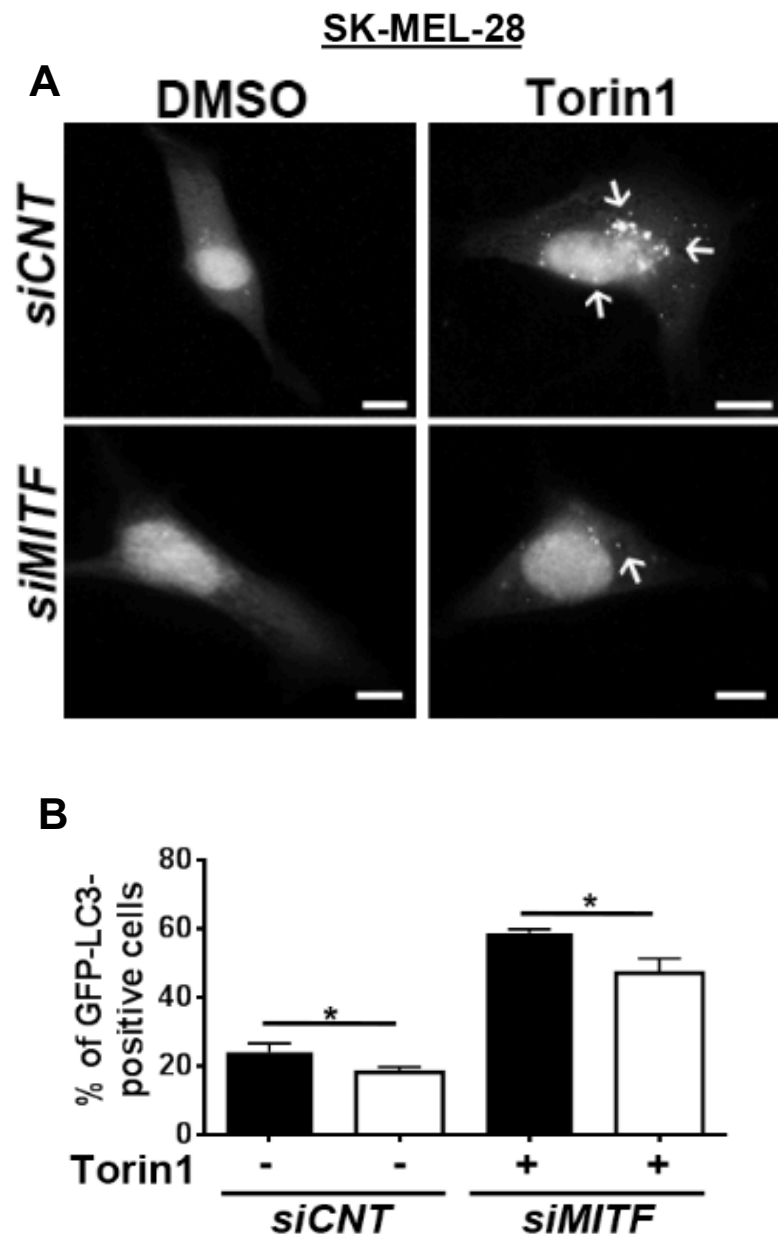


Figure 3.1.2 3: Effect of *siMITF* on GFP-LC3 dot formation following torin1 treatment in SK-MEL-28 cells. (A) SK-MEL-28 cells transiently transfected with either *siCNT* (control siRNA) or *siMITF*, incubated with torin1 (200 nM, 4 h) and analyzed under a fluorescence microscope. DMSO, carrier control. White arrows indicate the GFP-LC3 dots in the cells. Scale bar, 10 μ m. (B) Quantitative analysis of GFP-LC3 dots in the experimental set-up shown in A (mean \pm SD of n=3 independent experiments, **p<0.03, *p<0.05).

Moreover, MITF-dependence of autophagy was confirmed by LC3-II shift assays that were performed in torin1-treated HeLa cells in the presence or absence of E64D-pepstatin A (Figure 3.1.2 4). Knockdown of MITF significantly abolished LC3-II accumulation in torin1-induced autophagy.

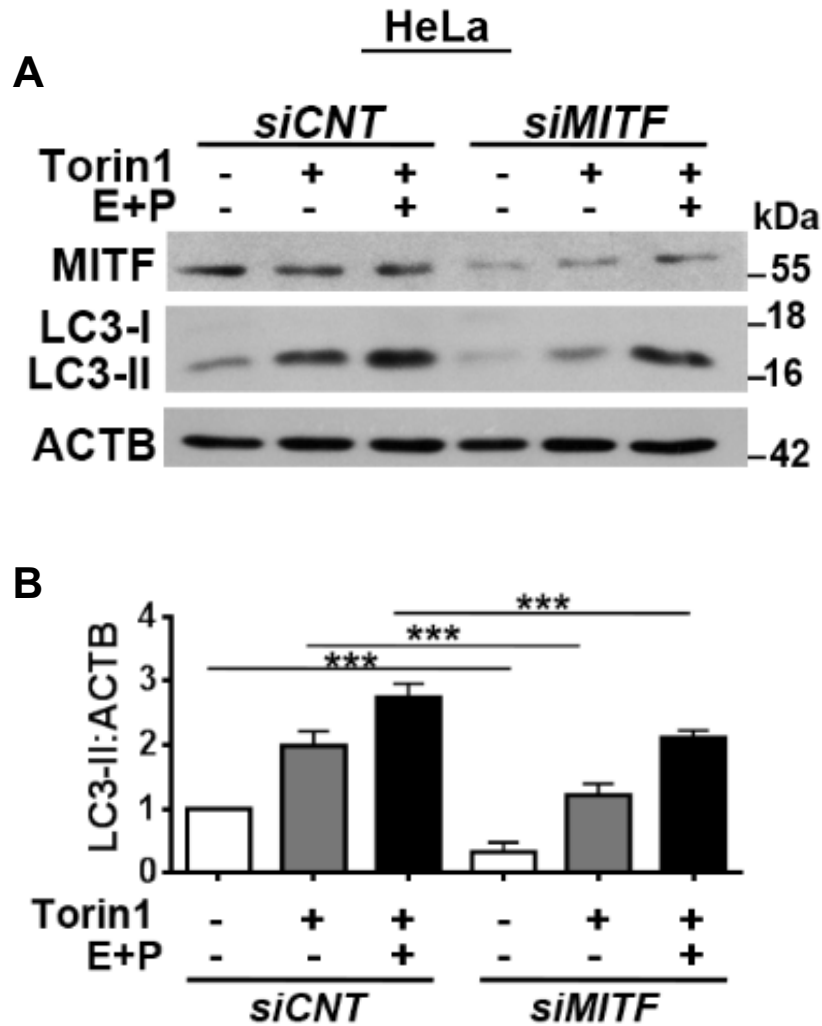


Figure 3.1.2 4: Effect of *siMITF* on LC3-II accumulation following torin1 treatment in HeLa cells. (A) Immunoblots of *siCNT*- or *siMITF*-transfected HeLa cells that were treated with DMSO or torin1 (200 nM, 4h). (B) Graph depicting quantification of LC3-II:ACTB ratios in the experimental set-up shown in A (mean±SD, n=3 independent experiments, ***p<0.01).

Additionally, the inhibitory effect of MITF knockdown on torin1-induced autophagy was confirmed in SK-MEL-28 cells using LC3-II shift assay (Figure 3.1.2 5).

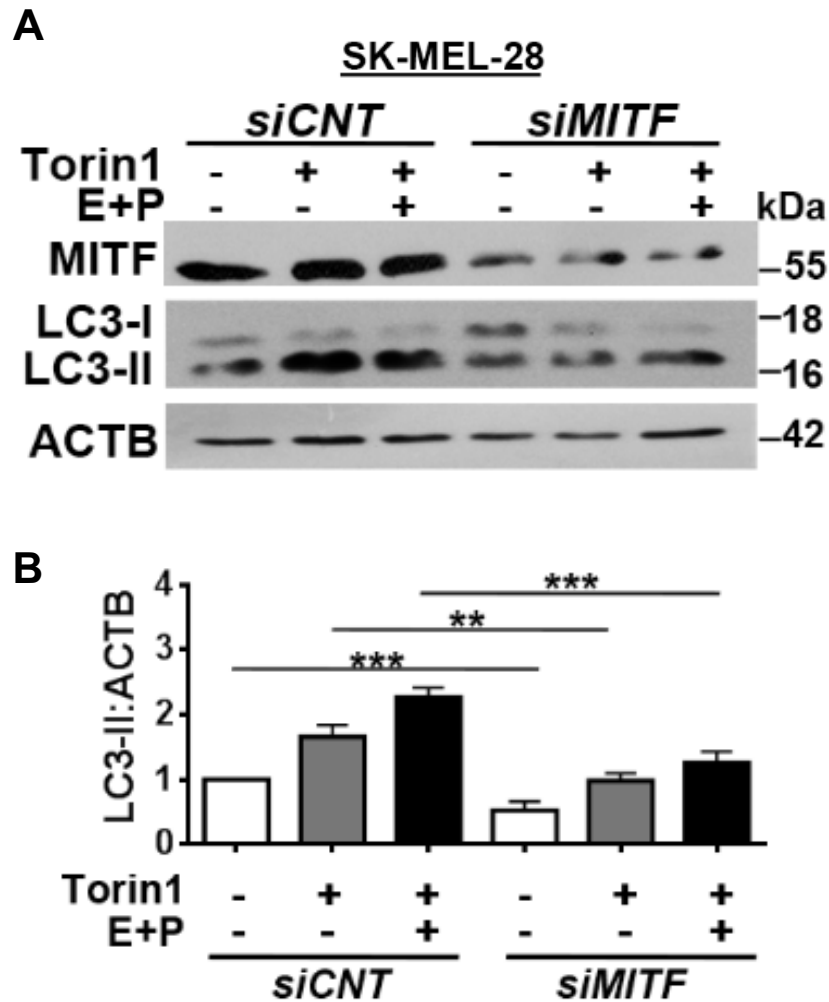


Figure 3.1.2 5: Effect of *siMITF* on LC3-II accumulation following torin1 treatment in SK-MEL-28 cells. (A) Immunoblots of *siCNT*- or *siMITF*-transfected SK-MEL-28 cells that were treated with DMSO or torin1 (200 nM, 4h). (B) Graph depicting quantification of LC3-II:ACTB ratios in the experimental set-up shown in A (mean±SD, n=3 independent experiments, ***p<0.01).

In order to verify the above results with another autophagy-inducing signal, the effect of MITF knockdown was analyzed under starvation conditions. Indeed, LC3-II shift analyses showed that MITF knockdown significantly attenuated both basal and starvation-induced autophagy in HeLa (Figure 3.1.2 6) and SK-MEL-28 (Figure 3.1.2.7) cells in the presence or absence of E64D-pepstatin A.

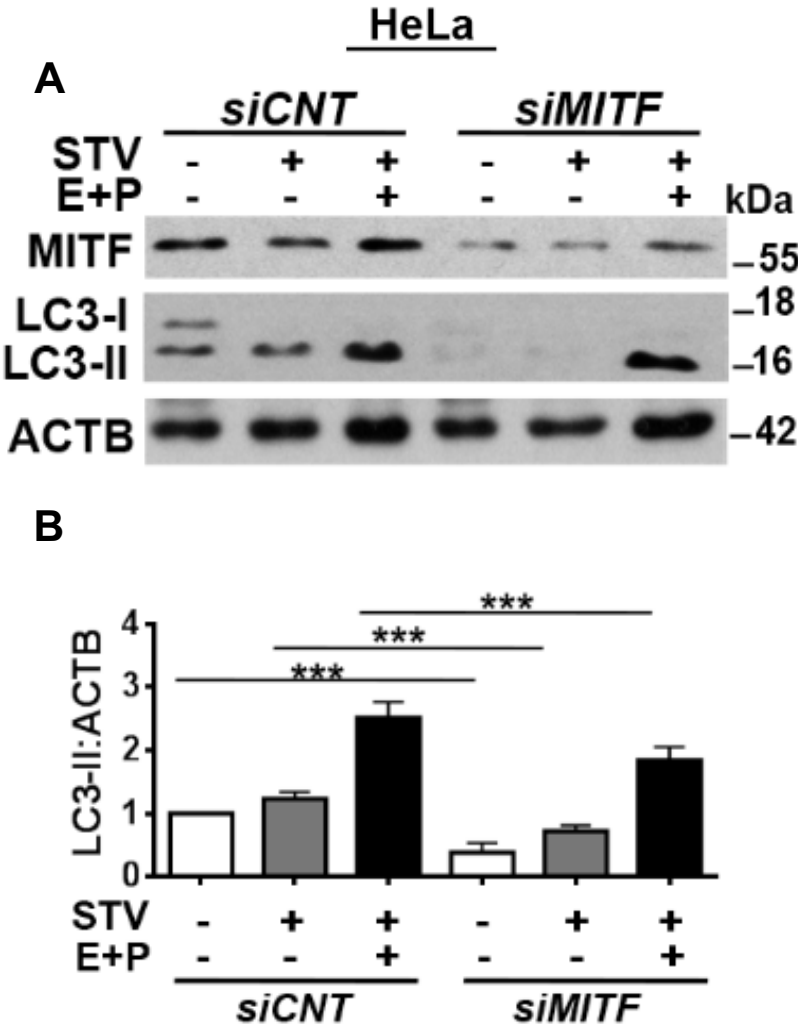


Figure 3.1.2 6: Effect of *siMITF* on LC3-II accumulation following starvation treatment in HeLa cells. (A) Immunoblots of *siCNT*- or *siMITF*-transfected HeLa cells that were non-starved or starved (EBSS, 4h). (B) Graph depicting quantification of LC3-II:ACTB ratios in the experimental set-up shown in A (mean±SD, n=3 independent experiments, ***p<0.01).

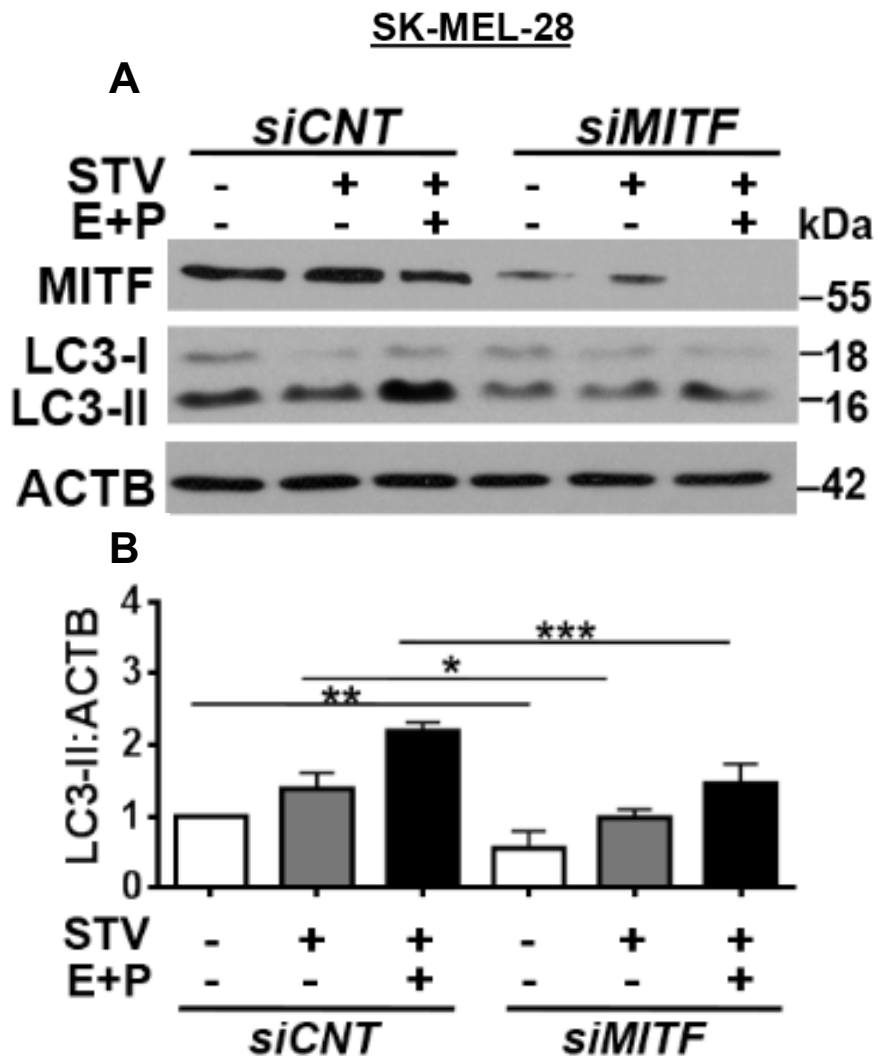


Figure 3.1.2 7: Effect of *siMITF* on LC3-II accumulation following starvation treatment in SK-MEL-28 cells. (A) Immunoblots of *siCNT*- or *siMITF*-transfected HeLa cells that were non-starved or starved (EBSS, 4h). (B) Graph depicting quantification of LC3-II:ACTB ratios in the experimental set-up shown in A (mean±SD, n=3 independent experiments, ***p<0.01).

Moreover, siRNA knockdown of MITF protein levels were confirmed and quantified for each and every experiment presented above and their triple replicates (Figure 3.1.2 8).

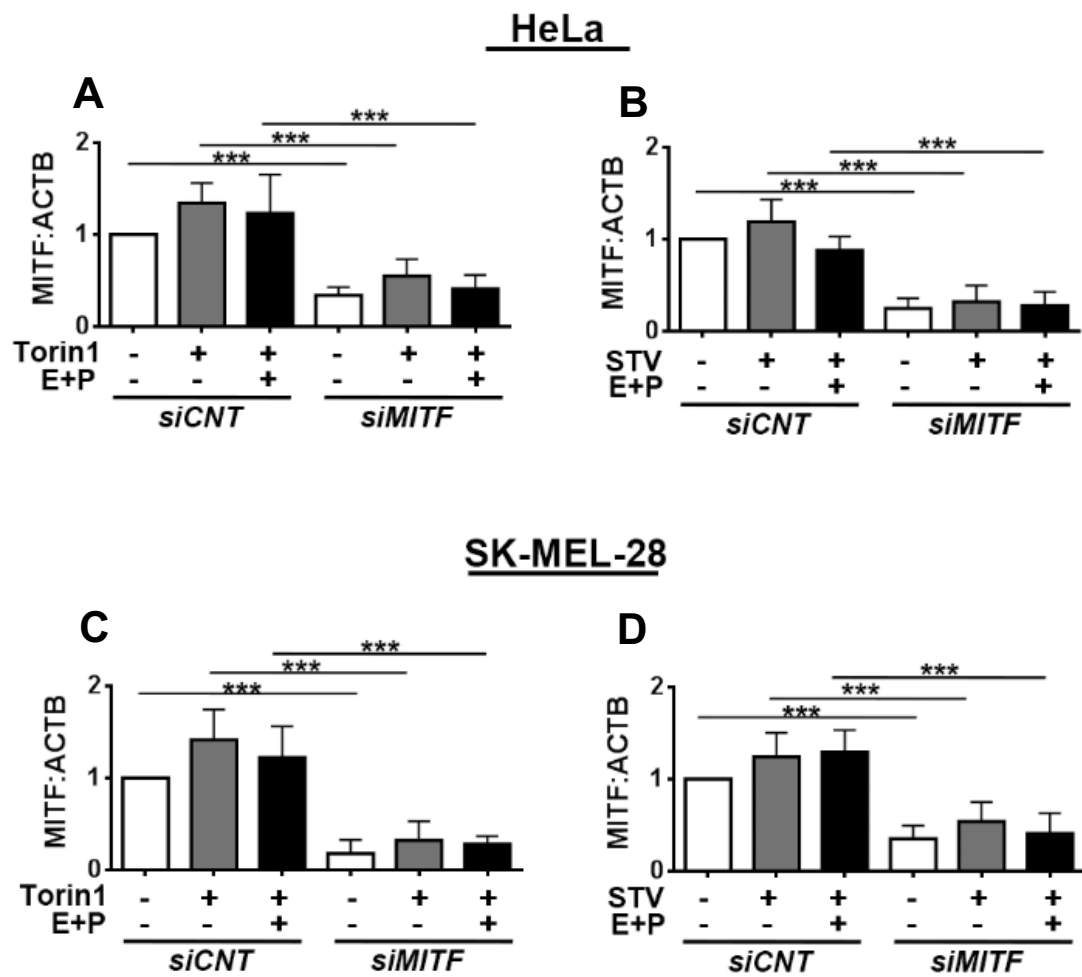


Figure 3.1.2 8: Confirmation of MITF knockdown using siRNA on MITF protein level. (A and B) Graph depicting quantification of MITF:ACTB protein ratios in the HeLa experiments shown in Figure 3.1.2 4 and Figure 3.1.2 6 (mean±SD, n=3 independent experiments,***p<0.01). (C and D) Graph depicting quantification of MITF:ACTB protein ratios in the SK-MEL-28 experiments shown in Figure 3.1.2 5 and Figure 3.1.2 7 (mean±SD, n=3 independent experiments,***p<0.01).

In addition to GFP-LC3 dot formation and LC3-II shift assays, effect of MITF knockdown on autophagy was also monitored through analysis of WIPI1 puncta formation. During autophagy activation, the phosphatidylinositol-3-phosphate (PtdIns3P) effector WIPI1 proteins are recruited to phagophores and form punctate patterns (Proikas-Cezanne, 2007). In line with LC3 tests, MITF knockdown significantly decreased GFP-WIPI1 dot formation

following torin1 treatment (Figure 3.1.2 9) or starvation (Figure 3.1.2 10). All these results clearly showed that MITF is required for the upregulation of autophagy in cells under stress.

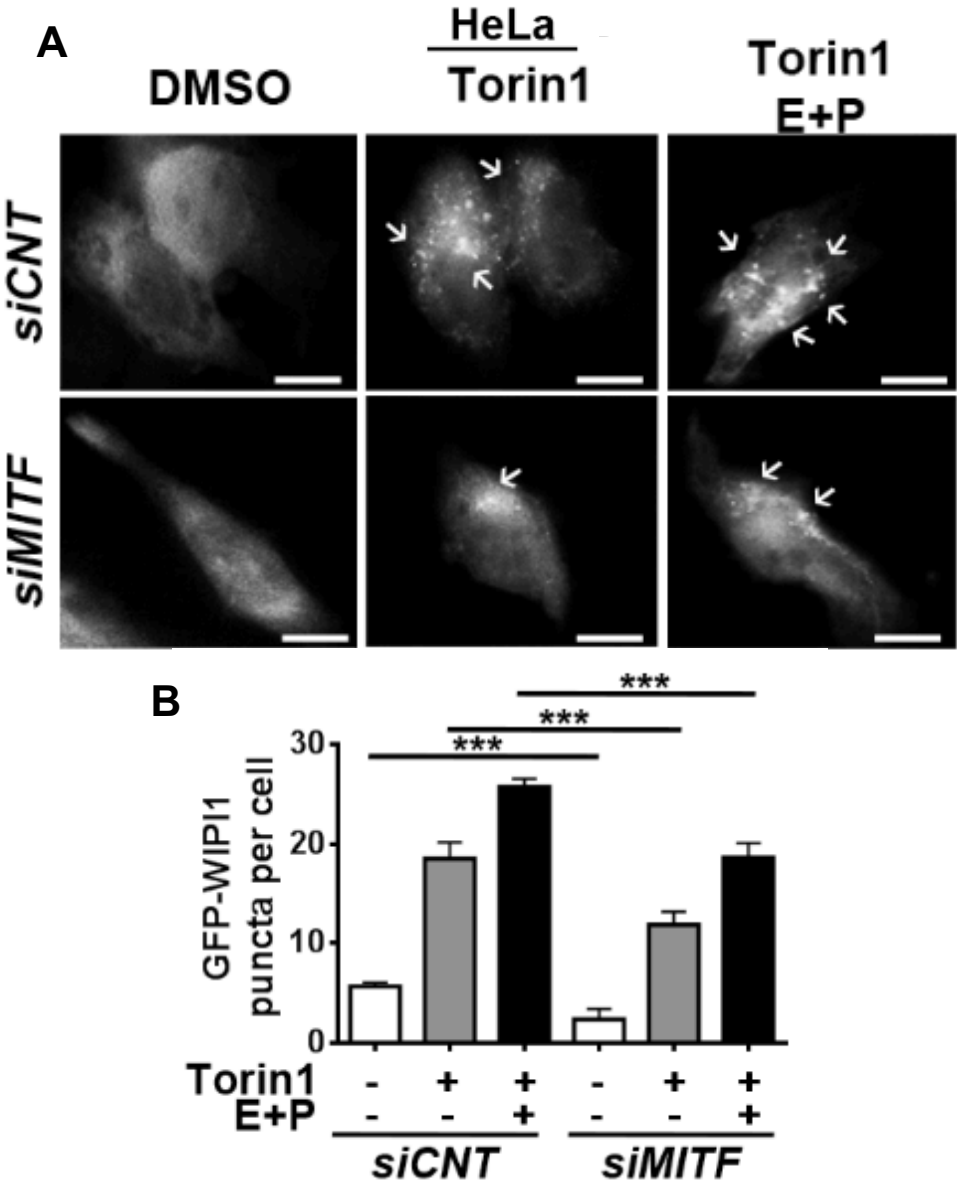


Figure 3.1.2.9: Effect of MITF knockdown on GFP-WIP11 puncta formation following torin1 treatment. (A) HeLa cells transiently transfected with GFP-WIP11 plasmid construct and either siCNT (control siRNA) or *siMITF*, then incubated with torin1 (200 nM, 4 h) and analyzed under a fluorescence microscope. DMSO, carrier control. White arrows indicate the GFP-WIP11 dots in the cells. Scale bar, 10 μ m. (B) Quantitative analysis of GFP-WIP11 puncta in the experimental set-up shown in A (mean \pm SD of n=3 independent experiments, ***p<0.01).

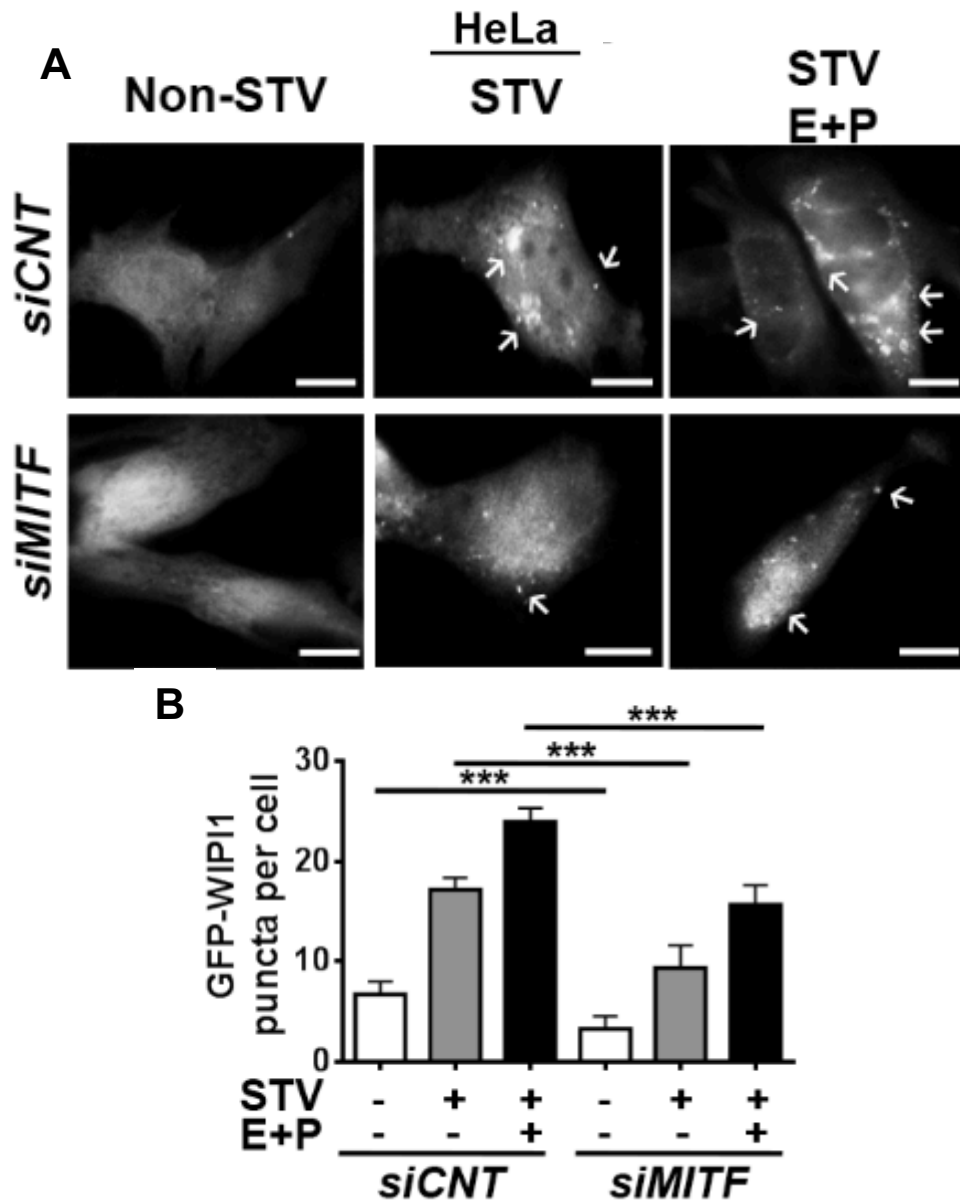


Figure 3.1.2.10: Effect of MITF knockdown on GFP-WIP1 puncta formation following starvation treatment. (A) HeLa cells transiently transfected with GFP-WIP1 plasmid construct and either siCNT (control siRNA) or *siMITF*, then incubated with torin1 (EBSS, 4 h) and analyzed under a fluorescence microscope. DMSO, carrier control. White arrows indicate the GFP-WIP1 dots in the cells. Scale bar, 10 μ m. (B) Quantitative analysis of GFP-WIP1 puncta in the experimental set-up shown in A (mean \pm SD of n=3 independent experiments, ***p<0.01).

All these results clearly showed that MITF is required for the upregulation of autophagy in cells under stress.

To further confirm that MITF did not block autophagosome-lysosome fusion and increased the autophagic flux, 2 independent approaches were used. The GFP-RFP-LC3 tandem fusion construct is commonly used to assess autophagosome and autolysosome numbers. Whereas GFP and RFP label autophagosomes, the GFP signal quenches in the lysosomes while the RFP signal remains, marking autolysosomes. Quantitative analysis of autophagosome and autolysosome numbers using this test showed that torin1 led to an increase in both autophagosome and autolysosome numbers, and the knockdown of MITF significantly decreased the numbers of both vesicle types (Figure 3.1.2 11).

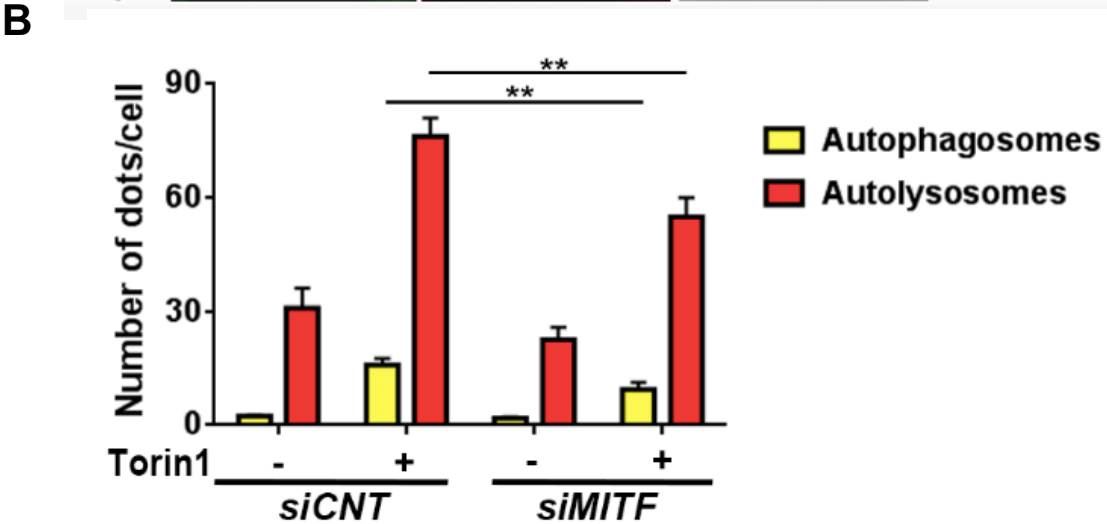
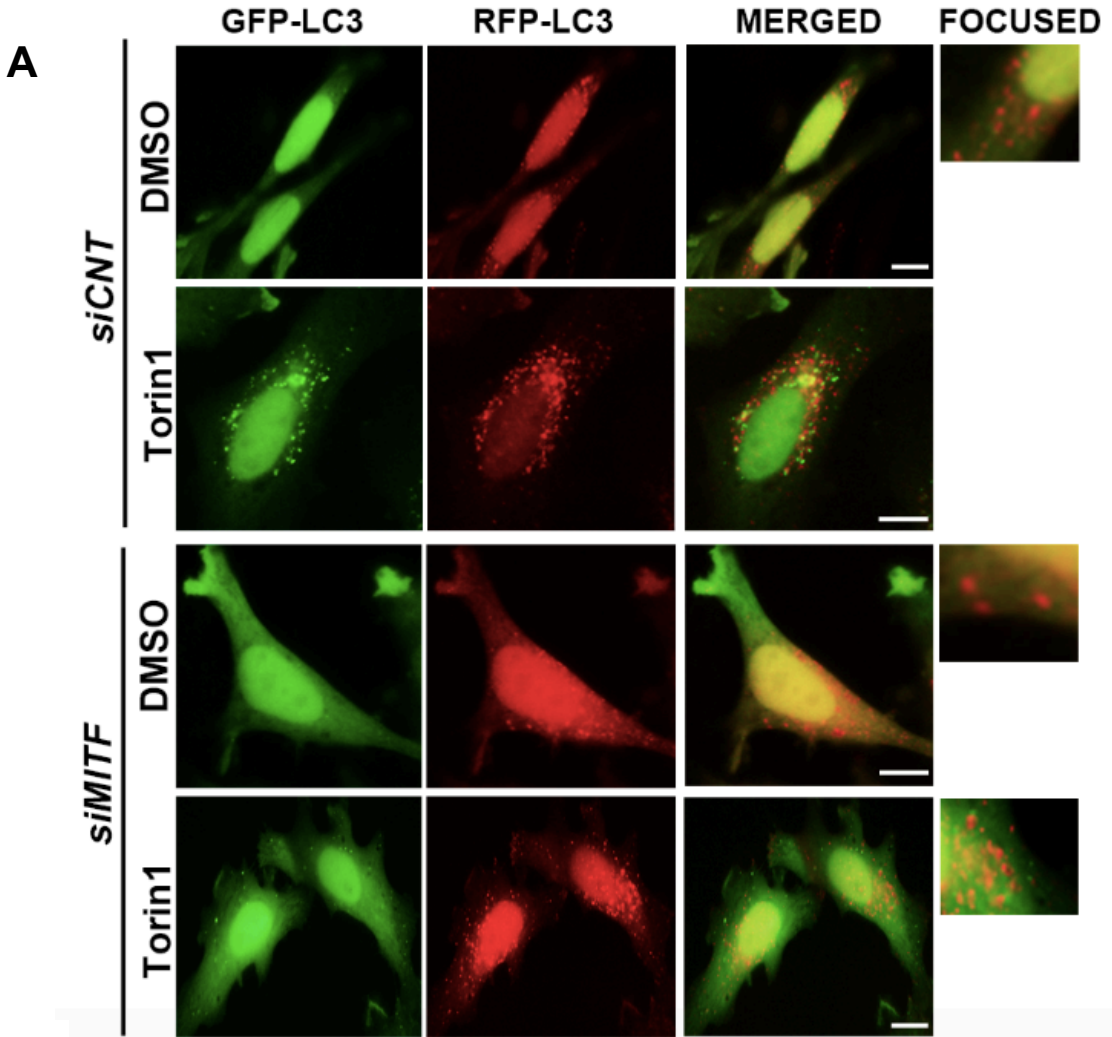


Figure 3.1.2 11: Effect of MITF knockdown on GFP-RFP-LC3 colocalization following torin1 treatment. (A) *siMITF*, but not *siCNT*, decreased the number of RFP⁺ GFP⁺ (yellow) and RFP⁺ GFP⁻ (red) dots per cell in torin1-treated HeLa cells. Yellow, autophagosomes; red, autolysosomes; merged, overlay of GFP-LC3 and RFP-LC3 signals; focused, higher magnification of a relevant region of the same cell. Scale bar, 10 μ m. (B) Quantitative analysis of autophagosome and autolysosome numbers in the experimental set-up shown in A (mean \pm SD, n=3 independent experiments, **p<0.03).

Additionally, we used another flux test that was suggested in the autophagy guidelines article (Klionsky, 2016), the GFP-LC3 lysosomal delivery and proteolysis test. Here, when GFP-LC3 is delivered to lysosomes, the LC3 part of the chimera is degraded, whereas the GFP protein that is relatively resistant to hydrolysis accumulates. Therefore, the appearance of free GFP on western blots can be used to monitor breakdown of the autophagosomal cargo. Using this test, we observed a robust accumulation of free GFP in torin1-treated cells, indicating increased flux and degradation. Knockdown of MITF almost completely abolished free GFP accumulation under these conditions.

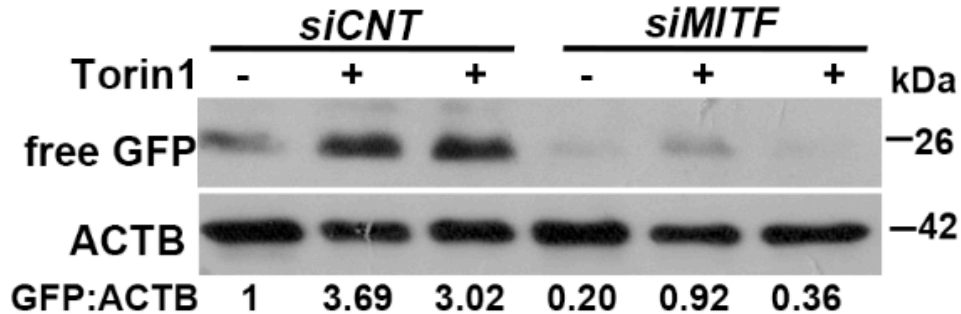


Figure 1.3.2 12: Effect of MITF knockdown on GFP-LC3 lysosomal delivery and proteolysis. HeLa cells were transiently co-transfected with a plasmid encoding GFP-LC3 and *siCNT* or *siMITF* and treated with DMSO (-) or torin1. Appearance of free GFP was analyzed in immunoblots. ACTB was used as a loading control. ImageJ analyses of free GFP:ACTB ratios are shown.

All of these results showed that MITF is required for autophagic activity in cells. Therefore, MITF is a key regulator of MTOR inhibition- and starvation-induced autophagy.

3.2 Role of MITF-dependent transcriptional activation in autophagy control

As presented in Section 3.1, MITF overexpression in various cell lines increases the number of autophagosomes, whereas depletion of endogenous MITF by RNAi reduces autophagosome numbers. Previous studies indicated that transcription of some autophagy-related genes, including *LC3B* and *ATG10*, are regulated in a MITF-dependent manner (Perera, 2015).

To confirm previous findings in our experimental conditions and to further analyze MITF-dependent transcriptional control of *LC3B* and *ATG10*, the expression of these autophagy-related genes following MITF knockdown under control, torin1 or starvation conditions were evaluated. Upon MITF knockdown, basal expression levels of *ATG10* and *LC3B* were significantly attenuated. Moreover, expression of these genes was increased upon autophagy induction by torin1 treatment and starvation, and knockdown of MITF significantly downregulated torin1- and starvation-induced expression of *ATG10* (Figure 3.2 1A and C) and *LC3B* (Figure 3.2 1B and D).

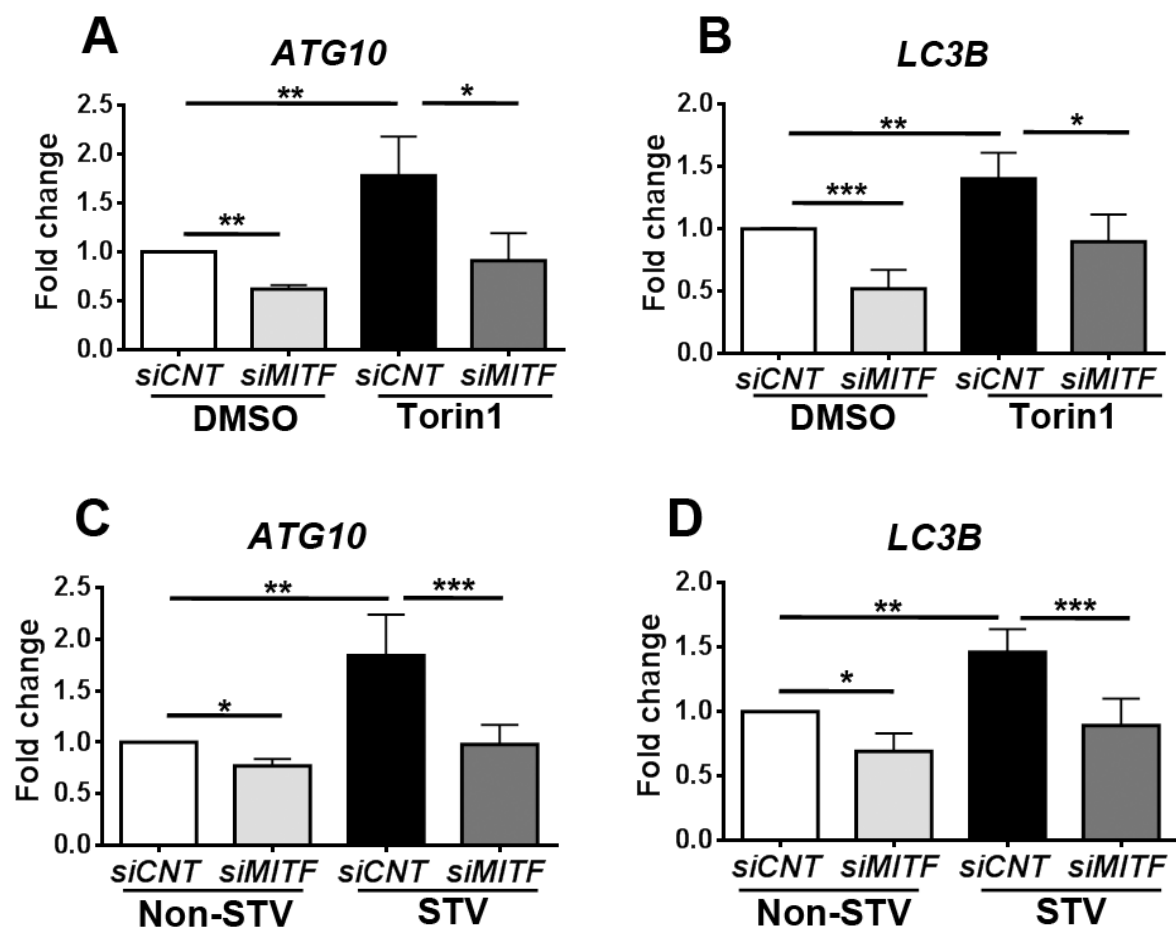


Figure 3.2 1: Effect of MITF silencing on expression of autophagy-related genes. (A-D) RT-qPCR analysis of mRNA levels of *ATG10* (A and C) and *LC3B* (B and D) in control siRNA (*siCNT*)- or *siMITF*-transfected HeLa cells following torin1 (A and B) or starvation (C and D) treatment (mean±SD of n=5 independent experiments ***p<0.01, **<0.03, *p<0.05). DMSO, carrier control. Data were normalized to *GAPDH*.

MIR211 was reported to be a direct transcriptional target of MITF in a melanoma invasion and metastasis context (Miller, 2004; Mazar 2010). Yet, whether MITF regulates *MIR211* under autophagy-inducing conditions in melanoma and epithelial cells, and whether it contributes to general autophagy control is not known. To confirm that *MIR211* was expressed in HeLa cells, qPCR analysis was performed following control, torin1 or starvation treatment. Torin1 treatment significantly induced *MIR211* expression in HeLa cells (Figure 3.2 2A). Under these conditions, introduction of *MITF* siRNA significantly decreased both basal and torin1-induced expression of *MIR211* (Figure 3.2 2A). Similar results were obtained when starvation used was used as an autophagy inducer (Figure 3.2 2B).

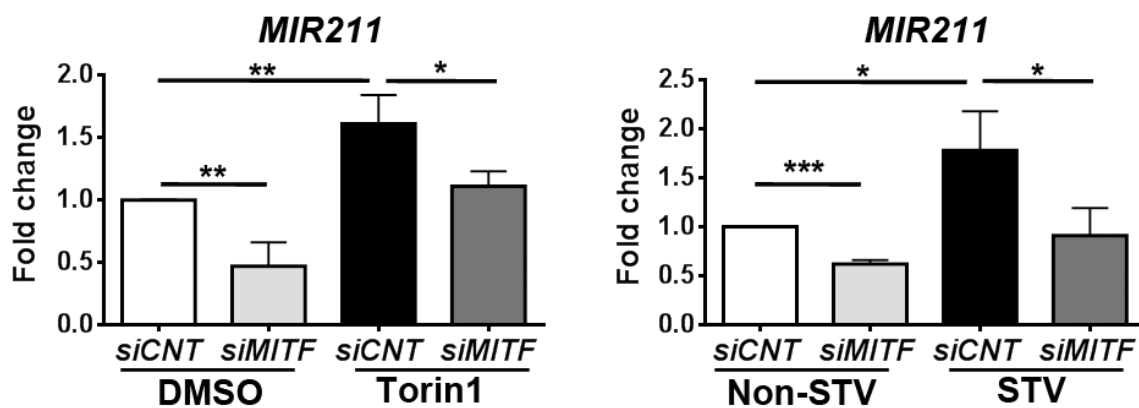


Figure 3.2 2: Effect of MITF silencing on *MIR211* expression. (A) TaqMan RT-qPCR analysis of *MIR211* expression in DMSO or torin1-treated (200 nm, 4h) HeLa cells (mean±SD of n=3 independent experiments, **p<0.03, *p<0.05). Data were normalized to *RNU6-1* (RNA, U6 small nuclear 1) (U6). (F) TaqMan RT-qPCR analysis of *MIR211* expression in non-starved (Non-STV) or starved (STV) (EBSS, 4h) HeLa cells (mean±SD of n=3 independent experiments, ***p<0.01, *p<0.05). Data were normalized to *RNU6-1*.

To confirm direct binding of MITF transcription factor to the promoter region of *MIR211*, chromatin immunoprecipitation (ChIP) experiments were performed. Chromatin IP identifies specific protein-DNA interactions within the cell, and to quantitate these interactions PCR or real-time PCR can be performed (Orlando V, 2000). Along with monitoring transcription regulation through histone modifications, ChIP can be also used to analyze the interaction of a transcription factor with a candidate target gene within the natural chromatin context of the cell. The overall protocol consists of various steps including crosslinking, cell lysis, chromatin shearing, immunoprecipitation with specific antibodies, DNA sample-clean up and PCR.

ChIP experiments performed in two different cell lines confirmed that MITF transcription factor interacts with the *MIR211* promoter region. Moreover, the amount of MITF protein bound to the *MIR211* promoter region was significantly increased upon autophagy induction by torin1 in HeLa (Figure 3.2 A) and SK-MEL-28 (Figure 3.2 B) cells.

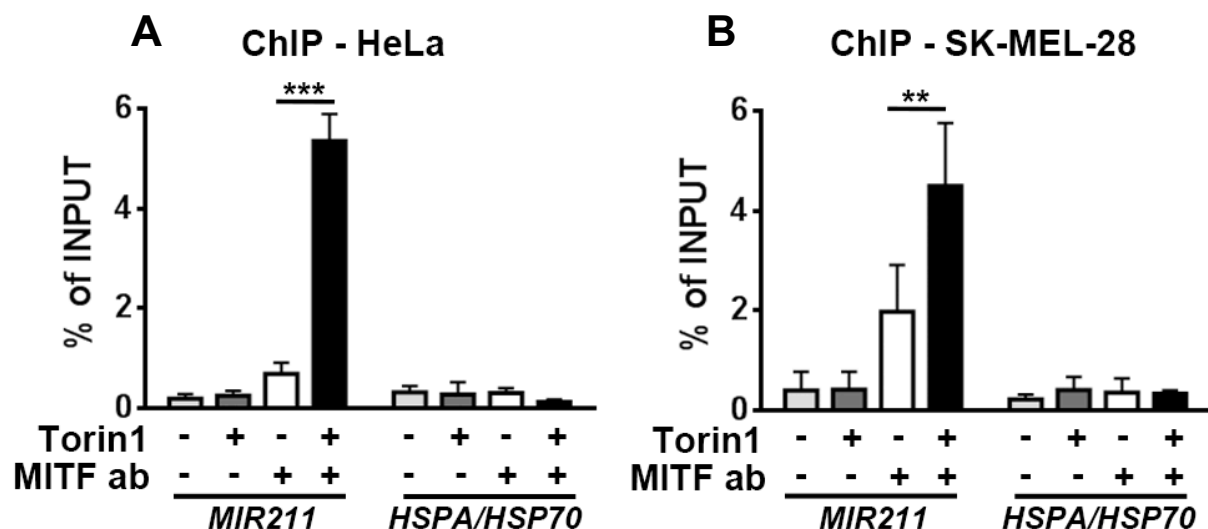


Figure 3.2 3: MITF-MIR211 promoter interaction analysis using ChIP assays. ChIP assays showing specific association of MITF with the *MIR211* promoter region in HeLa (A) and SK-MEL-28 (B) cells under DMSO or torin1-treated conditions. qPCR results of *MIR211* promoter primers were obtained from input (pre-IP) samples or following ChIP with MITF antibodies. Ct (threshold cycle) ratios were normalized (Ct^{ChIP}/Ct^{input}). In control (CNT) ChIP experiments, no antibody was added. *HSPA/HSP70* promoter primers were used as negative control (mean±SD of n=3 independent experiments, ***p<0.01, **p<0.03).

As presented in Figure 3.2 3, it was shown for the first time that MITF controlled basal and autophagic stress-induced *MIR211* levels in cells.

Moreover, in ChIP experiments, MITF could bind to the promoter of *LC3B* and, when autophagy was stimulated, MITF binding to the promoter was significantly increased in 2 different cell lines (Figure 3.2 4).

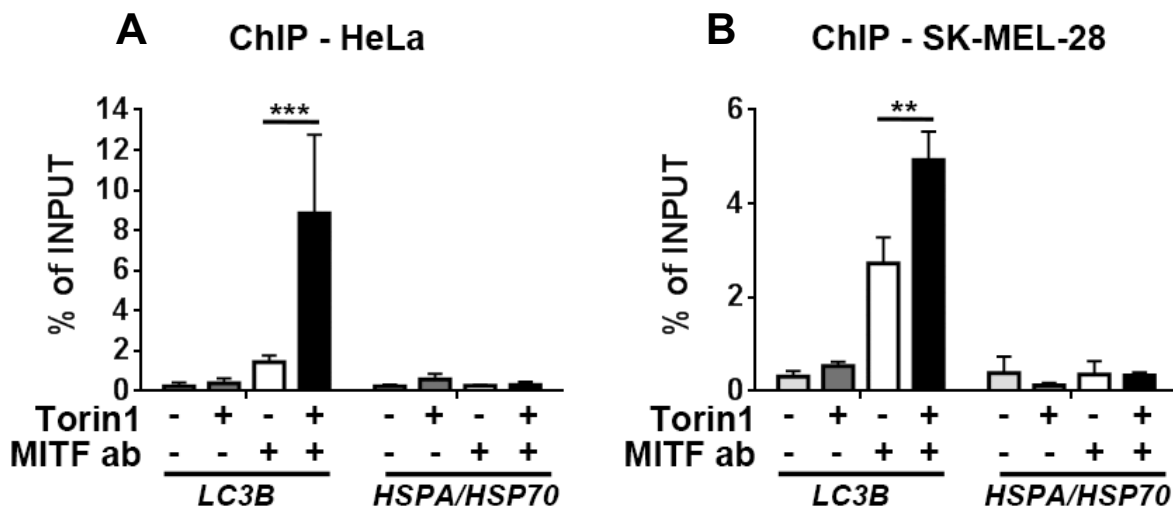


Figure 3.2 4: MITF-LC3 promoter interaction analysis using ChIP. Chromatin immunoprecipitation (ChIP). (A and B) ChIP assays showing specific association of MITF with the *LC3B* promoterregion in HeLa (A) and SK-MEL-28 (B) cells under DMSO-or torin1-treated conditions. qPCR results of *LC3B* promoter primers were obtained from input (pre-IP) samples or following ChIP with MITF antibodies. Ct (threshold cycle) ratios were normalized (Ct^{ChIP}/Ct^{input}). In control ChIP experiments, no antibody was added (MITF ab [-]). *HSPA/HSP70* promoter primers were used as a negative control (mean \pm SD of n=3 independent experiments, ***p<0.01, **p<0.03).

Next, to check whether the expression of MITF and its target *MIR211* is in correlation MITF and *MIR211* co-expression was analyzed in several cell lines originating from different tissue types. A positive correlation ($r=0.983$, $p=0.0004$) was found between *MIR211* and *MITF* mRNA expression in cell lines including MCF-7, SH-SY5, HEK293T, MDA-MB-231, HeLa

and SK-MEL-28 (Figure 3.2 5A). Moreover, MITF protein expression in all these cell lines was also confirmed by immunoblotting analysis with pan-MITF antibody which recognizes all isoforms (Figure 3.2 5B).

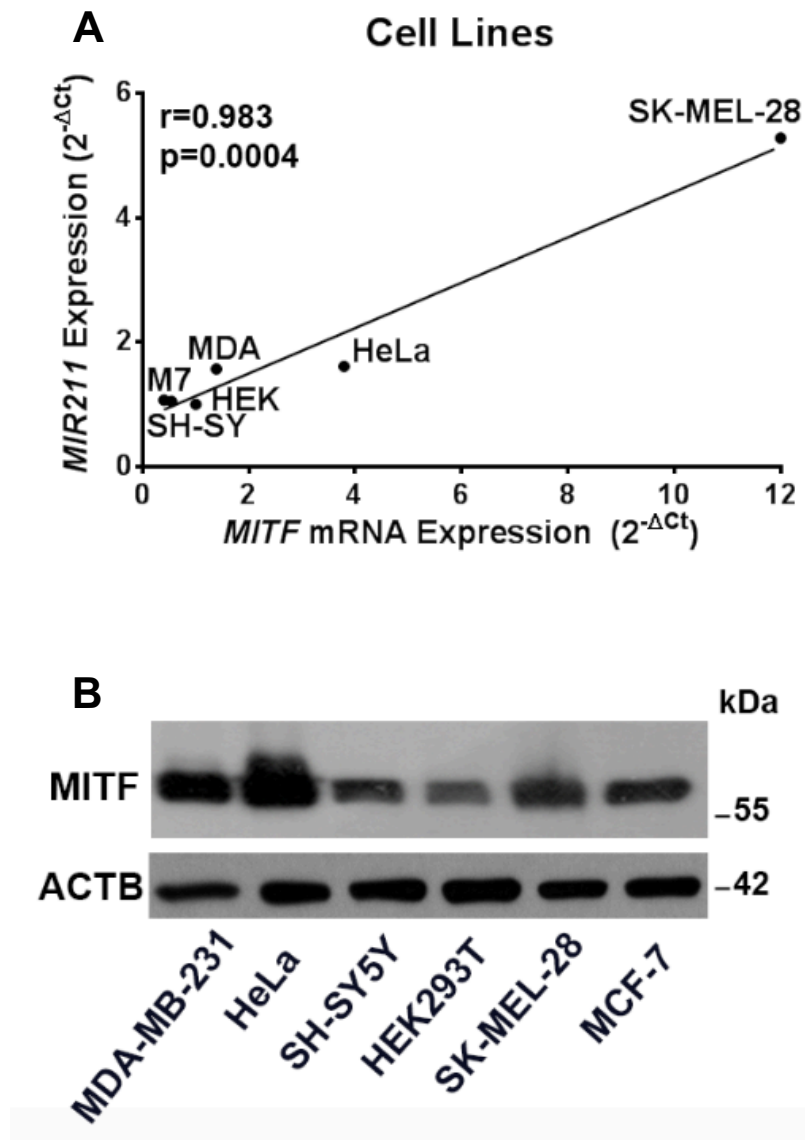


Figure 3.2 5: Correlation of endogenous *MIR211* and *MITF* mRNA levels in various cell lines. (A) A positive correlation between endogenous *MIR211* and *MITF* mRNA levels was determined by RT-qPCR in MDA-MB-231 (MDA), MCF-7 (M7), SH-SY5Y (SH-SY), HEK293T (HEK), HeLa and SK-MEL-28 cells. r , Pearson's correlation coefficient. ($r > 0$, positive correlation; p value=0.004). (B) Expression of MITF protein was detected in MDA-MB-231, HeLa, SH-SY5Y, HEK293T, SK-MEL-28, MCF-7 cells using a pan-MITF antibody.

Additionally, analyses of RNAs that were isolated from various human tissues showed a positive correlation ($r=0.729$, $p=0.0165$) between *MIR211* and *MITF* (Figure 3.2 6A). *MITF* protein expression was demonstrated in all studied human tissues as well (Figure 3.2 6B) and Fig. S3C).

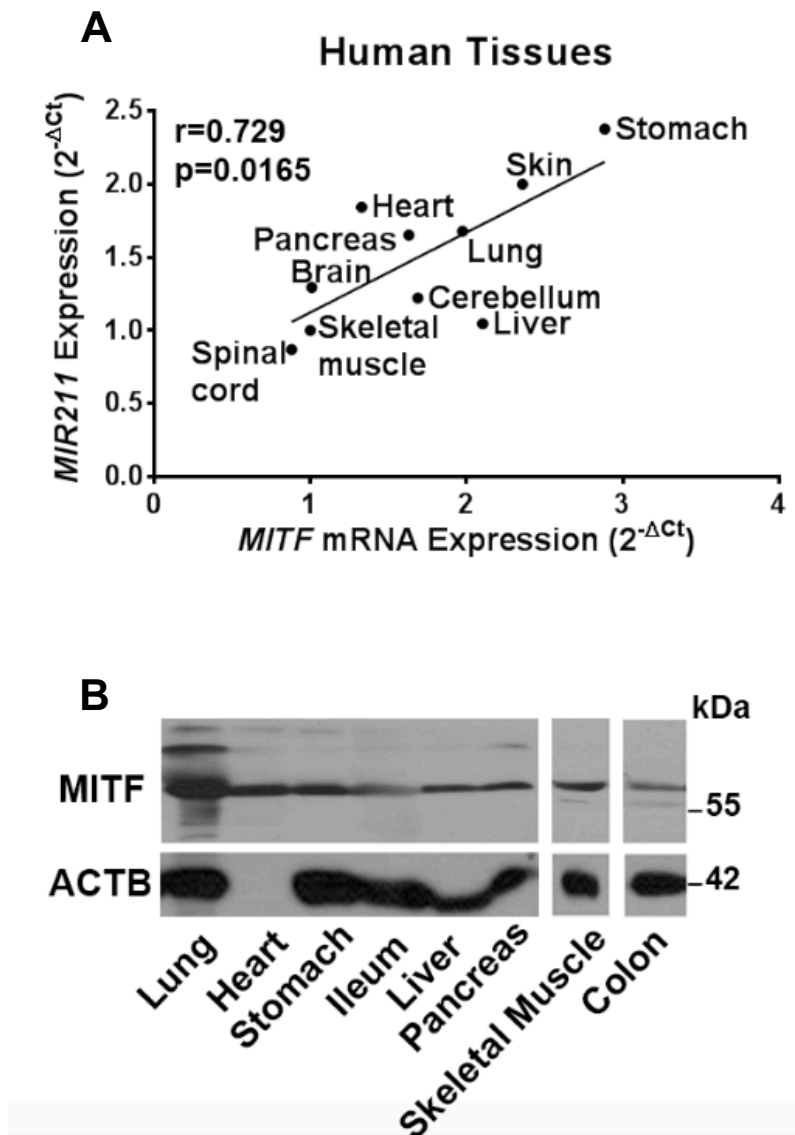


Figure 3.2 6: Correlation of endogenous *MIR211* and *MITF* mRNA levels in human tissues from 4 different cadavers. (A) A positive correlation between endogenous *MIR211* and *MITF* mRNA levels was determined by RT-qPCR in the indicated tissues (Pearson's r coefficient (r)= 0.729 , p value (p)= 0.0165). (B) Immunoblot analysis of tissue protein extracts from a cadaver using a pan-*MITF* antibody. ACTB was used as loading control.

To confirm our experimental results in larger datasets, correlation of *MIR211* and MITF expression was checked in publicly available expression data in different tissues and cell lines. First of all, NCI-60 datasets obtained from 60 different cancer cell lines showed that *MIR211* expression positively correlated with MITF expression in these cell lines (Figure 3.2 7) ($r=0.762$, $p<0.0001$).

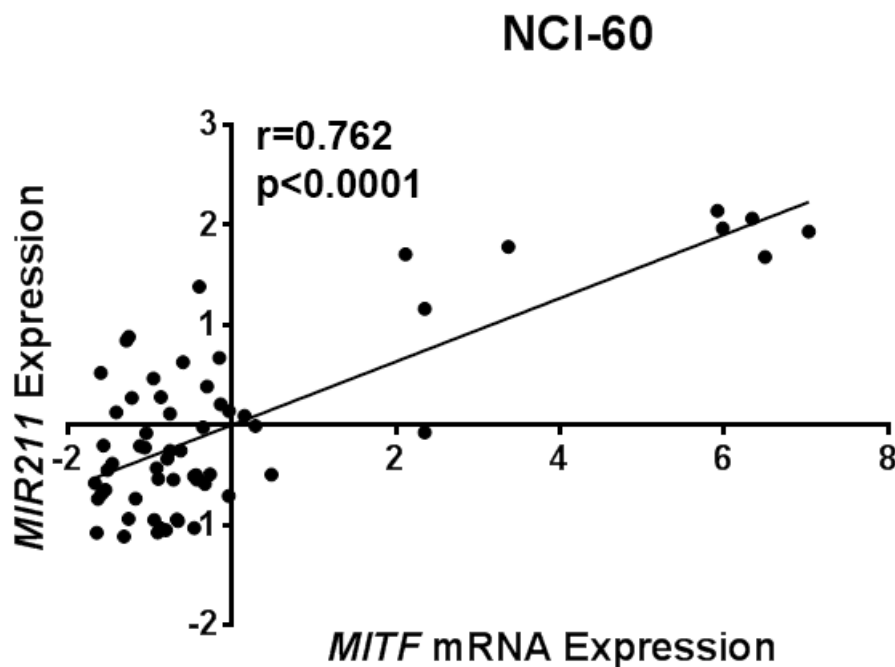


Figure 3.2 7: Correlation of *MIR211* and MITF mRNA expression using NCI-60 expression dataset. The correlation between miRNA and gene expression profile is quantified by computing the correlation coefficient using the NCI-60 expression profiling data (M) (Pearson's r coefficient (r)= 0.762 , p value (p) <0.0001)

The Cancer Genome Atlas (TCGA) cancer tissue data subsets were also analyzed. Subsets providing suitable sample size (see Materials and Methods) were skin cutaneous melanoma, pan-kidney cohort, testicular germ cell tumors, glioma and ovarian serous cystadenocarcinoma datasets. While a high correlation of *MIR211*-MITF expression was observed in the skin cutaneous melanoma subset ($r=0.745$, $p<0.0001$) (Figure 3.2 8), a variable but positive correlation was present in the pan-kidney cohort ($r=0.11$, $p=0.0052$), testicular germ cell tumors ($r=0.26$, $p=0.0034$) and glioma ($r=0.22$, $p<0.0001$) subsets. A similar tendency

was observed in the ovarian serous cystadenocarcinoma dataset ($r=0.13$, $p=0.0661$) (Figure 3.2 9).

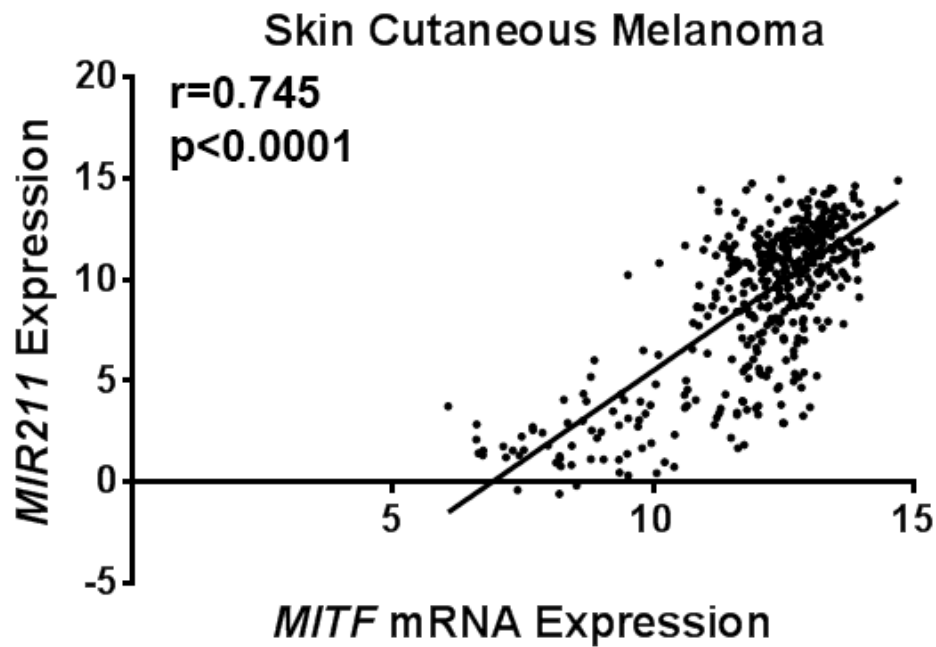


Figure 3.2 8: Correlation of MIR211 and MITF mRNA expression using TCGA SKCM expression dataset. The correlation between miRNA and gene expression profile is quantified by computing the correlation coefficient using TCGA Skin Cutaneous Melanoma (N) (Pearson's r coefficient (r)=0.745, p value (p)<0.0001) microRNA and gene expression data.

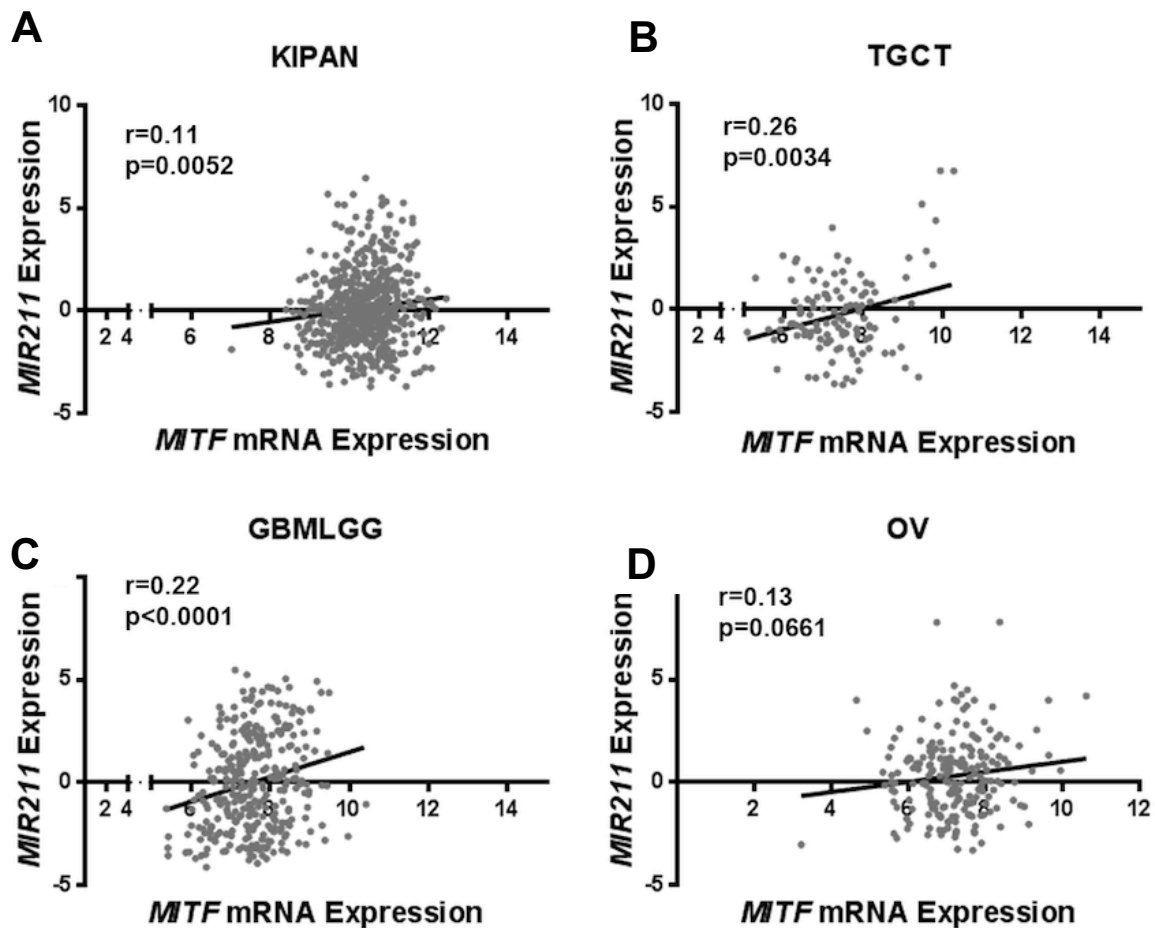


Figure 3.2 9: Correlation of MIR211 and MITF mRNA expression using various TCGA expression datasets. Analysis of TCGA pan-kidney cohort (KIPAN) (A), testicular germ cell tumors (TGCT) (B), glioma (GBMLGG) (C), ovarian serous cystadenocarcinoma (OV) (D) datasets for *MIR211* and *MITF* mRNA expression correlation.

Therefore, all of the above data demonstrated for the first time that, in addition to *LC3B* and *ATG10*, MITF regulated *MIR211* expression under autophagy-inducing conditions. Because both MITF and *MIR211* are co-expressed in cell lines and human tissues that were tested in this study, a MITF-*MIR211* axis might play a role in general autophagy control.

3.3 *MIR211* induced autophagy

Our results showed that MITF is indispensable for mTOR-mediated and starvation-induced autophagy. To clarify the role of *MIR211* in MITF-dependent autophagy regulation, several independent autophagy tests were performed (Figure 3.3 1)

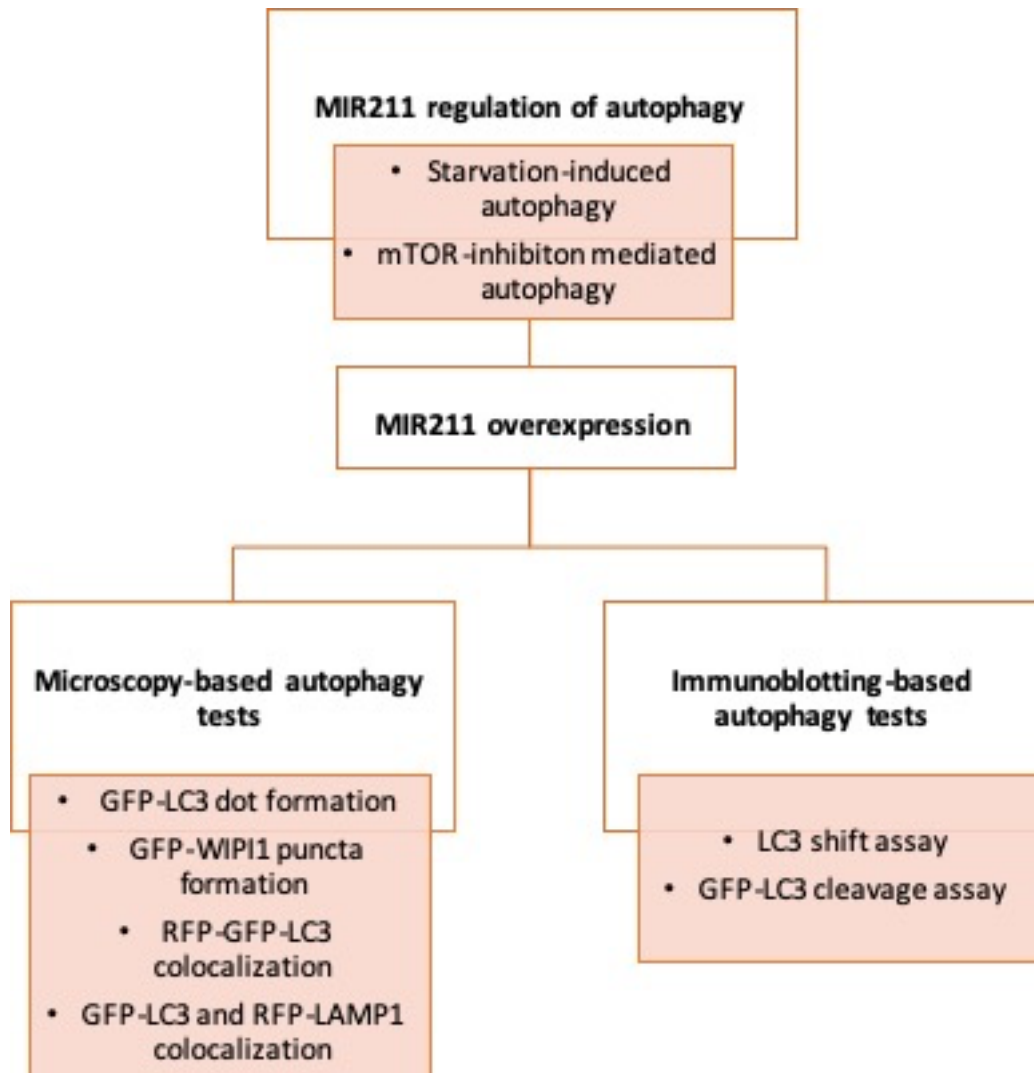


Figure 3.3 1: The pipeline of experiments demonstrating the effect *MIR211* overexpression on autophagy.

3.3.1 Effect of MIR211 on basal autophagy

In order to test the effect of *MIR211* on autophagy, we overexpressed miRNA mimic and control constructs in cells and checked for autophagic flux. Overexpression of *MIR211* but not the control construct (*MIR-CNT*) induced GFP-LC3 dot formation (Figure 3.3.1 1) under fed conditions in HeLa cells. Moreover, *MIR211* overexpression further increased GFP-LC3 dot formation upon lysosomal inhibition by E64D and pepstatin A. These results showed that *MIR211* stimulated autophagosome formation and did not prominently affect autophagosome-lysosome fusion (Figure 3.3.1 1).

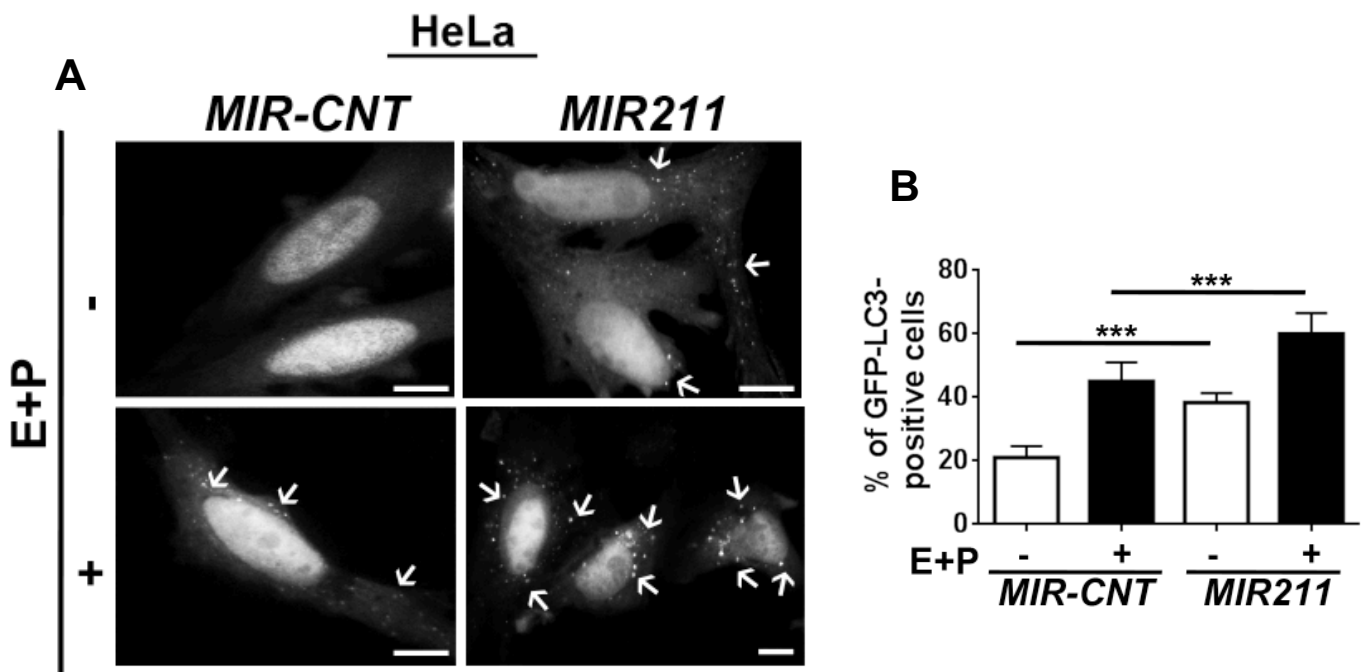


Figure 3.3.1 1: Effect of MIR211 on GFP-LC3 dot formation following lysosomal inhibition in HeLa cells. (A) HeLa-GFP-LC3 stable cells transfected with *MIR211* or a control construct (*MIR-CNT*), and autophagy was assessed in the presence and absence of lysosomal inhibitors. (Scale bar, 10 μ m. (B) Quantitative analysis of GFP-LC3 dots in the experimental set-up shown in A (mean \pm SD of n=3 independent experiments, ***p<0.01).

Similarly, immunoblotting experiments confirmed that *MIR211* overexpression promotes LC3-II accumulation in the presence of lysosomal inhibition, hence induces autophagosome-lysosome fusion in HeLa cells (Figure 3.3.1 2).

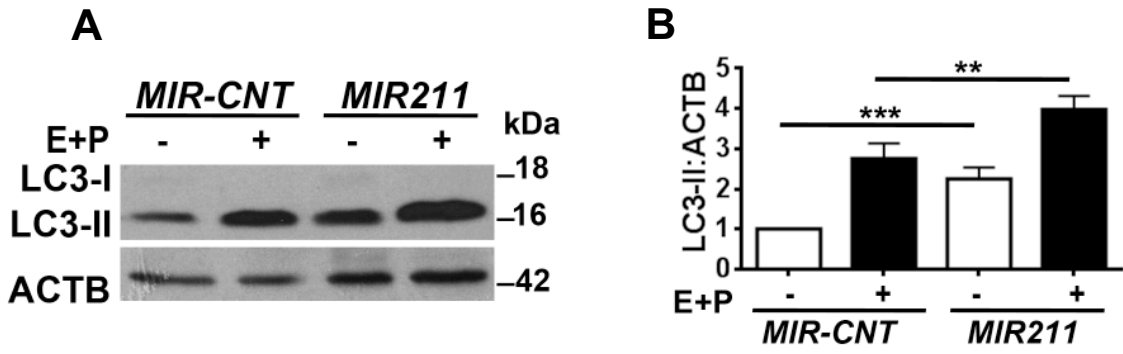


Figure 3.3.1 2: Effect of MIR211 on LC3-II accumulation following lysosomal inhibition in HeLa cells. (A) Autophagy-related LC3-II levels were analyzed in immunoblots of *MIR-CNT*-or *MIR211*-overexpressing HeLa cell extracts. (B) Graph depicting quantification of LC3-II:ACTB ratios in the experimental set-up shown in A (mean±SD, n=3 independent experiments, ***p<0.01, **p<0.03).

Next, the effect of *MIR211* overexpression on autophagic activity was also analyzed in SK-MEL-28 cells using immunofluorescence- and immunoblotting-based autophagy assays and the results are presented in Figure 3.3.1 3 and Figure 3.3.1 4, respectively.

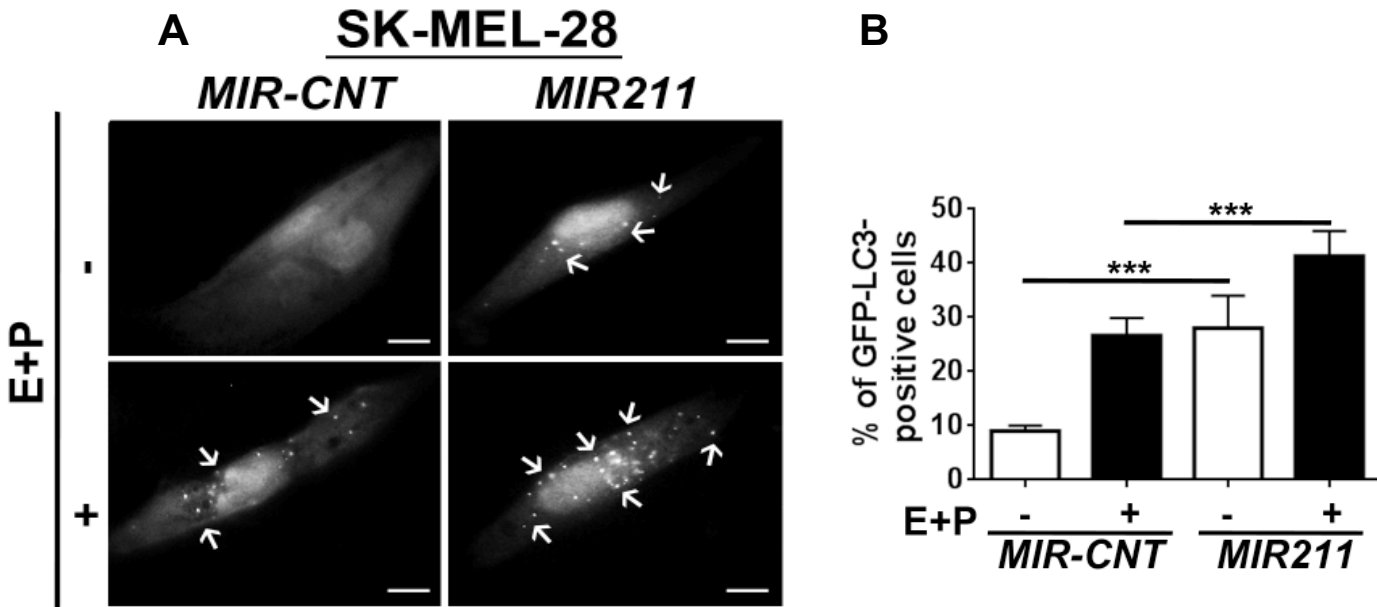


Figure 3.3.1 3: Effect of MIR211 on GFP-LC3 dot formation following lysosomal inhibition in SK-MEL-28 cells. (A) SK-MEL-28 cells transiently transfected with GFP-LC3 plasmid and *MIR211* or a control construct (*MIR-CNT*), and autophagy was assessed in the presence and absence of lysosomal inhibitors. *MIR211* overexpression increased GFP-LC3 dot formation. Scale bar, 10 μ m. (B) Quantitative analysis of GFP-LC3 dots in the experimental set-up shown in A (mean \pm SD of n=3 independent experiments, ***p<0.01).

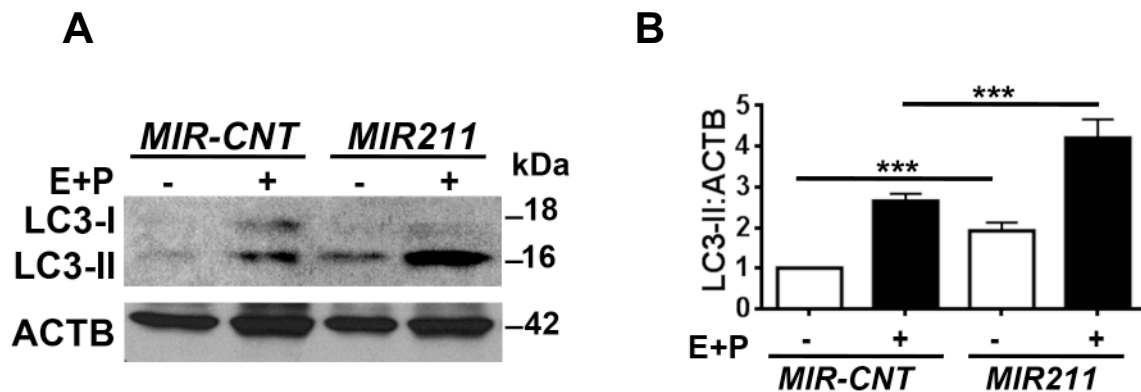


Figure 3.3.1 4: Effect of *MIR211* on LC3-II accumulation following lysosomal inhibition in SK-MEL-28 cells. (A) Autophagy-related LC3-II levels were analyzed in immunoblots of *MIR-CNT*- or *MIR211*-overexpressing SK-MEL-28 cell extracts. (B) Graph depicting quantification of LC3-II:ACTB ratios in the experimental set-up shown in A (mean \pm SD, n=3 independent experiments, ***p<0.01).

3.3.2 Effect of *MIR211* on torin1-induced autophagy

Moreover, the effect of *MIR211* on autophagy that was stimulated by torin1 treatment was checked in two different cell lines using LC3 shift assay. Torin1-induced autophagy was further induced in both HeLa (Figure 3.3.2 1) and SK-MEL-28 (Figure 3.3.2 2) cells following *MIR211* overexpression. Following lysosomal inhibition, LC3-II accumulation was further increased under these conditions upon *MIR211* overexpression.

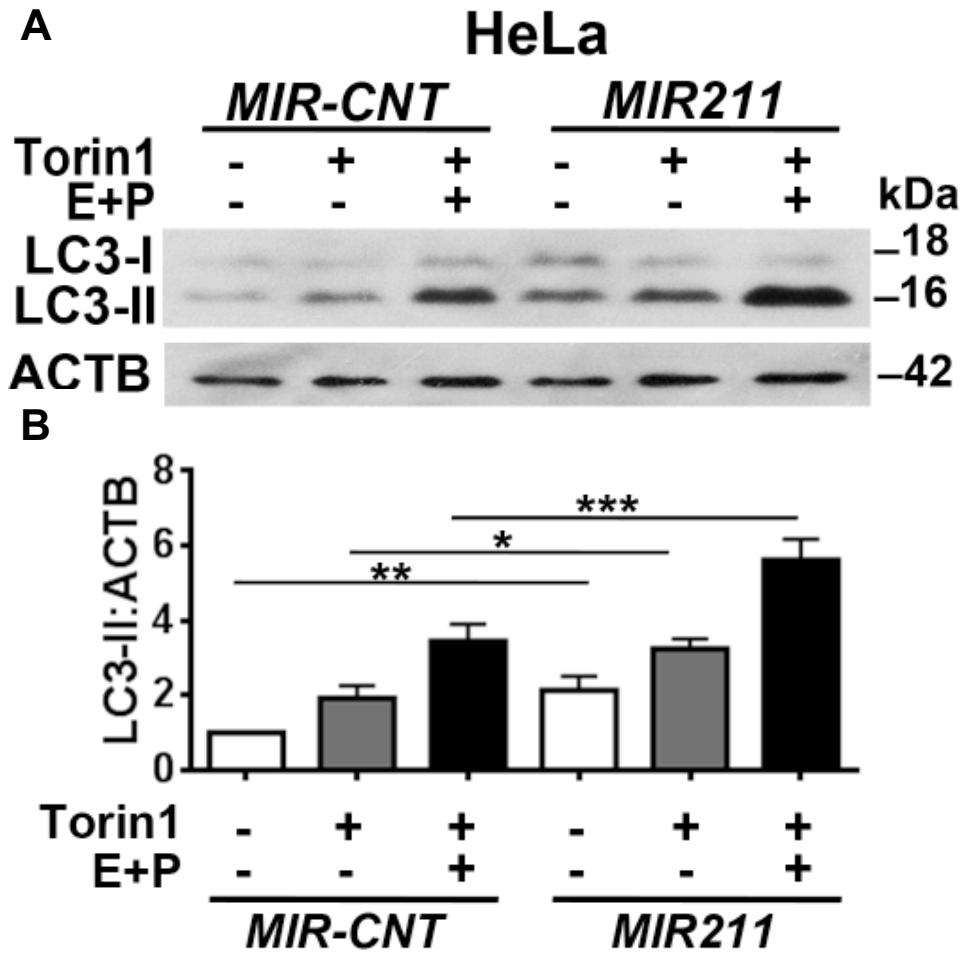


Figure 3.3.2 1: Effect of *MIR211* on LC3-II accumulation following torin1 treatment in HeLa cells. (A) Immunoblots of *MIR-CNT*- or *MIR211*-transfected HeLa cells that were treated with DMSO or torin1 (200 nM, 4h). (B) Graph depicting quantification of LC3-II:ACTB ratios in the experimental set-up shown in A (mean±SD, n=4 independent experiments, ***p<0.01, **<0.03, *p<0.05).

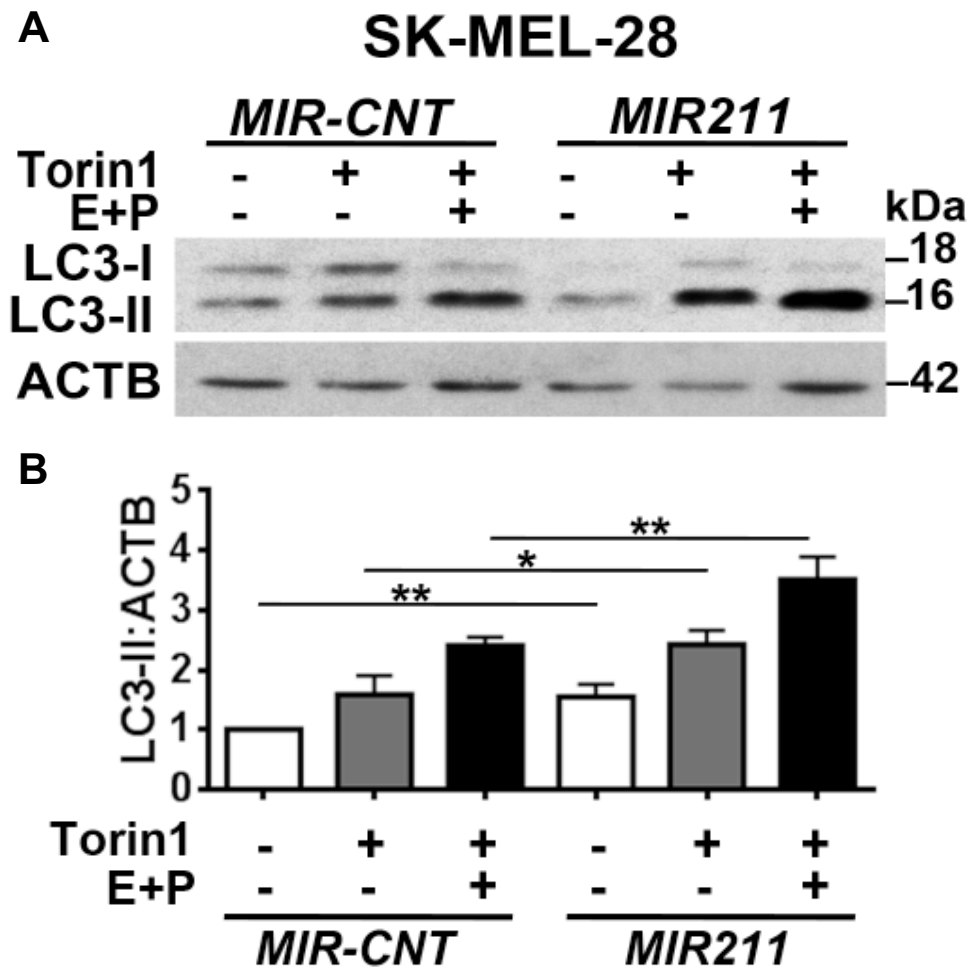


Figure 3.3.2 2: Effect of *MIR211* on LC3-II accumulation following torin1 treatment in SK-MEL-28 cells. (A) Immunoblots of *MIR-CNT*- or *MIR211*-transfected HeLa cells that were treated with DMSO or torin1 (200 nM, 4h). E+P, E64D and pepstatin A. (B) Graph depicting quantification of LC3-II:ACTB ratios in the experimental set-up shown in A (mean±SD, n=5 independent experiments, **p<0.03, *p<0.01).

To confirm the overexpression of *MIR211* in the above-mentioned immunoblotting experiments (Figure 3.3.2 1 and 3.3.2 2), RT-qPCR analyses were performed. Results for both HeLa and SK-MEL-28 cells are presented in Figure 3.3.2 3.

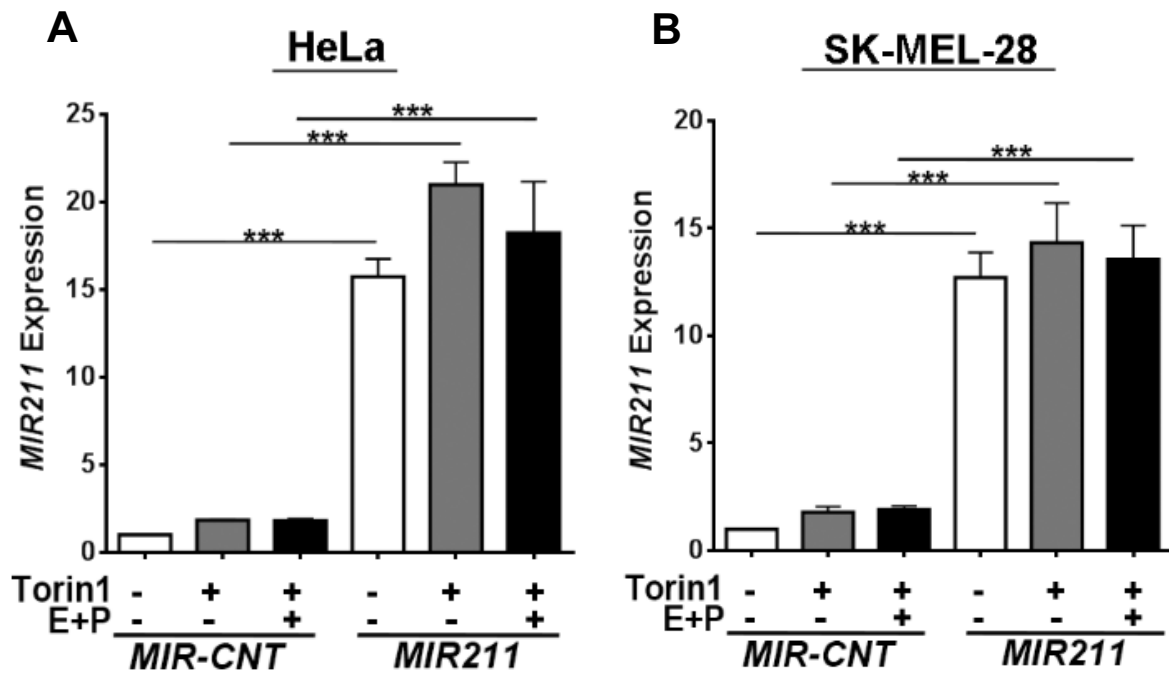


Figure 3.3.2 3: Confirmation of *MIR211* overexpression in Figure 3.3.2 1 and 3.3.2 2. *MIR211* levels were increased in HeLa (A, Figure 3.3.2 1) and SK-MEL-28 (B, Figure 3.3.2 2) cells following transfection with the *MIR211* expression plasmid (mean±SD, n=3 independent experiments, ***p<0.01).

Further analysis of the effect of *MIR211* on torin1-induced autophagy was carried out by GFP-WIPI1 dot formation assay. In line with LC3 tests, *MIR211* overexpression significantly increased GFP-WIPI1 dot formation following torin1 treatment (Figure 3.3.2 4) in HeLa cells.

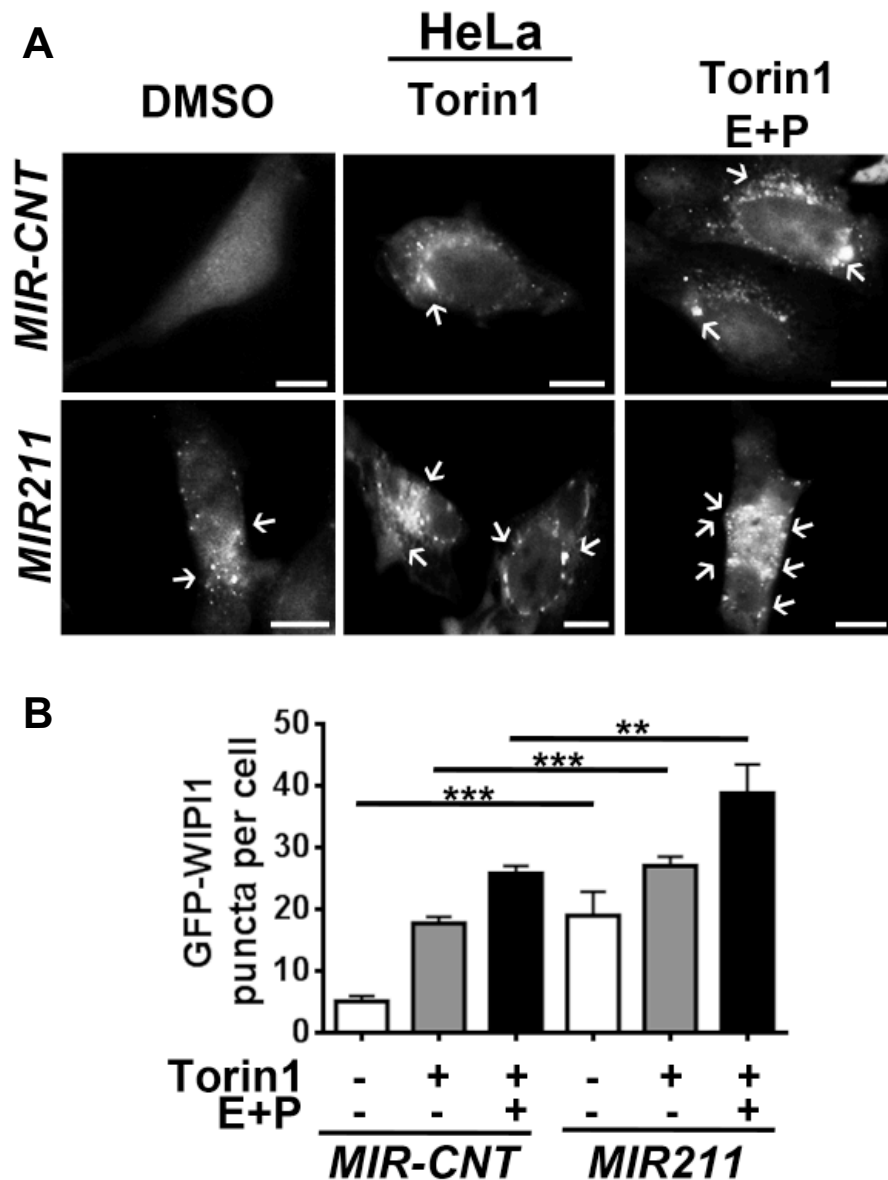


Figure 3.3.2 4: Effect of *MIR211* overexpression on GFP-WIPI1 puncta formation following torin1 treatment. (A) HeLa cells transiently transfected with GFP-WIPI1 plasmid construct and either *MIR-CNT* or *MIR211*, then incubated with torin1 (200 nM, 4 h) and analyzed under a fluorescence microscope. DMSO, carrier control. White arrows indicate the GFP-WIPI1 dots in the cells. Scale bar, 10 μ m. (B) Quantitative analysis of GFP-WIPI1 puncta in the experimental set-up shown in A (mean \pm SD of n=3 independent experiments, ***p<0.01, **<0.03).

3.3.3 Effect of *MIR211* on starvation-induced autophagy

Similar effect on LC3 shift in the presence of *MIR211* was obtained in starvation-induced autophagy. Autophagy that was stimulated by starvation was further upregulated in both HeLa (Figure 3.3.3 1) and SK-MEL-28 (Figure 3.3.3 2) cells when *MIR211* is introduced to the system. Following addition of lysosomal inhibitors, starvation-induced LC3-II was further accumulated upon *MIR211* overexpression.

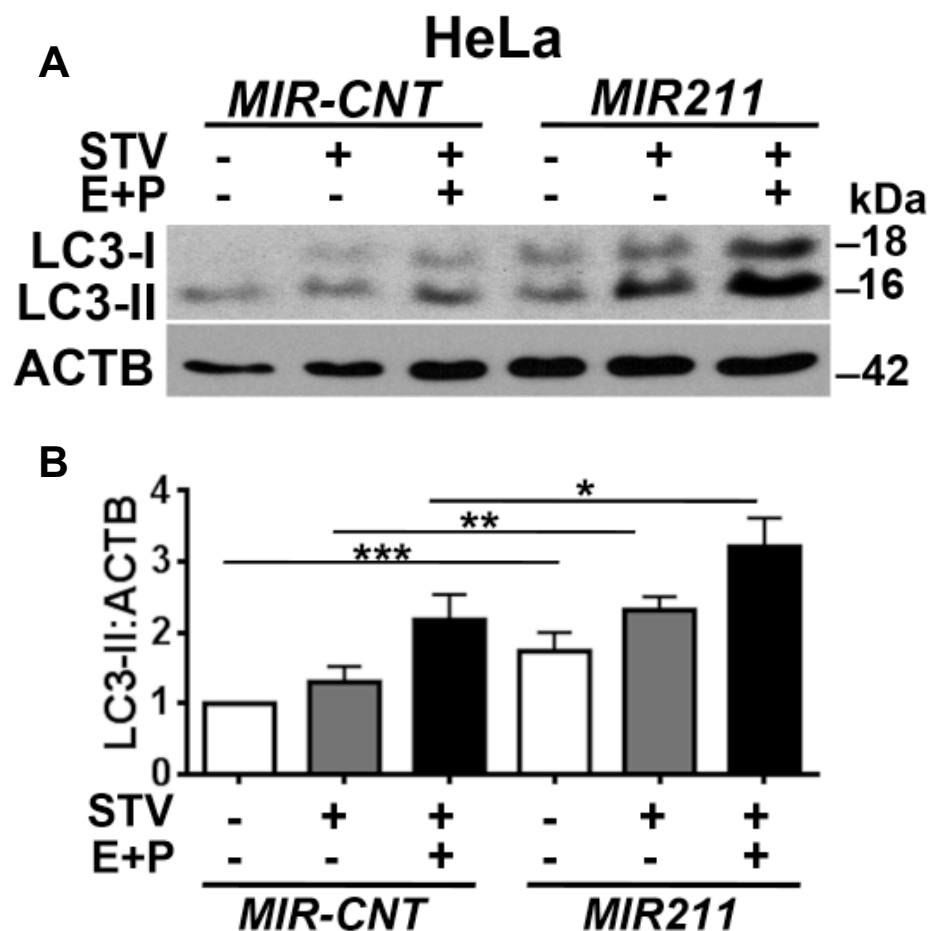


Figure 3.3.3 1: Effect of *MIR211* on LC3-II accumulation following starvation treatment in HeLa cells. (A) Immunoblots of HeLa cells transiently transfected with *MIR-CNT*- or *MIR211* and then non-starved or starved (STV) (EBSS, 4h). (B) Graph depicting quantification of LC3-II:ACTB ratios in the experimental set-up shown in A (mean±SD, n=3 independent experiments, ***p<0.01, **p<0.03, *p<0.05).

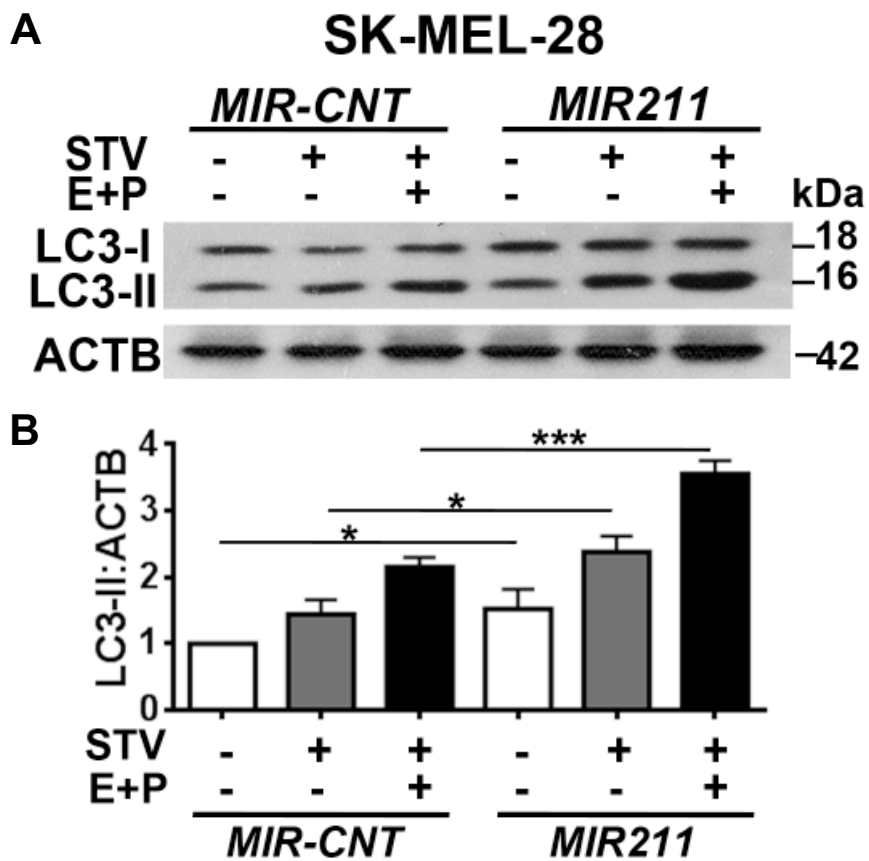


Figure 3.3.3 2 Effect of *MIR211* on LC3-II accumulation following starvation treatment in SK-MEL-28 cells. (A) Immunoblots of SK-MEL-28 cells transiently transfected with *MIR-CNT*- or *MIR211* and then non-starved or starved (STV) (EBSS, 4h). (B) Graph depicting quantification of LC3-II:ACTB ratios in the experimental set-up shown in A (mean±SD, n=3 independent experiments, ***p<0.01, *<0.05).

Moreover, overexpression of *MIR211* in the above-mentioned immunoblotting experiments (Figure 3.3.3 1 and 3.3.3 2) were confirmed using RT-qPCR. Results for both HeLa and SK-MEL-28 cells are presented in Figure 3.3.3 3.

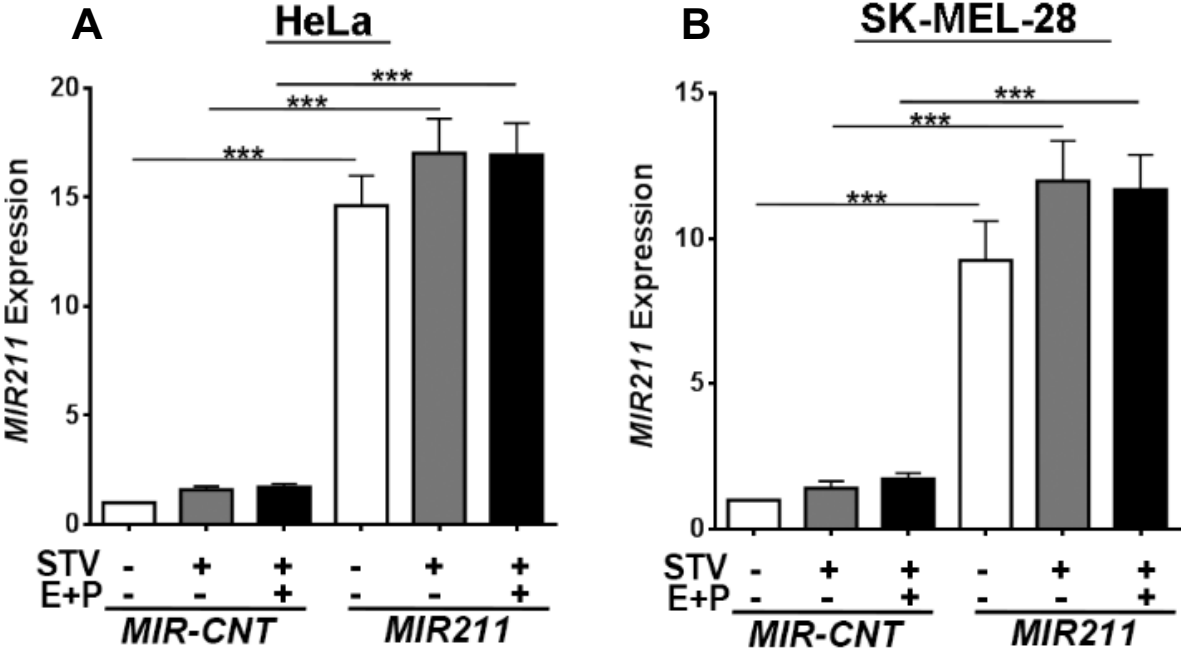


Figure 3.3.3 3: Confirmation of *MIR211* overexpression in Figure 3.3.3 1 and 3.3.3 2. *MIR211* levels were increased in HeLa (A) and SK-MEL-28 (B) cells following transfection with the *MIR211* expression plasmid (mean±SD, n=3 independent experiments, ***p<0.01).

These LC3 shift assay results were confirmed using another independent autophagy test, a GFP-WIP11 puncta formation assay following starvation treatment in HeLa cells (Figure 3.3.3 4).

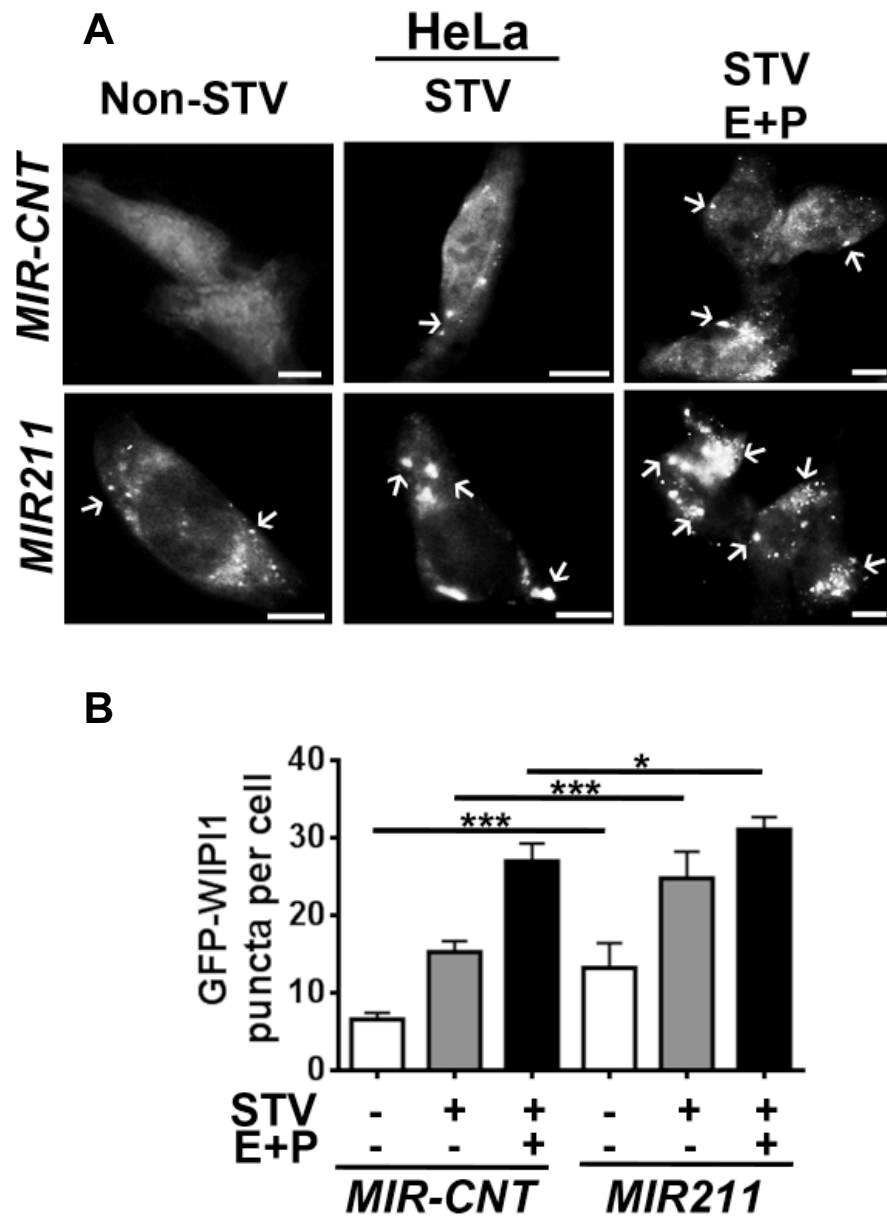
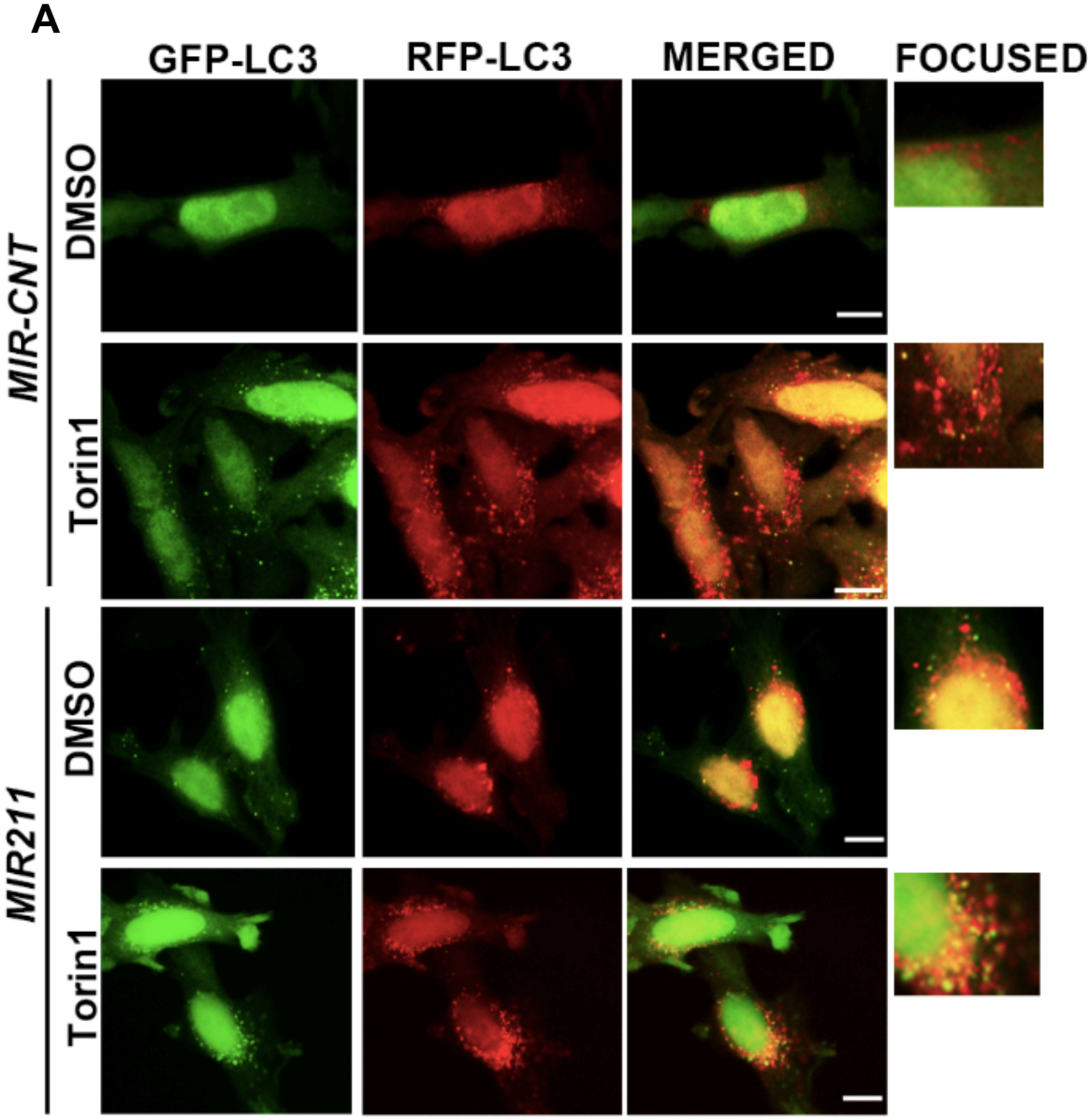


Figure 3.3.3 4: Effect of *MIR211* overexpression on GFP-WIP11 puncta formation following starvation. (A) HeLa cells transiently transfected with GFP-WIP11 plasmid construct and either *MIR-CNT* or *MIR211*, then non-starved or starved (EBSS, 4 h) and analyzed under a fluorescence microscope. STV, starvation. White arrows indicate the GFP-WIP11 dots in the cells. Scale bar, 10 μ m. (B) Quantitative analysis of GFP-WIP11 puncta in the experimental set-up shown in A (mean \pm SD of n=3 independent experiments, ***p<0.01, *<0.05).

To further provide evidence that *MIR211* stimulated productive autophagy that resulted in autophagosome-lysosome fusion and autophagic flux, quantitative GFP-RFP-LC3 analyses and GFP-LC3 and RFP-LAMP1 colocalization analyses were performed. *MIR211* overexpression stimulated an increase in both autophagosome and autolysosome numbers both in GFP-RFP-LC3 tests (Figure 3.3.3 5) and GFP-LC3 and RFP-LAMP1 colocalization analyses (Figure 3.3.3 6). All of these data showed that *MIR211* did not block autophagosome-lysosome fusion but rather stimulated autolysosome formation.



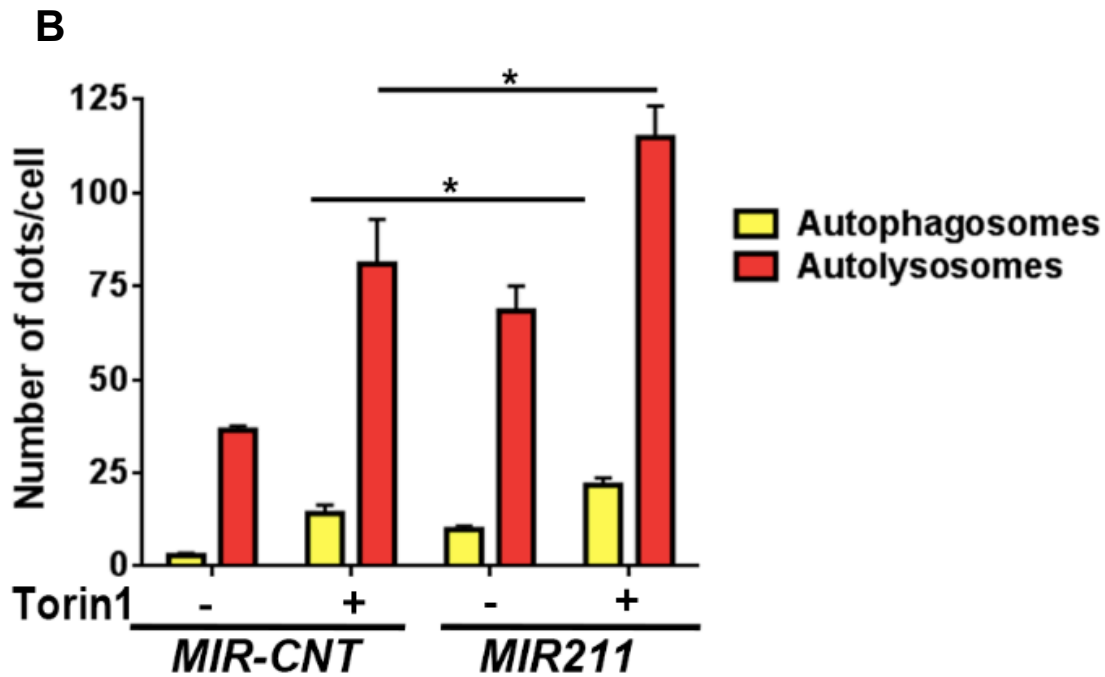


Figure 3.3.3 5: Effect of *MIR211* overexpression on GFP-RFP-LC3 colocalization following torin1 treatment. (A) *MIR211* overexpression increased the number of RFP⁺ GFP⁺ (yellow) and RFP⁺ GFP⁻ (red) dots per cell in DMSO- or torin1-treated HeLa cells. Yellow, autophagosomes; red, autolysosomes; merged, overlay of GFP-LC3 and RFP-LC3 signals; focused, higher magnification of a relevant region of the same cell. Scale bar, 10 μ m. (B) Quantitative analysis of autophagosome and autolysosome numbers in the experimental set-up shown in A (mean \pm SD, n=3 independent experiments, *p<0.01).

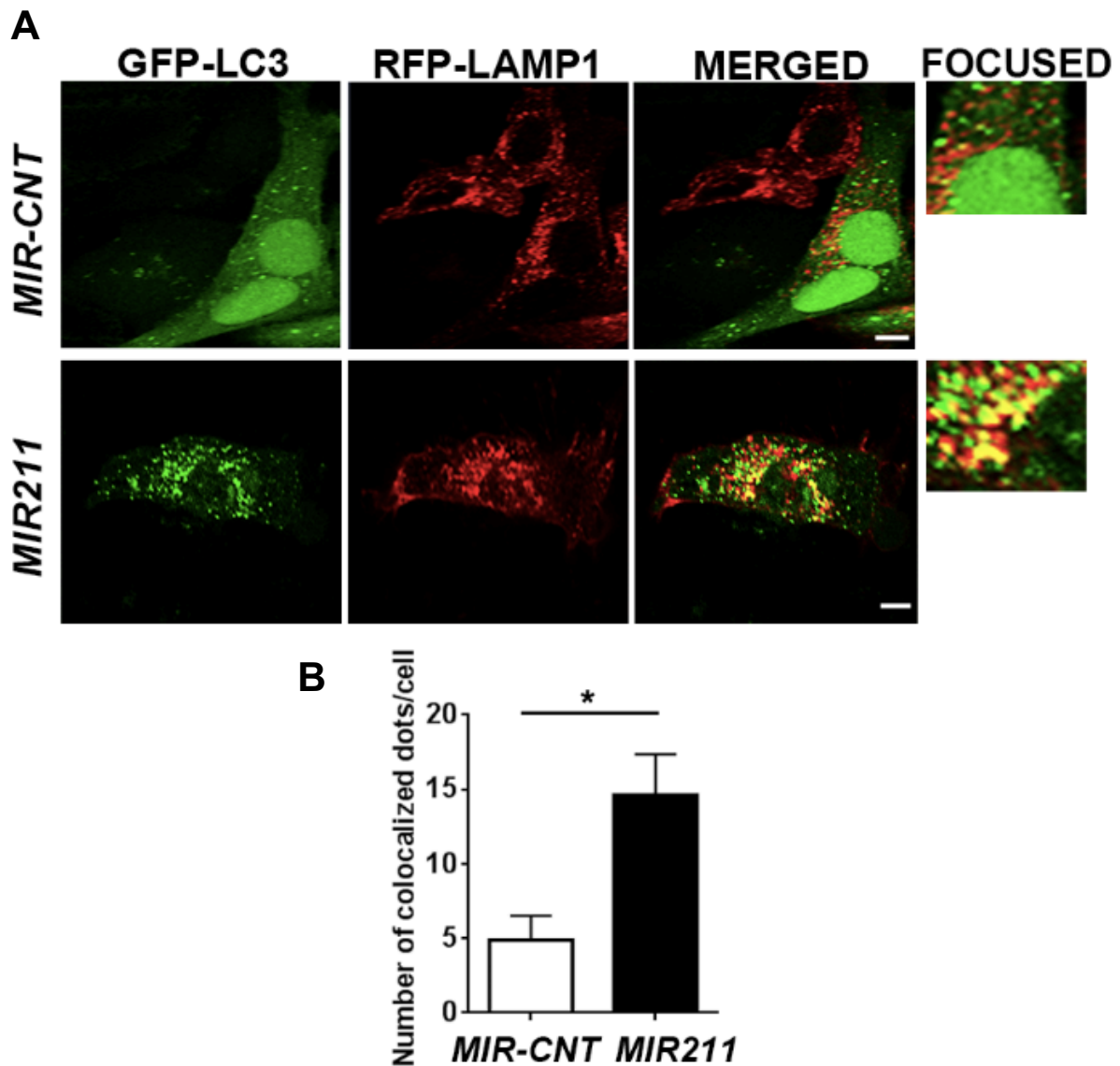


Figure 3.3.3 6: Effect of *MIR211* overexpression on GFP-LC3 and RFP-LAMP1 colocalization. (A) Colocalization of GFP-LC3 (autophagosomes) and RFP-LAMP1 (lysosomes) was stimulated by *MIR211* overexpression. Representative confocal microscopy images of *MIR-CNT* or *MIR211* transfected HeLa cells. Merged, overlay of GFP-LC3 and RFP-LAMP1 signals; yellow signal, colocalization; focused, higher magnification of a relevant region of the same cell. Scale bar, 10 μ m. (B) Quantitative analysis of colocalized autophagosomes and lysosomes in the experimental set-up shown in A (mean \pm SD, n=3 independent experiments, *p<0.05)

Finally, to monitor the effect of *MIR211* on breakdown of the autophagosomal cargo, GFP-LC3 lysosomal delivery and proteolysis tests were performed in the presence or absence of lysosomal inhibitors. These analyses showed that *MIR211* stimulated lysosome-dependent degradation of GFP-LC3. Free GFP accumulation was observed following *MIR211* overexpression, whereas inhibition of lysosomal proteases prominently decreased this accumulation (Figure 3.3.3 7).

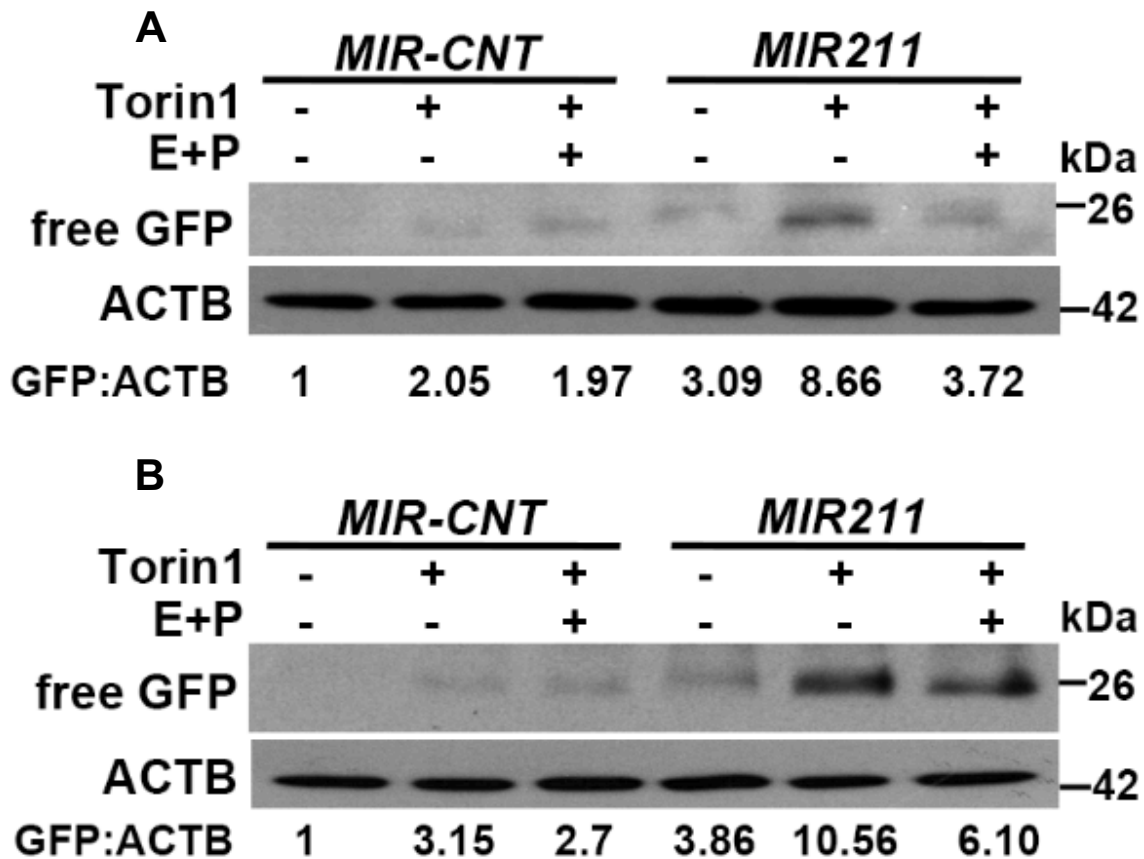


Figure 3.3.3 7: Effect of *MIR211* on GFP-LC3 lysosomal delivery and proteolysis. (A and B) HeLa cells were transiently co-transfected with GFP-LC3 and *MIR-CNT* or *MIR211* and treated with torin1 in the presence or absence of E64d and pepstatin A (E+P). Appearance of free GFP was analyzed in immunoblots. ACTB was used as a loading control. Results of 2 independent experiments (A and B) and ImageJ analyses of free GFP:ACTB ratios are shown.

Therefore, *MIR211* stimulated autophagosome and autolysosome formation and autophagic flux.

3.4 Inhibition of *MIR211* suppressed starvation- and MTOR-dependent autophagy.

To reveal the importance of endogenous *MIR211* in autophagy regulation, we inhibited endogenous miRNAs using chemically synthesized anti-*MIR211* antagomir oligonucleotides (*ANT211*) and checked torin1- or starvation-induced autophagy with GFP-LC3 and GFP-WIP1 dot formation tests and LC3 shift assay in the presence or absence of E64D-pepstatin A (Figure 3.4 1).

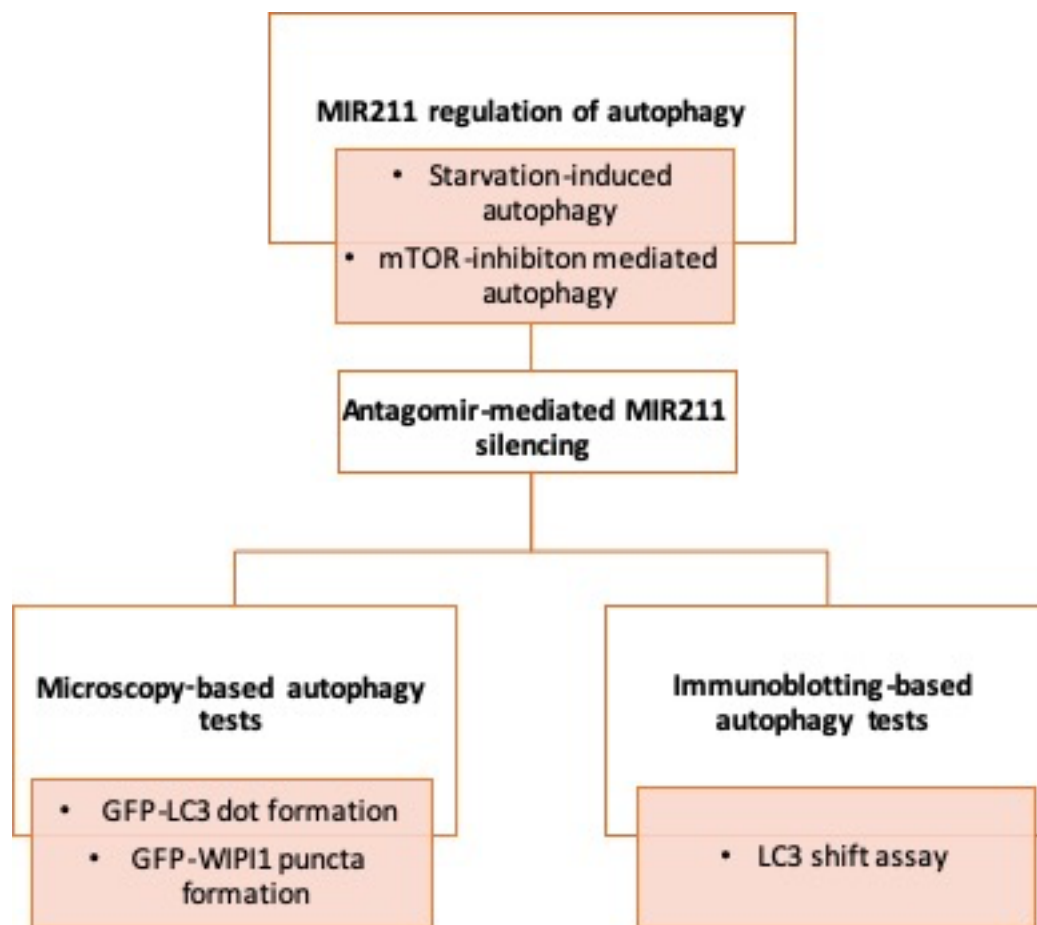


Figure 3.4 1: The pipeline of experiments demonstrating the effect of antagomir-mediated *MIR211* silencing on autophagy

First of all, introduction of specific antagomir nucleotides against *MIR211* was confirmed by checking endogenous *MIR211* expression levels in HeLa (Figure 3.4 2A) and SK-MEL28 (Figure 3.4 2B) cells.

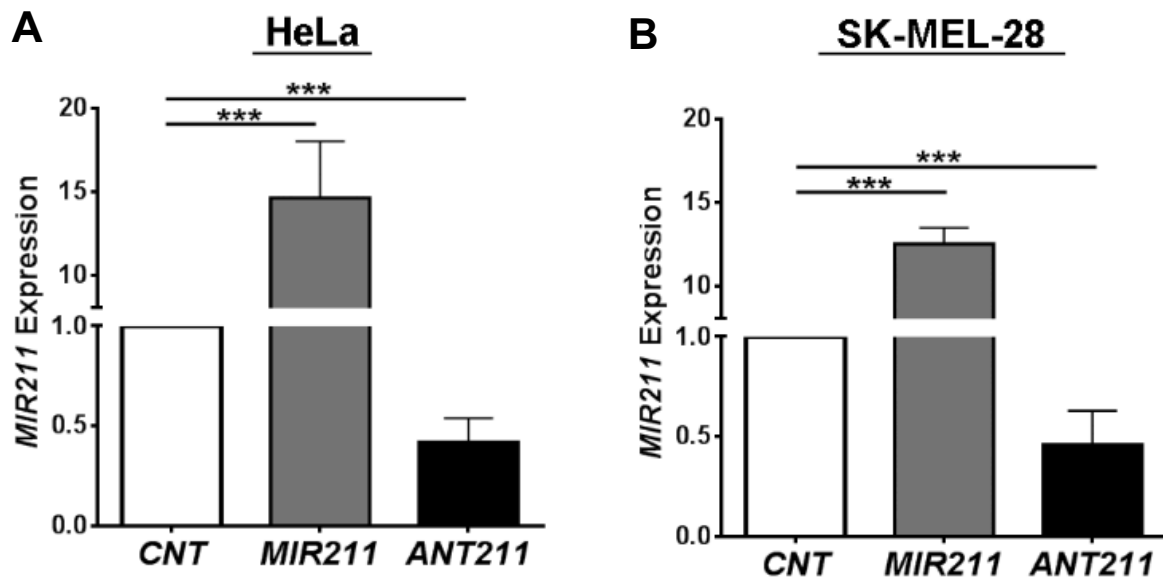


Figure 3.4 2: Confirmation of *MIR211* overexpression and antagomir (*ANT211*)-mediated silencing. *MIR211* levels were increased in HeLa (A) and SK-MEL-28 (B) cells following transfection with the *MIR211* construct whereas antagomir *ANT211* transfection significantly decreased endogenous *MIR211* levels in HeLa (A) and SK-MEL-28 (B) cells (mean±SD, n=3 independent experiments, ***p<0.01).

3.4.1 Effect of *ANT211* on torin1-induced autophagy

It was observed that introduction of *ANT211*, but not *ANT-CNT*, led to a decrease in GFP-LC3 dot numbers following torin1 treatment in HeLa (Figure 3.4.1 1) and SK-MEL-28 cells (Figure 3.4.1 2).

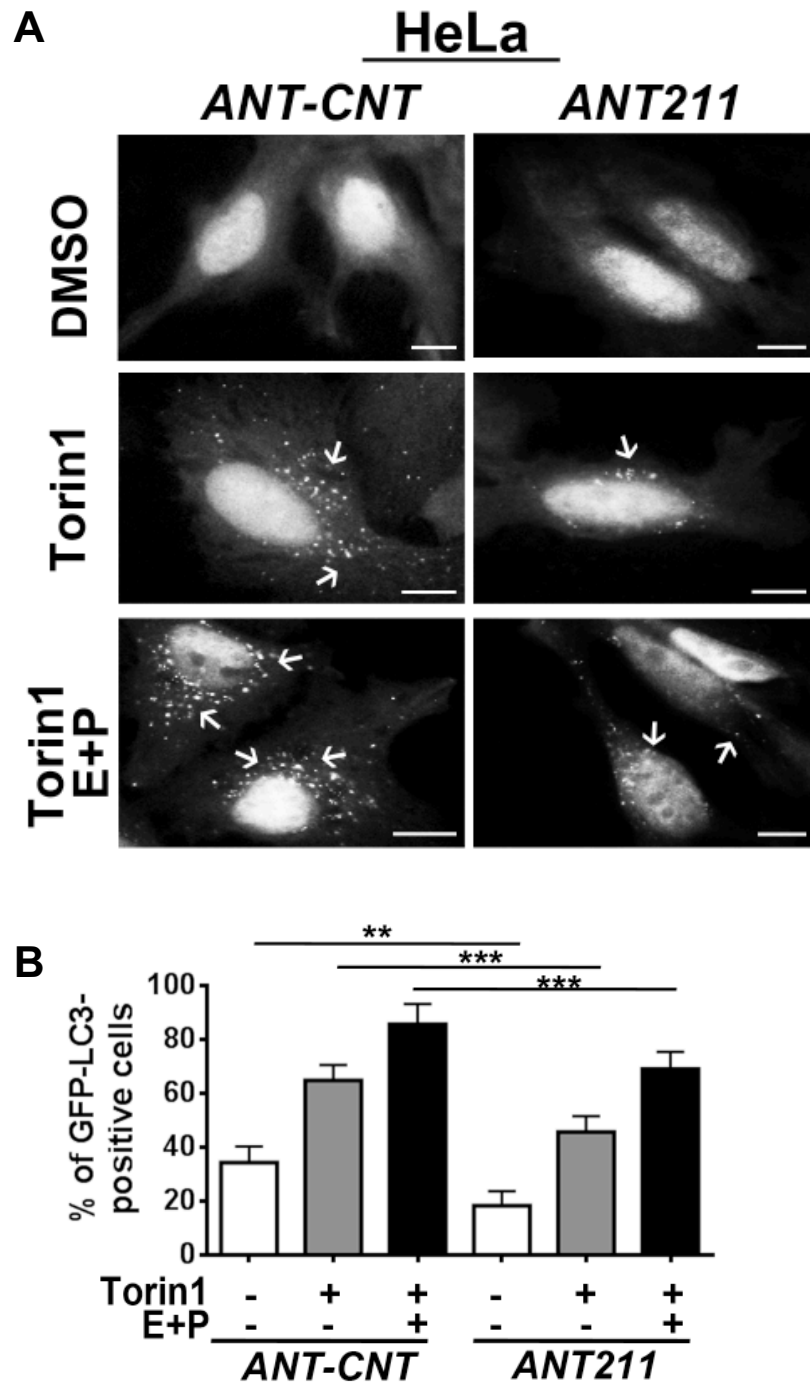


Figure 3.4.1 1: Effect of *ANT211* on GFP-LC3 dot formation following torin1 treatment in HeLa cells. (A) HeLa-GFP-LC3 stable cells transfected with either *ANT-CNT* (control antagomir) or *ANT211*, incubated with torin1 (200 nM, 4 h) and analyzed under a fluorescence microscope. DMSO, carrier control. White arrows indicate the GFP-LC3 dots in the cells. Scale bar, 10 μ m. (B) Quantitative analysis of GFP-LC3 dots in the experimental set-up shown in A (mean \pm SD of n=3 independent experiments, ***p<0.01, **p<0.03).

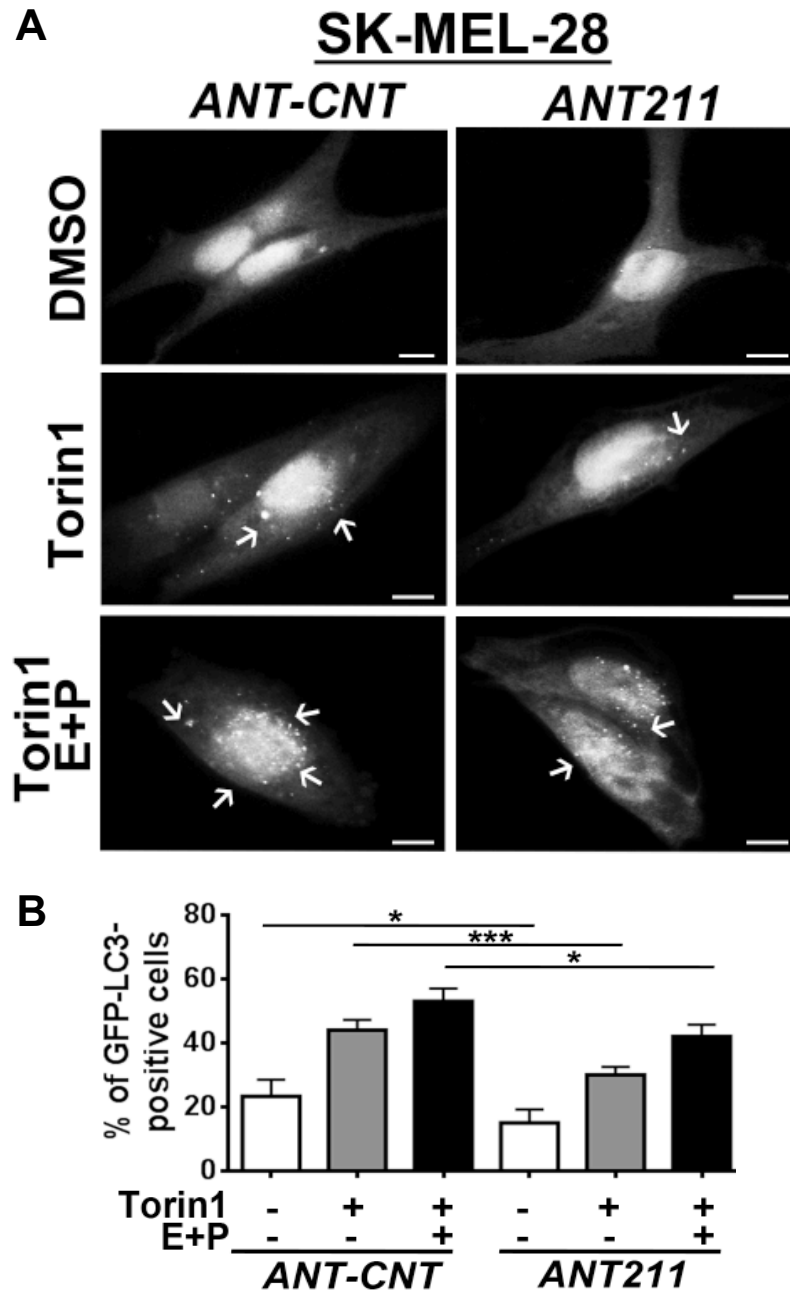


Figure 3.4.1 2: Effect of *ANT211* on GFP-LC3 dot formation following torin1 treatment in SK-MEL-28 cells. (A) SK-MEL-28 cells transiently transfected with either *ANT-CNT* (control antagomir) or *ANT211*, incubated with torin1 (200 nM, 4 h) and analyzed under a fluorescence microscope. DMSO, carrier control. White arrows indicate the GFP-LC3 dots in the cells. Scale bar, 10 μ m. (B) Quantitative analysis of GFP-LC3 dots in the experimental set-up shown in A (mean \pm SD of n=3 independent experiments, ***p<0.01, *p<0.05).

In line with GFP-LC3 dot formation results, the inhibitory effect of antagomir-mediated *MIR211* silencing on torin1-induced autophagy was confirmed using LC3 shift assay in HeLa (3.4.1 3) and SK-MEL-28 cells (Figure 3.4.1 4).

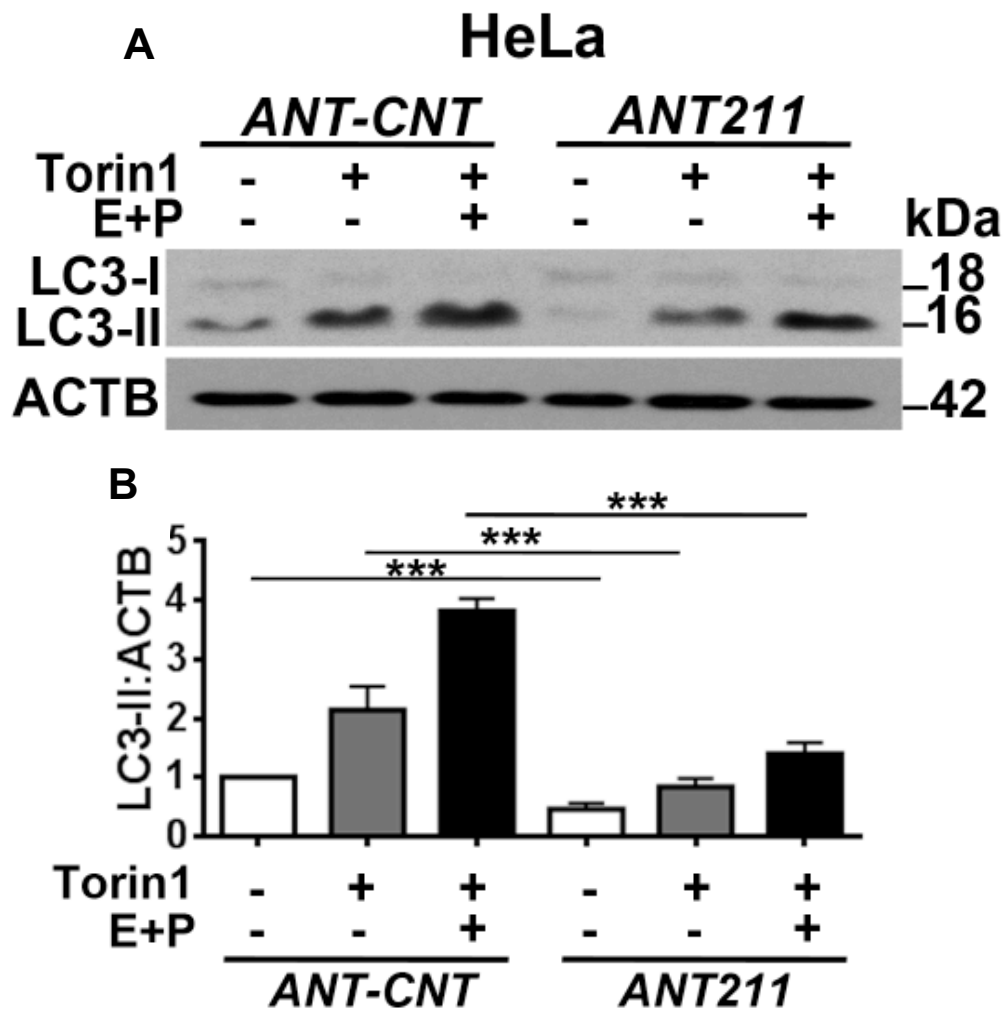


Figure 3.4.1 3: Effect of *ANT211* on LC3-II accumulation following torin1 treatment in HeLa cells. (A) Immunoblots of HeLa cells transiently transfected with either *ANT-CNT* (control antagomir) or *ANT211*, then incubated with DMSO or torin1 (200 nM, 4 h). (B) Graph depicting quantification of LC3-II:ACTB ratios in the experimental set-up shown in A (mean±SD, n=3 independent experiments, ***p<0.01).

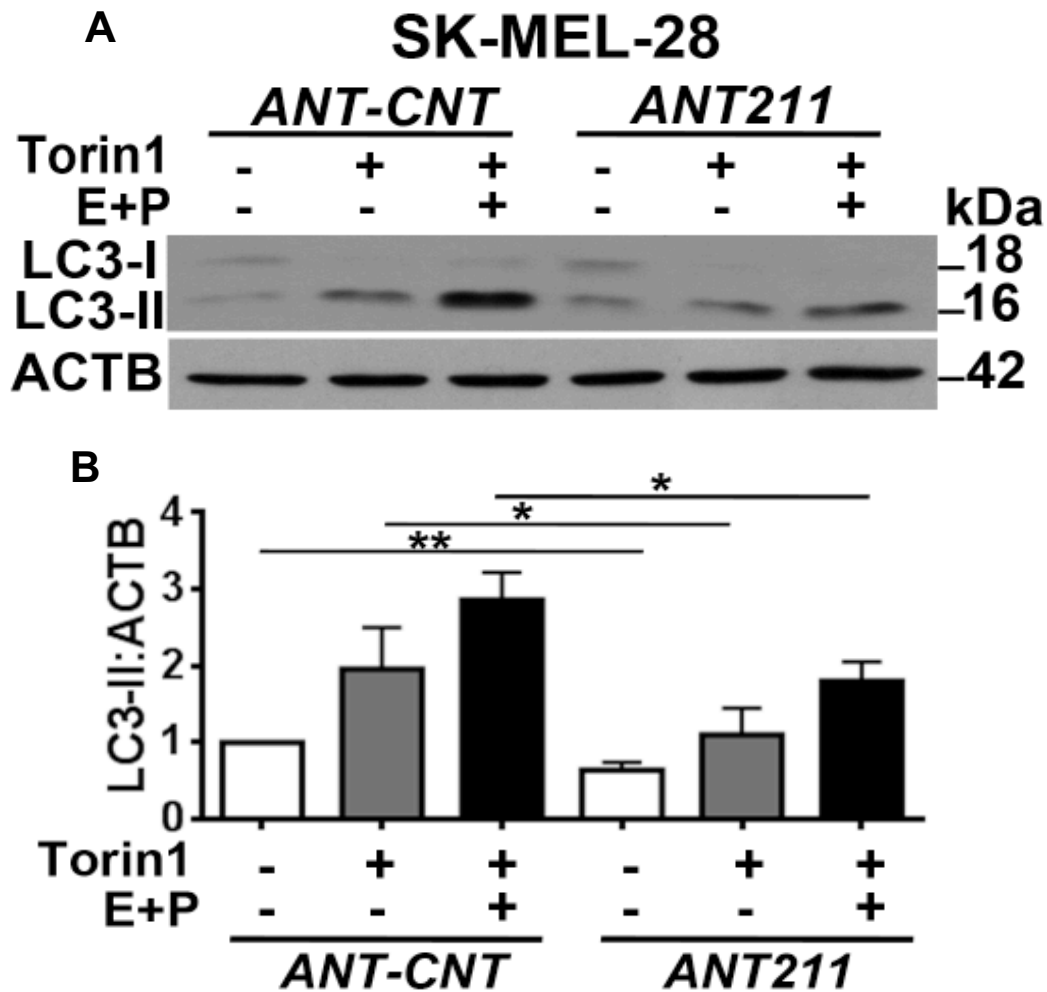


Figure 3.4.1 4: Effect of *ANT211* on LC3-II accumulation following torin1 treatment in SK-MEL-28 cells. (A) Immunoblots of SK-MEL-28 cells transiently transfected with either *ANT-CNT* (control antagomir) or *ANT211*, then incubated with DMSO or torin1 (200 nM, 4 h) (B) Graph depicting quantification of LC3-II:ACTB ratios in the experimental set-up shown in A (mean±SD, n=3 independent experiments, **p<0.03, *p<0.05).

MIR211-dependence of torin1-induced autophagy was also confirmed using GFP-WIP11 puncta formation tests (Figure 3.4.1 5).

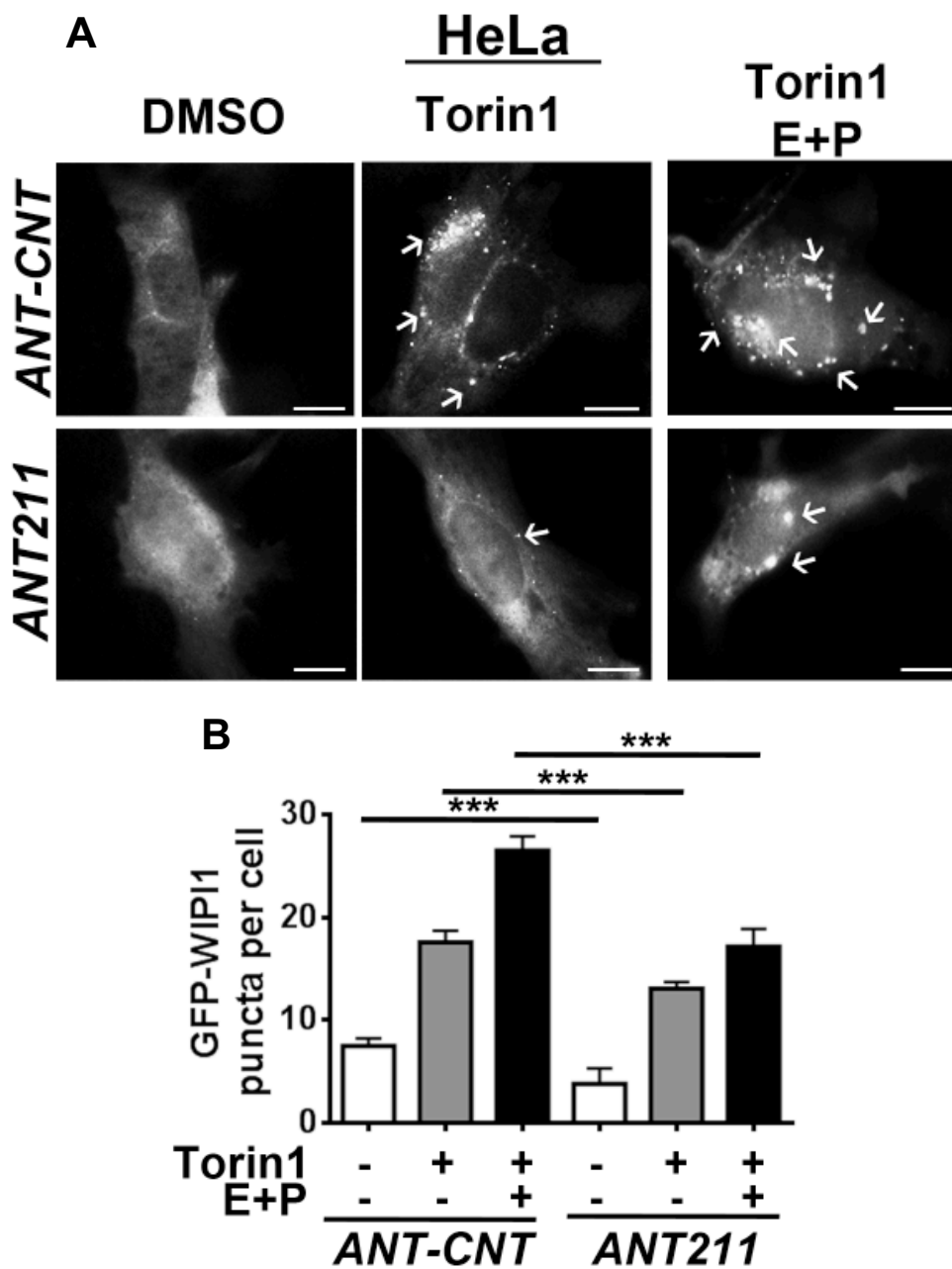


Figure 3.4.1 5: Effect of *ANT211* on GFP-WIP1 puncta formation following torin1 treatment. (A) HeLa cells transiently transfected with GFP-WIP1 plasmid construct and either *ANT-CNT* or *ANT211*, then incubated with torin1 (200 nM, 4 h) and analyzed under a fluorescence microscope. DMSO, carrier control. White arrows indicate the GFP-WIP1 dots in the cells. Scale bar, 10 μ m. (B) Quantitative analysis of GFP-WIP1 puncta in the experimental set-up shown in A (mean \pm SD of n=3 independent experiments, ***p<0.01).

3.4.2 Effect of *ANT211* on starvation-induced autophagy

When nutrient deprivation was used as an autophagy inducer, the level of LC3-II decreased in *ANT211*-transfected cells compared to control transfected counterparts in both HeLa (Figure 3.4.2 1) and SK-MEL-28 cells (Figure 3.4.2 2).

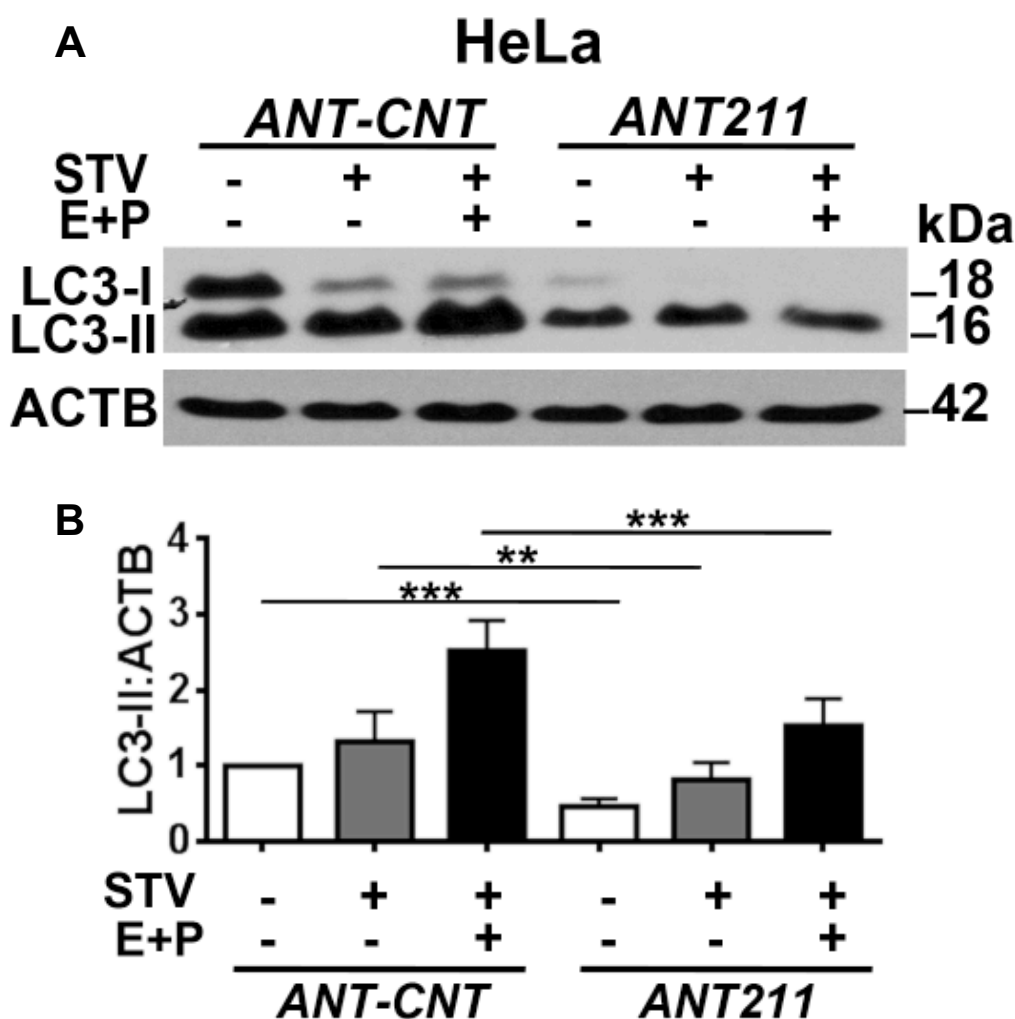


Figure 3.4.2 1: Effect of *ANT211* on LC3-II accumulation following starvation treatment in HeLa cells. (A) Immunoblots of *ANT-CNT* (control antagomir) or *ANT211*- transfected HeLa cells that were non-starved or starved (EBSS, 4h) (B) Graph depicting quantification of LC3-II:ACTB ratios in the experimental set-up shown in A (mean±SD, n=3 independent experiments, ***p<0.01, **p<0.03).

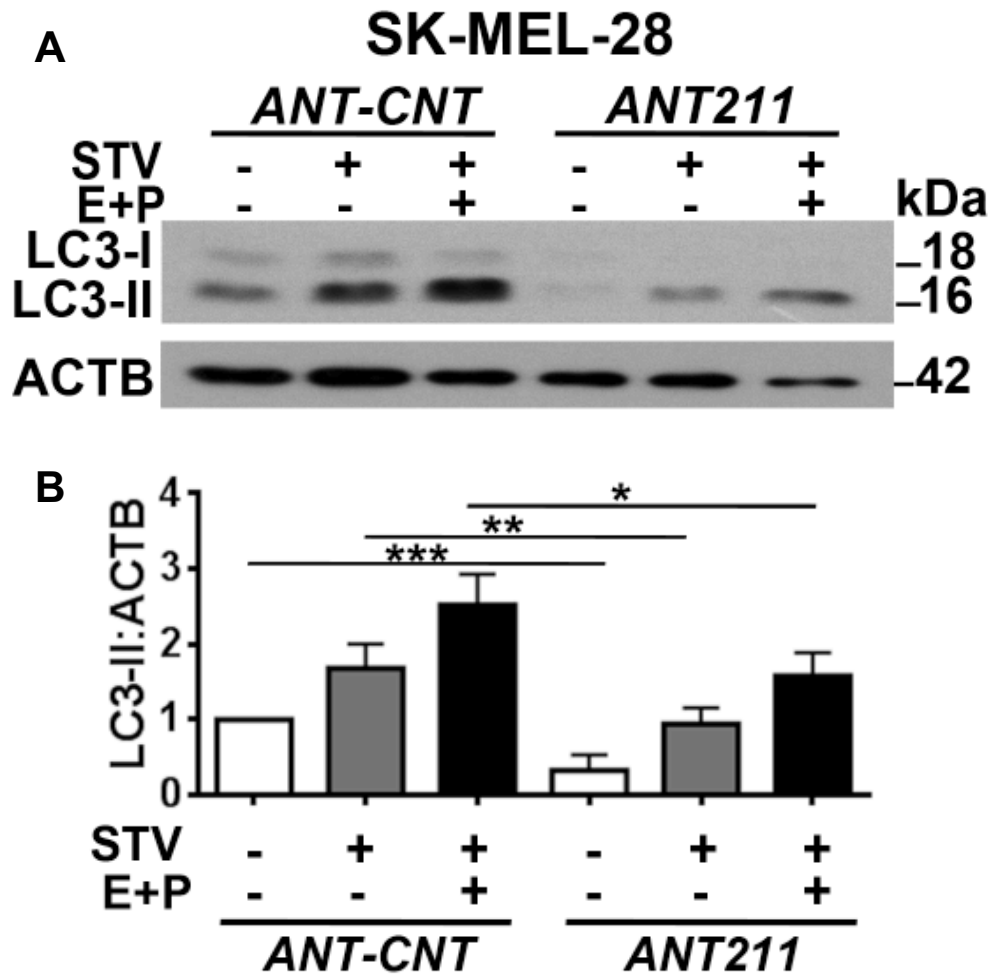


Figure 3.4.2 2: Effect of *ANT211* on LC3-II accumulation following starvation in SK-MEL-28 cells. (A) Immunoblots of *ANT-CNT* (control antagomir) or *ANT211*- transfected SK-MEL-28 cells that were non-starved or starved (EBSS, 4h) (B) Graph depicting quantification of LC3-II:ACTB ratios in the experimental set-up shown in A (mean±SD, n=3 independent experiments, ***p<0.01, **<0.03, *p<0.05).

Similarly, it was observed that starvation-induced accumulation of GFP-WIPI1 dots was attenuated in HeLa cells when endogenous *MIR211* is silenced (Figure 3.4.2 3).

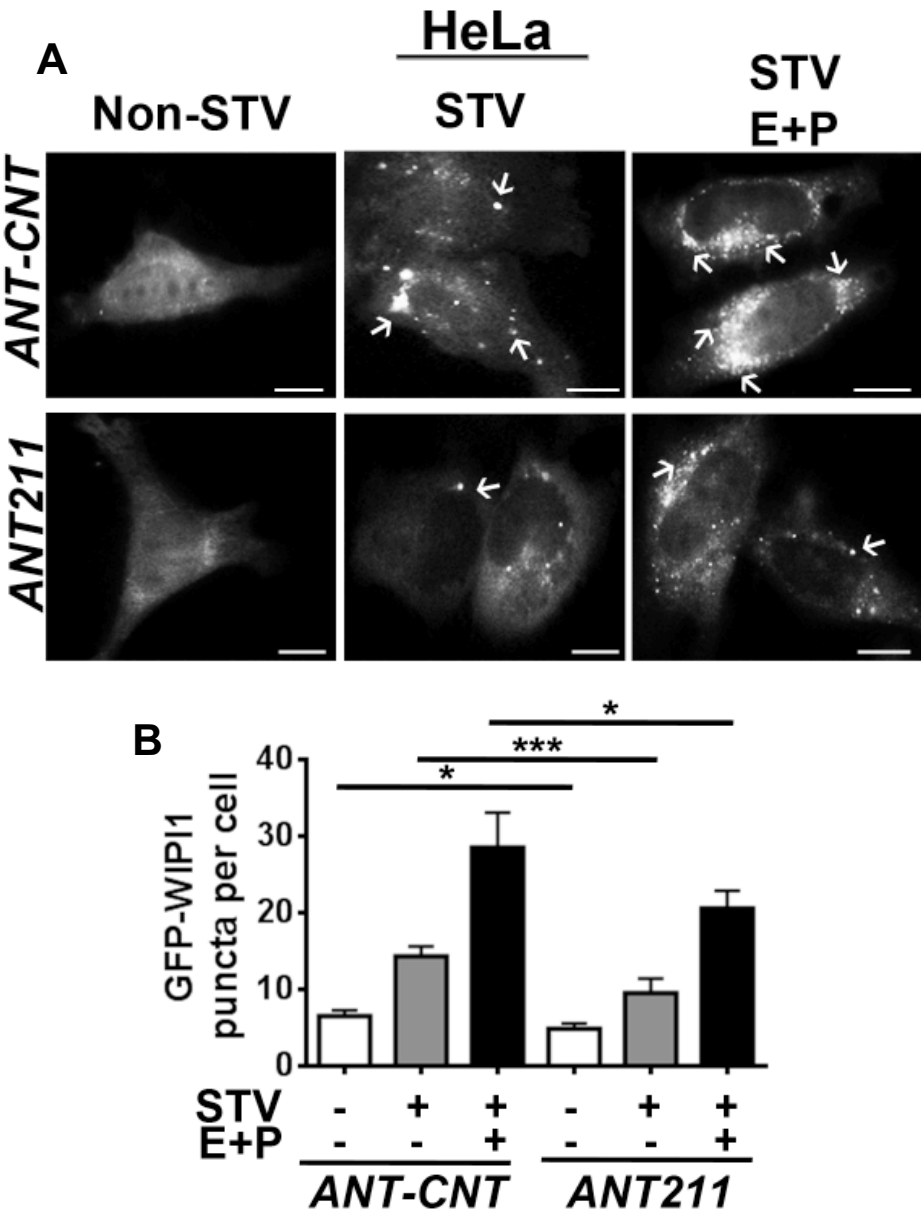


Figure 3.4.2 3: Effect of *ANT211* on GFP-WIPI1 puncta formation following starvation. (A) HeLa cells transiently transfected with GFP-WIPI1 plasmid construct and either *ANT-CNT* or *ANT211*, then non-starved or starved (EBSS, 4h) and analyzed under a fluorescence microscope. White arrows indicate the GFP-WIPI1 dots in the cells. Scale bar, 10 μ m. (B) Quantitative analysis of GFP-WIPI1 puncta in the experimental set-up shown in A (mean \pm SD of n=3 independent experiments, ***p<0.01).

3.4.3 Regulation of autophagy through MITF/*MIR211* axis

The most critical finding about the role of MITF and *MIR211* on autophagic activity was that *MIR211* silencing limited the increase in the amplitude of autophagy when MITF was overexpressed. This result clarified the critical role of this miRNA in MITF-dependent autophagy regulation.

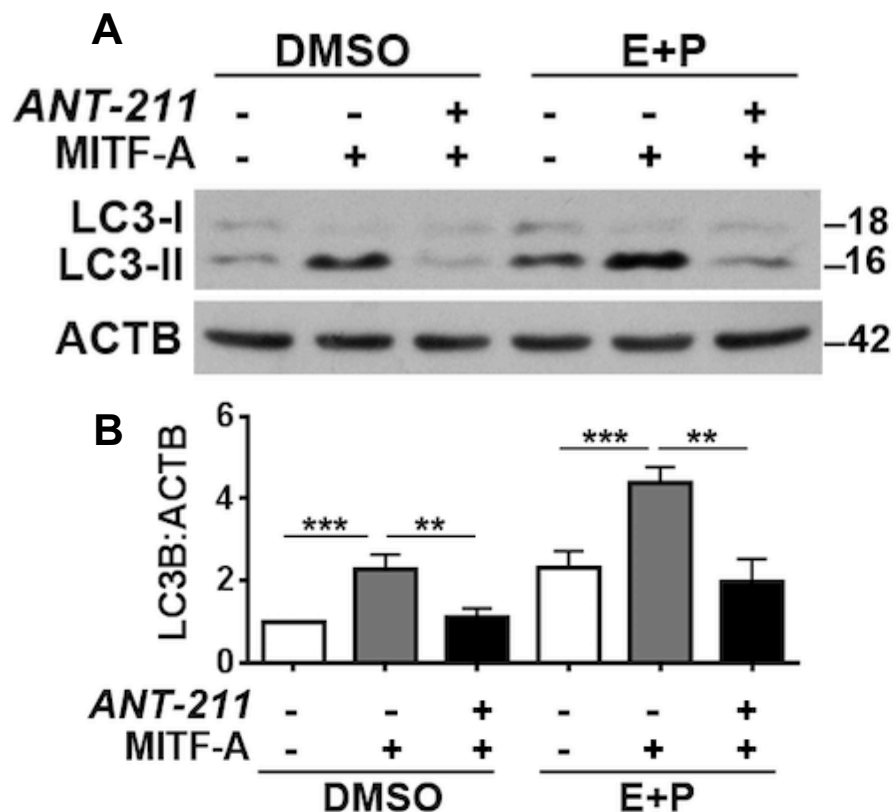


Figure 3.4.3 1: MITF regulates autophagy through *MIR211*. (A) Autophagy-related LC3-II levels were analyzed in immunoblots of HeLa cells that were co-transfected with a MITF-A-encoding plasmid, *ANT211* or controls as indicated in the presence or absence of E64D and pepstatin A (E+P). (B) Graph depicting quantification of LC3-II:ACTB ratios in the experimental set-up shown in A (mean±SD, n=4 independent experiments, ***p<0.01, **p<0.03).

These results indicate that endogenous *MIR211* levels are critical cellular factors regulating autophagy activation under cellular stress.

3.5 RICTOR was an autophagy-related target of *MIR211*

In order to understand the mechanism behind *MIR211* regulation of starvation and torin1 induced autophagy, autophagy-related target of the miRNA should be predicted and validated. Bioinformatics analysis was performed for miRNA-target interaction prediction. Then, the effect of *MIR211* on predicted target was validated through cellular analyses. To clarify whether the interaction is direct and target is the rate-limiting factor in the autophagy context, luciferase activity assay and rescue assay were performed, respectively (Figure 3.5 1).

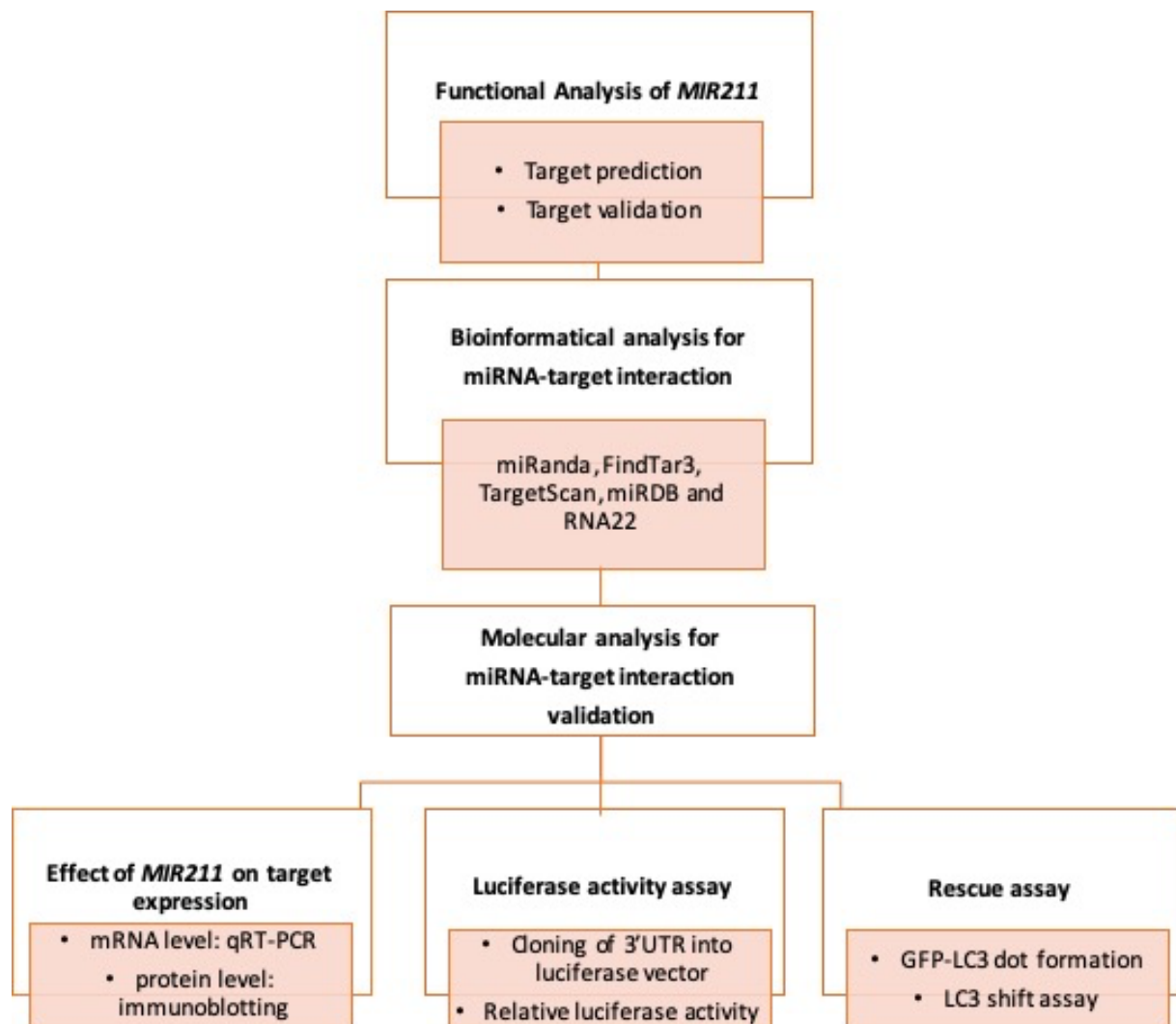


Figure 3.5 1: The pipeline of experiments demonstrating target prediction and validation for *MIR211* functional analysis.

3.5.1 Target prediction using bioinformatics tools

Autophagy-related genes with potential binding sites of *MIR211* in their 3'UTR were searched using the bioinformatics tools miRanda, FindTar3, TargetScan, miRDB and RNA22. All of these tools identified *RICTOR* (GenBank accession number: NM_152756) as a potential direct target of *MIR211*. Indeed, we could identify a *MIR211* miRNA response element (MRE) in the 3' UTR of the *RICTOR* mRNA (Base numbers: 4343-4349, Figure 3.5.1 1).

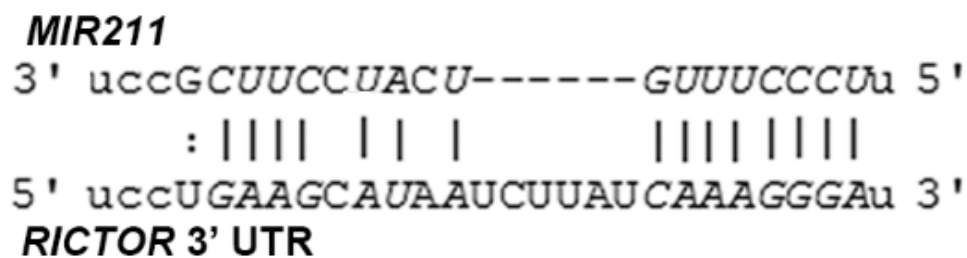


Figure 3.5.1 1: Target prediction using bioinformatics tools. *MIR211* target sequence in the 3' UTR of *RICTOR* mRNA. The *MIR211* seed sequence was marked in *italics*.

3.5.2 Effect of *MIR211* on target mRNA and protein levels

To confirm the bioinformatic prediction, *RICTOR* mRNA and protein levels were analyzed by real time PCR and immunoblotting, respectively.

MIR211 overexpression but not *MIR-CNT* resulted in the downregulation of *RICTOR* mRNA levels in both HeLa and SK-MEL-28 cells (Figure 3.5.2 1).

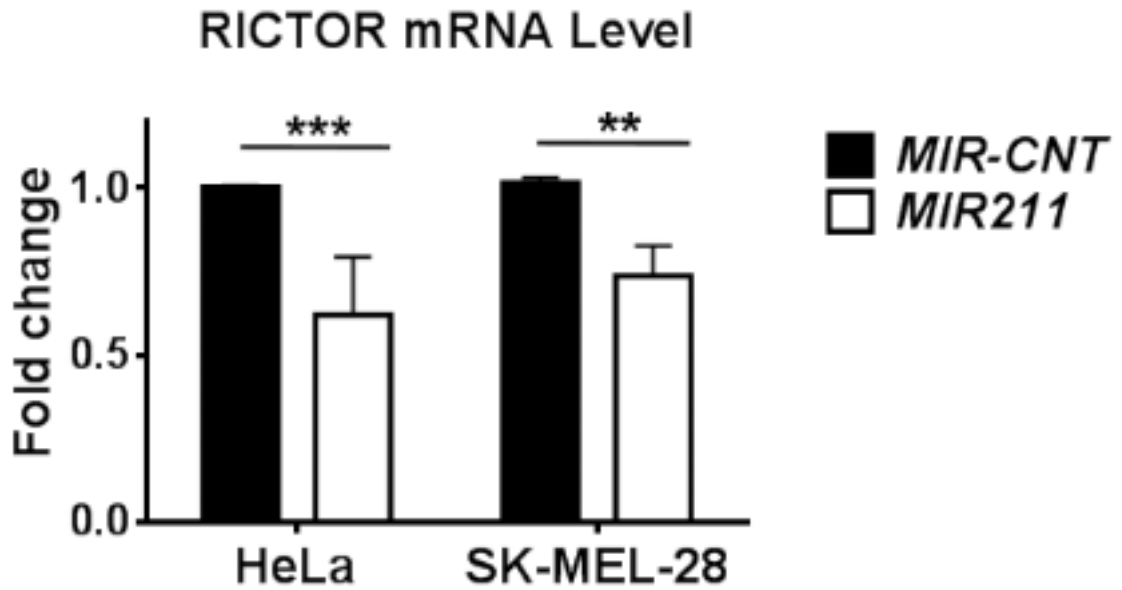


Figure 3.5.2 1: Effect of *MIR211* overexpression on RICTOR mRNA levels. RT-qPCR analysis of *RICTOR* mRNA levels in control (*MIR-CNT*)- or *MIR211*-transfected HeLa or SK-MEL-28 cells (mean±SD, n=3 independent experiments, **p<0.03, ***p<0.01). Data were normalized using *GAPDH* mRNA as a control.

Moreover, protein extracts from either control or *MIR211*-overexpressed cells were immunoblotted for RICTOR. It was found that overexpression of the miRNA decreased RICTOR protein levels (Figure 3.5.2 2) and downregulation of endogenous *MIR211* using antagomirs resulted in the accumulation of RICTOR protein level in cells (Figure 3.5.2 3).

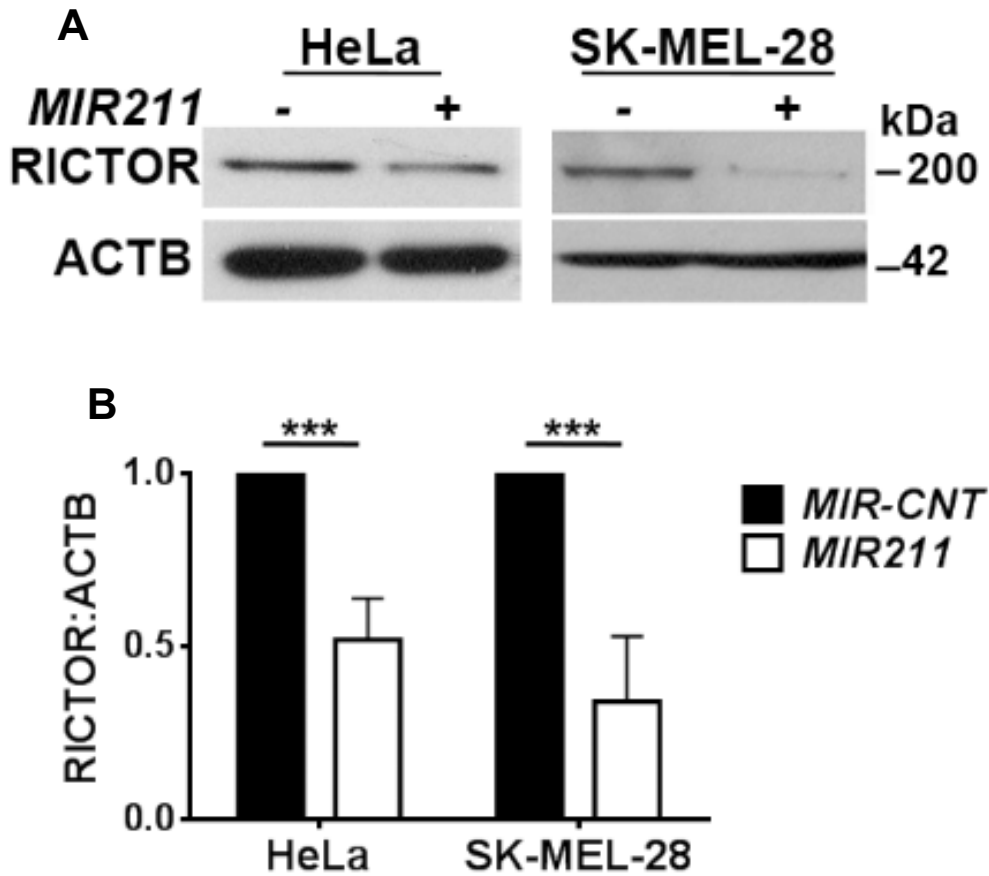


Figure 3.5.2 2: Effect of *MIR211* overexpression on RICTOR protein levels. Effect of Immunoblots of *MIR-CNT* or *MIR211* transfected cells. RICTOR protein levels decreased following *MIR211* overexpression in HeLa or SK-MEL-28 cells. (B) Graph depicting quantification of RICTOR:ACTB ratios in the experimental set-up shown in A (mean±SD, n=3 independent experiments, ***p<0.01).

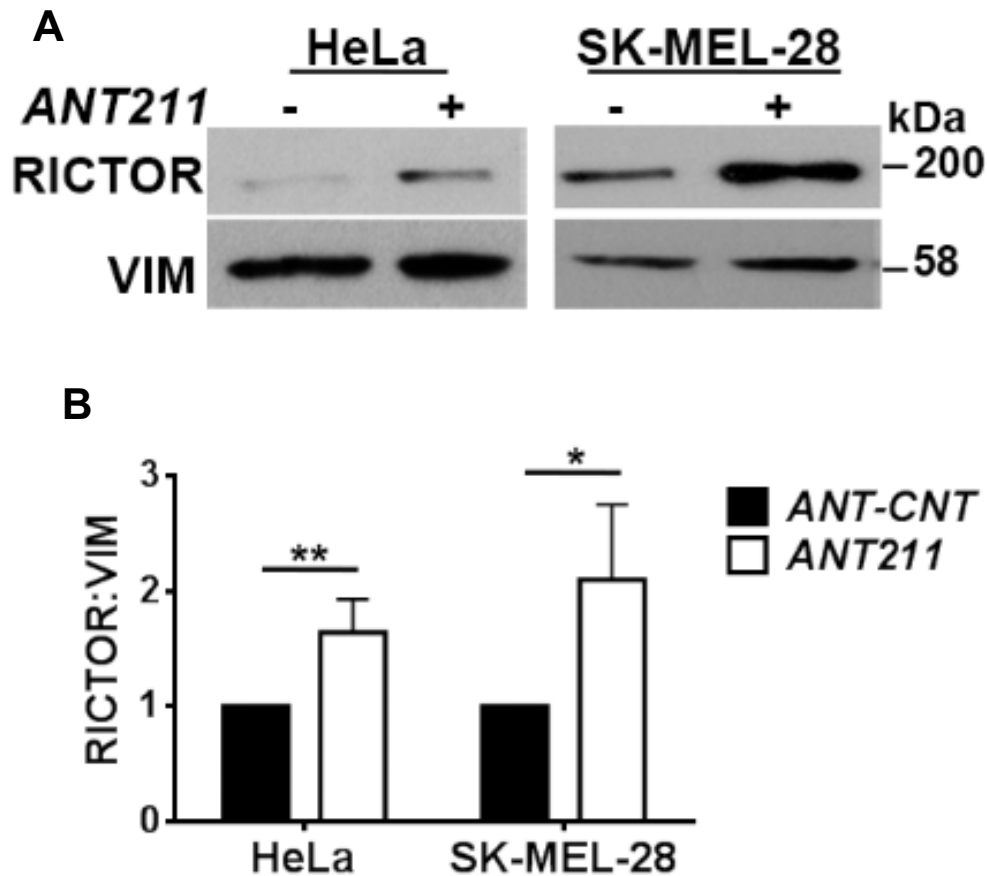


Figure 3.5.2 3: Effect of *ANT211* on RICTOR protein levels. (A) Immunoblots of *ANT-CNT* or *ANT211* transfected cells. RICTOR protein levels decreased following *ANT211* in HeLa or SK-MEL-28 cells. (B) Graph depicting quantification of RICTOR:VIM ratios in the experimental set-up shown in A (mean±SD, n=3 independent experiments, **p<0.03, *p<0.05).

As a conclusion, RICTOR transcript and protein levels in cells are regulated through *MIR211*.

3.5.3 Luciferase activity assay to demonstrate direct binding of *MIR211* to RICTOR

To validate that the MRE sequence in the 3'UTR of *RICTOR* mRNA was responsive to *MIR211*, the region of 3'UTR of *RICTOR* mRNA containing a potential *MIR211* binding site was cloned to luciferase vector. Linker primer cloning method was used (Figure 3.5.3 1). Additionally, a mutant version of this construct by introducing base changes to putative miRNA seed sequence binding region was created (Figure 3.5.3 2)

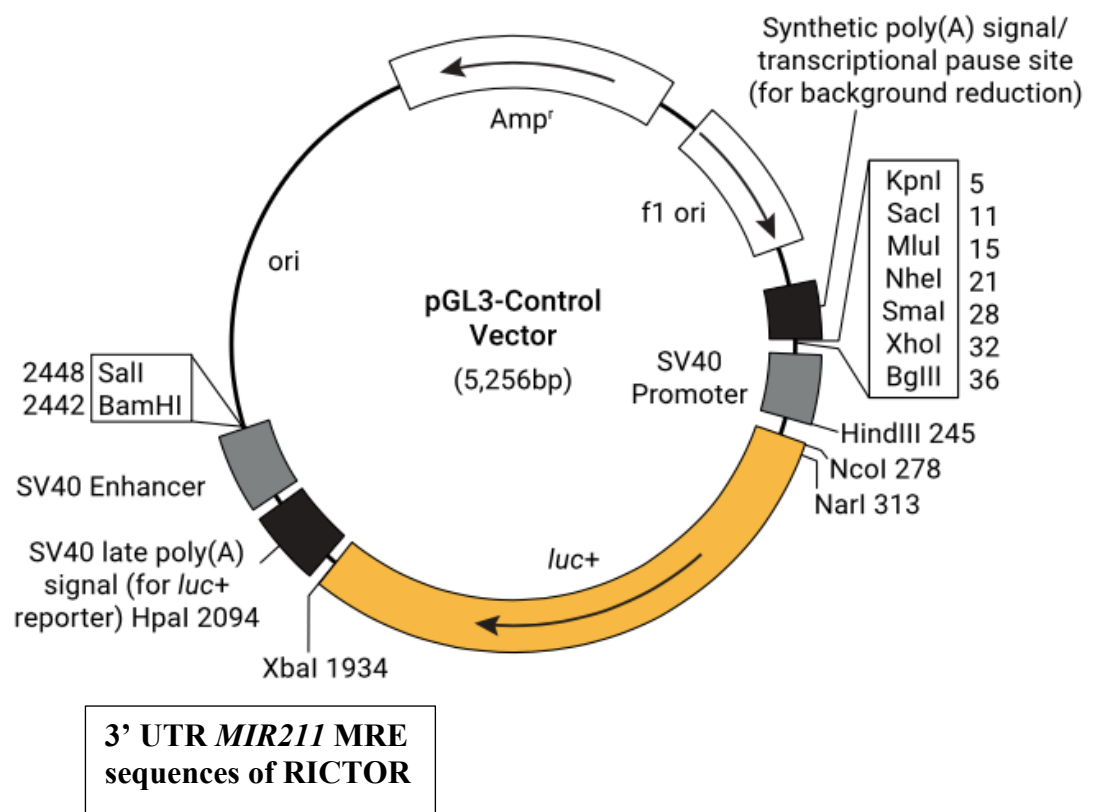


Figure 3.5.3 1: Linker primer cloning strategy for RICTOR 3'UTR into luciferase vector. pGL3 control vector was used for cloning of the portion of 3'UTR of RICTOR that *MIR211* binds. (Promega-pGL3-Control Vector map)

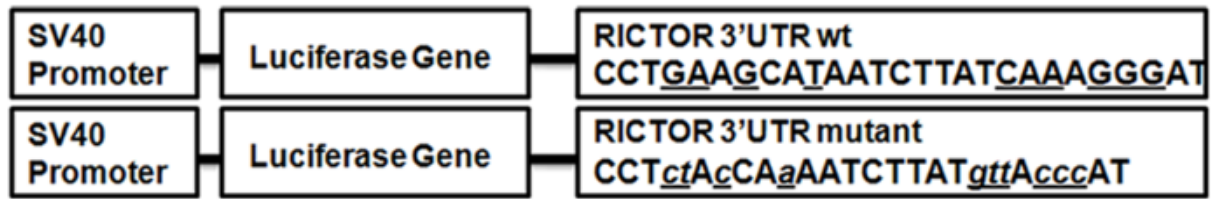


Figure 3.5.3 2: A scheme representing luciferase constructs. Wild-type (WT) or mutant *MIR211* target 3' UTR MRE sequences of *RICTOR*. Mutations were marked in lowercase letters.

Co-transfection of *MIR211* together with the wild-type luciferase construct into HEK293T (Figure 3.5.3 3), HeLa and SK-MEL-28 (Figure 3.5.3 4) cells resulted in a significant decrease in luciferase activity. However, when *MIR211* was co-transfected with the mutant construct, luciferase activity was similar to control levels.

Moreover, luciferase activity assay was performed after suppression of endogenous *MIR211* by *ANT211* in HeLa and SK-MEL-28 cells. A significant increase above control levels was observed in the luciferase activity of *ANT211*-transfected cells, while this effect was not observed in cells transfected with the mutant construct (Figure 3.5.3 4).

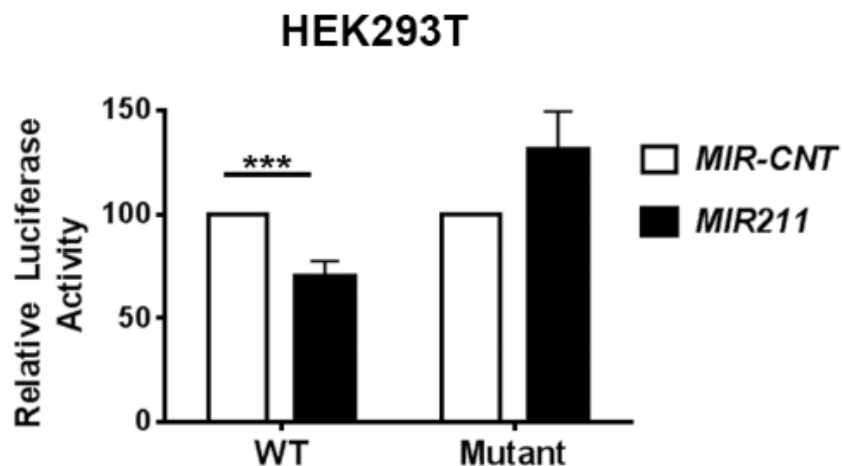


Figure 3.5.3 3: Luciferase activity assay in HEK293T cells. Normalized luciferase activity in lysates from HEK293T cells that were co-transfected with wild-type or mutant *RICTOR*-luciferase constructs and *MIR211* or *MIR-CNT* (mean±SD, n=5 independent experiments, ***p<0.01).

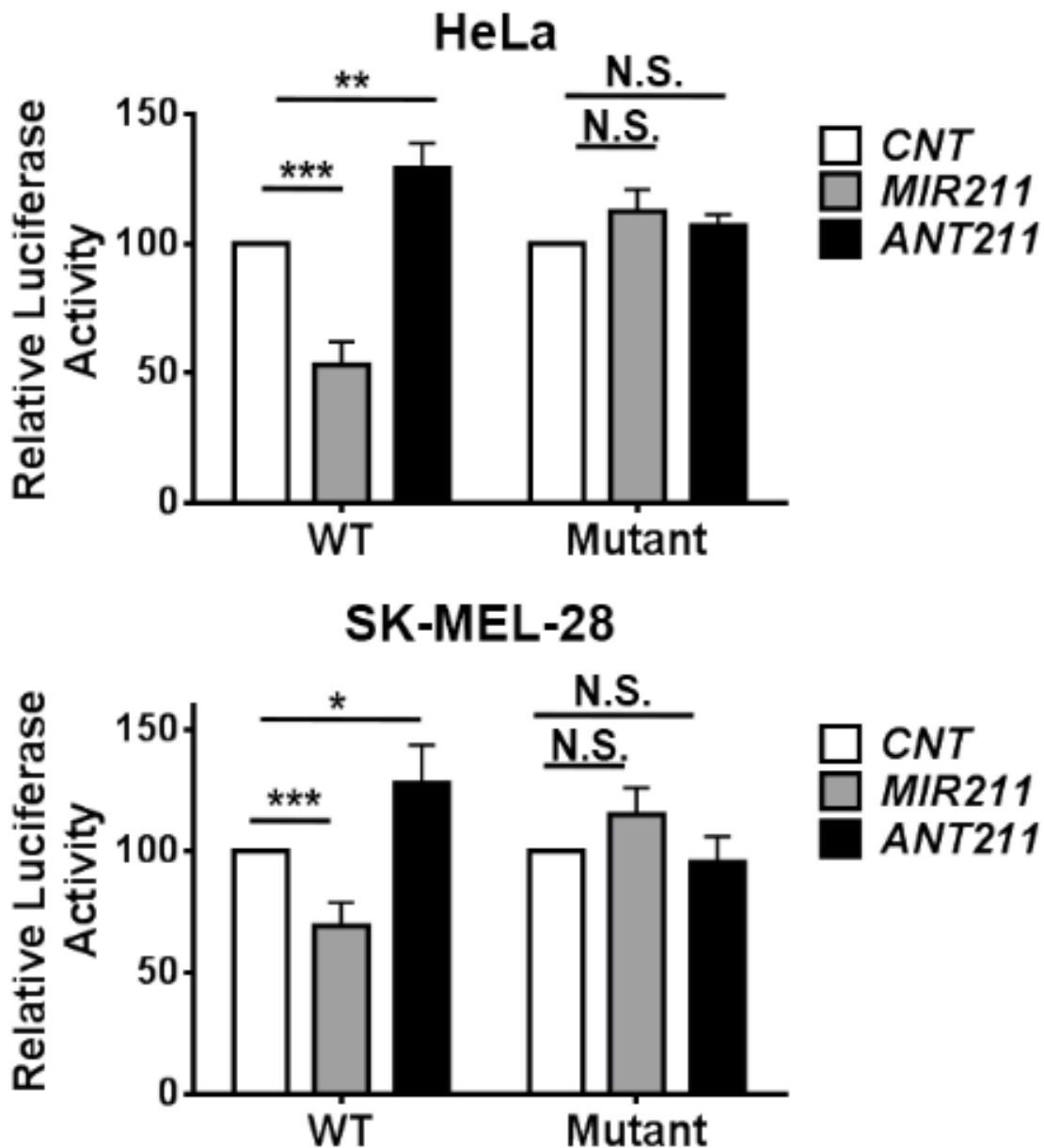


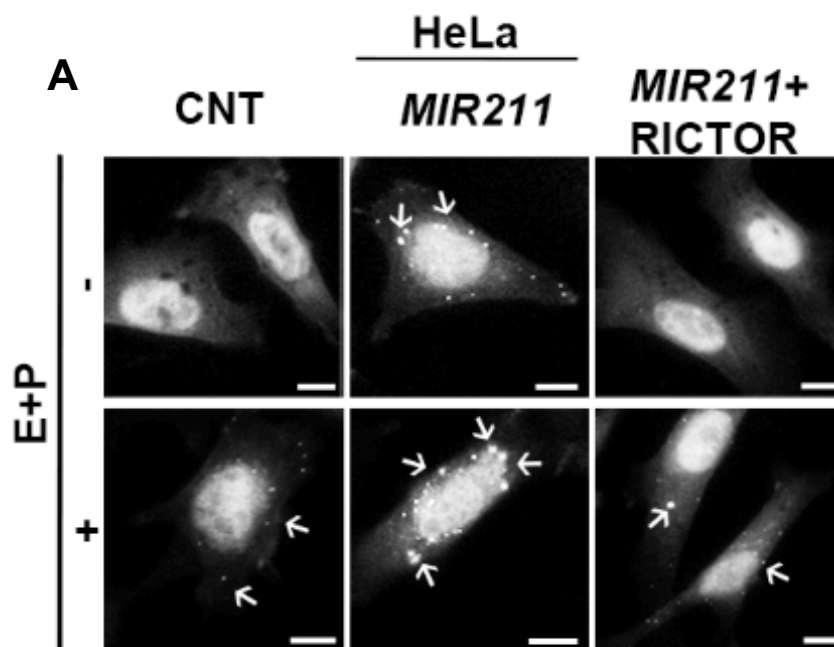
Figure 3.5.3 4: Luciferase activity assay in HeLa and SK-MEL28. Normalized luciferase activity in lysates from HeLa and SK-MEL-28 cells that were co-transfected with wild-type or mutant RICTOR-luciferase constructs and *MIR211* or *ANT211* (mean \pm SD of independent experiments, n=4, *p<0.05, **p<0.03, ***p<0.01, N.S., not significant).

These results indicated that *MIR211* controlled RICTOR gene expression through directly binding to its 3'UTR.

3.5.4 Rescue assay to demonstrate RICTOR is a rate-limiting target

Since microRNAs may target at least dozens of genes at once. In order to prove that a gene is a rate-limiting target in a defined biological event, rescue experiment should be performed. Here, a miRNA-resistant expression construct encoding the target protein is introduced to the system that overexpresses the miRNA. If the effect of miRNA on the biological event is reversed, then it can be concluded that target protein of interest is a key player in the miRNA-mediated effect.

Hence, rescue experiments were performed to validate that RICTOR downregulation was responsible for the autophagy-related effects of *MIR211*. For this purpose, RICTOR protein was overexpressed from a plasmid lacking the MRE region, and therefore resistant to miRNA-mediated silencing. Then, for autophagy analysis, GFP-LC3 puncta formation assays were performed in HeLa cells in the presence or absence of E64D-pepstatin A. Under these conditions, GFP-LC3 dot formation assay revealed that *MIR211*-induced autophagy could be reversed by reintroduction of the RICTOR protein (Figure 3.5.4 1).



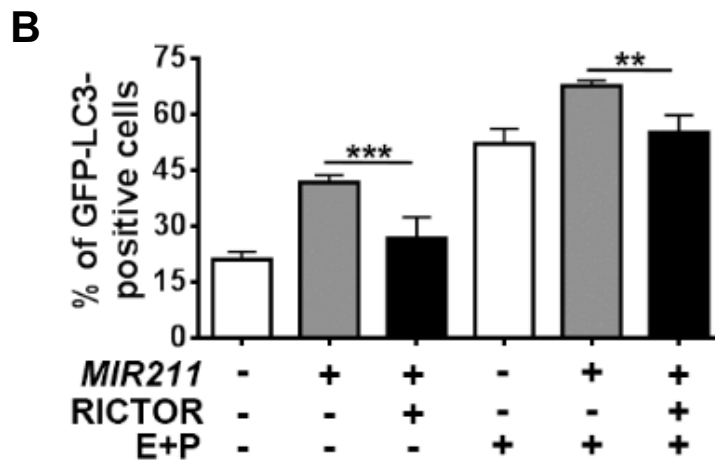


Figure 3.5.4 1: Rescue assay and GFP-LC3 dot formation assay. (A) RICTOR overexpression was sufficient to revert *MIR211*-mediated autophagy induction. HeLa cells were co-transfected with *MIR211* or *MIR-CNT* and a RICTOR expression plasmid lacking the *MIR211* target MRE region (*MIR211*-resistant RICTOR plasmid). GFP-LC3 dot formation was evaluated in the presence or absence of E64D and pepstatin A (E+P). Scale bar, 10 μ m. (B) Quantitative analysis of GFP-LC3 dots in the experimental set-up shown in A (mean \pm SD of n=3 independent experiments, ***p<0.01, **p<0.03).

In line with these results, an increase in LC3-II protein levels that was observed upon *MIR211* overexpression, was attenuated when the RICTOR protein was reintroduced, and these effects were enhanced by lysosomal inhibitors (Figure 3.5.4 2).

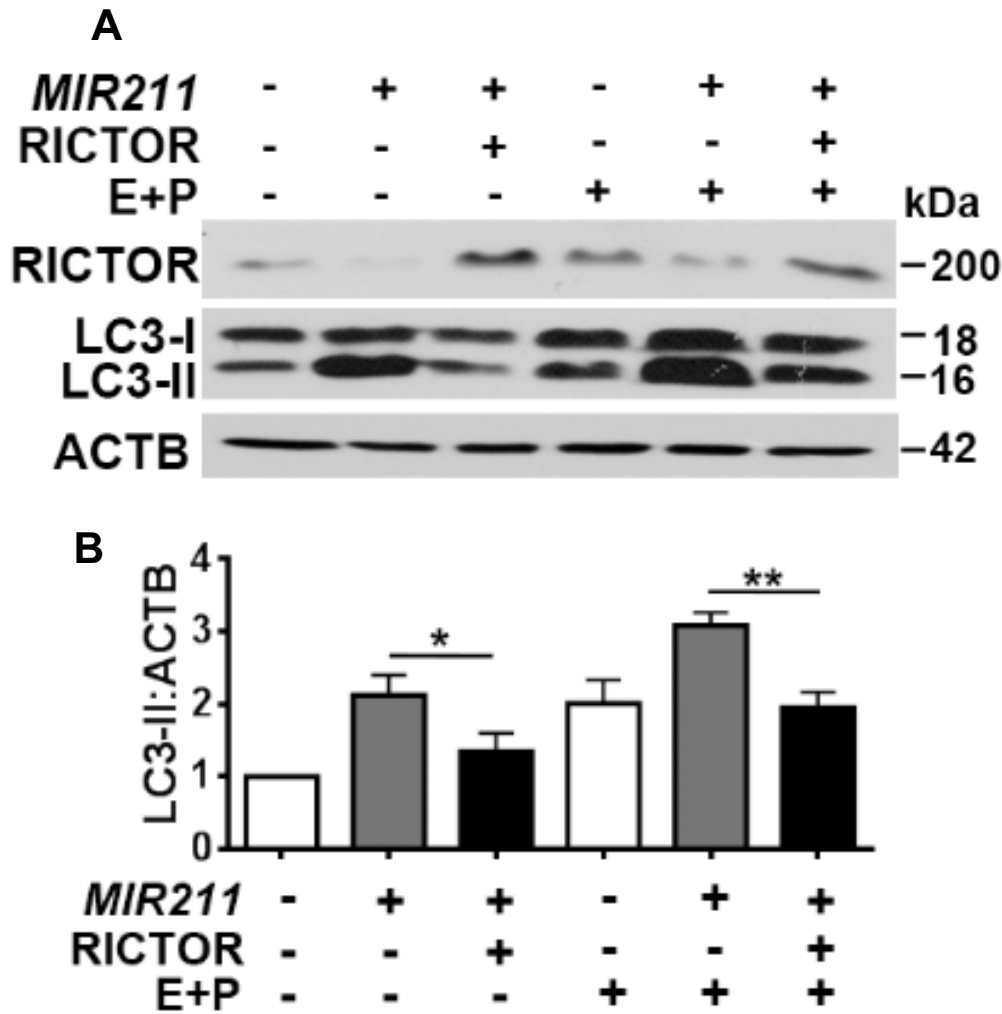


Figure 3.5.4 2: Rescue assay and LC3 shift assay. (A) Immunoblots of extracts from cells transfected with *MIR-CNT*, *MIR211* or *MIR211* together with the *MIR211*-resistant RICTOR expression plasmid. (B) Graph depicting quantification of LC3B:ACTB ratios in the experimental set-up shown in B (mean±SD, n=3 independent experiments, **p<math><0.03</math>, *p<math><0.05</math>)

Hence, expression of RICTOR alone was sufficient for autophagy suppression even in the presence of elevated *MIR211* levels.

The above presented data demonstrated for the first time that RICTOR is a rate-limiting target of the MIF-regulated microRNA *MIR211*, in the context of autophagy.

3.6 *MIR211* regulated the mTORC1 pathway through RICTOR

mTORC2 was directly linked to mTORC1 regulation and autophagy control through AKT phosphorylation. The serine 473 (Ser473) residue on the AKT protein was identified as a direct target of the mTORC2-associated mTOR Ser/Thr kinase (Sarbasov, 2005). Because it was established that RICTOR, a major regulator of mTORC2 activity, was directly downregulated by *MIR211*, we checked whether AKT Ser473 phosphorylation was affected by overexpression of the miRNA.

Figure 3.6.1 shows that *MIR211* overexpression prominently decreased AKT phosphorylation. Torin1 was used as a positive control.

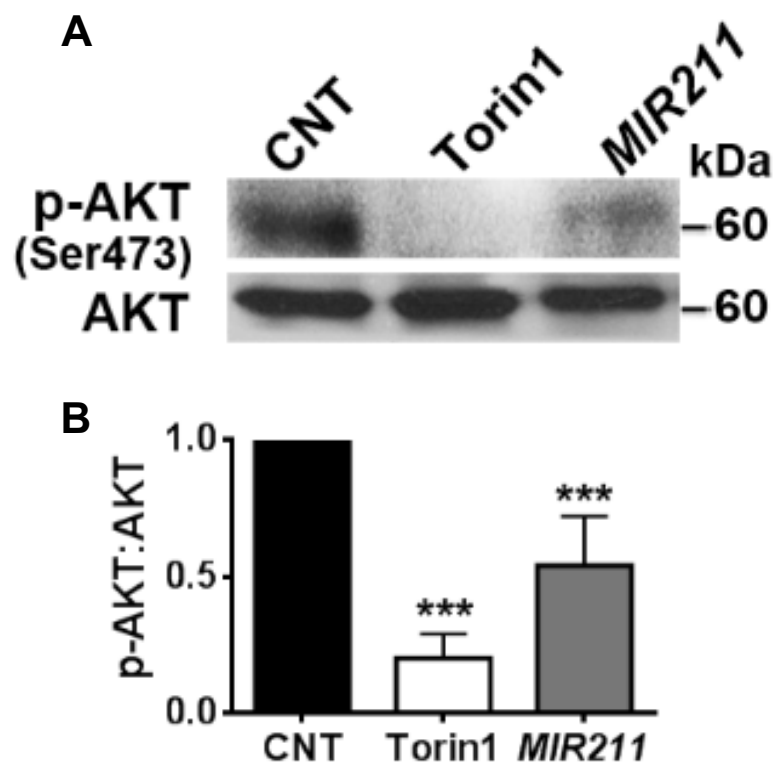


Figure 3.6 1: Effect of *MIR211* overexpression on AKT phosphorylation. (A) MTORC2-mediated AKT Ser473 phosphorylation was decreased in HeLa cells overexpressing *MIR211*. (B) Graph depicting quantification of p-AKT:AKT ratios in the experimental set-up shown in A (mean±SD, n=3 independent experiments, ***p<0.01).

In the same experimental context, *MIR211* overexpression blocked the activation of mTORC1 by AKT through mTOR Ser2448 phosphorylation (Figure 3.6.2). Furthermore, the miRNA also led to a decrease in RPS6KB1 phosphorylation by mTORC1 at Thr389, confirming the inhibition of mTORC1 activity under these conditions.

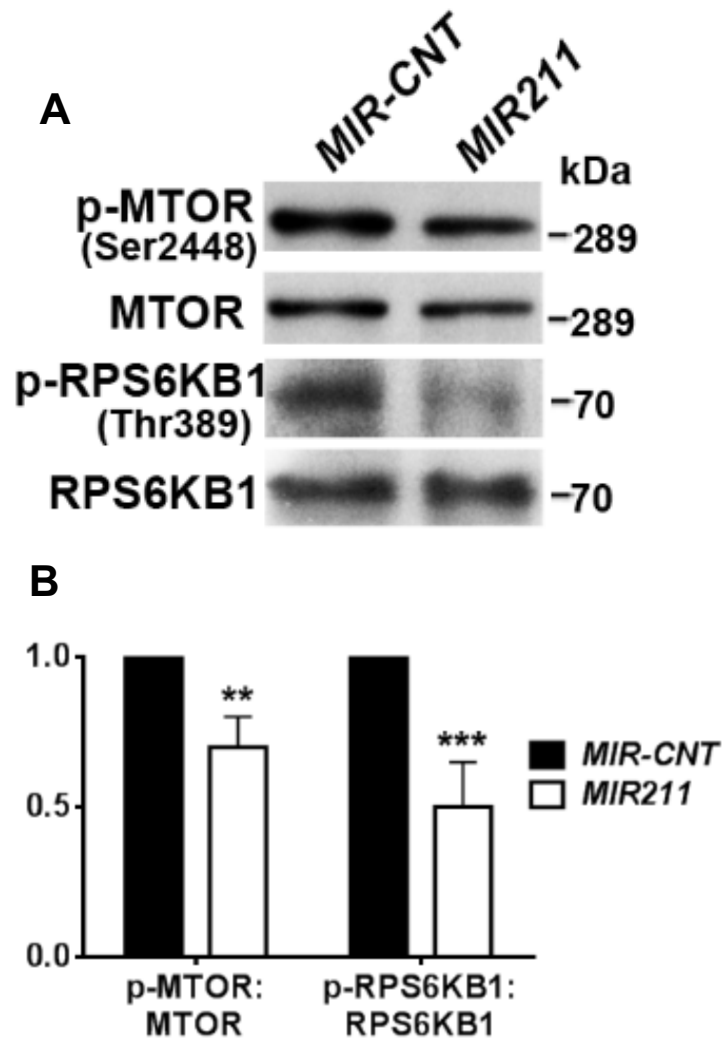


Figure 3.6 2: Effect of *MIR211* overexpression on MTOR pathway. MTOR phospho-Ser2448 (p-MTOR) and RPS6KB1 phospho-Thr389 levels were decreased following *MIR211* overexpression in HeLa cells. (D) Graph depicting quantification of p-MTOR:MTOR and p-RPS6KB1:RPS6KB1 ratios in the experimental set-up shown in C (mean±SD, n=3 independent experiments, ***p<0.01, **<0.03).

Above-mentioned results were confirmed by checking the effect of RICTOR on mTOR pathway. It was clarified that RICTOR downregulation *per se* was responsible for mTORC1 inhibition by the miRNA. Indeed, introduction of an shRNA against *RICTOR* (*shRICTOR*) resulted in mTOR Ser2448 and RPS6KB1 Thr389 dephosphorylation, and hence mTORC1 inhibition (Figure 3.6.3).

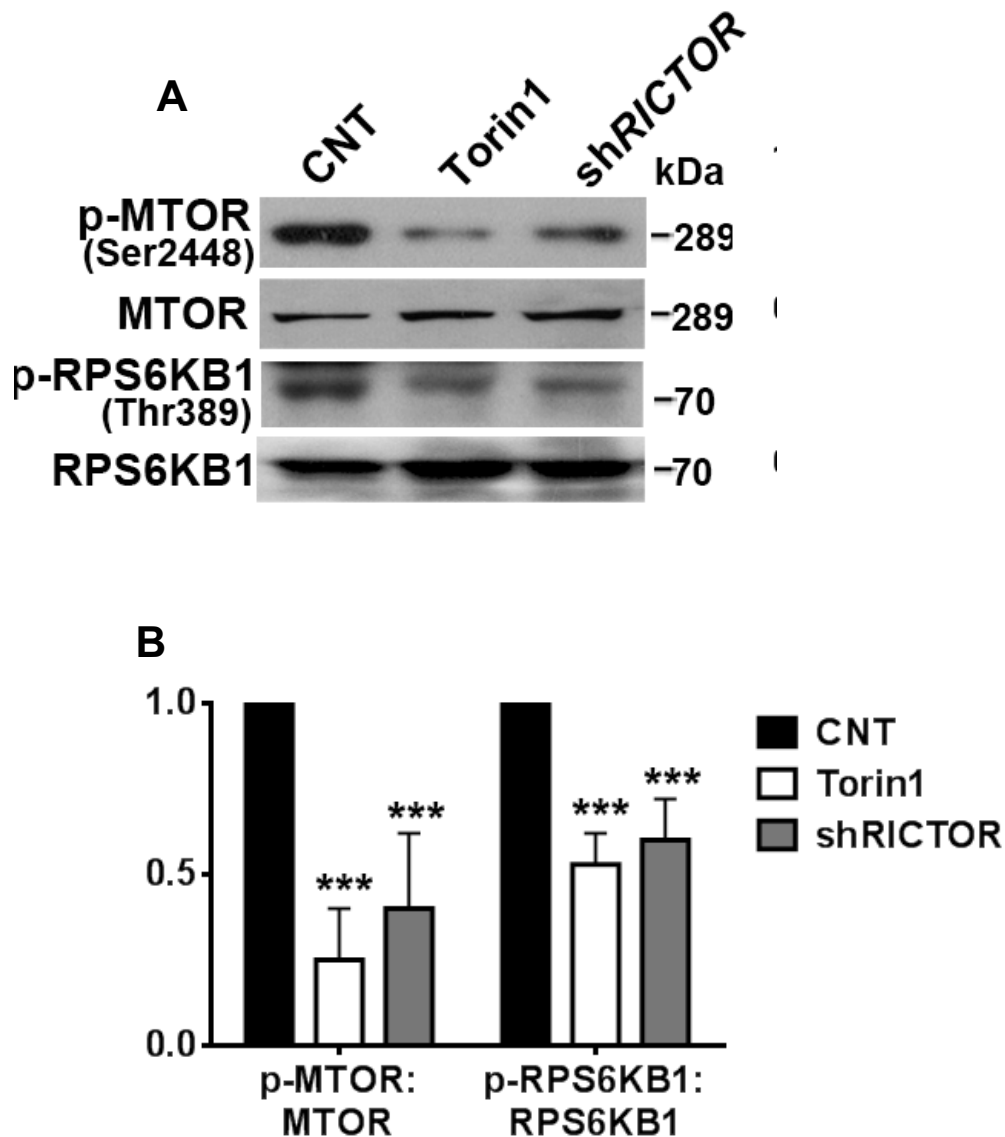


Figure 3.6.3: Effect of *shRICTOR* on mTOR pathway. (A) Knockdown of RICTOR by shRNA (*shRICTOR*) decreased p-mTOR and p-RPS6KB1 levels. Torin1, positive control. (B) Graph depicting quantification of p-mTOR:mTOR and p-RPS6KB1:RPS6KB1 ratios in the experimental set-up shown in E (mean±SD, n=3 independent experiments, ***p<0.01).

Similarly, overexpression of RICTOR from a *MIR211*-resistant construct increased mTORC2-related AKT Ser 473 phosphorylation (Figure 3.6 4).

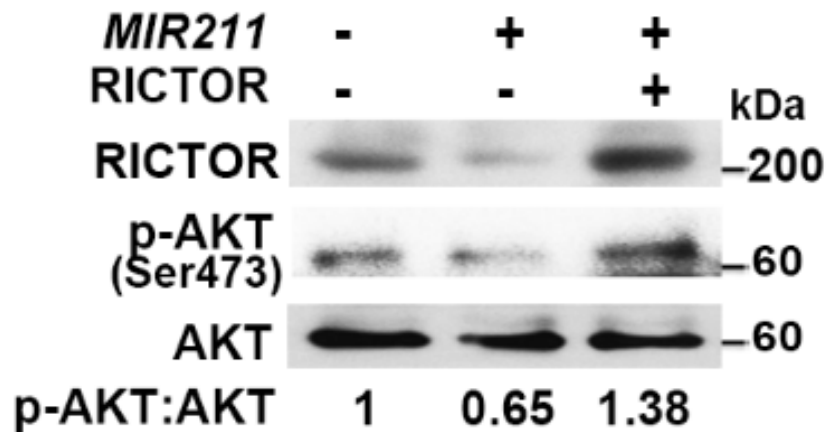


Figure 3.6 4: Determination of RICTOR activity on AKT phosphorylation. RICTOR activity was determined as AKT Ser473 phosphorylation following *MIR211* overexpression or *MIR211*-resistant RICTOR plasmid co-overexpression with the miRNA. *MIR211* overexpression led to a decrease in p-AKT levels, whereas AKT Ser473 phosphorylation increased following overexpression of RICTOR from plasmid lacking the *MIR211* target MRE region, indicating that overexpressed RICTOR indeed stimulated MTORC2 activity.

Finally, autophagy-related consequences of mTORC1 inhibition upon RICTOR downregulation were explored. Indeed, transfection of *shRICTOR* alone stimulated GFP-LC3 puncta formation in the presence of lysosomal inhibitors, hence autophagic flux (Figure 3.6 5).

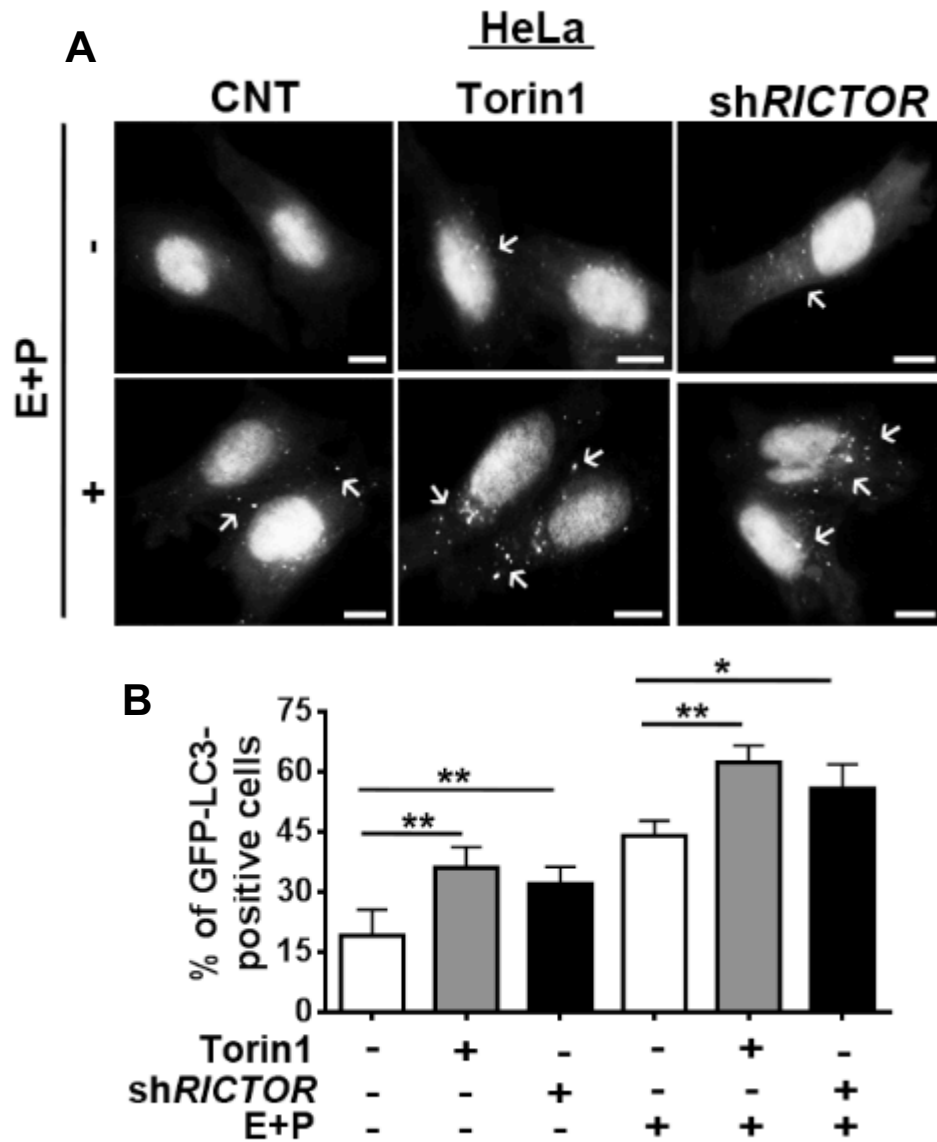


Figure 3.6 5 Effect of RICTOR knockdown on GFP-LC3 puncta formation. (A) Knockdown of RICTOR increased GFP-LC3 dot formation. Torin1, positive control. E+P, E64D and pepstatin A. Scale bar, 10 μ m. (B) Quantitative analysis of GFP-LC3 dots in the experimental set-up shown in A (mean \pm SD of n=3 independent experiments, **p<0.03, *p<0.05).

Furthermore, to support GFP-LC3 formation experiment results, LC3 shift test was also performed in HeLa cells. As illustrated in Figure 3.6 6, RICTOR downregulation by sh*RICTOR* promoted LC3-II accumulation. Considering that the knockdown efficiency was approximately 50%, we can conclude that sh*RICTOR* activated autophagy to a comparable level as mTORC1 and mTORC2 inhibitor torin1 treatment (Figure 3.6.6).

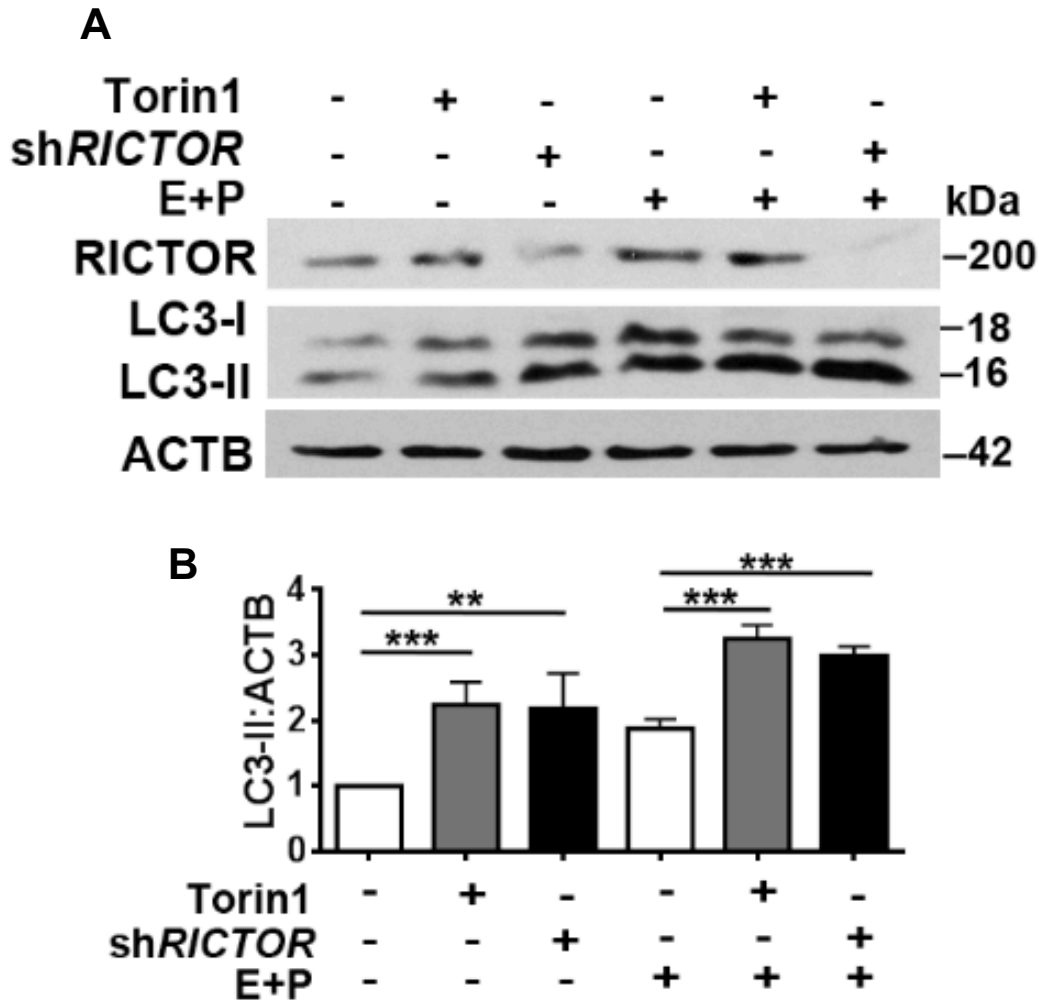


Figure 3.6 6 Effect of RICTOR knockdown on LC3-II accumulation. (A) Immunoblots of HeLa cells following knockdown of RICTOR. Torin1, positive control. (B) Graph depicting quantification of LC3B:ACTB ratios in the experimental set-up shown in A (mean±SD, n=3 independent experiments, ***p<0.01, **p<0.03).

All of these data conclude that *MIR211*-mediated RICTOR downregulation resulted in a strong inhibition of the mTORC2-AKT-mTORC1 pathway, leading to the stimulation of autophagy.

3.7 *MIR211* overexpression resulted in MITF translocation to the nucleus.

As previously shown in literature and also in our results, mTORC1 inhibition led to the translocation of TFEB and MITF to the nucleus under autophagy-inducing stress conditions (Figure 3.1.1 1 and Figure 3.1.1 2 and as shown in reference Martina, 2013). Having demonstrated that *MIR211* inhibited mTORC1 pathway, immunofluorescence experiments were performed to clarify whether mere overexpression of the miRNA would lead to a similar outcome. As illustrated in Figure 3.7 1, endogenous TFEB proteins translocated to the nuclei in a significant fraction of cells following *MIR211* overexpression (Figure 3.7 1).

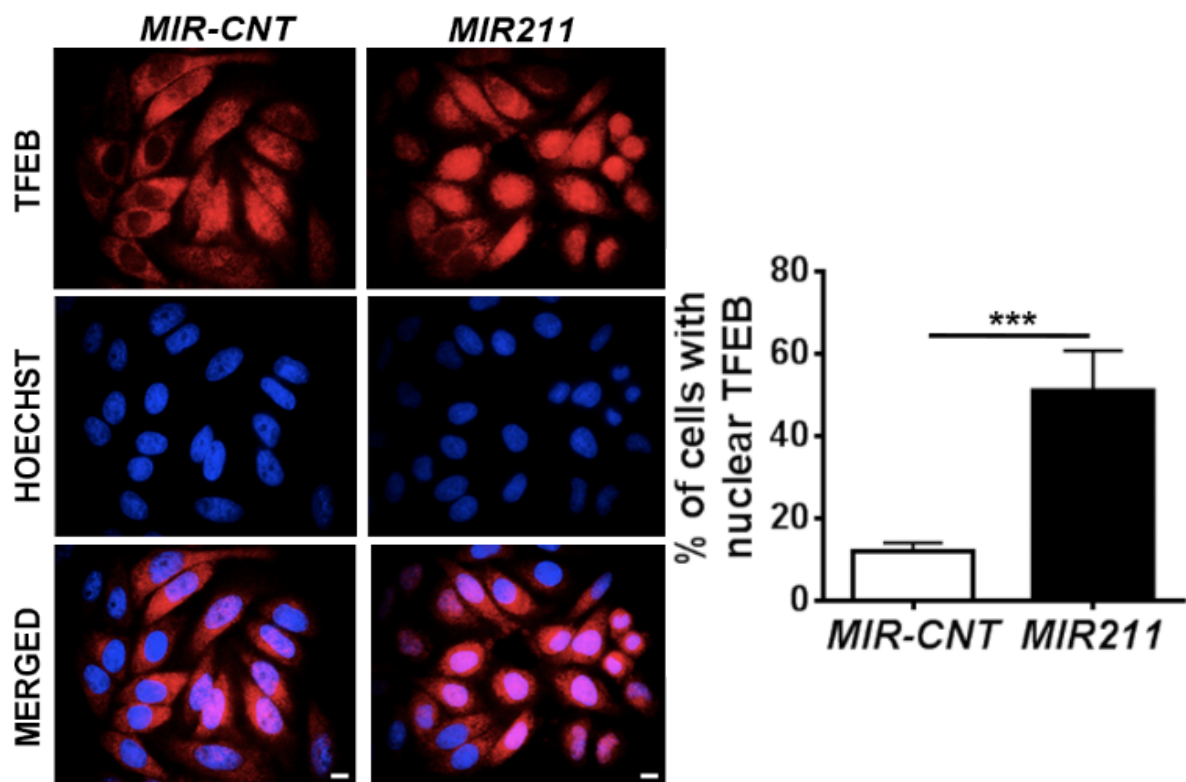


Figure 3.7 1: Effect of *MIR211* overexpression of TFEB nuclear translocation. (A) Endogenous TFEB subcellular localizations were analyzed using indirect immunostaining with specific antibodies in HeLa cells transfected with *MIR-CNT* or *MIR211*. Scale bar, 10 μ m. (B) Quantification of endogenous TFEB (nuclear localization (mean \pm SD, n=3 independent experiments, ***p<0.01).

Moreover, it was found that *MIR211* overexpression also led to MITF nuclear translocation in more than 50% of cells.

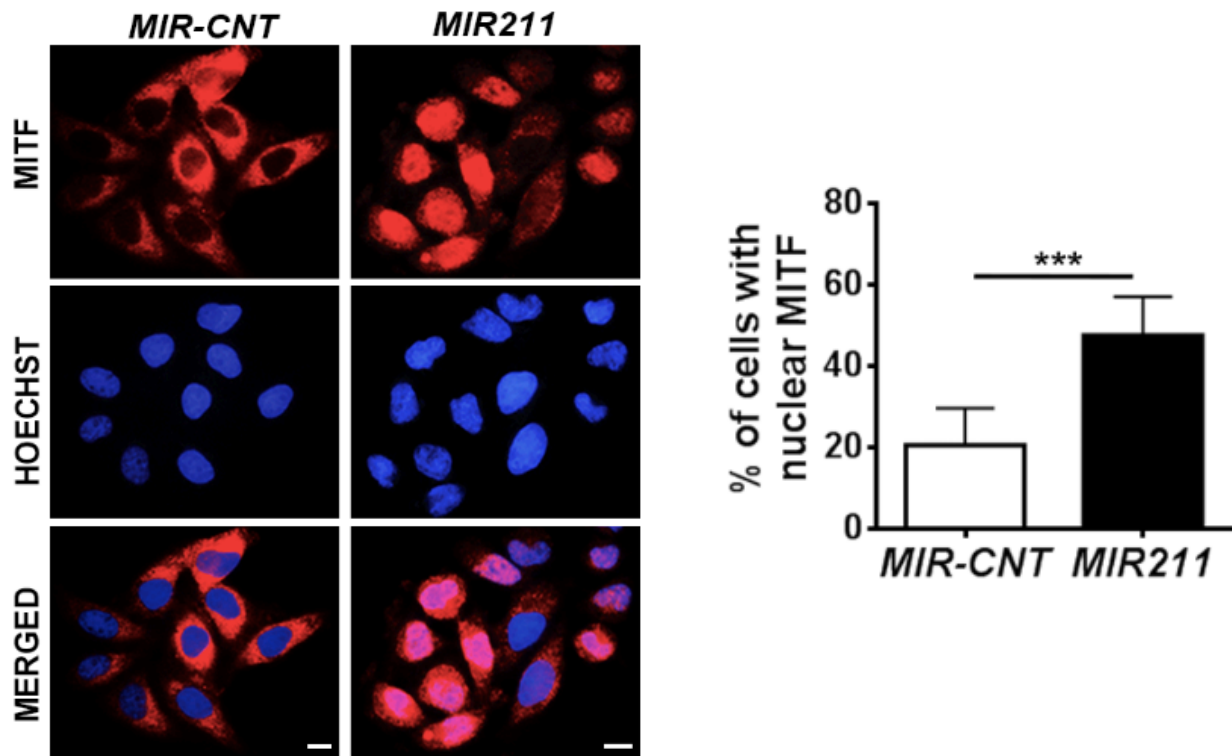


Figure 3.7 2: Effect of *MIR211* overexpression of MITF nuclear translocation. (A) Endogenous MITF subcellular localizations were analyzed using indirect immunostaining with specific antibodies in HeLa cells transfected with *MIR-CNT* or *MIR211*. Scale bar, 10 μ m. (B) Quantification of endogenous MITF (nuclear localization (mean \pm SD, n=3 independent experiments, ***p<0.01).

Of note, miRNA transfection efficiency was approximately 60% for HeLa cells, indicating that translocation occurred in most of the transfected cells (Figure 3.7 1 and 3.7 2).

MIR211 overexpression was sufficient for the stimulation of TFEB and MITF translocation to nuclei, and it did so through direct targeting of RICTOR and inhibition of the mTORC2 and mTORC1 pathways.

3.8 Other autophagy-related miRNAs targeting RICTOR

Up to now, 4 different miRNAs, namely *MIR155* (Wan et al., 2014), *MIR15A* (N. Huang et al., 2015), *MIR16* (N. Huang et al., 2015) and *MIR185* (Zhou et al., 2017) were shown to target RICTOR in an autophagy context.

MIR155 was shown to have a role in hypoxia-induced autophagy through inhibition of mTOR pathway components (Wan et al., 2014). Direct targets of *MIR155* were described as RHEB, RICTOR and RPS6KB2, and dysregulation of the mTOR pathway by miRNA resulted in autophagic activation and conducted cell cycle arrest. *MIR15A/MIR16* was reported to be directly targeting RICTOR and decreasing the phosphorylation of mTOR and p70S6K in HeLa cells. Overexpression of these miRNAs also inhibited cell proliferation and G1/S cell cycle transition (N. Huang et al., 2015). *MIR185* was shown to directly interact with 3' UTRs of several genes in AKT pathway, including AKT1, RICTOR and RHEB, and its overexpression induced autophagy in hepatocellular carcinoma cell (Zhou et al., 2017).

In none of the studies was RICTOR shown as a rate-limiting target for autophagy induction. Moreover, binding regions of these miRNAs in the 3'UTR region of *RICTOR* mRNA were different and non-overlapping with that of the *MIR211* binding region that we have identified (Figure 3.5.1 1).

Furthermore, in our hands, none of these miRNAs were shown to be regulated by starvation or MTOR-inhibition (Figure 3.8 1), indicating that *MIR211* plays a special and specific role that is different from other *RICTOR*-targeting miRNAs in autophagy control.

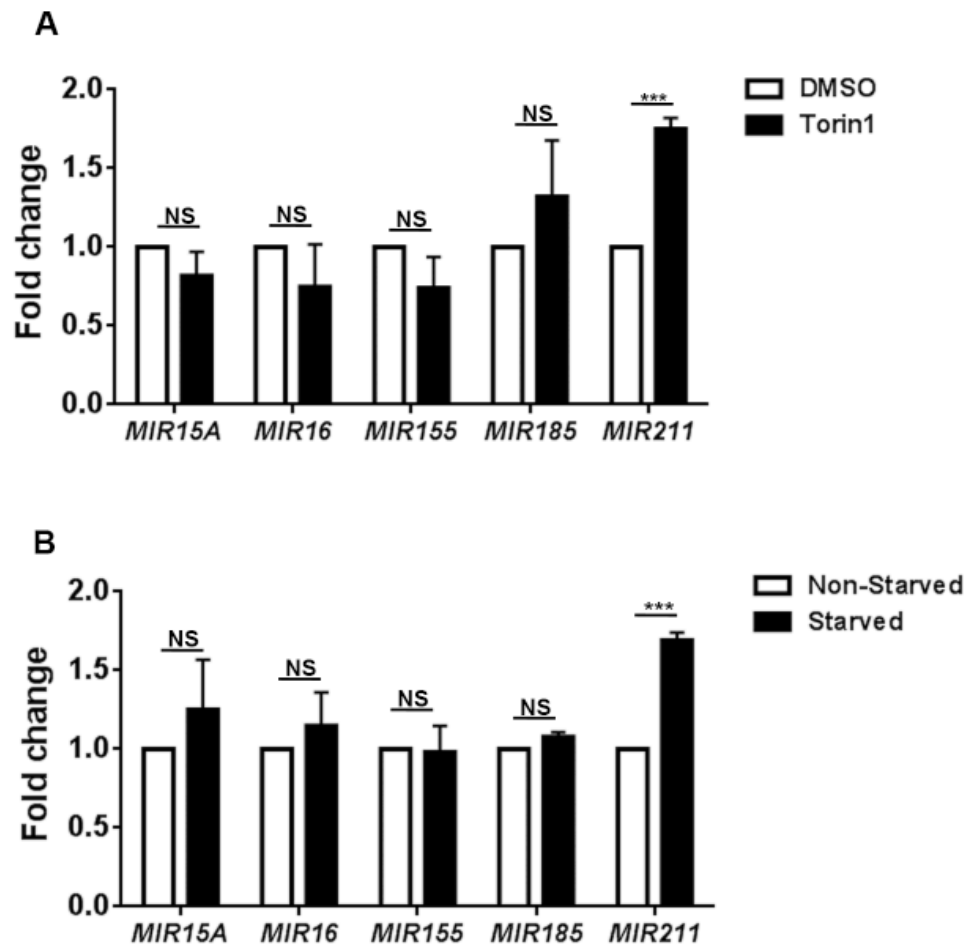


Figure 3.8 1: Regulation of other RICTOR targeting miRNAs upon torin1 treatment and starvation. (A and B) Expression of previously identified RICTOR-targeting microRNAs *MIR16*, *MIR15A*, *MIR185* and *MIR155* were determined by RT-qPCR and compared to that of *MIR211* following torin1 (A) or starvation (B) treatment. Data were normalized to *RNU6-1* (mean±SD, n=4 independent experiments, ***p<0.01, NS, not significant).

RICTOR targeting miRNAs other than *MIR211* are not regulated by torin1- or starvation-induced autophagy.

3.9 Model for novel autophagy-regulating axis during cellular stress: MITF/MIR211

All of these data proposed that MITF-*MIR211* axis is a universal amplifier of the autophagy signal in cells, through a feed-forward mechanism involving the MITF-*MIR211*-RICTOR-MTORC1 axis (Figure 3.9 1). Downregulation of RICTOR by *MIR211* blocks MTORC2 activity, leading to AKT inhibition that is followed by MTORC1 blockage. Under these conditions, MITF that was sequestered in the cytosol migrates to the nucleus and contributes to the transactivation of autophagy-related genes as well as *MIR211*. Upregulation of the miRNA under these conditions creates a feed-forward loop that amplifies and sustains autophagy during stress. Although, we have shown here that RICTOR was a direct and rate-limiting target of *MIR211* in autophagy control, additional direct or indirect connections involving other *MIR211* targets (e.g., *ATG14*) might also be contributing to the further amplification of the autophagic activity.

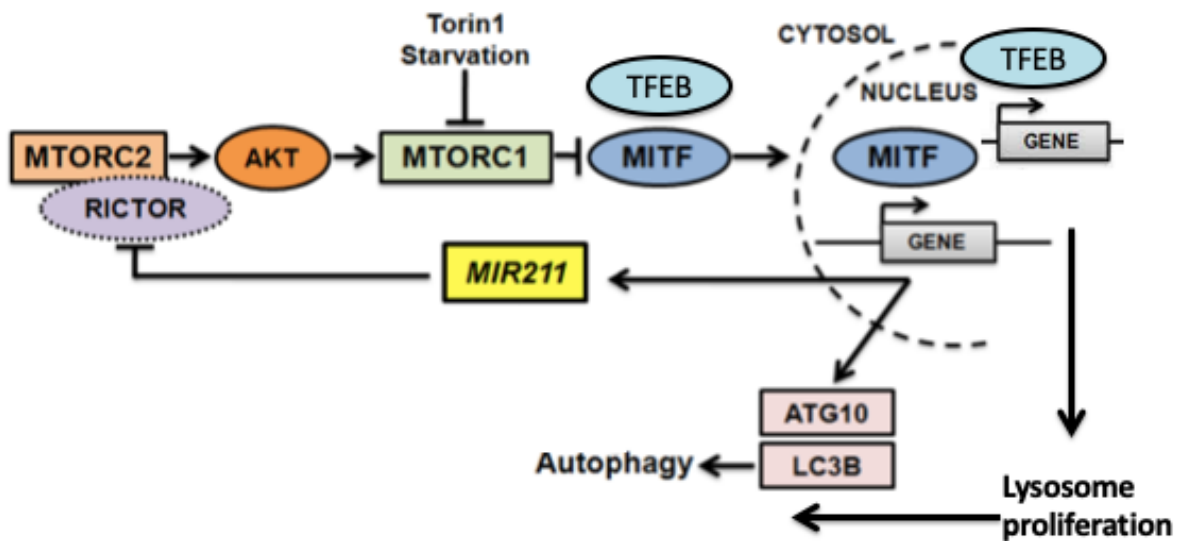


Figure 3.9 1: A model depicting the MITF-*MIR211* autophagy feed-forward regulation pathway.

4. DISCUSSION

Autophagy is an evolutionarily conserved catabolic pathway to maintain cellular homeostasis by degrading cellular constituents such as long-lived proteins and intracellular organelles. Being a highly complex process, autophagy is mediated through autophagy-related ATG proteins, and also several key upstream pathways regulate including mTOR pathway regulate autophagy. Dysregulation of autophagy causes multiple human pathologies such as cancer, lysosomal disorder diseases, neurodegenerative diseases and infection. Thus, autophagy requires constant fine-tuning and tight regulation at multiple levels including transcriptional and post-transcriptional. The research on transcriptional regulation of autophagy has gained importance as TFEB, the member of MITF/TFE family of transcription factors, is identified as master regulator of lysosomal biogenesis and autophagy. Hence, TFEB and other factors of the MITF/TFE family, MITF and TFE3, have the ability to rapidly induce autophagy by transcriptionally targeting autophagy-related proteins that are involved in all steps of the process.

miRNAs are important regulators in various biological processes by targeting genes in different signaling pathways including autophagy. Indeed, independent studies demonstrated that, core autophagy-related genes (*ATG* genes) and upstream mediators were targeted by microRNAs, revealing the presence of a novel and intricate miRNA network that is tightly regulating autophagy under physiological conditions. Moreover, dysregulation of miRNA expression was reported under various pathological conditions, including cancer, neurodegenerative diseases, cardiac and metabolic disorders. Most autophagy-related miRNAs were shown to be up or down-regulated in response to autophagy-inducing stress signals. In order to achieve a dynamic and context-dependent regulation, stress responsiveness may be an important property of autophagy modulation by miRNAs.

In this thesis, we demonstrated that MITF plays a crucial role in starvation and MTOR inhibition mediated autophagy. In addition to controlling the expression of lysosome-related genes, we showed that MITF is a key regulator of autophagic signal amplification through a MITF-*MIR211* axis.

We showed that:

i. Following autophagy-inducing stress, TFEB as well as MITF translocated to the nuclei of cells.

ii. MITF knockdown significantly downregulated the amplitude of autophagy that was activated by starvation and torin1.

iii. MITF overexpression potentiated starvation- and torin1-stimulated autophagy.

iv. Following translocation to the nuclei, MITF transactivated autophagy-related targets as well as *MIR211* expression.

v. Both MITF and *MIR211* were co-expressed in tested cell lines, human tissue samples and in various tumor datasets.

vi. Overexpression of *MIR211* stimulated autophagosome and autolysosome formation, and autophagic degradation.

vii. Knockdown of endogenous *MIR211* limited the increase in the amplitude of autophagy under these conditions, indicating a key role for this miRNA in autophagy regulation.

viii. *MIR211* overexpression was sufficient for the stimulation of TFEB and MITF translocation to nuclei, and it did so through direct targeting of RICTOR and inhibition of the MTORC2 and MTORC1 pathways.

All of these data demonstrated that MITF is a universal amplifier of the autophagy signal in cells, through a feed-forward mechanism involving the MITF-*MIR211*-RICTOR-MTORC1 axis.

MITF is a member of the MITF/TFE family of bHLH-Zip transcription factors, that include TFEB, TFEC, and TFE3. Studies until now implicated TFEB, and to a certain extent TFE3, in the transcriptional regulation of autophagosome and lysosome biogenesis via activation of the genes of crucial proteins, including subunits of the v-ATPase, lysosomal transporters and hydrolases. Additionally, some autophagy-related genes such as *BECN1*, *WIPI*, *GABARAP*, *HIF1A*, *VPS11* and *VPS18* were also reported to be transcriptional targets of TFEB (Palmieri et al., 2011; Perera et al., 2015; Settembre et al., 2011). Similar to TFEB, TFE3 was shown to perform overlapping gene regulatory functions (José A. Martina, Diab, Lishu, et al., 2014; Palmieri et al., 2011).

In contrast, study of MITF function in an autophagy context was limited to the analysis of MITF transcriptional targets, and most studies in the literature on MITF concentrated on its function in melanocyte differentiation and melanoma invasion (Hartman & Czyz, 2015). Although MITF has been implicated in lysosomal biogenesis and shown to regulate some overlapping genes with TFEB and TFE3, including autophagy genes *ATG10*, *ATG16L1*, *SQSTM1*, *ATG9B* and *UVRAG*, whether MITF played a non-redundant and specific function in autophagy regulation was not established so far. Strikingly, none of the studies that were published to date clearly showed the importance of independent contribution of MITF to autophagy regulation. Based on several independent autophagy assays performed under basal conditions or with autophagy inducers and in the presence or absence of the lysosomal inhibitors, MITF is required for autophagic activity in cells. Therefore, our study establishes for the first time a MITF-specific role in autophagic control through a feed-forward autophagy amplification loop involving a MITF-*MIR211* axis.

Transcriptional activation of *MIR211* by MITF was previously reported in a melanoma invasion and metastasis context (Levy et al., 2010; Mazar et al., 2010; Miller et al., 2004), we confirmed by chromatin IP experiments that *MIR211* expression was dependent on MITF expression because MITF moved to the nuclei and bound to the *MIR211* promoter under autophagy-stimulating conditions. Furthermore, knockdown of MITF led to a drop in endogenous *MIR211* levels. Conversely, antagomir-mediated silencing of *MIR211* limited the increase in the amplitude of autophagy when MITF was overexpressed, demonstrating the critical role of this miRNA in MITF-dependent autophagy regulation. This data demonstrated for the first time that, in addition to *LC3B* and *ATG10*, MITF regulated *MIR211* expression under autophagy-inducing conditions. The results obtained from several independent autophagy assays indicate that endogenous *MIR211* levels are critical cellular factors regulating autophagy activation.

MITF is subject to alternative splicing and differential promoter usage, giving rise to multiple isoforms. A tissue-specific expression pattern was reported for different MITF isoforms. For example, MITF-M is preferentially expressed in melanoblasts and melanocytes, while MITF-A is more ubiquitously expressed in several tissues and cell lines including HeLa and SK-MEL-28 cells. *MIR211* was previously reported to be a MITF-M target. In this study, we used a pan-MITF antibody that recognized all isoforms, including MITF-A and MITF-M. Since the M isoform is not expressed in HeLa cells, MITF-A that is strongly expressed in this

cell type, was responsible for autophagy-related phenotype that we observed. On the other hand, MITF-A and MITF-M are present in SK-MEL-28 cells, and both isoforms possibly contribute to autophagy regulation in this cell type. In spite of sequence variations, since domains that are responsible for DNA binding are shared between the different isoforms, they all seem to target similar genes (Hemesath et al., 1994). While MITF-A was cytosolic under basal conditions, and its nuclear translocation was directly regulated by mTORC1, melanocyte-specific MITF-M was reported to be in the nucleus at all times because it lacks the N-terminal interaction site with mTORC1. Yet, mTORC1 also controls indirectly MITF-M transcription, and hence active nuclear protein levels (Ho, Kapadia, Al-Tahan, Ahmad, & Ganesan, 2011).

Although mTORC1 was the focus of majority of studies on autophagy control, mTORC2 was also shown to be involved under certain settings. In most cases, mTORC2 exerts its autophagy-related effects through mTORC1 regulation. AKT activation through Ser473 phosphorylation by mTORC2 is among key connections between the two mTOR complexes. (Sarbasov, Ali, et al., 2005). AKT can mediate multi-site phosphorylation, and inactivation of TSC2, an inhibitor of RHEB, thus leading to mTORC1 phosphorylation at Ser 2448 and activation (Inoki, Li, Zhu, Wu, & Guan, 2002). Moreover, GSK3, a kinase that activates TSC1/2 and that inhibits mTORC1, is directly phosphorylated and inactivated by AKT (Cross, Alessi, Cohen, Andjelkovich, & Hemmings, 1995; Inoki et al., 2006). AKT can also activate mTORC1 in a TSC1/2-independent manner through phosphorylation PRAS40, an mTORC1 inhibitor, and causing its dissociation from the complex (Sancak et al., 2007). Therefore, inhibition of AKT is directly connected to mTORC1 inhibition through various upstream regulatory proteins and complex components.

Here, RICTOR was identified as a direct and rate-limiting target of *MIR211* in an autophagy context because the 3'UTR region of the gene contained a *MIR211*-responsive sequence element, and, in rescue assays, reintroduction of RICTOR protein attenuated autophagy activation by the miRNA. Moreover, we showed that RICTOR downregulation by *MIR211* or specific shRNAs, resulted in the attenuation of the mTORC2 activity and decreased AKT Ser473 phosphorylation. mTOR Ser2448 phosphorylation as well as phosphorylation of the downstream effector p70S6K1 were prominently suppressed by *MIR211* or shRICTOR. Under these conditions, TFEB and MITF translocated to the nuclei of cells, further increasing *MIR211* levels in a MITF-dependent manner, and activating a gene expression program that determines the amplitude of the autophagic signal. In line with our results, RICTOR

downregulation and/or inhibition of mTORC2/AKT was associated with autophagy stimulation in several independent studies under different experimental conditions (Arias et al., 2015; Chin et al., 2010; Dhar, Batinic-Haberle, & Clair, 2019; N. Huang et al., 2015; Seo et al., 2018; Zhou et al., 2017). Therefore, mTORC2 is a universal negative regulator of autophagy. Our results confirm and underline the importance of the mTORC2/AKT axis in autophagy control and introduce *MIR211* as a key regulator of cellular RICTOR levels, and hence autophagy. During the osteogenic differentiation of human induced pluripotent stem cells, a correlation between *MIR211* expression and ATG14 upregulation was suggested, but relevance of this observation for autophagy regulation so far remained obscure (Ozeki et al., 2017).

There are 4 different miRNAs targeting RICTOR in an autophagy context: MIR155, MIR15A, MIR16 and MIR185. In none of the studies was RICTOR shown as a rate-limiting target for autophagy induction. Moreover, binding regions of these miRNAs in the 3'UTR region of *RICTOR* mRNA were different and non-overlapping with that of the *MIR211* binding region that we have identified. Furthermore, in our hands, none of these miRNAs were shown to be regulated by starvation or MTOR-inhibition indicating that *MIR211* plays a special and specific role that is different from other *RICTOR*-targeting miRNAs in autophagy control.

Here we showed for the first time, the role of a MITF-specific axis, the MITF-*MIR211* axis, in the control of starvation- and MTOR-inhibition-mediated autophagy. Considering the co-existence of MITF and *MIR211* in various cell lines and tissues, our results suggest that the MITF-*MIR211* axis is a universal determinant of autophagy amplitude under stress conditions.

5. CONCLUSION and FUTURE PROSPECTS

In this thesis, MITF/MIR211 axis was introduced as a novel feed-forward mechanism that amplifies autophagy under cellular stress. Detailed analysis of MITF function in mTOR inhibition- and starvation-induced autophagy was shown for the first time. Further analysis revealed for the first time that, in addition to autophagy-related genes *LC3B* and *ATG10*, MITF regulated *MIR211* expression under autophagy-inducing conditions. Several independent autophagic activity analyses showed that endogenous *MIR211* is a critical component of stress-induced autophagy activation. Functional analyses identified mTORC2 component RICTOR, as a rate limiting direct target of *MIR211*. RICTOR downregulation by the *MIR211* attenuated mTORC1 signal through AKT-mediated crosstalk, and stimulated autophagy. Under these conditions, MITF translocated to the nucleus and activate autophagy transcriptional network and *MIR211*. Downregulation of either MITF or *MIR211* resulted in a decrease in the amplitude of stress induced autophagy. Therefore, we can conclude that the MITF-*MIR211*-MTORC2-AKT-MTORC1 axis is functional and important for autophagy regulation under various biological contexts, and in different cell and tissue types.

We believe that findings from this thesis will first clarify the rate-limiting function of MITF in autophagy regulation. Since MITF is involved in cellular clearance pathway, it should be an attractive therapeutic target for human diseases associated with cellular storage disorders such as Parkinson's and Alzheimer's. Although there are multiple studies providing compelling evidence that stimulation of autophagy through genetic or pharmacological TFEB activation is a critical therapeutic approach, there are still remaining questions about MITF. In vivo preclinical studies should be carried out for several diseases to provide promising perspectives for MITF in robust protection and disease modifying effect.

Although MITF/TFE family of transcription factors still share a group of target genes, the individual family members, MITF, TFEB and TFE3, each have acquired more specific roles by targeting different subset of genes. Moreover, the role and significance of localization and heterodimerization of MITF isoforms, TFEB and TFE3 remains to be explored.

Autophagy-related miRNAs constitute a very important control layer on top of all other autophagy regulatory mechanisms that were described so far. In the last few years, there is an exponential increase in the number of articles studying miRNA-autophagy connection. These efforts will eventually result in the construction of a detailed and functional map of autophagy-related miRNA networks. Accumulation of knowledge on miRNA-mediated control of autophagy under physiological and pathological conditions might lead to the development of new approaches that can be used for the diagnosis, treatment and follow-up of serious health problems involving autophagy abnormalities, including cancer. Therefore, considering the emerging role of autophagy abnormalities in cancer and other diseases, determination of the contribution of autophagy regulation problems arising from miRNA dysregulation under disease-related conditions, might contribute to a better understanding of the mechanisms of major health problems, and provide new disease markers and/or drug-targets.

6. REFERENCES

- Abràmoff, M. D., Magalhães, P. J., & Ram, S. J. (2004). Image processing with imageJ. *Biophotonics International*.
- Aksan, I., & Goding, C. R. (2015). Targeting the Microphthalmia Basic Helix-Loop-Helix–Leucine Zipper Transcription Factor to a Subset of E-Box Elements In Vitro and In Vivo. *Molecular and Cellular Biology*. <https://doi.org/10.1128/mcb.18.12.6930>
- Amae, S., Fuse, N., Yasumoto, K. I., Sato, S., Yajima, I., Yamamoto, H., ... Shibahara, S. (1998). Identification of a novel isoform of microphthalmia-associated transcription factor that is enriched in retinal pigment epithelium. *Biochemical and Biophysical Research Communications*. <https://doi.org/10.1006/bbrc.1998.8838>
- Amaravadi, R. K., Yu, D., Lum, J. J., Bui, T., Christophorou, M. A., Evan, G. I., ... Thompson, C. B. (2007). Autophagy inhibition enhances therapy-induced apoptosis in a Myc-induced model of lymphoma. *Journal of Clinical Investigation*. <https://doi.org/10.1172/JCI28833>
- Aoyama, T., Matsui, T., Novikov, M., Park, J., Hemmings, B., & Rosenzweig, A. (2005). Serum and glucocorticoid-responsive kinase-1 regulates cardiomyocyte survival and hypertrophic response. *Circulation*. <https://doi.org/10.1161/01.CIR.0000160352.58142.06>
- Apel, A., Herr, I., Schwarz, H., Rodemann, H. P., & Mayer, A. (2008). Blocked autophagy sensitizes resistant carcinoma cells to radiation therapy. *Cancer Research*. <https://doi.org/10.1158/0008-5472.CAN-07-0562>
- Argani, P. (2015). MiT family translocation renal cell carcinoma. *Seminars in Diagnostic Pathology*. <https://doi.org/10.1053/j.semmp.2015.02.003>
- Arias, E., Koga, H., Diaz, A., Mocholi, E., Patel, B., & Cuervo, A. M. (2015). Lysosomal mTORC2/PHLPP1/Akt Regulate Chaperone-Mediated Autophagy. *Molecular Cell*. <https://doi.org/10.1016/j.molcel.2015.05.030>
- Asuthkar, S., Velpula, K. K., Chetty, C., Gorantla, B., & Rao, J. S. (2012). Epigenetic Regulation of miRNA-211 by MMP-9 Governs Glioma Cell Apoptosis, Chemosensitivity and Radiosensitivity. *Oncotarget*. <https://doi.org/10.18632/oncotarget.683>
- B., R., S., S., J.E., D., M., F., M., G.-A., Z.W., G.-T., ... D.C., R. (2010). Regulation of mammalian autophagy in physiology and pathophysiology. *Physiological Reviews*.
- Ballabio, A. (2016). The awesome lysosome. *EMBO Molecular Medicine*. <https://doi.org/10.15252/emmm.201505966>
- Bartel, D. P. (2004). MicroRNAs: Genomics, Biogenesis, Mechanism, and Function. *Cell*. [https://doi.org/10.1016/S0092-8674\(04\)00045-5](https://doi.org/10.1016/S0092-8674(04)00045-5)

- Beckmann, H., Su, L. K., & Kadesch, T. (1990). TFE3: A helix-loop-helix protein that activates transcription through the immunoglobulin enhancer μ E3 motif. *Genes and Development*. <https://doi.org/10.1101/gad.4.2.167>
- Bell, R. E., Khaled, M., Netanel, D., Schubert, S., Golan, T., Buxbaum, A., ... Levy, C. (2014). Transcription factor/microRNA axis blocks melanoma invasion program by miR-211 targeting NUA1. *Journal of Investigative Dermatology*. <https://doi.org/10.1038/jid.2013.340>
- Bellot, G., Garcia-Medina, R., Gounon, P., Chiche, J., Roux, D., Pouyssegur, J., & Mazure, N. M. (2009). Hypoxia-Induced Autophagy Is Mediated through Hypoxia-Inducible Factor Induction of BNIP3 and BNIP3L via Their BH3 Domains. *Molecular and Cellular Biology*. <https://doi.org/10.1128/MCB.00166-09>
- Berry, D. L., & Baehrecke, E. H. (2007). Growth Arrest and Autophagy Are Required for Salivary Gland Cell Degradation in *Drosophila*. *Cell*. <https://doi.org/10.1016/j.cell.2007.10.048>
- Borchert, G. M., Lanier, W., & Davidson, B. L. (2006). RNA polymerase III transcribes human microRNAs. *Nature Structural and Molecular Biology*. <https://doi.org/10.1038/nsmb1167>
- Bouché, V., Espinosa, A. P., Leone, L., Sardiello, M., Ballabio, A., & Botas, J. (2016). *Drosophila* Mitf regulates the V-ATPase and the lysosomal-autophagic pathway. *Autophagy*. <https://doi.org/10.1080/15548627.2015.1134081>
- Boyle, G. M., Woods, S. L., Bonazzi, V. F., Stark, M. S., Hacker, E., Aoude, L. G., ... Hayward, N. K. (2011). Melanoma cell invasiveness is regulated by miR-211 suppression of the BRN2 transcription factor. *Pigment Cell and Melanoma Research*. <https://doi.org/10.1111/j.1755-148X.2011.00849.x>
- Bronisz, A. (2006). Microphthalmia-associated Transcription Factor Interactions with 14-3-3 Modulate Differentiation of Committed Myeloid Precursors. *Molecular Biology of the Cell*. <https://doi.org/10.1091/mbc.e06-05-0470>
- Brugarolas, J., Lei, K., Hurley, R. L., Manning, B. D., Reiling, J. H., Hafen, E., ... Kaelin, W. G. (2004). Regulation of mTOR function in response to hypoxia by REDD1 and the TSC1/TSC2 tumor suppressor complex. *Genes and Development*. <https://doi.org/10.1101/gad.1256804>
- Brunn, G. J., Hudson, C. C., Sekulić, A., Williams, J. M., Hosoi, H., Houghton, P. J., ... Abraham, R. T. (1997). Phosphorylation of the translational repressor PHAS-I by the mammalian target of rapamycin. *Science*. <https://doi.org/10.1126/science.277.5322.99>
- Cai, C., Ashktorab, H., Pang, X., Zhao, Y., Sha, W., Liu, Y., & Gu, X. (2012). MicroRNA-211 expression promotes colorectal cancer cell growth in vitro and in Vivo by targeting tumor suppressor CHD5. *PLoS ONE*. <https://doi.org/10.1371/journal.pone.0029750>
- Carlsson, S. R., & Simonsen, A. (2015). Membrane dynamics in autophagosome biogenesis. *Journal of Cell Science*. <https://doi.org/10.1242/jcs.141036>
- Carreira, S., Goodall, J., Denat, L., Rodriguez, M., Nuciforo, P., Hoek, K. S., ... Goding, C.

- R. (2006). Mitf regulation of Dial controls melanoma proliferation and invasiveness. *Genes and Development*. <https://doi.org/10.1101/gad.406406>
- Chang, K. W., Liu, C. J., Chu, T. H., Cheng, H. W., Hung, P. S., Hu, W. Y., & Lin, S. C. (2008). Association between high miR-211 microRNA expression and the poor prognosis of oral carcinoma. *Journal of Dental Research*. <https://doi.org/10.1177/154405910808701116>
- Chen, Y. S., Song, H. X., Lu, Y., Li, X., Chen, T., Zhang, Y., ... Fu, T. (2011). Autophagy inhibition contributes to radiation sensitization of esophageal squamous carcinoma cells. *Diseases of the Esophagus*. <https://doi.org/10.1111/j.1442-2050.2010.01156.x>
- Cheng, A. M., Byrom, M. W., Shelton, J., & Ford, L. P. (2005). Antisense inhibition of human miRNAs and indications for an involvement of miRNA in cell growth and apoptosis. *Nucleic Acids Research*. <https://doi.org/10.1093/nar/gki200>
- Chiang, H. L., Terlecky, S. R., Plant, C. P., & Dice, J. F. (1989). A role for a 70-kilodalton heat shock protein in lysosomal degradation of intracellular proteins. *Science*. <https://doi.org/10.1126/science.2799391>
- Chin, T. Y., Kao, C. H., Wang, H. Y., Huang, W. P., Ma, K. H., & Chueh, S. H. (2010). Inhibition of the mammalian target of rapamycin promotes cyclic AMP-induced differentiation of NG108-15 cells. *Autophagy*. <https://doi.org/10.4161/auto.6.8.13564>
- Chitnis, N. S., Pytel, D., Bobrovnikova-Marjon, E., Pant, D., Zheng, H., Maas, N. L., ... Diehl, J. A. (2012). MiR-211 Is a Prosurvival MicroRNA that Regulates chop Expression in a PERK-Dependent Manner. *Molecular Cell*. <https://doi.org/10.1016/j.molcel.2012.08.025>
- Choudhury, S., Kolukula, V. K., Preet, A., Albanese, C., & Avantaggiati, M. L. (2013). Dissecting the pathways that destabilize mutant p53: The proteasome or autophagy? *Cell Cycle*. <https://doi.org/10.4161/cc.24128>
- Ciani, B., Layfield, R., Cavey, J. R., Sheppard, P. W., & Searle, M. S. (2003). Structure of the ubiquitin-associated domain of p62 (SQSTM1) and implications for mutations that cause Paget's disease of bone. *Journal of Biological Chemistry*. <https://doi.org/10.1074/jbc.M307416200>
- Cross, D. A. E., Alessi, D. R., Cohen, P., Andjelkovich, M., & Hemmings, B. A. (1995). Inhibition of glycogen synthase kinase-3 by insulin mediated by protein kinase B. *Nature*. <https://doi.org/10.1038/378785a0>
- Cuervo, A. M., & Dice, J. F. (1996). A receptor for the selective uptake and degradation of proteins by lysosomes. *Science*. <https://doi.org/10.1126/science.273.5274.501>
- Degenhardt, K., Mathew, R., Beaudoin, B., Bray, K., Anderson, D., Chen, G., ... White, E. (2006). Autophagy promotes tumor cell survival and restricts necrosis, inflammation, and tumorigenesis. *Cancer Cell*. <https://doi.org/10.1016/j.ccr.2006.06.001>
- Denli, A. M., Tops, B. B. J., Plasterk, R. H. A., Ketting, R. F., & Hannon, G. J. (2004). Processing of primary microRNAs by the Microprocessor complex. *Nature*. <https://doi.org/10.1038/nature03049>

- Deosaran, E., Larsen, K. B., Hua, R., Sargent, G., Wang, Y., Kim, S., ... Kim, P. K. (2013). NBR1 acts as an autophagy receptor for peroxisomes. *Journal of Cell Science*. <https://doi.org/10.1242/jcs.114819>
- Dhar, S. K., Batinic-Haberle, I., & Clair, D. K. S. (2019). UVB-induced inactivation of manganese-containing superoxide dismutase promotes mitophagy via ROS-mediated mTORC2 pathway activation. *Journal of Biological Chemistry*. <https://doi.org/10.1074/jbc.RA118.006595>
- Dibble, C. C., & Manning, B. D. (2010). The TSC1-TSC2 complex. A key signal-integrating node upstream of TOR. In *Enzymes*. [https://doi.org/10.1016/S1874-6047\(10\)28002-2](https://doi.org/10.1016/S1874-6047(10)28002-2)
- Dikic, I., & Elazar, Z. (2018). Mechanism and medical implications of mammalian autophagy. *Nature Reviews Molecular Cell Biology*. <https://doi.org/10.1038/s41580-018-0003-4>
- Dorrello, N. V., Peschiaroli, A., Guardavaccaro, D., Colburn, N. H., Sherman, N. E., & Pagano, M. (2006). S6k1- and β TRCP-mediated degradation of PDCD4 promotes protein translation and cell growth. *Science*. <https://doi.org/10.1126/science.1130276>
- Dos, D. S., Ali, S. M., Kim, D. H., Guertin, D. A., Latek, R. R., Erdjument-Bromage, H., ... Sabatini, D. M. (2004). Rictor, a novel binding partner of mTOR, defines a rapamycin-insensitive and raptor-independent pathway that regulates the cytoskeleton. *Current Biology*. <https://doi.org/10.1016/j.cub.2004.06.054>
- Dubouloz, F., Deloche, O., Wanke, V., Cameroni, E., & De Virgilio, C. (2005). The TOR and EGO protein complexes orchestrate microautophagy in yeast. *Molecular Cell*. <https://doi.org/10.1016/j.molcel.2005.05.020>
- Dunlop, E. A., Hunt, D. K., Acosta-Jaquez, H. A., Fingar, D. C., & Tee, A. R. (2011). ULK1 inhibits mTORC1 signaling, promotes multisite Raptor phosphorylation and hinders substrate binding. *Autophagy*. <https://doi.org/10.4161/auto.7.7.15491>
- Duran, A., Linares, J. F., Galvez, A. S., Wikenheiser, K., Flores, J. M., Diaz-Meco, M. T., & Moscat, J. (2008). The Signaling Adaptor p62 Is an Important NF- κ B Mediator in Tumorigenesis. *Cancer Cell*. <https://doi.org/10.1016/j.ccr.2008.02.001>
- Düvel, K., Yecies, J. L., Menon, S., Raman, P., Lipovsky, A. I., Souza, A. L., ... Manning, B. D. (2010). Activation of a metabolic gene regulatory network downstream of mTOR complex 1. *Molecular Cell*. <https://doi.org/10.1016/j.molcel.2010.06.022>
- Elgendy, M., Sheridan, C., Brumatti, G., & Martin, S. J. (2011). Oncogenic Ras-Induced Expression of Noxa and Beclin-1 Promotes Autophagic Cell Death and Limits Clonogenic Survival. *Molecular Cell*. <https://doi.org/10.1016/j.molcel.2011.02.009>
- Ferron, M., Settembre, C., Shimazu, J., Lacombe, J., Kato, S., Rawlings, D. J., ... Karsenty, G. (2013). A RANKL-PKC β -TFEB signaling cascade is necessary for lysosomal biogenesis in osteoclasts. *Genes and Development*. <https://doi.org/10.1101/gad.213827.113>
- Foley, C. J., Freedman, H., Choo, S. L., Onyskiw, C., Fu, N. Y., Yu, V. C., ... Baksh, S. (2008). Dynamics of RASSF1A/MOAP-1 Association with Death Receptors. *Molecular*

- and Cellular Biology*. <https://doi.org/10.1128/mcb.02011-07>
- Frankel, L. B., & Lund, A. H. (2012). MicroRNA regulation of autophagy. *Carcinogenesis*. <https://doi.org/10.1093/carcin/bgs266>
- Fred Dice, J. (1990). Peptide sequences that target cytosolic proteins for lysosomal proteolysis. *Trends in Biochemical Sciences*. [https://doi.org/10.1016/0968-0004\(90\)90019-8](https://doi.org/10.1016/0968-0004(90)90019-8)
- Friedman, R. C., Farh, K. K. H., Burge, C. B., & Bartel, D. P. (2009). Most mammalian mRNAs are conserved targets of microRNAs. *Genome Research*. <https://doi.org/10.1101/gr.082701.108>
- Füllgrabe, J., Ghislat, G., Cho, D.-H., & Rubinsztein, D. C. (2016). Transcriptional regulation of mammalian autophagy at a glance. *Journal of Cell Science*. <https://doi.org/10.1242/jcs.188920>
- Funderburk, S. F., Wang, Q. J., & Yue, Z. (2010). The Beclin 1-VPS34 complex - at the crossroads of autophagy and beyond. *Trends in Cell Biology*. <https://doi.org/10.1016/j.tcb.2010.03.002>
- Fung, C., Lock, R., Gao, S., Salas, E., & Debnath, J. (2007). Induction of Autophagy during Extracellular Matrix Detachment Promotes Cell Survival. *Molecular Biology of the Cell*. <https://doi.org/10.1091/mbc.e07-10-1092>
- Fuse, N., Yasumoto, K. I., Suzuki, H., Takahashi, K., & Shibahara, S. (1996). Identification of a melanocyte-type promoter of the microphthalmia-associated transcription factor gene. *Biochemical and Biophysical Research Communications*. <https://doi.org/10.1006/bbrc.1996.0298>
- Fuse, N., Yasumoto, K. I., Takeda, K., Amae, S., Yoshizawa, M., Udono, T., ... Shibahara, S. (1999). Molecular cloning of cDNA encoding a novel microphthalmia-associated transcription factor isoform with a distinct amino-terminus. *Journal of Biochemistry*. <https://doi.org/10.1093/oxfordjournals.jbchem.a022548>
- García-Martínez, J. M., & Alessi, D. R. (2008). mTOR complex 2 (mTORC2) controls hydrophobic motif phosphorylation and activation of serum- and glucocorticoid-induced protein kinase 1 (SGK1). *Biochemical Journal*. <https://doi.org/10.1042/BJ20081668>
- Garraway, L. A., Widlund, H. R., Rubin, M. A., Getz, G., Berger, A. J., Ramaswamy, S., ... Sellers, W. R. (2005). Integrative genomic analyses identify MITF as a lineage survival oncogene amplified in malignant melanoma. *Nature*. <https://doi.org/10.1038/nature03664>
- Gewirtz, D. A. (2009). Autophagy, senescence and tumor dormancy in cancer therapy. *Autophagy*. <https://doi.org/10.4161/auto.5.8.9896>
- Gingras, A. C., Gygi, S. P., Raught, B., Polakiewicz, R. D., Abraham, R. T., Hoekstra, M. F., ... Sonenberg, N. (1999). Regulation of 4E-BP1 phosphorylation: A novel two step mechanism. *Genes and Development*. <https://doi.org/10.1101/gad.13.11.1422>
- Goode, A., Long, J. E., Shaw, B., Ralston, S. H., Visconti, M. R., Gianfrancesco, F., ...

- Layfield, R. (2014). Paget disease of bone-associated UBA domain mutations of SQSTM1 exert distinct effects on protein structure and function. *Biochimica et Biophysica Acta - Molecular Basis of Disease*.
<https://doi.org/10.1016/j.bbadis.2014.03.006>
- Goussetis, D. J., Gounaris, E., Wu, E. J., Vakana, E., Sharma, B., Bogyo, M., ... Platanias, L. C. (2012). Autophagic degradation of the BCR-ABL oncoprotein and generation of antileukemic responses by arsenic trioxide. *Blood*. <https://doi.org/10.1182/blood-2012-01-402578>
- Gozuacik, D., Bialik, S., Raveh, T., Mitou, G., Shohat, G., Sabanay, H., ... Kimchi, A. (2008). DAP-kinase is a mediator of endoplasmic reticulum stress-induced caspase activation and autophagic cell death. *Cell Death and Differentiation*.
<https://doi.org/10.1038/cdd.2008.121>
- Gozuacik, Devrim, Akkoc, Y., Ozturk, D. G., & Kocak, M. (2017). Autophagy-Regulating microRNAs and Cancer. *Frontiers in Oncology*. <https://doi.org/10.3389/fonc.2017.00065>
- Gozuacik, Devrim, & Kimchi, A. (2004). Autophagy as a cell death and tumor suppressor mechanism. *Oncogene*. <https://doi.org/10.1038/sj.onc.1207521>
- Guertin, D. A., Stevens, D. M., Thoreen, C. C., Burds, A. A., Kalaany, N. Y., Moffat, J., ... Sabatini, D. M. (2006). Ablation in Mice of the mTORC Components raptor, rictor, or mLST8 Reveals that mTORC2 Is Required for Signaling to Akt-FOXO and PKC α , but Not S6K1. *Developmental Cell*. <https://doi.org/10.1016/j.devcel.2006.10.007>
- Gugnoni, M., Sancisi, V., Manzotti, G., Gandolfi, G., & Ciarrocchi, A. (2016). Autophagy and epithelial-mesenchymal transition: an intricate interplay in cancer. *Cell Death & Disease*. <https://doi.org/10.1038/cddis.2016.415>
- Gwinn, D. M., Shackelford, D. B., Egan, D. F., Mihaylova, M. M., Mery, A., Vasquez, D. S., ... Shaw, R. J. (2008). AMPK Phosphorylation of Raptor Mediates a Metabolic Checkpoint. *Molecular Cell*. <https://doi.org/10.1016/j.molcel.2008.03.003>
- Haar, E. Vander, Lee, S. il, Bandhakavi, S., Griffin, T. J., & Kim, D. H. (2007). Insulin signalling to mTOR mediated by the Akt/PKB substrate PRAS40. *Nature Cell Biology*.
<https://doi.org/10.1038/ncb1547>
- Hagiwara, A., Cornu, M., Cybulski, N., Polak, P., Betz, C., Trapani, F., ... Hall, M. N. (2012). Hepatic mTORC2 activates glycolysis and lipogenesis through Akt, glucokinase, and SREBP1c. *Cell Metabolism*. <https://doi.org/10.1016/j.cmet.2012.03.015>
- Hallsson, J. H., Haflidadóttir, B. S., Stivers, C., Odenwald, W., Arnheiter, H., Pignoni, F., & Steingrímsson, E. (2004). The basic helix-loop-helix leucine zipper transcription factor Mitf is conserved in Drosophila and functions in eye development. *Genetics*.
<https://doi.org/10.1534/genetics.167.1.233>
- Han, J., Lee, Y., Yeom, K. H., Kim, Y. K., Jin, H., & Kim, V. N. (2004). The Drosha-DGCR8 complex in primary microRNA processing. *Genes and Development*.
<https://doi.org/10.1101/gad.1262504>
- Hanada, T., Noda, N. N., Satomi, Y., Ichimura, Y., Fujioka, Y., Takao, T., ... Ohsumi, Y.

- (2007). The Atg12-Atg5 conjugate has a novel E3-like activity for protein lipidation in autophagy. *Journal of Biological Chemistry*. <https://doi.org/10.1074/jbc.C700195200>
- Haq, R., & Fisher, D. E. (2011). Biology and clinical relevance of the microphthalmia family of transcription factors in human cancer. *Journal of Clinical Oncology*. <https://doi.org/10.1200/JCO.2010.32.6223>
- Hara, K., Maruki, Y., Long, X., Yoshino, K. ichi, Oshiro, N., Hidayat, S., ... Yonezawa, K. (2002). Raptor, a binding partner of target of rapamycin (TOR), mediates TOR action. *Cell*. [https://doi.org/10.1016/S0092-8674\(02\)00833-4](https://doi.org/10.1016/S0092-8674(02)00833-4)
- Harrington, L. S., Findlay, G. M., Gray, A., Tolkacheva, T., Wigfield, S., Rebholz, H., ... Lamb, R. F. (2004). The TSC1-2 tumor suppressor controls insulin-PI3K signaling via regulation of IRS proteins. *Journal of Cell Biology*. <https://doi.org/10.1083/jcb.200403069>
- Hartman, M. L., & Czyz, M. (2015). MITF in melanoma: Mechanisms behind its expression and activity. *Cellular and Molecular Life Sciences*. <https://doi.org/10.1007/s00018-014-1791-0>
- He, C., & Klionsky, D. J. (2009). Regulation mechanisms and signaling pathways of autophagy. *Annual Review of Genetics*. <https://doi.org/10.1146/annurev-genet-102808-114910>
- Hemesath, T. J., Steingrímsson, E., McGill, G., Hansen, M. J., Vaught, J., Hodgkinson, C. A., ... Fisher, D. E. (1994). microphthalmia, A critical factor in melanocyte development, defines a discrete transcription factor family. *Genes and Development*. <https://doi.org/10.1101/gad.8.22.2770>
- Hershey, C. L., & Fisher, D. E. (2004). Mitf and Tfe3: Members of a b-HLH-ZIP transcription factor family essential for osteoclast development and function. *Bone*. <https://doi.org/10.1016/j.bone.2003.08.014>
- Hershey, C. L., & Fisher, D. E. (2005). Genomic analysis of the Microphthalmia locus and identification of the MITF-J/Mitf-J isoform. *Gene*. <https://doi.org/10.1016/j.gene.2004.12.002>
- Ho, H., Kapadia, R., Al-Tahan, S., Ahmad, S., & Ganesan, A. K. (2011). WIPI1 coordinates melanogenic gene transcription and melanosome formation via TORC1 inhibition. *Journal of Biological Chemistry*. <https://doi.org/10.1074/jbc.M110.200543>
- Hodgkinson, C. A., Moore, K. J., Nakayama, A., Steingrímsson, E., Copeland, N. G., Jenkins, N. A., & Arnheiter, H. (1993). Mutations at the mouse microphthalmia locus are associated with defects in a gene encoding a novel basic-helix-loop-helix-zipper protein. *Cell*. [https://doi.org/10.1016/0092-8674\(93\)90429-T](https://doi.org/10.1016/0092-8674(93)90429-T)
- Holz, M. K., Ballif, B. A., Gygi, S. P., & Blenis, J. (2005). mTOR and S6K1 mediate assembly of the translation preinitiation complex through dynamic protein interchange and ordered phosphorylation events. *Cell*. <https://doi.org/10.1016/j.cell.2005.10.024>
- Hosokawa, N., Sasaki, T., Iemura, S. I., Natsume, T., Hara, T., & Mizushima, N. (2009). Atg101, a novel mammalian autophagy protein interacting with Atg13. *Autophagy*.

<https://doi.org/10.4161/auto.5.7.9296>

- Hsu, C. L., Lee, E. X., Gordon, K. L., Paz, E. A., Shen, W. C., Ohnishi, K., ... La Spada, A. R. (2018). MAP4K3 mediates amino acid-dependent regulation of autophagy via phosphorylation of TFEB. *Nature Communications*. <https://doi.org/10.1038/s41467-018-03340-7>
- Hsu, P. P., Kang, S. A., Rameseder, J., Zhang, Y., Ottina, K. A., Lim, D., ... Sabatini, D. M. (2011). The mTOR-regulated phosphoproteome reveals a mechanism of mTORC1-mediated inhibition of growth factor signaling. *Science*. <https://doi.org/10.1126/science.1199498>
- Huang, J., & Manning, B. D. (2008). The TSC1–TSC2 complex: a molecular switchboard controlling cell growth. *Biochemical Journal*. <https://doi.org/10.1042/bj20080281>
- Huang, N., Wu, J., Qiu, W., Lyu, Q., He, J., Xie, W., ... Zhang, Y. (2015). MiR-15a and miR-16 induce autophagy and enhance chemosensitivity of Camptothecin. *Cancer Biology and Therapy*. <https://doi.org/10.1080/15384047.2015.1040963>
- Huntzinger, E., & Izaurralde, E. (2011). Gene silencing by microRNAs: contributions of translational repression and mRNA decay. *Nature Reviews. Genetics*. <https://doi.org/10.1038/nrg2936>
- Inbal, B., Bialik, S., Sabanay, I., Shani, G., & Kimchi, A. (2002). DAP kinase and DRP-1 mediate membrane blebbing and the formation of autophagic vesicles during programmed cell death. *Journal of Cell Biology*. <https://doi.org/10.1083/jcb.200109094>
- Inoki, K., Li, Y., Xu, T., & Guan, K. L. (2003). Rheb GTPase is a direct target of TSC2 GAP activity and regulates mTOR signaling. *Genes and Development*. <https://doi.org/10.1101/gad.1110003>
- Inoki, K., Li, Y., Zhu, T., Wu, J., & Guan, K. L. (2002). TSC2 is phosphorylated and inhibited by Akt and suppresses mTOR signalling. *Nature Cell Biology*. <https://doi.org/10.1038/ncb839>
- Inoki, K., Ouyang, H., Zhu, T., Lindvall, C., Wang, Y., Zhang, X., ... Guan, K. L. (2006). TSC2 Integrates Wnt and Energy Signals via a Coordinated Phosphorylation by AMPK and GSK3 to Regulate Cell Growth. *Cell*. <https://doi.org/10.1016/j.cell.2006.06.055>
- Inoki, K., Zhu, T., & Guan, K.-L. (2003). TSC2 mediates cellular energy response to control cell growth and survival. *Cell*.
- Ionov, Y., Nowak, N., Perucho, M., Markowitz, S., & Cowell, J. K. (2004). Manipulation of nonsense mediated decay identifies gene mutations in colon cancer cells with microsatellite instability. *Oncogene*. <https://doi.org/10.1038/sj.onc.1207178>
- Jacinto, E., Facchinetti, V., Liu, D., Soto, N., Wei, S., Jung, S. Y., ... Su, B. (2006). SIN1/MIP1 maintains rictor-mTOR complex integrity and regulates Akt phosphorylation and substrate specificity. *Cell*. <https://doi.org/10.1016/j.cell.2006.08.033>
- Jager, S. (2004). Role for Rab7 in maturation of late autophagic vacuoles. *Journal of Cell Science*. <https://doi.org/10.1242/jcs.01370>

- Jounai, N., Takeshita, F., Kobiyama, K., Sawano, A., Miyawaki, A., Xin, K.-Q., ... Okuda, K. (2007). The Atg5 Atg12 conjugate associates with innate antiviral immune responses. *Proceedings of the National Academy of Sciences*. <https://doi.org/10.1073/pnas.0704014104>
- Kabeya, Y. (2000). LC3, a mammalian homologue of yeast Apg8p, is localized in autophagosome membranes after processing. *The EMBO Journal*. <https://doi.org/10.1093/emboj/19.21.5720>
- Kabeya, Y. (2004). LC3, GABARAP and GATE16 localize to autophagosomal membrane depending on form-II formation. *Journal of Cell Science*. <https://doi.org/10.1242/jcs.01131>
- Kaushik, S., & Cuervo, A. M. (2012). Chaperone-mediated autophagy: A unique way to enter the lysosome world. *Trends in Cell Biology*. <https://doi.org/10.1016/j.tcb.2012.05.006>
- Khvorova, A., Reynolds, A., & Jayasena, S. D. (2003). Functional siRNAs and miRNAs exhibit strand bias. *Cell*.
- Kim, D. H., Sarbassov, D. D., Ali, S. M., King, J. E., Latek, R. R., Erdjument-Bromage, H., ... Sabatini, D. M. (2002). mTOR interacts with raptor to form a nutrient-sensitive complex that signals to the cell growth machinery. *Cell*. [https://doi.org/10.1016/S0092-8674\(02\)00808-5](https://doi.org/10.1016/S0092-8674(02)00808-5)
- Kim, John, Krichevsky, A., Grad, Y., Hayes, G. D., Kosik, K. S., Church, G. M., & Ruvkun, G. (2004). Identification of many microRNAs that copurify with polyribosomes in mammalian neurons. *Proceedings of the National Academy of Sciences of the United States of America*. <https://doi.org/10.1073/pnas.2333854100>
- Kim, Joungmok, Kundu, M., Viollet, B., & Guan, K.-L. (2011). AMPK and mTOR regulate autophagy through direct phosphorylation of Ulk1. *Nature Cell Biology*. <https://doi.org/10.1038/ncb2152>
- Kim, K. W., Paul, P., Qiao, J., Lee, S., & Chung, D. H. (2013). Enhanced autophagy blocks angiogenesis via degradation of gastrin-releasing peptide in neuroblastoma cells. *Autophagy*. <https://doi.org/10.4161/auto.25987>
- Kim, S. G., Buel, G. R., & Blenis, J. (2013). Nutrient regulation of the mTOR complex 1 signaling pathway. *Molecules and Cells*. <https://doi.org/10.1007/s10059-013-0138-2>
- Kim, Y. C., & Guan, K. L. (2015). mTOR: A pharmacologic target for autophagy regulation. *Journal of Clinical Investigation*. <https://doi.org/10.1172/JCI73939>
- Kimura, S., Fujita, N., Noda, T., & Yoshimori, T. (2009). Chapter 1 Monitoring Autophagy in Mammalian Cultured Cells through the Dynamics of LC3. *Methods in Enzymology*. [https://doi.org/10.1016/S0076-6879\(08\)03201-1](https://doi.org/10.1016/S0076-6879(08)03201-1)
- Kirisako, T., Ichimura, Y., Okada, H., Kabeya, Y., Mizushima, N., Yoshimori, T., ... Ohsumi, Y. (2000). The reversible modification regulates the membrane-binding state of Apg8/Aut7 essential for autophagy and the cytoplasm to vacuole targeting pathway. *Journal of Cell Biology*. <https://doi.org/10.1083/jcb.151.2.263>

- Kocalis, H. E., Hagan, S. L., George, L., Turney, M. K., Siuta, M. A., Laryea, G. N., ... Niswender, K. D. (2014). Rictor/mTORC2 facilitates central regulation of energy and glucose homeostasis. *Molecular Metabolism*. <https://doi.org/10.1016/j.molmet.2014.01.014>
- Komatsu, M., Waguri, S., Koike, M., Sou, Y. shin, Ueno, T., Hara, T., ... Tanaka, K. (2007). Homeostatic Levels of p62 Control Cytoplasmic Inclusion Body Formation in Autophagy-Deficient Mice. *Cell*. <https://doi.org/10.1016/j.cell.2007.10.035>
- Koren, I., Reem, E., & Kimchi, A. (2010). DAP1, a novel substrate of mTOR, negatively regulates autophagy. *Current Biology*. <https://doi.org/10.1016/j.cub.2010.04.041>
- Korkmaz, G., Ayse Tekirdag, K., Gulfem Ozturk, D., Kosar, A., Ugur Sezerman, O., & Gozuacik, D. (2013). MIR376A is a regulator of starvation-induced autophagy. *PLoS ONE*. <https://doi.org/10.1371/journal.pone.0082556>
- Korkmaz, G., Le Sage, C., Tekirdag, K. A., Agami, R., & Gozuacik, D. (2012). miR-376b controls starvation and mTOR inhibition-related autophagy by targeting ATG4C and BECN1. *Autophagy*. <https://doi.org/10.4161/auto.8.2.18351>
- Koscianska, E., Starega-Roslan, J., & Krzyzosiak, W. J. (2011). The role of dicer protein partners in the processing of microRNA precursors. *PLoS ONE*. <https://doi.org/10.1371/journal.pone.0028548>
- Kozomara, A., Birgaoanu, M., & Griffiths-Jones, S. (2019). MiRBase: From microRNA sequences to function. *Nucleic Acids Research*. <https://doi.org/10.1093/nar/gky1141>
- Lamark, T., & Johansen, T. (2012). Aggrephagy: Selective Disposal of Protein Aggregates by Macroautophagy. *International Journal of Cell Biology*. <https://doi.org/10.1155/2012/736905>
- Lamy, L., Ngo, V. N., Emre, N. C. T., Shaffer, A. L., Yang, Y., Tian, E., ... Staudt, L. M. (2013). Control of autophagic cell death by caspase-10 in multiple myeloma. *Cancer Cell*. <https://doi.org/10.1016/j.ccr.2013.02.017>
- Laplante, M., & Sabatini, D. M. (2012). MTOR signaling in growth control and disease. *Cell*. <https://doi.org/10.1016/j.cell.2012.03.017>
- Lazarou, M., Sliter, D. A., Kane, L. A., Sarraf, S. A., Wang, C., Burman, J. L., ... Youle, R. J. (2015). The ubiquitin kinase PINK1 recruits autophagy receptors to induce mitophagy. *Nature*. <https://doi.org/10.1038/nature14893>
- Lee, D. F., Kuo, H. P., Chen, C. Te, Hsu, J. M., Chou, C. K., Wei, Y., ... Hung, M. C. (2007). IKK β Suppression of TSC1 Links Inflammation and Tumor Angiogenesis via the mTOR Pathway. *Cell*. <https://doi.org/10.1016/j.cell.2007.05.058>
- Lee, H., Lee, S., Bae, H., Kang, H. S., & Kim, S. J. (2016). Genome-wide identification of target genes for miR-204 and miR-211 identifies their proliferation stimulatory role in breast cancer cells. *Scientific Reports*. <https://doi.org/10.1038/srep25287>
- Lee, J. W., Park, S., Takahashi, Y., & Wang, H. G. (2010). The association of AMPK with ULK1 regulates autophagy. *PLoS ONE*. <https://doi.org/10.1371/journal.pone.0015394>

- Lee, R. C., Feinbaum, R. L., & Ambros, V. (1993). The *C. elegans* heterochronic gene *lin-4* encodes small RNAs with antisense complementarity to *lin-14*. *Cell*.
[https://doi.org/10.1016/0092-8674\(93\)90529-Y](https://doi.org/10.1016/0092-8674(93)90529-Y)
- Lee, S. J., Kim, H. P., Jin, Y., Choi, A. M. K., & Ryter, S. W. (2011). Beclin 1 deficiency is associated with increased hypoxia-induced angiogenesis. *Autophagy*.
<https://doi.org/10.4161/auto.7.8.15598>
- Lee, Y., Ahn, C., Han, J., Choi, H., Kim, J., Yim, J., ... Kim, V. N. (2003). The nuclear RNase III Droscha initiates microRNA processing. *Nature*.
<https://doi.org/10.1038/nature01957>
- Levine, B., & Yuan, J. (2005). Autophagy in cell death: An innocent convict? *Journal of Clinical Investigation*. <https://doi.org/10.1172/JCI26390>
- Levy, C., Khaled, M., & Fisher, D. E. (2006). MITF: master regulator of melanocyte development and melanoma oncogene. *Trends in Molecular Medicine*.
<https://doi.org/10.1016/j.molmed.2006.07.008>
- Levy, C., Khaled, M., Iliopoulos, D., Janas, M. M., Schubert, S., Pinner, S., ... Novina, C. D. (2010). Intronic miR-211 Assumes the Tumor Suppressive Function of Its Host Gene in Melanoma. *Molecular Cell*. <https://doi.org/10.1016/j.molcel.2010.11.020>
- Li, J., Hou, N., Faried, A., Tsutsumi, S., Takeuchi, T., & Kuwano, H. (2009). Inhibition of autophagy by 3-MA enhances the effect of 5-FU-induced apoptosis in colon cancer cells. *Annals of Surgical Oncology*. <https://doi.org/10.1245/s10434-008-0260-0>
- Li, W. W., Li, J., & Bao, J. K. (2012). Microautophagy: Lesser-known self-eating. *Cellular and Molecular Life Sciences*. <https://doi.org/10.1007/s00018-011-0865-5>
- Li, Y., Xu, M., Ding, X., Yan, C., Song, Z., Chen, L., ... Yang, C. (2016). Protein kinase C controls lysosome biogenesis independently of mTORC1. *Nature Cell Biology*.
<https://doi.org/10.1038/ncb3407>
- Liang, C., Feng, P., Ku, B., Dotan, I., Canaani, D., Oh, B. H., & Jung, J. U. (2006). Autophagic and tumour suppressor activity of a novel Beclin1-binding protein UVRAG. *Nature Cell Biology*. <https://doi.org/10.1038/ncb1426>
- Liu, X. D., Yao, J., Tripathi, D. N., Ding, Z., Xu, Y., Sun, M., ... Jonasch, E. (2015). Autophagy mediates HIF2 α degradation and suppresses renal tumorigenesis. *Oncogene*.
<https://doi.org/10.1038/onc.2014.199>
- Lock, R., Kenific, C. M., Leidal, A. M., Salas, E., & Debnath, J. (2014). Autophagy-dependent production of secreted factors facilitates oncogenic RAS-Driven invasion. *Cancer Discovery*. <https://doi.org/10.1158/2159-8290.CD-13-0841>
- Löffler, A. S., Alers, S., Dieterle, A. M., Keppeler, H., Franz-Wachtel, M., Kundu, M., ... Stork, B. (2011). Ulk1-mediated phosphorylation of AMPK constitutes a negative regulatory feedback loop. *Autophagy*. <https://doi.org/10.4161/auto.7.7.15451>
- Long, X., Ortiz-Vega, S., Lin, Y., & Avruch, J. (2005). Rheb binding to mammalian target of rapamycin (mTOR) is regulated by amino acid sufficiency. *Journal of Biological*

Chemistry. <https://doi.org/10.1074/jbc.C500169200>

- Lu, K., Psakhye, I., & Jentsch, S. (2014). Autophagic clearance of PolyQ proteins mediated by ubiquitin-Atg8 adaptors of the conserved CUET protein family. *Cell*. <https://doi.org/10.1016/j.cell.2014.05.048>
- Lu, Z., Luo, R. Z., Lu, Y., Zhang, X., Yu, Q., Khare, S., ... Bast, R. C. (2008). The tumor suppressor gene ARHI regulates autophagy and tumor dormancy in human ovarian cancer cells. *Journal of Clinical Investigation*. <https://doi.org/10.1172/JCI35512>
- M., P., R., P., H.R., N., P., L., G.R., S., M.L., S., ... Sardiello, M. (2017). MTORC1-independent TFEB activation via Akt inhibition promotes cellular clearance in neurodegenerative storage diseases. *Nature Communications*. <https://doi.org/10.1038/ncomms14338>
- Ma, X. M., Yoon, S. O., Richardson, C. J., Jülich, K., & Blenis, J. (2008). SKAR Links Pre-mRNA Splicing to mTOR/S6K1-Mediated Enhanced Translation Efficiency of Spliced mRNAs. *Cell*. <https://doi.org/10.1016/j.cell.2008.02.031>
- Ma, Y., Chen, B., Xu, X., & Lin, G. (2013). Prospective nested case-control study of feature genes related to leukemic evolution of myelodysplastic syndrome. *Molecular Biology Reports*. <https://doi.org/10.1007/s11033-012-2082-1>
- MacFarlane, L.-A., & R. Murphy, P. (2010). MicroRNA: Biogenesis, Function and Role in Cancer. *Current Genomics*. <https://doi.org/10.2174/138920210793175895>
- Macintosh, R. L., Timpson, P., Thorburn, J., Anderson, K. I., Thorburn, A., & Ryan, K. M. (2012). Inhibition of autophagy impairs tumor cell invasion in an organotypic model. *Cell Cycle*. <https://doi.org/10.4161/cc.20424>
- Maes, H., Kuchnio, A., Peric, A., Moens, S., Nys, K., DeBock, K., ... Carmeliet, P. (2014). Tumor vessel normalization by chloroquine independent of autophagy. *Cancer Cell*. <https://doi.org/10.1016/j.ccr.2014.06.025>
- Majeski, A. E., & Fred Dice, J. (2004). Mechanisms of chaperone-mediated autophagy. *International Journal of Biochemistry and Cell Biology*. <https://doi.org/10.1016/j.biocel.2004.02.013>
- Mammucari, C., Milan, G., Romanello, V., Masiero, E., Rudolf, R., Del Piccolo, P., ... Sandri, M. (2007). FoxO3 Controls Autophagy in Skeletal Muscle In Vivo. *Cell Metabolism*. <https://doi.org/10.1016/j.cmet.2007.11.001>
- Mansky, K. C., Sankar, U., Han, J., & Ostrowski, M. C. (2002). Microphthalmia transcription factor is a target of the p38 MAPK pathway in response to receptor activator of NF-κB ligand signaling. *Journal of Biological Chemistry*. <https://doi.org/10.1074/jbc.M111696200>
- Mariño, G., Salvador-Montoliu, N., Fueyo, A., Knecht, E., Mizushima, N., & López-Otín, C. (2007). Tissue-specific autophagy alterations and increased tumorigenesis in mice deficient in Atg4C/autophagin-3. *Journal of Biological Chemistry*. <https://doi.org/10.1074/jbc.M701194200>

- Martina, J. A., Diab, H. I., Brady, O. A., & Puertollano, R. (2016). TFEB and TFE3 are novel components of the integrated stress response. *The EMBO Journal*.
<https://doi.org/10.15252/emj.201593428>
- Martina, Jose A., Chen, Y., Gucek, M., & Puertollano, R. (2012). MTORC1 functions as a transcriptional regulator of autophagy by preventing nuclear transport of TFEB. *Autophagy*. <https://doi.org/10.4161/auto.19653>
- Martina, José A., Diab, H. I., Li, H., & Puertollano, R. (2014). Novel roles for the MiTF/TFE family of transcription factors in organelle biogenesis, nutrient sensing, and energy homeostasis. *Cellular and Molecular Life Sciences*. <https://doi.org/10.1007/s00018-014-1565-8>
- Martina, José A., Diab, H. I., Lishu, L., Jeong-A, L., Patange, S., Raben, N., & Puertollano, R. (2014). The nutrient-responsive transcription factor TFE3 promotes autophagy, lysosomal biogenesis, and clearance of cellular debris. *Science Signaling*.
<https://doi.org/10.1126/scisignal.2004754>
- Mathelier, A., & Carbone, A. (2013). Large scale chromosomal mapping of human microRNA structural clusters. *Nucleic Acids Research*.
<https://doi.org/10.1093/nar/gkt112>
- Mathew, R., Karp, C. M., Beaudoin, B., Vuong, N., Chen, G., Chen, H. Y., ... White, E. (2009). Autophagy Suppresses Tumorigenesis through Elimination of p62. *Cell*.
<https://doi.org/10.1016/j.cell.2009.03.048>
- Mauthe, M., Jacob, A., Freiberger, S., Hentschel, K., Stierhof, Y. D., Codogno, P., & Proikas-Cezanne, T. (2011). Resveratrol-mediated autophagy requires WIPI-1-regulated LC3 lipidation in the absence of induced phagophore formation. *Autophagy*.
<https://doi.org/10.4161/auto.7.12.17802>
- Mazar, J., de Young, K., Khaitan, D., Meister, E., Almodovar, A., Goydos, J., ... Perera, R. J. (2010). The Regulation of miRNA-211 Expression and Its Role in Melanoma Cell Invasiveness. *PLoS ONE*. <https://doi.org/10.1371/journal.pone.0013779>
- Medina, D. L., Di Paola, S., Peluso, I., Armani, A., De Stefani, D., Venditti, R., ... Ballabio, A. (2015). Lysosomal calcium signalling regulates autophagy through calcineurin and TFEB. *Nature Cell Biology*. <https://doi.org/10.1038/ncb3114>
- Medina, D. L., Fraldi, A., Bouche, V., Annunziata, F., Mansueto, G., Spampinato, C., ... Ballabio, A. (2011). Transcriptional activation of lysosomal exocytosis promotes cellular clearance. *Developmental Cell*. <https://doi.org/10.1016/j.devcel.2011.07.016>
- Mehrpour, M., Esclatine, A., Beau, I., & Codogno, P. (2010). Autophagy in health and disease. 1. Regulation and significance of autophagy: an overview. *American Journal of Physiology-Cell Physiology*. <https://doi.org/10.1152/ajpcell.00507.2009>
- Menon, S., Dibble, C. C., Talbott, G., Hoxhaj, G., Valvezan, A. J., Takahashi, H., ... Manning, B. D. (2014). Spatial control of the TSC complex integrates insulin and nutrient regulation of mTORC1 at the lysosome. *Cell*.
<https://doi.org/10.1016/j.cell.2013.11.049>

- Mijaljica, D., Prescott, M., & Devenish, R. J. (2011). Microautophagy in mammalian cells: Revisiting a 40-year-old conundrum. *Autophagy*. <https://doi.org/10.4161/auto.7.7.14733>
- Miller, A. J., Du, J., Rowan, S., Hershey, C. L., Widlund, H. R., & Fisher, D. E. (2004). Transcriptional Regulation of the Melanoma Prognostic Marker Melastatin (TRPM1) by MITF in Melanocytes and Melanoma. *Cancer Research*. <https://doi.org/10.1158/0008-5472.CAN-03-2440>
- Mizushima, N. (2010). The role of the Atg1/ULK1 complex in autophagy regulation. *Current Opinion in Cell Biology*. <https://doi.org/10.1016/j.ceb.2009.12.004>
- Mizushima, N., & Komatsu, M. (2011). Autophagy: Renovation of cells and tissues. *Cell*. <https://doi.org/10.1016/j.cell.2011.10.026>
- Monteys, A. M., Spengler, R. M., Wan, J., Tecedor, L., Lennox, K. A., Xing, Y., & Davidson, B. L. (2010). Structure and activity of putative intronic miRNA promoters. *RNA*. <https://doi.org/10.1261/rna.1731910>
- Nakahira, K., Haspel, J. A., Rathinam, V. A. K., Lee, S. J., Dolinay, T., Lam, H. C., ... Choi, A. M. K. (2011). Autophagy proteins regulate innate immune responses by inhibiting the release of mitochondrial DNA mediated by the NALP3 inflammasome. *Nature Immunology*. <https://doi.org/10.1038/ni.1980>
- Nakatogawa, H., Suzuki, K., Kamada, Y., & Ohsumi, Y. (2009). Dynamics and diversity in autophagy mechanisms: Lessons from yeast. *Nature Reviews Molecular Cell Biology*. <https://doi.org/10.1038/nrm2708>
- Napolitano, G., & Ballabio, A. (2016). TFEB at a glance. *Journal of Cell Science*. <https://doi.org/10.1242/jcs.146365>
- Nazio, F., Strappazzon, F., Antonioli, M., Bielli, P., Cianfanelli, V., Bordi, M., ... Cecconi, F. (2013). mTOR inhibits autophagy by controlling ULK1 ubiquitylation, self-association and function through AMBRA1 and TRAF6. *Nature Cell Biology*. <https://doi.org/10.1038/ncb2708>
- Nezich, C. L., Wang, C., Fogel, A. I., & Youle, R. J. (2015). MiT/TFE transcription factors are activated during mitophagy downstream of Parkin and Atg5. *Journal of Cell Biology*. <https://doi.org/10.1083/jcb.201501002>
- Nezis, I. P., Simonsen, A., Sagona, A. P., Finley, K., Gaumer, S., Contamine, D., ... Brech, A. (2008). Ref(2)P, the Drosophila melanogaster homologue of mammalian p62, is required for the formation of protein aggregates in adult brain. *Journal of Cell Biology*. <https://doi.org/10.1083/jcb.200711108>
- Ngeow, K. C., Friedrichsen, H. J., Li, L., Zeng, Z., Andrews, S., Volpon, L., ... Goding, C. R. (2018). BRAF/MAPK and GSK3 signaling converges to control MITF nuclear export. *Proceedings of the National Academy of Sciences*. <https://doi.org/10.1073/pnas.1810498115>
- Oh, W. J., & Jacinto, E. (2011). mTOR complex 2 signaling and functions. *Cell Cycle*. <https://doi.org/10.4161/cc.10.14.16586>

- Oh, W. J., Wu, C. C., Kim, S. J., Facchinetti, V., Julien, L. A., Finlan, M., ... Jacinto, E. (2010). MTORC2 can associate with ribosomes to promote cotranslational phosphorylation and stability of nascent Akt polypeptide. *EMBO Journal*. <https://doi.org/10.1038/emboj.2010.271>
- Okada, C., Yamashita, E., Lee, S. J., Shibata, S., Katahira, J., Nakagawa, A., ... Tsukihara, T. (2009). A high-Resolution structure of the pre-miRNA nuclear export machinery. *Science*. <https://doi.org/10.1126/science.1178705>
- Okamoto, K., Kondo-Okamoto, N., & Ohsumi, Y. (2009). Mitochondria-Anchored Receptor Atg32 Mediates Degradation of Mitochondria via Selective Autophagy. *Developmental Cell*. <https://doi.org/10.1016/j.devcel.2009.06.013>
- Oku, M., Maeda, Y., Kagohashi, Y., Kondo, T., Yamada, M., Fujimoto, T., & Sakai, Y. (2017). Evidence for ESC RT- and clathrin-dependent microautophagy. *Journal of Cell Biology*. <https://doi.org/10.1083/jcb.201611029>
- Oral, O., Akkoc, Y., Bayraktar, O., & Gozuacik, D. (2016). Physiological and pathological significance of the molecular cross-talk between autophagy and apoptosis. *Histology and Histopathology*. <https://doi.org/10.14670/HH-11-714>
- Orenstein, S. J., & Cuervo, A. M. (2010). Chaperone-mediated autophagy: Molecular mechanisms and physiological relevance. *Seminars in Cell and Developmental Biology*. <https://doi.org/10.1016/j.semcdb.2010.02.005>
- Ozeki, N., Hase, N., Hiyama, T., Yamaguchi, H., Kawai-Asano, R., Nakata, K., & Mogi, M. (2017). MicroRNA-211 and autophagy-related gene 14 signaling regulate osteoblast-like cell differentiation of human induced pluripotent stem cells. *Experimental Cell Research*. <https://doi.org/10.1016/j.yexcr.2017.01.018>
- Ozsolak, F., Poling, L. L., Wang, Z., Liu, H., Liu, X. S., Roeder, R. G., ... Fisher, D. E. (2008). Chromatin structure analyses identify miRNA promoters. *Genes and Development*. <https://doi.org/10.1101/gad.1706508>
- Palmieri, M., Impey, S., Kang, H., di Ronza, A., Pelz, C., Sardiello, M., & Ballabio, A. (2011). Characterization of the CLEAR network reveals an integrated control of cellular clearance pathways. *Human Molecular Genetics*. <https://doi.org/10.1093/hmg/ddr306>
- Pankiv, S., Clausen, T. H., Lamark, T., Brech, A., Bruun, J. A., Outzen, H., ... Johansen, T. (2007). p62/SQSTM1 binds directly to Atg8/LC3 to facilitate degradation of ubiquitinated protein aggregates by autophagy*[S]. *Journal of Biological Chemistry*. <https://doi.org/10.1074/jbc.M702824200>
- Pastore, N., Brady, O. A., Diab, H. I., Martina, J. A., Sun, L., Huynh, T., ... Puertollano, R. (2016). TFEB and TFE3 cooperate in the regulation of the innate immune response in activated macrophages. *Autophagy*. <https://doi.org/10.1080/15548627.2016.1179405>
- Pastore, N., Vainshtein, A., Klisch, T. J., Armani, A., Huynh, T., Herz, N. J., ... Ballabio, A. (2017). TFE3 regulates whole-body energy metabolism in cooperation with TFEB. *EMBO Molecular Medicine*. <https://doi.org/10.15252/emmm.201607204>
- Peng, Y. F., Shi, Y. H., Ding, Z. Bin, Ke, A. W., Gu, C. Y., Hui, B., ... Fan, J. (2013).

- Autophagy inhibition suppresses pulmonary metastasis of HCC in mice via impairing anoikis resistance and colonization of HCC cells. *Autophagy*.
<https://doi.org/10.4161/auto.26398>
- Perera, R. M., Stoykova, S., Nicolay, B. N., Ross, K. N., Fitamant, J., Boukhali, M., ... Bardeesy, N. (2015). Transcriptional control of autophagy-lysosome function drives pancreatic cancer metabolism. *Nature*. <https://doi.org/10.1038/nature14587>
- Peterson, T. R., Laplante, M., Thoreen, C. C., Sancak, Y., Kang, S. A., Kuehl, W. M., ... Sabatini, D. M. (2009). DEPTOR Is an mTOR Inhibitor Frequently Overexpressed in Multiple Myeloma Cells and Required for Their Survival. *Cell*.
<https://doi.org/10.1016/j.cell.2009.03.046>
- Peterson, T. R., Sengupta, S. S., Harris, T. E., Carmack, A. E., Kang, S. A., Balderas, E., ... Sabatini, D. M. (2011). mTOR complex 1 regulates lipin 1 localization to control the SREBP pathway. *Cell*. <https://doi.org/10.1016/j.cell.2011.06.034>
- Pietrocola, F., Izzo, V., Niso-Santano, M., Vacchelli, E., Galluzzi, L., Maiuri, M. C., & Kroemer, G. (2013). Regulation of autophagy by stress-responsive transcription factors. *Seminars in Cancer Biology*. <https://doi.org/10.1016/j.semcancer.2013.05.008>
- Ploper, D., & De Robertis, E. M. (2015). The MITF family of transcription factors: Role in endolysosomal biogenesis, Wnt signaling, and oncogenesis. *Pharmacological Research*.
<https://doi.org/10.1016/j.phrs.2015.04.006>
- Ploper, D., Taelman, V. F., Robert, L., Perez, B. S., Titz, B., Chen, H.-W., ... De Robertis, E. M. (2015). MITF drives endolysosomal biogenesis and potentiates Wnt signaling in melanoma cells. *Proceedings of the National Academy of Sciences*.
<https://doi.org/10.1073/pnas.1424576112>
- Pogenberg, V., Ögmundsdóttir, M. H., Bergsteinsdóttir, K., Schepsky, A., Phung, B., Deineko, V., ... Wilmanns, M. (2012). Restricted leucine zipper dimerization and specificity of DNA recognition of the melanocyte master regulator MITF. *Genes and Development*. <https://doi.org/10.1101/gad.198192.112>
- Porstmann, T., Santos, C. R., Griffiths, B., Cully, M., Wu, M., Leever, S., ... Schulze, A. (2008). SREBP activity is regulated by mTORC1 and contributes to Akt-dependent cell growth. *Cell Metabolism*. <https://doi.org/10.1016/j.cmet.2008.07.007>
- Puertollano, R., Ferguson, S. M., Brugarolas, J., & Ballabio, A. (2018). The complex relationship between TFEB transcription factor phosphorylation and subcellular localization. *The EMBO Journal*. <https://doi.org/10.15252/embj.201798804>
- Qu, X., Yu, J., Bhagat, G., Furuya, N., Hibshoosh, H., Troxel, A., ... Levine, B. (2003). Promotion of tumorigenesis by heterozygous disruption of the beclin 1 autophagy gene. *Journal of Clinical Investigation*. <https://doi.org/10.1172/JCI20039>
- Ramphal, R., Pappo, A., Zielenska, M., Grant, R., & Ngan, B. Y. (2006). Pediatric renal cell carcinoma: Clinical, pathologic, and molecular abnormalities associated with the members of the MITF transcription factor family. *American Journal of Clinical Pathology*. <https://doi.org/10.1309/98YE9E442AR7LX2X>

- Rehli, M., Den Elzen, N., Cassady, A. I., Ostrowski, M. C., & Hume, D. A. (1999). Cloning and characterization of the murine genes for bHLH-ZIP transcription factors TFEC and TFEB reveal a common gene organization for all MiT subfamily members. *Genomics*. <https://doi.org/10.1006/geno.1998.5588>
- Reinhold, W. C., Sunshine, M., Liu, H., Varma, S., Kohn, K. W., Morris, J., ... Pommier, Y. (2012). CellMiner: A web-based suite of genomic and pharmacologic tools to explore transcript and drug patterns in the NCI-60 cell line set. *Cancer Research*. <https://doi.org/10.1158/0008-5472.CAN-12-1370>
- Robitaille, A. M., Christen, S., Shimobayashi, M., Cornu, M., Fava, L. L., Moes, S., ... Hall, M. N. (2013). Quantitative phosphoproteomics reveal mTORC1 activates de novo pyrimidine synthesis. *Science*. <https://doi.org/10.1126/science.1228771>
- Roczniak-Ferguson, A., Petit, C. S., Froehlich, F., Qian, S., Ky, J., Angarola, B., ... Ferguson, S. M. (2012). The transcription factor TFEB links mTORC1 signaling to transcriptional control of lysosome homeostasis. *Science Signaling*. <https://doi.org/10.1126/scisignal.2002790>
- Rout, A. K., Strub, M. P., Piszczek, G., & Tjandra, N. (2014). Structure of transmembrane domain of lysosome-associated membrane protein type 2a (LAMP-2A) reveals key features for substrate specificity in chaperone-mediated autophagy. *Journal of Biological Chemistry*. <https://doi.org/10.1074/jbc.M114.609446>
- Rubinsztein, D. C., Shpilka, T., & Elazar, Z. (2012). Mechanisms of autophagosome biogenesis. *Current Biology*. <https://doi.org/10.1016/j.cub.2011.11.034>
- Russell, R. C., Fang, C., & Guan, K.-L. (2011). An emerging role for TOR signaling in mammalian tissue and stem cell physiology. *Development*. <https://doi.org/10.1242/dev.058230>
- Saitoh, T., Fujita, N., Hayashi, T., Takahara, K., Satoh, T., Lee, H., ... Akira, S. (2009). Atg9a controls dsDNA-driven dynamic translocation of STING and the innate immune response. *Proceedings of the National Academy of Sciences of the United States of America*. <https://doi.org/10.1073/pnas.0911267106>
- Samie, M., & Cresswell, P. (2015). The transcription factor TFEB acts as a molecular switch that regulates exogenous antigen-presentation pathways. *Nature Immunology*. <https://doi.org/10.1038/ni.3196>
- Sancak, Y., Bar-Peled, L., Zoncu, R., Markhard, A. L., Nada, S., & Sabatini, D. M. (2010). Ragulator-rag complex targets mTORC1 to the lysosomal surface and is necessary for its activation by amino acids. *Cell*. <https://doi.org/10.1016/j.cell.2010.02.024>
- Sancak, Y., Peterson, T. R., Shaul, Y. D., Lindquist, R. A., Thoreen, C. C., Bar-Peled, L., & Sabatini, D. M. (2008). The rag GTPases bind raptor and mediate amino acid signaling to mTORC1. *Science*. <https://doi.org/10.1126/science.1157535>
- Sancak, Y., Thoreen, C. C., Peterson, T. R., Lindquist, R. A., Kang, S. A., Spooner, E., ... Sabatini, D. M. (2007). PRAS40 Is an Insulin-Regulated Inhibitor of the mTORC1 Protein Kinase. *Molecular Cell*. <https://doi.org/10.1016/j.molcel.2007.03.003>

- Sarbassov, D. D., Ali, S. M., & Sabatini, D. M. (2005). Growing roles for the mTOR pathway. *Current Opinion in Cell Biology*. <https://doi.org/10.1016/j.ceb.2005.09.009>
- Sarbassov, D. D., Ali, S. M., Sengupta, S., Sheen, J. H., Hsu, P. P., Bagley, A. F., ... Sabatini, D. M. (2006). Prolonged Rapamycin Treatment Inhibits mTORC2 Assembly and Akt/PKB. *Molecular Cell*. <https://doi.org/10.1016/j.molcel.2006.03.029>
- Sarbassov, D. D., Guertin, D. A., Ali, S. M., & Sabatini, D. M. (2005). Phosphorylation and regulation of Akt/PKB by the rictor-mTOR complex. *Science*. <https://doi.org/10.1126/science.1106148>
- Sardiello, M., & Ballabio, A. (2009). Lysosomal enhancement: A CLEAR answer to cellular degradative needs. *Cell Cycle*. <https://doi.org/10.4161/cc.8.24.10263>
- Sarraf, S. A., Raman, M., Guarani-Pereira, V., Sowa, M. E., Huttlin, E. L., Gygi, S. P., & Harper, J. W. (2013). Landscape of the PARKIN-dependent ubiquitylome in response to mitochondrial depolarization. *Nature*. <https://doi.org/10.1038/nature12043>
- Sato, S., Roberts, K., Gambino, G., Cook, A., Kouzarides, T., & Goding, C. R. (1997). CBP/p300 as a co-factor for the Microphthalmia transcription factor. *Oncogene*. <https://doi.org/10.1038/sj.onc.1201298>
- Saxton, R. A., & Sabatini, D. M. (2017). mTOR Signaling in Growth, Metabolism, and Disease. *Cell*. <https://doi.org/10.1016/j.cell.2017.02.004>
- Schwarz, T., Murphy, S., Sohn, C., & Mansky, K. C. (2010). C-TAK1 interacts with microphthalmia-associated transcription factor, Mitf, but not the related family member Tfe3. *Biochemical and Biophysical Research Communications*. <https://doi.org/10.1016/j.bbrc.2010.03.034>
- Seibenhener, M. L., Babu, J. R., Geetha, T., Wong, H. C., Krishna, N. R., & Wooten, M. W. (2004). Sequestosome 1/p62 Is a Polyubiquitin Chain Binding Protein Involved in Ubiquitin Proteasome Degradation. *Molecular and Cellular Biology*. <https://doi.org/10.1128/mcb.24.18.8055-8068.2004>
- Selvakumaran, M., Amaravadi, R. K., Vasilevskaya, I. A., & O'Dwyer, P. J. (2013). Autophagy inhibition sensitizes colon cancer cells to antiangiogenic and cytotoxic therapy. *Clinical Cancer Research*. <https://doi.org/10.1158/1078-0432.CCR-12-1542>
- Selzer, E., Wacheck, V., Lucas, T., Heere-Ress, E., Wu, M., Weilbaecher, K. N., ... Jansen, B. (2002). The melanocyte-specific isoform of the microphthalmia transcription factor affects the phenotype of human melanoma. *Cancer Research*.
- Seo, S. U., Woo, S. M., Lee, H. S., Kim, S. H., Min, K. jin, & Kwon, T. K. (2018). mTORC1/2 inhibitor and curcumin induce apoptosis through lysosomal membrane permeabilization-mediated autophagy. *Oncogene*. <https://doi.org/10.1038/s41388-018-0345-6>
- Settembre, C., De Cegli, R., Mansueto, G., Saha, P. K., Vetrini, F., Visvikis, O., ... Ballabio, A. (2013). TFEB controls cellular lipid metabolism through a starvation-induced autoregulatory loop. *Nature Cell Biology*. <https://doi.org/10.1038/ncb2718>

- Settembre, C., Di Malta, C., Polito, V. A., Arencibia, M. G., Vetrini, F., Erdin, S., ... Ballabio, A. (2011). TFEB links autophagy to lysosomal biogenesis. *Science*. <https://doi.org/10.1126/science.1204592>
- Settembre, C., Zoncu, R., Medina, D. L., Vetrini, F., Erdin, S., Erdin, S., ... Ballabio, A. (2012). A lysosome-to-nucleus signalling mechanism senses and regulates the lysosome via mTOR and TFEB. *EMBO Journal*. <https://doi.org/10.1038/emboj.2012.32>
- Shah, O. J., Wang, Z., & Hunter, T. (2004). Inappropriate activation of the TSC/Rheb/mTOR/S6K cassette induces IRS1/2 depletion, insulin resistance, and cell survival deficiencies. *Current Biology*. <https://doi.org/10.1016/j.cub.2004.08.026>
- Shang, L., & Wang, X. (2011). AMPK and mTOR coordinate the regulation of Ulk1 and mammalian autophagy initiation. *Autophagy*. <https://doi.org/10.4161/auto.7.8.15860>
- Shende, P., Xu, L., Morandi, C., Pentassuglia, L., Heim, P., Lebboukh, S., ... Brink, M. (2016). Cardiac mTOR complex 2 preserves ventricular function in pressure-overload hypertrophy. *Cardiovascular Research*. <https://doi.org/10.1093/cvr/cvv252>
- Sherer, N. M., Lehmann, M. J., Jimenez-Soto, L. F., Ingmundson, A., Horner, S. M., Cicchetti, G., ... Mothes, W. (2003). Visualization of retroviral replication in living cells reveals budding into multivesicular bodies. *Traffic*. <https://doi.org/10.1034/j.1600-0854.2003.00135.x>
- Shibahara, S. (2001). Microphthalmia-associated transcription factor (MITF): Multiplicity in structure, function, and regulation. *Journal of Investigative Dermatology Symposium Proceedings*. <https://doi.org/10.1046/j.0022-202x.2001.00010.x>
- Shpilka, T., Weidberg, H., Pietrokovski, S., & Elazar, Z. (2011). Atg8: An autophagy-related ubiquitin-like protein family. *Genome Biology*. <https://doi.org/10.1186/gb-2011-12-7-226>
- Smith, S. D., Kelley, P. M., Kenyon, J. B., & Hoover, D. (2000). Tietz syndrome (hypopigmentation/deafness) caused by mutation of MITF. *Journal of Medical Genetics*.
- Soria, L. R., & Brunetti-Pierri, N. (2018). Targeting autophagy for therapy of hyperammonemia. *Autophagy*. <https://doi.org/10.1080/15548627.2018.1444312>
- Sotelo, J., Briceño, E., & López-González, M. A. (2006). Adding chloroquine to conventional treatment for glioblastoma multiforme: A randomized, double-blind, placebo-controlled trial. *Annals of Internal Medicine*. <https://doi.org/10.7326/0003-4819-144-5-200603070-00008>
- Spampanato, C., Feeney, E., Li, L., Cardone, M., Lim, J. A., Annunziata, F., ... Raben, N. (2013). Transcription factor EB (TFEB) is a new therapeutic target for Pompe disease. *EMBO Molecular Medicine*. <https://doi.org/10.1002/emmm.201202176>
- Steingrimsson, E., Tessarollo, L., Pathak, B., Hou, L., Arnheiter, H., Copeland, N. G., & Jenkins, N. A. (2002). Mitf and Tfe3, two members of the Mitf-Tfe family of bHLH-Zip transcription factors, have important but functionally redundant roles in osteoclast development. *Proceedings of the National Academy of Sciences*. <https://doi.org/10.1073/pnas.072071099>

- Steingrímsson, E, Tessarollo, L., Reid, S. W., Jenkins, N. A., & Copeland, N. G. (1998). The bHLH-Zip transcription factor Tfeb is essential for placental vascularization. *Development (Cambridge, England)*.
- Steingrímsson, Eiríkur, Copeland, N. G., & Jenkins, N. A. (2004). Melanocytes and the *Microphthalmia* Transcription Factor Network. *Annual Review of Genetics*. <https://doi.org/10.1146/annurev.genet.38.072902.092717>
- Strohecker, A. M., Guo, J. Y., Karsli-Uzunbas, G., Price, S. M., Chen, G. J., Mathew, R., ... White, E. (2013). Autophagy sustains mitochondrial glutamine metabolism and growth of Braf V600E -driven lung tumors. *Cancer Discovery*. <https://doi.org/10.1158/2159-8290.CD-13-0397>
- Svenning, S., & Johansen, T. (2013). Selective autophagy. *Essays In Biochemistry*. <https://doi.org/10.1042/bse0550079>
- Takahashi, Y., Coppola, D., Matsushita, N., Cualing, H. D., Sun, M., Sato, Y., ... Wang, H. G. (2007). Bif-1 interacts with Beclin 1 through UVRAG and regulates autophagy and tumorigenesis. *Nature Cell Biology*. <https://doi.org/10.1038/ncb1634>
- Takamura, A., Komatsu, M., Hara, T., Sakamoto, A., Kishi, C., Waguri, S., ... Mizushima, N. (2011). Autophagy-deficient mice develop multiple liver tumors. *Genes and Development*. <https://doi.org/10.1101/gad.2016211>
- Takeda, K. (2000). Ser298 of MITF, a mutation site in Waardenburg syndrome type 2, is a phosphorylation site with functional significance. *Human Molecular Genetics*. <https://doi.org/10.1093/hmg/9.1.125>
- Takeda, Kazuhisa, Yasumoto, K. I., Kawaguchi, N., Udono, T., Watanabe, K. I., Saito, H., ... Shibahara, S. (2002). Mitf-D, a newly identified isoform, expressed in the retinal pigment epithelium and monocyte-lineage cells affected by Mitf mutations. *Biochimica et Biophysica Acta - Gene Structure and Expression*. [https://doi.org/10.1016/S0167-4781\(01\)00339-6](https://doi.org/10.1016/S0167-4781(01)00339-6)
- Takemoto, C. M., Yoon, Y. J., & Fisher, D. E. (2002). The identification and functional characterization of a novel mast cell isoform of the microphthalmia-associated transcription factor. *The Journal of Biological Chemistry*. <https://doi.org/10.1074/jbc.M201441200>
- Tanaka, Y., Guhde, G., Suter, A., Eskelinen, E. L., Hartmann, D., Lüllmann-Rauch, R., ... Saftig, P. (2000). Accumulation of autophagic vacuoles and cardiomyopathy LAMP-2-deficient mice. *Nature*. <https://doi.org/10.1038/35022595>
- Tanida, I., Ueno, T., & Kominami, E. (2004). Human light chain 3/MAP1LC3B Is cleaved at its carboxyl-terminal Met 121 to expose Gly120 for lipidation and targeting to autophagosomal membranes. *Journal of Biological Chemistry*. <https://doi.org/10.1074/jbc.M407016200>
- Tassabehji, M., Newton, V. E., & Read, A. P. (1994). Waardenburg syndrome type 2 caused by mutations in the human microphthalmia (MITF) gene. *Nature Genetics*. <https://doi.org/10.1038/ng1194-251>

- Tekirdag, K. A., Akkoc, Y., Kosar, A., & Gozuacik, D. (2016). MIR376 family and cancer. *Histology and Histopathology*. <https://doi.org/10.14670/HH-11-752>
- Tekirdag, K. A., Korkmaz, G., Ozturk, D. G., Agami, R., & Gozuacik, D. (2013). MIR181A regulates starvation-and rapamycininduced autophagy through targeting of ATG5. *Autophagy*. <https://doi.org/10.4161/auto.23117>
- Thurston, T. L. M. (2009). The tbk1 adaptor and autophagy receptor ndp52 restricts the proliferation of ubiquitin-coated bacteria. *Nature Immunology*. <https://doi.org/10.1038/ni.1800>
- Till, A., Lakhani, R., Burnett, S. F., & Subramani, S. (2012). Pexophagy: The selective degradation of peroxisomes. *International Journal of Cell Biology*. <https://doi.org/10.1155/2012/512721>
- Torisu, T., Torisu, K., Lee, I. H., Liu, J., Malide, D., Combs, C. A., ... Finkel, T. (2013). Autophagy regulates endothelial cell processing, maturation and secretion of von Willebrand factor. *Nature Medicine*. <https://doi.org/10.1038/nm.3288>
- Tsunemi, T., Ashe, T. D., Morrison, B. E., Soriano, K. R., Au, J., Roque, R. A. V., ... La Spada, A. R. (2012). PGC-1 α rescues Huntington's disease proteotoxicity by preventing oxidative stress and promoting TFEB function. *Science Translational Medicine*. <https://doi.org/10.1126/scitranslmed.3003799>
- Udono, T., Yasumoto, K. I., Takeda, K., Amae, S., Watanabe, K. I., Saito, H., ... Shibahara, S. (2000). Structural organization of the human microphthalmia-associated transcription factor gene containing four alternative promoters. *Biochimica et Biophysica Acta - Gene Structure and Expression*. [https://doi.org/10.1016/S0167-4781\(00\)00051-8](https://doi.org/10.1016/S0167-4781(00)00051-8)
- Vega-Rubin-de-Celis, S., Peña-Llopis, S., Konda, M., & Brugarolas, J. (2017). Multistep regulation of TFEB by MTORC1. *Autophagy*. <https://doi.org/10.1080/15548627.2016.1271514>
- Viry, E., Paggetti, J., Baginska, J., Mgrditchian, T., Berchem, G., Moussay, E., & Janji, B. (2014). Autophagy: An adaptive metabolic response to stress shaping the antitumor immunity. *Biochemical Pharmacology*. <https://doi.org/10.1016/j.bcp.2014.07.006>
- Voorhoeve, P. M., Sage, C. Le, Schrier, M., Gillis, A. J. M., Stoop, H., Nagel, R., ... Agami, R. (2007). A genetic screen implicates miRNA-372 and miRNA-373 as oncogenes in testicular germ cell tumors. *Advances in Experimental Medicine and Biology*. https://doi.org/10.1007/978-0-387-69116-9_2
- Wan, G., Xie, W., Liu, Z., Xu, W., Lao, Y., Huang, N., ... Zhang, Y. (2014). Hypoxia-induced MIR155 is a potent autophagy inducer by targeting multiple players in the MTOR pathway. *Autophagy*. <https://doi.org/10.4161/auto.26534>
- Wang, L., Harris, T. E., Roth, R. A., & Lawrence, J. C. (2007). PRAS40 regulates mTORC1 kinase activity by functioning as a direct inhibitor of substrate binding. *Journal of Biological Chemistry*. <https://doi.org/10.1074/jbc.M702376200>
- Weidberg, H., Shvets, E., & Elazar, Z. (2011). Biogenesis and Cargo Selectivity of Autophagosomes. *Annual Review of Biochemistry*. <https://doi.org/10.1146/annurev->

- Weilbaecher, K. N., Motyckova, G., Huber, W. E., Takemoto, C. M., Hemesath, T. J., Xu, Y., ... Fisher, D. E. (2001). Linkage of M-CSF signaling to Mitf, TFE3, and the osteoclast defect in Mitfmi/mi mice. *Molecular Cell*. [https://doi.org/10.1016/S1097-2765\(01\)00360-4](https://doi.org/10.1016/S1097-2765(01)00360-4)
- Wightman, B., Ha, I., & Ruvkun, G. (1993). Posttranscriptional regulation of the heterochronic gene lin-14 by lin-4 mediates temporal pattern formation in *C. elegans*. *Cell*. [https://doi.org/10.1016/0092-8674\(93\)90530-4](https://doi.org/10.1016/0092-8674(93)90530-4)
- Wild, P., Farhan, H., McEwan, D. G., Wagner, S., Rogov, V. V., Brady, N. R., ... Dikic, I. (2011). Phosphorylation of the autophagy receptor optineurin restricts Salmonella growth. *Science*. <https://doi.org/10.1126/science.1205405>
- Wileman, T. (2013). Autophagy as a defence against intracellular pathogens. *Essays In Biochemistry*. <https://doi.org/10.1042/bse0550153>
- Wing, S. S., Chiang, H. L., Goldberg, A. L., & Dice, J. F. (1991). Proteins containing peptide sequences related to Lys-Phe-Glu-Arg-Gln are selectively depleted in liver and heart, but not skeletal muscle, of fasted rats. *The Biochemical Journal*.
- Wu, M., Hemesath, T. J., Takemoto, C. M., Horstmann, M. A., Wells, A. G., Price, E. R., ... Fisher, D. E. (2000). c-Kit triggers dual phosphorylations, which couple activation and degradation of the essential melanocyte factor Mi. *Genes and Development*.
- Xia, B., Yang, S., Liu, T., & Lou, G. (2015). miR-211 suppresses epithelial ovarian cancer proliferation and cell-cycle progression by targeting Cyclin D1 and CDK6. *Molecular Cancer*. <https://doi.org/10.1186/s12943-015-0322-4>
- Yang, H., Rudge, D. G., Koos, J. D., Vaidialingam, B., Yang, H. J., & Pavletich, N. P. (2013). mTOR kinase structure, mechanism and regulation. *Nature*. <https://doi.org/10.1038/nature12122>
- Yoda, M., Kawamata, T., Paroo, Z., Ye, X., Iwasaki, S., Liu, Q., & Tomari, Y. (2010). ATP-dependent human RISC assembly pathways. *Nature Structural and Molecular Biology*. <https://doi.org/10.1038/nsmb.1733>
- Young, A. R. J. (2006). Starvation and ULK1-dependent cycling of mammalian Atg9 between the TGN and endosomes. *Journal of Cell Science*. <https://doi.org/10.1242/jcs.03172>
- Young, Andrew R.J., Narita, M., Ferreira, M., Kirschner, K., Sadaie, M., Darot, J. F. J., ... Narita, M. (2009). Autophagy mediates the mitotic senescence transition. *Genes and Development*. <https://doi.org/10.1101/gad.519709>
- Yu, Y., Yoon, S. O., Poulogiannis, G., Yang, Q., Ma, X. M., Villén, J., ... Blenis, J. (2011). Phosphoproteomic analysis identifies Grb10 as an mTORC1 substrate that negatively regulates insulin signaling. *Science*. <https://doi.org/10.1126/science.1199484>
- Yuan, H. X., & Guan, K. L. (2015). The SIN1-PH domain connects mTORC2 to PI3K. *Cancer Discovery*. <https://doi.org/10.1158/2159-8290.CD-15-1125>

- Yuan, H. X., Russell, R. C., & Guan, K. L. (2013). Regulation of PIK3C3/VPS34 complexes by MTOR in nutrient stress-induced autophagy. *Autophagy*. <https://doi.org/10.4161/auto.26058>
- Yue, Z., Jin, S., Yang, C., Levine, A. J., & Heintz, N. (2003). Beclin 1, an autophagy gene essential for early embryonic development, is a haploinsufficient tumor suppressor. *Proceedings of the National Academy of Sciences*. <https://doi.org/10.1073/pnas.2436255100>
- Zaffagnini, G., & Martens, S. (2016). Mechanisms of Selective Autophagy. *Journal of Molecular Biology*. <https://doi.org/10.1016/j.jmb.2016.02.004>
- Zhang, T., Zhou, Q., Ogmundsdottir, M. H., Moller, K., Siddaway, R., Larue, L., ... Pignoni, F. (2015). Mitf is a master regulator of the v-ATPase, forming a control module for cellular homeostasis with v-ATPase and TORC1. *Journal of Cell Science*. <https://doi.org/10.1242/jcs.173807>
- Zhang, X., Cheng, X., Yu, L., Yang, J., Calvo, R., Patnaik, S., ... Xu, H. (2016). MCOLN1 is a ROS sensor in lysosomes that regulates autophagy. *Nature Communications*. <https://doi.org/10.1038/ncomms12109>
- Zhao, D., Ma, Y., Li, X., & Lu, X. (2019). microRNA-211 promotes invasion and migration of colorectal cancer cells by targeting FABP4 via PPAR γ . *Journal of Cellular Physiology*. <https://doi.org/10.1002/jcp.28190>
- Zhiqi, S., Soltani, M. H., Bhat, K. M. R., Sangha, N., Fang, D., Hunter, J. J., & Setaluri, V. (2004). Human melastatin 1 (TRPM1) is regulated by MITF and produces multiple polypeptide isoforms in melanocytes and melanoma. *Melanoma Research*. <https://doi.org/10.1097/00008390-200412000-00011>
- Zhou, L., Liu, S., Han, M., Feng, S., Liang, J., Li, Z., ... Cheng, J. (2017). MicroRNA-185 induces potent autophagy via AKT signaling in hepatocellular carcinoma. *Tumor Biology*. <https://doi.org/10.1177/1010428317694313>
- Zhu, H., Wu, H., Liu, X., Li, B., Chen, Y., Ren, X., ... Yang, J.-M. (2009). Regulation of autophagy by a beclin 1-targeted microRNA, miR-30a, in cancer cells. *Autophagy*.
- Zinzalla, V., Stracka, D., Oppliger, W., & Hall, M. N. (2011). Activation of mTORC2 by association with the ribosome. *Cell*. <https://doi.org/10.1016/j.cell.2011.02.014>
- Zitvogel, L., Kepp, O., Galluzzi, L., & Kroemer, G. (2012). Inflammasomes in carcinogenesis and anticancer immune responses. *Nature Immunology*. <https://doi.org/10.1038/ni.2224>
- Zoncu, R., Bar-Peled, L., Efeyan, A., Wang, S., Sancak, Y., & Sabatini, D. M. (2011). mTORC1 senses lysosomal amino acids through an inside-out mechanism that requires the vacuolar H⁺-ATPase. *Science*. <https://doi.org/10.1126/science.1207056>

APPENDIX A – Chemical and material list

| Name of Material/ Equipment | Company | Catalog Number |
|-------------------------------------|-----------------------|-----------------------|
| Acrylamide/Bis-Acrylamide Solution | Sigma | A3574 |
| Anti mouse IgG, HRP conjugated | Jackson Immuno. | 115035003 |
| Anti-Mouse IgG Alexa Fluor 594 | Invitrogen | A11005 |
| Anti-rabbit IgG HRP conjugated | Jackson Immuno. | 1110305144 |
| Anti-Rabbit IgG Alexa Fluor 594 | Invitrogen | A11002 |
| Anti-LC3B | Novus | 2331 |
| Anti-RICTOR | CST | 2114S |
| Anti-phospho-mTOR (Ser2448) | CST | 5336 |
| Anti-mTOR | CST | 2972 |
| Anti-phospho-RPS6KB/p70S6K (Thr389) | CST | 9205 |
| Anti-RPS6KB/p70S6K | CST | 2708 |
| Anti-phospho-AKT | CST | 587F11 |
| Anti-AKT | CST | 9272S |
| Anti-MITF clone 5 | Millipore | MAB3747-I |
| Anti-TFEB | CST | 4240 |
| Anti-GFP | Roche | 11814460001 |
| Anti-ACTB | Sigma | A5441 |
| Anti-Vimentin | Sigma | V6630 |
| Ampicillin | Roche | 10835269001 |
| Bradford Solution | Sigma | B6916 |
| Bromophenol blue | Applichem | A3640.0005 |
| BSA | Sigma | A4503 |
| Coumeric Acid | Sigma | C9008 |
| Coverslides | Jena Bioscience | CSL-103 |
| DMEM (high glucose) | PAN Biotech | P04-03500 |
| DMEM (low glucose) | PAN Biotech | P04-03501 |
| DMSO | Sigma | VWRSAD2650 |
| Dual luciferase reporter assay kit | Promega | E1910 |
| E64D | Santa Cruz | SC201280A |
| Ethanol | Sigma | 32221 |
| EBSS | Biological Industries | BI02-010-1A |
| Fetal bovine serum (FBS) | Biowest | S1810-500 |

| | | |
|----------------------------------|-----------------------|--------------------|
| G418 | Sigma | A1720 |
| Glutaraldehyde | Sigma | G5882 |
| Glycerol | Applichem | A4453 |
| Hoechst 33342 | Invitrogen | H3570 |
| Hydrogen Peroxide | Merck | K35522500604 |
| Isopropanol | Sigma | 24137 |
| Kanamycin | Promega | A1493 |
| LB Agar | Sigma | L2897 |
| LB Broth | Sigma | L302214 |
| L-glutamine | Biological Industries | BI03-020-1B |
| Luminol | Fluka | 9253 |
| MOPS | Sigma | M1254 |
| Methanol | Sigma | 24229 |
| Nitocellulose membrane | GE Healthcare | A10083108 |
| Non-essential aminoacids | Gibco | 11140-035 |
| Nonfat milk powder | Applichem | A0830 |
| NP-40 | Applichem | A16694.0250 |
| Pepstatin A | Sigma | P5318 |
| Paraformaldehyde (PFA) | Sigma | 15812-7 |
| PBS | PAN Biotech | P04-36500 |
| Penicillin/streptomycin solution | Biological Industries | 03-031-1B |
| PEI | Polysciences Inc | 23966 |
| Phenol red | Sigma | 114537-5G |
| PMSF | Sigma | P7627 |
| Poly-L-Lysine | Sigma | P8920 |
| Potassium Chloride | Sigma | P9333 |
| Protease inhibitor cocktail | Sigma | P8340 |
| Propidium iodide | Invitrogen | P3566 |
| Proteinase K | Promega | V302B |
| RNase Away | Sigma | 83931 |
| Saponin | Sigma | 84510 |
| siRNA MITF | Dharmacon | M-010347-02-0005 5 |
| siRNA Non-targeting | Dharmacon | D-0011210-02-20 |
| Slides | Isolab | I.075.02.005 |
| Sodium azide | Riedel de Haen | 13412 |
| Sodium chloride | Applichem | A9242.5000 |

| | | |
|---------------------------------|-----------------------|----------------|
| Sodium deoxycholate | Sigma | 30970 |
| Sodium hydroxide | Merck | 1.064.625.000 |
| Sodium dodecyl sulphate (SDS) | Biochemika | A2572 |
| Sodium orthovanadate | Sigma | 450243 |
| Sucrose | Sigma | S0389 |
| SYBR Green qRT-PCR Kit | Roche | 04-913-914-001 |
| Taqman Universal PCR Master Mix | Roche | 4304437 |
| TEMED | Sigma | T7024 |
| Torin | Tocris | 4247 |
| TRIzol Reagent | Sigma | T9424 |
| Triton-X | Applichem | 4975 |
| Trizma Base | Sigma | T1503 |
| Trypan Blue | Sigma | A4503 |
| Trypsin EDTA Solution A | Biological Industries | BI03-050-1A |
| Tween 20 | Sigma | P5927 |
| X-ray Films | Fujifilm | 47410 19289 |

APPENDIX B- Publications

Research and Review Articles

^X Corresponding author. * Authors with equal contribution.

Ozturk DG, Kocak M, Akcay A, Kinoglu K, Kara E, Buyuk Y, Kazan H and Gozuacik D ^X. MITF/MIR211 axis is a novel autophagy amplifier system during cellular stress. **Autophagy**, 2019 Mar;15(3):375-390. doi: 10.1080/15548627.2018.1531197. Epub 2018 Oct 16.

Ozturk DG, Kocak M, Gozuacik D ^X. Cloning of Autophagy-Related MicroRNAs. **Springer Protocols: Methods Mol Biol**. 2017 Oct 12. doi: 10.1007/7651_2017_83.

Gozuacik D ^X, Akkoc Y*, **Ozturk DG***, Kocak M. Autophagy, MicroRNAs and Cancer. In the special issue: Self-eating on demand: Autophagy in Cancer and Cancer Therapy (Eds. Agostinis P and Lane J). **Frontiers in Oncology**, 2017

Demir F, Hocaoglu I, **Ozturk DG**, Kiraz A, Gozuacik D^x, Acar HY^x. Highly Luminescent and Cytocompatible Cationic Ag₂S NIR-emitting Quantum Dots for Gene Transfection and Optical Imaging. **Nanoscale**. 2015 Jul 14;7(26):11352-62. doi: 10.1039/c5nr00189g.

Tekirdag KA, **Ozturk DG**, Gozuacik D^x. Regulation of autophagy by miRNAs. In the book: **Autophagy: Cancer, Other Pathologies, Inflammation, Immunity, and Infection**. Elsevier Academic Press. 2014. ISBN: 9780124055308, Book chapter.

Tekirdag KA, **Ozturk DG**, Gozuacik D^x. Alterations in autophagic-lysosomal potential during ageing and neurological diseases: The miRNA perspective. **Current Pathobiology Reports**, 2013 December 2013, Volume 1, Issue 4, pp 247-261.

Korkmaz G*, Tekirdag AK*, **Ozturk DG**, Kosar A, Sezerman OU and Gozuacik D ^X. MIR376A is a regulator of starvation-induced autophagy. **PLoS ONE**, 2013, 8(12): e82556. doi:10.1371/journal.pone.0082556.

Tekirdag AK*, Korkmaz G*, **Ozturk DG**, Agami R, Gozuacik D^x. miR-181a regulates starvation- and rapamycin-induced autophagy through targeting of ATG5. **Autophagy**, 2013 March; 9(3): 1-12.

Poster Presentations

1. **Ozturk DG**, Kocak M, Gozuacik D. MITF/MIR211 axis is a novel autophagy amplifier system during cellular stress. **Gordon Research Conference**, 2018 Autophagy in Stress, Development and Disease (GRS), Renaissance Tuscany Il Ciocco in Lucca (Barga) Italy, March 19-23, 2018
2. **Ozturk DG**, Kocak M, Gozuacik D. MITF/MIR211 axis is a novel autophagy amplifier system during cellular stress. **Gordon Research Seminar**, 2018 Autophagy in Stress, Development and Disease (GRS), Renaissance Tuscany Il Ciocco in Lucca (Barga) Italy, March 18-19
3. Oral O, İtah Z, **Ozturk DG** and Gozuacik D. Cleavage of Atg3 protein by caspase-8 regulates autophagy during receptor-activated cell death. FEBS Advanced Lecture Course: 360 Lysosome, Kusadasi, Turkey, October 23-28 2014

Patents

Stress-incuded microRNAs as novel diagnostic markers of cancer (SIM-Marker)
(SUP147-PCT/TR2019/050004)

MITF-MIR211 axis is a novel autophagy amplifier system during cellular stress

Deniz Gulfem Ozturk^a, Muhammed Kocak^a, Arzu Akcay^b, Kubilay Kinoglu^b, Erdogan Kara^b, Yalcin Buyuk^b, Hilal Kazan^c, and Devrim Gozuacik^{a,d,e}

^aSabanci University, Faculty of Engineering and Natural Sciences, Molecular Biology, Genetics and Bioengineering Program, Orhanli-Tuzla, Turkey; ^bCouncil of Forensic Medicine, Ministry of Justice, Bahcelievler, Turkey; ^cAntalya Bilim University, Faculty of Engineering, Department of Computer Engineering, Antalya, Turkey; ^dCenter of Excellence for Functional Surfaces and Interfaces for Nano Diagnostics (EFSUN) Orhanli-Tuzla, Turkey; ^eSabanci University Nanotechnology Research and Application Center (SUNUM), Sabanci University, Orhanli-Tuzla, Turkey

ABSTRACT

Macroautophagy (autophagy) is an evolutionarily conserved recycling and stress response mechanism. Active at basal levels in eukaryotes, autophagy is upregulated under stress providing cells with building blocks such as amino acids. A lysosome-integrated sensor system composed of RAG GTPases and MTOR complex 1 (MTORC1) regulates lysosome biogenesis and autophagy in response to amino acid availability. Stress-mediated inhibition of MTORC1 results in the dephosphorylation and nuclear translocation of the TFE/ MITF family of transcriptional factors, and triggers an autophagy- and lysosomal-related gene transcription program. The role of family members TFEB and TFE3 have been studied in detail, but the importance of MITF proteins in autophagy regulation is not clear so far. Here we introduce for the first time a specific role for MITF in autophagy control that involves upregulation of *MIR211*. We show that, under stress conditions including starvation and MTOR inhibition, a MITF-MIR211 axis constitutes a novel feed-forward loop that controls autophagic activity in cells. Direct targeting of the MTORC2 component RICTOR by *MIR211* led to the inhibition of the MTORC1 pathway, further stimulating MITF translocation to the nucleus and completing an autophagy amplification loop. In line with a ubiquitous function, MITF and *MIR211* were co-expressed in all tested cell lines and human tissues, and the effects on autophagy were observed in a cell-type independent manner. Thus, our study provides direct evidence that MITF has rate-limiting and specific functions in autophagy regulation. Collectively, the MITF-MIR211 axis constitutes a novel and universal autophagy amplification system that sustains autophagic activity under stress conditions.

Abbreviations: ACTB: actin beta; AKT: AKT serine/threonine kinase; AKT1S1/PRAS40: AKT1 substrate 1; AMPK: AMP-activated protein kinase; ATG: autophagy-related; BECN1: beclin 1; DEPTOR: DEP domain containing MTOR interacting protein; GABARAP: GABA type A receptor-associated protein; HIF1A: hypoxia inducible factor 1 subunit alpha; LAMP1: lysosomal associated membrane protein 1; MAP1LC3B/LC3B: microtubule associated protein 1 light chain 3 beta; MAPKAP1/SIN1: mitogen-activated protein kinase associated protein 1; MITF: melanogenesis associated transcription factor; MLST8: MTOR associated protein, LST8 homolog; MRE: miRNA response element; MTOR: mechanistic target of rapamycin kinase; MTORC1: MTOR complex 1; MTORC2: MTOR complex 2; PRR5/Protor 1: proline rich 5; PRR5L/Protor 2: proline rich 5 like; RACK1: receptor for activated C kinase 1; RPTOR: regulatory associated protein of MTOR complex 1; RICTOR: RPTOR independent companion of MTOR complex 2; RPS6KB/p70S6K: ribosomal protein S6 kinase; RT-qPCR: quantitative reverse transcription-polymerase chain reaction; SQSTM1: sequestosome 1; STK11/LKB1: serine/threonine kinase 11; TFE3: transcription factor binding to IGHM enhancer 3; TFEB: transcription factor EB; TSC1/2: TSC complex subunit 1/2; ULK1: unc-51 like autophagy activating kinase 1; UVRAG: UV radiation resistance associated; VIM: vimentin; VPS11: VPS11, CORVET/HOPS core subunit; VPS18: CORVET/HOPS core subunit; WIP1: WD repeat domain, phosphoinositide interacting 1

ARTICLE HISTORY

Received 18 September 2017
Revised 21 September 2018
Accepted 26 September 2018

KEYWORDS

Autophagy; cellular stress;
lysosome; microRNA; MITF;
MTOR; RICTOR



Autophagy-Regulating microRNAs and Cancer

Devrim Gozuacik^{1,2*}, Yunus Akkoc^{1†}, Deniz Gulfem Ozturk^{1†} and Muhammed Kocak¹

¹Molecular Biology, Genetics and Bioengineering Program, Faculty of Engineering and Natural Sciences, Sabanci University, Istanbul, Turkey; ²Center of Excellence for Functional Surfaces and Interfaces for Nano Diagnostics (EFSUN), Sabanci University, Istanbul, Turkey

OPEN ACCESS

Edited by:

Patrizia Agostinis,
State University of Leuven, Belgium

Reviewed by:

Giovanni Blandino,
Istituti Fisioterapici Ospitalieri
(IROCCS), Italy
Stefano Fais,
Istituto Superiore di Sanità, Italy
Francesco Di Raimondo,
University of Catania, Italy

*Correspondence:

Devrim Gozuacik
dgozuacik@sabanciuniv.edu

[†]These authors have contributed
equally to this work as second
authors.

Macroautophagy (autophagy herein) is a cellular stress response and a survival pathway that is responsible for the degradation of long-lived proteins, protein aggregates, as well as damaged organelles in order to maintain cellular homeostasis. Consequently, abnormalities of autophagy are associated with a number of diseases, including Alzheimer's disease, Parkinson's disease, and cancer. According to the current view, autophagy seems to serve as a tumor suppressor in the early phases of cancer formation, yet in later phases, autophagy may support and/or facilitate tumor growth, spread, and contribute to treatment resistance. Therefore, autophagy is considered as a stage-dependent dual player in cancer. microRNAs (miRNAs) are endogenous non-coding small RNAs that negatively regulate gene expression at a post-transcriptional level. miRNAs control several fundamental biological processes, and autophagy is no exception. Furthermore, accumulating data in the literature indicate that dysregulation of miRNA expression contribute to the mechanisms of cancer formation, invasion, metastasis, and affect responses to chemotherapy or radiotherapy. Therefore, considering the importance of autophagy for cancer biology, study of autophagy-regulating miRNA in cancer will allow a better understanding of malignancies and lead to the development of novel disease markers and therapeutic strategies. The potential to provide study of some of these cancer-related miRNAs were also implicated in autophagy regulation. In this review, we will focus on autophagy, miRNA, and cancer connection, and discuss its implications for cancer biology and cancer treatment.

Keywords: autophagy, microRNA, post-transcriptional control, cancer growth, metastasis, chemotherapy, radiotherapy, biomarker

ARTICLE

Highly luminescent and cytocompatible cationic Ag₂S NIR-emitting quantum dots for optical imaging and gene transfection

Cite this: DOI: 10.1039/x0xx00000x

Received 00th January 2012,
Accepted 00th January 2012

DOI: 10.1039/x0xx00000x

www.rsc.org/

Fatma Demir Duman,^a Ibrahim Hocaoglu,^a Deniz Gulfem Ozturk,^b Devrim Gozuacik,^b Alper Kiraz^{a,c} and Havva Yagci Acar^{a,d,e}

Development of non-toxic theranostic nanoparticles capable of delivering a therapeutic cargo and providing a means for diagnosis is one of the most challenging tasks in front of the nanobiotechnology. Gene therapy is a very important mode of therapy and polyethylenimine (PEI) is one of the most successful vehicles for gene transfection, yet pose a significant toxicity. Optical imaging utilizing quantum dots is one of the newer but fast growing diagnostic modality, which requires non-toxic, highly luminescent materials, preferentially active in the near infrared region. Ag₂S NIRQDs fit to this profile perfectly. Here, we demonstrate the aqueous synthesis of cationic Ag₂S NIRQDs with a mixed coating of 2-mercaptopropionic acid (2MPA) and PEI (branched, 25 kDa), that are highly luminescent in the NIR-I window ($\lambda_{em} = 810-840$ nm) as new theranostic nanoparticles. Synergistic stabilization of QD surface via simultaneous use of a small molecule and a polymeric material provided the highest quantum yield, 150 % (with respect to LDS 798 at pH 7.4), reported in the literature for Ag₂S. These cationic particles show dramatic improvement in cytocompatibility even without PEGylation, strong optical signal easily detected by confocal laser microscopy and effective conjugation and transfection of green fluorescence protein plasmid (pGFP) to HeLa and MCF-7 cell lines (40 % efficiency). Overall, these Ag₂S NIRQDs demonstrate great potential as new theranostics.

Alteration in Autophagic-lysosomal Potential During Aging and Neurological Diseases: The microRNA Perspective

Kumsal Ayse Tekirdag · Deniz Gulfem Ozturk · Devrim Gozuacik

Published online: 1 October 2013
© Springer Science+Business Media New York 2013

Abstract Macroautophagy (hereafter referred to as autophagy) is an evolutionary conserved degradation pathway that targets cytoplasmic substrates, including long-lived proteins, protein aggregates and damaged organelles, and leads to their degradation in lysosomes. Beyond its role in adaptation to cellular stresses, such as nutrient deprivation, hypoxia and toxins, recent studies attributed a central role to autophagy in aging and life span determination. Moreover, alterations and abnormalities of autophagy may contribute to a number of important health problems, including cancer, myopathies, metabolic disorders and, the focus of this review, aging-related neurodegenerative diseases. Some disease-related, mutant and aggregation-prone proteins may be cleared by autophagy; on the other hand, dysregulation of the autophagy pathways may also contribute to neurotoxicity observed in degenerative pathologies. microRNAs (miRNAs) are endogenous regulators of gene expression, and their deregulation was reported in several aging-related conditions. Studies in the last few years introduced miRNAs as novel and potent regulators of autophagy. In this review article, we will summarize the connection between autophagy, aging and Alzheimer's, Parkinson's and Huntington's diseases, and discuss the role of autophagy-related miRNAs in this context.

Introduction

Aging is an evolutionarily conserved and biologically regulated natural phenomenon, leading to changes that eventually result in the death of organisms. As the human life span is increasing due to higher living standards, medical care and preventive measures, aging-related diseases have become widespread in societies. Therefore, a better understanding of molecular, cellular and organismal changes accompanying aging and aging-related diseases is required.

Recent studies underline the importance of changes and abnormalities in autophagy pathways during aging and disease [1]. In fact, autophagy is a cellular recycling mechanism and a key biological phenomenon in cell survival and death. Two major types of autophagy were involved in aging and related diseases, namely macroautophagy and chaperone-mediated autophagy (CMA). Macroautophagy is characterized by sequestration in double membrane vesicles (autophagic vesicles or autophagosomes) of cytosolic components, such as long-lived proteins, organelles (e.g., mitochondria) and abnormal aggregates, followed by their delivery into lysosomes (now becoming autolysosomes) [2, 3]. Once degraded by lyso-

4

Regulation of Autophagy by microRNAs

Kumsal Ayse Tekirdag, Deniz Gulfem Ozturk
and Devrim Gozuacik

OUTLINE

| | | | |
|---|----|---|----|
| Introduction | 82 | <i>microRNAs</i> | 88 |
| Molecular Mechanisms of Autophagy | 82 | <i>microRNA Biogenesis</i> | 88 |
| <i>Initiation and Formation of the Autophagosome</i> | 83 | microRNAs: Novel Regulators of Autophagy | 90 |
| <i>Elongation of the Autophagosome</i> | 84 | <i>miRNA Regulation of Signals Upstream to Autophagy Pathways</i> | 90 |
| <i>Maturation and Fusion with the Lysosomes</i> | 85 | <i>miRNA Regulation of Autophagosome Initiation and Formation</i> | 94 |
| Major Signaling Pathways Regulating Autophagy | 85 | <i>miRNA Regulation of the Autophagosome Elongation Step</i> | 95 |
| <i>mTOR Pathway</i> | 85 | <i>miRNA Regulation of Vesicular Transport Events, Autophagosome Maturation and Fusion with Lysosomes</i> | 96 |
| <i>AKT/PKB and Growth Factors</i> | 86 | microRNA Regulation of Autophagy-Related Signaling Pathways | 96 |
| <i>FoxO Regulation of Autophagy</i> | 86 | Conclusion | 97 |
| <i>AMPK Pathway</i> | 86 | Acknowledgments | 99 |
| <i>Inositol Pathway</i> | 86 | References | 99 |
| <i>Stress-Responsive BECN1/BCL2 Complex</i> | 87 | | |
| <i>Hypoxia, ROS and Autophagy</i> | 87 | | |
| <i>P53 Pathway</i> | 87 | | |
| Small Regulators: microRNAs, their Biogenesis and Biological Functions | 88 | | |

MIR376A Is a Regulator of Starvation-Induced Autophagy

Gozde Korkmaz^{1*}, Kumsal Ayse Tekirdag¹, Deniz Gulfem Ozturk, Ali Kosar, Osman Ugur Sezerman, Devrim Gozuacik²

Faculty of Engineering and Natural Sciences, Sabanci University, Istanbul, Turkey

Abstract

Background: Autophagy is a vesicular trafficking process responsible for the degradation of long-lived, misfolded or abnormal proteins, as well as damaged or surplus organelles. Abnormalities of the autophagic activity may result in the accumulation of protein aggregates, organelle dysfunction, and autophagy disorders were associated with various diseases. Hence, mechanisms of autophagy regulation are under exploration.

Methods: Over-expression of hsa-miR-376a1 (shortly *MIR376A*) was performed to evaluate its effects on autophagy. Autophagy-related targets of the miRNA were predicted using Microcosm Targets and MIRanda bioinformatics tools and experimentally validated. Endogenous miRNA was blocked using antagomirs and the effects on target expression and autophagy were analyzed. Luciferase tests were performed to confirm that 3' UTR sequences in target genes were functional. Differential expression of *MIR376A* and the related *MIR376B* was compared using TaqMan quantitative PCR.

Results: Here, we demonstrated that, a microRNA (miRNA) from the *DLK1/GTL2* gene cluster, *MIR376A*, played an important role in autophagy regulation. We showed that, amino acid and serum starvation-induced autophagy was blocked by *MIR376A* overexpression in MCF-7 and Huh7 cells. *MIR376A* shared the same seed sequence and had overlapping targets with *MIR376B*, and similarly blocked the expression of key autophagy proteins ATG4C and BECN1 (Beclin 1). Indeed, 3' UTR sequences in the mRNA of these autophagy proteins were responsive to *MIR376A* in luciferase assays. Antagomir tests showed that, endogenous *MIR376A* was participating to the control of *ATG4C* and *BECN1* transcript and protein levels. Moreover, blockage of endogenous *MIR376A* accelerated starvation-induced autophagic activity. Interestingly, *MIR376A* and *MIR376B* levels were increased with different kinetics in response to starvation stress and tissue-specific level differences were also observed, pointing out to an overlapping but miRNA-specific biological role.

Conclusions: Our findings underline the importance of miRNAs encoded by the *DLK1/GTL2* gene cluster in stress-response control mechanisms, and introduce *MIR376A* as a new regulator of autophagy.

Citation: Korkmaz G, Tekirdag KA, Ozturk DG, Kosar A, Sezerman OU, et al. (2013) *MIR376A* Is a Regulator of Starvation-Induced Autophagy. PLoS ONE 8(12): e82556. doi:10.1371/journal.pone.0082556

Editor: Sebastien Pfeffer, French National Center for Scientific Research - Institut de biologie moléculaire et cellulaire, France

Received: August 23, 2013; **Accepted:** October 29, 2013; **Published:** December 16, 2013

Copyright: © 2013 Korkmaz et al. This is an open-access article distributed under the terms of the Creative Commons Attribution License, which permits unrestricted use, distribution, and reproduction in any medium, provided the original author and source are credited.

Funding: This work was supported by The Scientific and Technological Research Council of Turkey (TUBITAK) 1001 Grant and Sabanci University. D.G. and A.K. are recipients of the Turkish Academy of Sciences (TUBA) GEBIP Award. D.G. is a recipient of the EMBO Strategical Development and Installation Grant (EMBO-SDIG) and A.K. is a recipient of the TUBITAK Incentive Award. G.K. and K.A.T. are recipients of Yousef Jameel and TUBITAK-BIDEB PhD Scholarships, respectively. The funders had no role in study design, data collection and analysis, decision to publish, or preparation of the manuscript.

Competing Interests: The authors have declared that no competing interests exist.

* E-mail: dgozuacik@sabanciuniv.edu

† These authors contributed equally to this work.

‡ Current address: Division of Gene Regulation, The Netherlands Cancer Institute, Amsterdam, The Netherlands

MIR181A regulates starvation- and rapamycin-induced autophagy through targeting of ATG5

Kumsal Ayse Tekirdag,^{1,†} Gozde Korkmaz,^{1,‡} Deniz Gulfem Ozturk,¹ Reuven Agami² and Devrim Gozuacik^{1,*}

¹Faculty of Engineering and Natural Sciences; Biological Sciences and Bioengineering Program; Sabanci University; Istanbul, Turkey; ²Division of Gene Regulation; The Netherlands Cancer Institute; Amsterdam, The Netherlands

[†]These authors contributed equally to this work.

Keywords: macroautophagy, mammalian autophagy regulation, microRNA, hsa-miR-181a, ATG5, starvation, rapamycin, MTOR

Abbreviations: ACTB, actin beta; *ATG5*, autophagy-related 5; ATG12, autophagy-related 12; ATG16L1, autophagy-related 16-like 1; BECN1, Beclin 1; miRNA, microRNA; LC3, microtubule-associated protein 1 light chain 3; *MIR181A*, human microRNA-181A and its gene; PE, phosphatidylethanolamine; MTOR, mechanistic target of rapamycin; MRE, miRNA-response element; BCL2, B-cell lymphoma 2; RPS6KB/P70S6K, ribosomal protein S6 kinase; SQSTM1/P62, sequestosome 1; RAP, rapamycin; STV, starvation; E+P, E64d/pepstatin A; RT-PCR, reverse transcriptase-polymerase chain reaction; MTT, thiazolyl blue tetrazolium blue; Ant-181a, *MIR181A*-specific antagomir; CNT-Ant, control antagomir; TRIzol, trizol Reagent; PEI, polyethylenimine; DMSO, dimethyl sulfoxide; *U6*, U6 small nuclear 1 (RNU6-1); GFP, green fluorescent protein; *MIR376B*, human microRNA-376B and its gene; EBSS, Earle's Balanced Salt Solution; *MIR30A*, human microRNA-30A and its gene; QPCR, quantitative PCR; *GAPDH*, glyceraldehyde-3-phosphate dehydrogenase

Macroautophagy (autophagy herein) is a cellular catabolic mechanism activated in response to stress conditions including starvation, hypoxia and misfolded protein accumulation. Abnormalities in autophagy were associated with pathologies including cancer and neurodegenerative diseases. Hence, elucidation of the signaling pathways controlling autophagy is of utmost importance. Recently we and others described microRNAs (miRNAs) as novel and potent modulators of the autophagic activity. Here, we describe *MIR181A* (hsa-miR-181a-1) as a new autophagy-regulating miRNA. We showed that overexpression of *MIR181A* resulted in the attenuation of starvation- and rapamycin-induced autophagy in MCF-7, Huh-7 and K562 cells. Moreover, antagomir-mediated inactivation of endogenous miRNA activity stimulated autophagy. We identified *ATG5* as an *MIR181A* target. Indeed, *ATG5* cellular levels were decreased in cells upon *MIR181A* overexpression and increased following the introduction of antagomirs. More importantly, overexpression of *ATG5* from a miRNA-insensitive cDNA construct rescued autophagic activity in the presence of *MIR181A*. We also showed that the *ATG5* 3' UTR contained functional *MIR181A* responsive sequences sensitive to point mutations. Therefore, *MIR181A* is a novel and important regulator of autophagy and *ATG5* is a rate-limiting miRNA target in this effect.